Alma Mater Studiorum – Università di Bologna

DOTTORATO DI RICERCA

Science for Conservation

Ciclo **XXII**

Settore/i scientifico disciplinari di afferenza: CHIM/12

TITOLO TESI

DURABILITY OF CRYSTALLINE MONUMENTAL STONES IN TERMS OF THEIR PETROPHYSICAL CHARACTERISTICS

Presentata da: Timea Kovács

Coordinatore Dottorato

Relatore

Prof. Rosa María Esbert Alemany

Prof. Rocco Mazzeo

Prof. Modesto Montoto San Miguel

Esame finale anno 2009

Universidad de Oviedo
Departamento de Geología

Durability of crystalline monumental stones in terms of their petrophysical characteristics

PhD Thesis

Timea Kovács

Supervisors:

Rosa María Esbert Alemany **Modesto Montoto San Miguel**

Oviedo, 2009

Acknowledgements

First of all I would like to thank my supervisors, Rosa María Esbert and Modesto Montoto. Despite of all the difficulties we had to face during these three years I could always count on their support and I could turn to them with any questions or doubts.

The research was carried out at the Department of Geology of the University of Oviedo and I received a lot of professional help from the professors of the Petrophysics and Alteration Group and in general the Petrology and Geochemistry Area of this Department, especially from Javier Alonso Rodríguez. I am very grateful for it.

My fellow workers from the same group also deserve my gratitude, especially Felix Mateos, without whom I would have never learnt and achieved the half of what I did. Patricia, Marta, Lucía, Héctor, Edgar and all the others who worked with me for longer or shorter intervals were also of great help either in professional or personal terms. Thank you all.
Luis Valdeón and Araceli Rojo also helped me a lot with their wide professional and practical experience.
From the same department I have to express my thanks to the technical staff for the several dozens of thin sections they prepared for me.
From Servicios Científico-Técnicos of the University of Oviedo I am especially grateful to Angel Martínez Nistal and Marta Alonso Guervós from the Digital Image Processing group; to Alfredo Quintana from the Scanning Electron Microscopy service; to Emilio Ariño from the XRD-XRF service and to Alfonso Fernández González from the X-ray Photoelectron Spectrometry laboratory.

Other measurements were carried out at the Instituto Nacional del Carbón in Oviedo and at the University of Barcelona, I would like to thank their work also.

During my few days stay at the University of Alicante I learnt a lot from David Benavente, Nora Cueto and Javier Martínez; I am very grateful to them to welcome me so warmly and to be willing to co-operate any time.
Also my short visit to AIDICO proved to be very useful and interesting; many thanks to Ángel López Buendía and José Manuel Cuevas.

From Hungary I can still any time count on the professional and emotional support of my former supervisors, Szakmány György and T. Biró Katalin. Józsa Sándor and Pintér Farkas also helped me a lot to be able to start this research, and I could always turn to them for help or encouragement. Köszönöm szépen mindőtöknek.

This research was part of the EPISCON project, which is a Marie Curie Action. Without the coordination of Rocco Mazzeo and of the University of Bologna and the financial support of the European Community, this work and this fantastic international project would never have been possible. From the "Ravenna-days" the continuous help and care of Anna Missiroli must be mentioned on the first place. I also would like to give my thanks to all of my EPISCON fellows. I think we formed a great team and I hope to keep in touch with all of you.

También quiero dar las gracias a todas las personas en Oviedo que me ayudaron a adaptarme a esta cultura y sociedad tan maravillosa pero tan lejana de la mía y que hacían que me sienta en casa. Aparte de las que ya están mencionadas gracias a Alberto, Esther, Matthias y a muchos más.

Köszönöm barátaimnak azoknak is, akik otthon vannak és azoknak is, akik szintén távol az otthonuktól, hogy mellettem álltak, és hogy nem hagyták elveszni a barátságot a távolság ellenére sem. Köszönöm Szilvinek, Jánosnak, Péternek, Daninak, a lányoknak Egerből és mindenki másnak.

Végül, de egyátalán nem utolsó sorban szeretném megköszönni nektek, anya, apa és Judit, hogy elengedtetek ilyen messzire, bár tudom, nem örültetek neki, és köszönöm, hogy mindig támogattok, akármit is vegyek a fejembe…

Köszönöm mindenkinek!
Thank you all!
¡Gracias a todos!

Index

Abstract

The durability of stone building materials is an issue of utmost importance in the field of monument conservation. In order to be able to preserve our built cultural heritage, the thorough knowledge of its constituent materials and the understanding of the processes that affect them are indispensable.

The main objective of this research was to evaluate the durability of a special stone type, the crystalline stones, in correlation with their intrinsic characteristics, the petrophysical properties.

The crystalline stones are differentiated from the cemented stones on the basis of textural features. Their most important specific property is the usually low, fissure-like porosity. Stone types of significant monumental importance, like the marble or granite belong to this group. The selected materials for this investigation, indeed, are a marble (Macael marble, Spain) and a granite (Silvestre Vilachán granite, Spain). In addition, an andesite (Szob andesite, Hungary) also of significant monumental importance was selected. This way a wide range of crystalline rocks is covered in terms of petrogenesis: stones of metamorphic, magmatic and volcanic origin, which can be of importance in terms of mineralogical, petrological or physical characteristics.

After the detailed characterization of the petrophysical characteristics of the selected stones, their durability was assessed by means of artificial ageing. The applied ageing tests were: the salt crystallization, the frost resistance in pure water and in the presence of soluble salts, the salt mist and the action of SO_2 in the presence of humidity.

The research aimed at the understanding of the mechanisms of each weathering process and at finding the petrophysical properties most decisive in the degradation of these materials.

Among the several weathering mechanisms, the most important ones seem to be the physical stress due to crystallization pressure of both salt and ice, the thermal fatigue due to cyclic temperature changes and the chemical reactions (mostly the acidic attack) between the mineral phases and the external fluids.

The properties that fundamentally control the degradation processes, and thus the durability of stones were found to be: the mineralogical and chemical composition; the hydraulic properties especially the water uptake, the permeability and the drying; the void space structure, especially the void size and aperture size distribution and the connectivity of the porous space; and the thermal and mechanical properties.

The mineralogical and chemical composition was decisive in the resistance to chemical attack, controlled by the solubility of each mineral phase (e.g. calcite in acidic solutions) or the

presence of other chemical reactions (e.g. the catalyzation of SO_2 by the iron content of the stone). On the other hand, the mechanical properties of each mineral phase and the possible presence of minerals especially susceptible to physical stress (like phyllosilicates) influence the resistance to physical degradation also.

The mentioned hydraulic properties control the process of salt weathering both during the salt crystallization and the salt mist tests. Therefore, stones with fast fluid kinetics – both in the liquid and the vapour phase – and with high degree of water uptake have the highest susceptibility to this kind of weathering. The properties of the void space structure determine the hydraulic properties on one hand, and on the other, they play fundamental role in other aspects of weathering, such as the freezing point depression, the crystallization pressure, etc. This had an influence mostly on the frost and the salt weathering. Of two stone types with very similar open porosity values (granite ~4% and andesite ~4,5%), the one with a well-communicating porous network and larger apertures proved to be highly susceptible to salt and frost weathering; while the other with extremely slow fluid kinetics is highly durable under the same conditions.

The thermal properties have an important control over the deterioration whenever cyclic thermal changes occur. The marble of this research, with anisotropic thermal properties, suffered thermal degradation even after a small number of cycles of 40°C temperature range.

Finally, the mechanical properties, which were not investigated deeply in this research, determine the resistance of stones to physical damage.

Because of the complexity of the processes and the high number of determining properties, no mechanisms or characteristics could be identified as typical for crystalline stones. The durability or alterability of each stone type must be assessed according to its properties and not according to the textural or petrophysical classification they belong to.

Finally, a critical review of standardized methods is presented, based on which an attempt was made for recommendations of the most adequate methodology for the characterization and durability assessment of crystalline stones.

1. Introduction

1. Introduction – State of the art

"Durability is a complex term that can only be defined and understood in relation to its context." (Inkpen et al., 2004).

According to an early definition (Anon., 1983), durability is the ability of a material to maintain its characteristics of strength, resistance to decay and appearance in relation to a specific manner, purpose and environment of use. This definition summarizes the aspects that must be taken into consideration when dealing with natural stone used in construction. These aspects do not only include the distinct and already numerous properties of the material itself, but a set of environmental, architectonical, social and economical factors, which all have their determining influence on the value of a building material. Besides, the evolution of the performance has been pointed out as another important issue in durability (Nireki, 1980; Duffy and O'Brien, 1996), which highlights the continuous variability of this property both in time and space (Turkington, 2002).

This leads to the conclusion that durability is not a definite and constant property of a material, and thus, it cannot be determined by a single test or described by a single value. According to Miglio and Willmott (1997) "the assessment of durability will have to be taken on the basis of skilled interpretation based on the results of a series of tests" and always taking into account the purpose, motion and circumstances of the use of the material.

Natural stone, besides its significant economical and industrial importance, has an incontrovertible cultural and historical value. It can be considered the most important building material all along the history of humanity, a major part of the built Cultural Heritage being constructed of it. As expressed by Lewin (1983) "Stone … is and has been employed by humans for recording, embellishing, advertising or preserving the facts of their lives and their spiritual and artistic visions, as well as to satisfy their practical needs for shelter, protection and secure storage." And thus, today's scientists and conservators have the responsibility to reserve all these memories of the past – monuments, sculptures and religious relics – for future generations, as the deterioration of these objects is an urgent and serious issue.

The conservation and restoration of our Cultural Heritage, the build heritage included, is becoming a concept of more and more acknowledged importance all over the world. By the second half of the 19th and the beginning of the 20th century the first public organizations and legal regulations were created for the protection of heritage (Poblador, 2001). In the 1970es several groups and committees of experts in European countries started the systematic scientific study of topics related to stone conservation, like the RILEM with the outstanding contribution of Mamillan, the Instituto per il Restauro of Rome, under the direction of Brandi or the Centro "Cesare Gnudi" of Bologna, under the direction of Rossi-Manaresi. The scientific results of these and several other groups have been and are still published in the

series of congresses under the name of "International Congress on the Deterioration and Conservation of Stone".

The Italian Charter for the Restoration of Historic Monuments or "Carta del Restauro" from 1972 (Brandi, 1977) was one of the first to officially establish "general principles and doctrines relating to the protection of monuments". The IPHE (Instituto del Patrimonio Histórico Español) in 2003 synthesised the stages, methods and procedures of stone conservation (Esbert and Losada, 2003), which today are official guidelines to follow in conservation-restoration works in Spain and the countries of South-America. Recommendations are introduced in Europe also for the longest possible preservation of monuments from the inevitable stone decay.

Conservation in general is a multidisciplinary field, and so is stone conservation. The later, besides the owners, the legal organisms and the stakeholders, involves geomorphologists, geologists, stone conservators, engineers and architects. The co-operation among these professionals and the application of interdisciplinary solutions is not at all an easy task due to the problems of communication and distinct approaches. Scientific conservation aims at building a bridge among the different groups and employing the knowledge of natural sciences and engineering directly to the service of conservation/restoration. The fundamentals of natural processes must be taken into consideration whenever a consolidating treatment is applied, a new material is assessed for replacement or the decay rate and causes of the elements of a monument are established.

The weathering of stone materials is a natural and continuous process due to differences between the conditions of their formation and the conditions to which they are exposed on the surface of the Earth. It is a result of physical, chemical and biological mechanisms conditioned by the interaction of the rock and the atmospheric agents (Amoroso and Fassina, 1983; Kühnel, 2004). The most important physical driving forces of damage are the pressure and temperature changes or fluctuations (Camuffo, 1995); the chemical ones are the redox reactions, the hydration-dehydration, and the dissolution and precipitation (Esbert et al., 1997); and finally, the biogenic ones are mostly connected to the growth of micro- or higher plants (Caneva et al., 1991). Besides, stones used in man-made constructions are subject to another type of deterioration which can be classified as anthropogenic. This includes all the human activities, starting from the quarrying of the stone till the effects of vandalism or warfare on built constructions (Siegesmund et al. 2002) including the indirect consequences of air pollution etc. A more detailed discussion about the weathering agents can be found in the chapter 6.1 of this thesis.

The deterioration is a function of the rock properties and the aggressiveness of the external conditions (Esbert et al., 1982; Kühnel, 2002). Rocks, by definition, are solids composed of one or more types of minerals joined to one another in a more or less tight fabric. The term 'stone' is used for rocks shaped and used by man (Winkler, 1997). The above definition reveals the two most basic properties of rocks: the mineralogical composition and the texture. Originating from these two basic characteristics, a series of further properties can be defined,

such as the chemical composition, the grain size and shape, the void space properties, the microstructure etc – that altogether can be called petrophysical properties (Montoto, 1983).

Field and laboratory observations during the past decades of scientific investigation of stone weathering proved that among the numerous properties that characterize a stone material, there are a few that has an especially important role in the degradation (Esbert and Ordaz, 1985).

Hirschwald already in 1908 defined a coefficient based on the saturation kinetics of the stone material, which he proposed for the assessment of stones to frost weathering. Hatsagortsian, in 1985, published a theory of the assessment of stone durability based on the pore space structure.

These two early works point out the importance of two fundamental characteristics, which are in strong connection to each other: the void space and the hydraulic properties of the material. The total, open and effective porosity, the void size distribution, the connectivity and permeability of the void space to different fluids, the shape and position of voids, the pore to fissure ratio, the fissure density, the velocity of fluid movement during wetting, drying or circulating inside the material etc. are the most important of these characteristics. These properties, which determine the behaviour and movement of water in the stone, the specific surface exposed to chemical reactions, the stresses building up by the movement or formation of foreign liquid or solid substances, were proved to be fundamental by several further investigations (Delgado Rodrigues, 1983, Hoffmann and Niesel, 1992; Valdeón et al., 1992; Bromblet et al., 1996; Jeannette, 1997; Ordóñez et al., 1997; Iñingo et al., 2000; Mosquera et al., 2000; Nicholson, 2001; Chabas and Jeannette, 2001; Begonha and Braga, 2002; Moropoulou et al., 2002b; Sousa et al., 2005 etc.).

As a great part of the deteriorating agents are connected to water, such as the soluble salts, the effects of freezing or the wet deposition of atmospheric pollutants, evidently the above mentioned hydraulic properties will play a crucial part in the weathering processes, but they are not the only ones to control the durability of a stone material.

The mechanical strength of a rock determines its ability to resist physical stress. The most fundamental mechanical property of stone material is the tensile strength, because it is significantly lower than the compressive strength, and it is more affected by weathering (Gupta and Seshagiri Rao, 1998; Arikan et al., 2007). Nevertheless the compressive strength, the acoustic wave propagation and the moduli of elasticity were also found to be important parameters to assess the durability or the weathering degree (Spetzler, 1978; Allison, 1988; Eberhardt et al., 1999; Winkler and Murphy, 1995; Goudie, 1999; Martínez-Martínez, 2008).

Microstructural characteristics, which include the grain size, grain shape, the grain boundary shape, the grain interlocking, the anisotropies and inhomogeneities like larger fossils or stylolites in limestones or any changes in the texture (Dürrast and Siegesmund, 1999;

Nicholson and Nicholson, 2000; Lindqvist et al., 2007a, b), is another important group of properties influencing the rate and degree of weathering.

The already mentioned mineralogical and chemical composition, besides determining the reactivity of the stone material in front of chemical processes (mostly acidic attack) (Grossi et al., 1994; Simão et al., 2006), raise other aspects such as the problems of swelling clay minerals (Esbert and Valdeón, 1985; Sebastián et al., 2008), the leaching of Fe-oxides that can cause unsightly discolorations (Bams and Dewaele, 2007) etc.

And finally, another important issue, also strongly connected to the mineralogical composition, is the thermal behaviour of the stone material, which especially in carbonate stones, is one of the most serious causes of degradation (Hall, 1999; Koch and Siegesmund, 2004; Takarli, 2008).

From the above literature survey, we can conclude that a wide spectrum of properties – the petrophysical properties – will influence the response of a given stone material under given conditions (Esbert and Montoto, 1998). Moreover, these properties will act simultaneously and may have a synergetic effect on each other, therefore the combined effects of decay functions has to be considered when assessing the durability (Benavente et al., 2008).

A series of standardized and non-standardized laboratory tests exist for the study of stone decay by artificial weathering. The so-called ageing tests are relatively simple procedures that aim at the simulation of natural weathering environment to a greater or lesser extent; at inducing breakdown and at testing hypotheses (Nicholson, 2002). These tests usually intend to accelerate the rate of natural weathering by exposing the samples to fast cycling of extremely varying conditions of temperature, stress or chemical solutions (Hudec, 1998) in order to define the decay processes, to identify the crucial stone properties and/or to evaluate the effectiveness of treatments (Tabasso and Simon, 2005; Rivas Brea et al., 2008). Although they are the best methods for the experimental testing of stone weathering, these tests have many disadvantages: they focus on only one or maximum two weathering agents at a time; the intended acceleration often fundamentally changes the real processes, and, as they are designed for an "average" material, very often they are not suitable for the assessment of any one given kind of stone. The standardization, which is intended to serve as an aid for the users in the academic and industrial field, further decreases the possibilities of the investigation of special rock types.

Generally speaking, the porous rocks – rocks with high open porosity, low density and low mechanical resistance – which means mostly given types of limestones and sandstones, are the most susceptible to weathering, due to the usually fast water kinetics and high specific surface and storability determined by their pore space (Montoto, 2003). These stone types, due to their high abundance and easy workability, have been and still are very popular for human use (Winkler, 1997). Therefore, the standardized ageing tests are usually designed for the testing of these types of materials. Nevertheless, there exists another important stone group, the crystalline rocks, also exceedingly used in monumental and modern constructions including

the marble and the granite, two of the most popular ornamental stone types. The term 'crystalline rock' is a petrophysical term that refers to given textural and physical characteristics. These stones are usually of magmatic or metamorphic origin, but the most important aspect of their classification is the interlocking character of the mineral grains. The magmatic and the metamorphic rocks are formed under high temperature and/or pressure by crystallization or re-crystallization. This results in a dense fabric constructed of more or less euhedral rock-forming minerals with a strong, "welded" interlocking (Montoto, 2003). This formation does not leave space to large, spherical pores, so typical in cemented rocks, so the primary porosity of these rock types is usually very low. During the lifetime of the rock closer to the Earth's surface or already in an artificial construction, another type, a secondary porosity can evolve. This may be due to chemical degradation of the mineral phases, which usually results in equi-dimensional pores, but more typically it is due to mechanical stresses and results in cracks and fractures. This fissure like porosity, which is characterized by discontinuities of sheet-like appearance having two of their dimensions much larger than the third one, is the responsible for the striking difference of behaviour between crystalline and cemented rocks (Delgado Rodrigues, 1983; Montoto and Esbert, 1999). In this thesis, all the investigated stones belong to the crystalline group.

2. Objectives

2. Objectives

According to the aspects detailed in the Introduction, the objectives of this thesis are the followings.

1) **The main objective was to evaluate the overall durability of crystalline stones in correlation with their intrinsic properties, the petrophysical characteristics.**

In order to reach this principal goal, further objectives were determined:

2) **To assess the durability of the three selected crystalline stones**

The main objective will be completed via the investigation of the three stone types selected for research. They were chosen to represent the widest possible variation within the crystalline stone group as far as the petrophysical properties are concerned in order to provide general conclusions about the whole group.

3) **To understand the mechanisms of the different weathering processes**

The behaviour of the damaging agent and mechanism by which it forms are key elements in the understanding of the deterioration. The ways of ice or salt formation in porous materials have been investigated for many decades but still there are several unclear points in the processes. The principles of other agents, such as the frost damage in the presence of soluble salts, are even less clear yet.

4) **To understand what is the effect of different weathering agents on different stones**

Due to the specific behaviour of each weathering agent and the specific properties of each stone type, the effect of the same process can be very diverse on different stones or the same stone can act very distinctly to different agents. Therefore, all the stone - weathering agent combinations must be handled and understood independently.

5) **To identify those petrophysical parameters of the stone that are most responsible for the decay**

The term 'petrophysical property' includes almost all the stone characteristics from the mineralogical, chemical composition till the mechanical properties. All these characteristics have their role in the overall durability of the stone but some of them are more decisive than others. The recognition of these key properties would give a tool to both the academic

research and the stone industry to assess the durability and alterability of given stone materials more directly and simply.

6) **To identify which feature of the porosity and void space structure most influences the degradation processes**

The characteristics of the void space structure are part of the petrophysical properties, nevertheless the number of features belonging to this group is so high and their importance in the great majority of degradation processes is so significant that they deserve special attention in the assessment of durability of stone. Moreover, the most fundamental differences between the crystalline and cemented stone types are due to their differing void space structure.

7) **To understand the principle mechanisms of deterioration of crystalline stones**

Crystalline stones are differentiated from cemented stones on basis of their texture and their void space structure. The characteristic features of their void space cause their special behaviour towards water and other deteriorating agents. Therefore, their alterability is a distinct and independent issue within the field of stone durability. This research focuses on processes of crystalline stones only.

8) **To find the most adequate methodology both for the characterization and the durability assessment of crystalline stones**

Due to the specific features of crystalline stones their characterization as much as the assessment of their durability or the monitoring of the processes that take place during their degradation often requires special methodology and techniques. Large part of standardized methods, as well as non-standardized measurements is designed for the investigation of cemented rocks with high porosity. The theoretical models usually presume spherical or cylindrical pore shapes for the calculations. Therefore, techniques and models so adequate for cemented rocks must be applied circumspectly for crystalline stones and often smaller or larger modifications are necessary in order to get reliable results. This thesis also aims at the assessment of the efficacy of generally used methods for the investigation of crystalline rocks and at the suggestions of modifications for their improvement or of the selection of the most adequate ones.

3. Stone selection

3. Stone selection

3.1 Criteria for the selection

For the selection of the stone types to investigate in this thesis, we had two important criteria to keep in mind.

The first one was to choose stone types that are frequently used as monumental stones. This means that the type of stone is used world-wide and also that the stone has a local, regional or general importance with significant monuments in Spain or in Hungary.

The second criterion was that they belonged to the crystalline rock group. The members of this group – as it was explained in the Introduction – are generally characterized by their typical textural properties: the "welded" grain interlocking, the low primary porosity, the fissure type secondary porosity etc. The differences within the group are mainly provided by the genesis of the rocks on one hand, which will determine their chemical and mineralogical composition, their grain size, the possible anisotropies etc; and on the other hand, by the weathering, which can cause alterations in the chemical-, mineralogical composition and in the void space. In order to take into account this variety, rocks of different genesis were considered for the research and finally, a metamorphic (marble), a plutonic (granite) and a volcanic rock (andesite) were selected.

3.2 Selected stones – Historical and geological background

The aim of scientific conservation is to complete and help the work of conservators with additional and background information originating from the detailed, scientific knowledge of the materials and processes. In the field of stone conservation, the precognition of stone as a geological entity is indispensable; all conservation and/or restoration works must start with the collection and synthetization of the geological information about the material. Another fundamental step is the consideration of the historical, cultural importance of the monument, where the stone was applied. Therefore, in the following subchapters the historical and the geological background of the selected stones are discussed together.

3.2.1. Macael marble

This marble is a white calcitic rock from Macael, Southern Spain. Its occurrence is in one of the several valleys of the Alpujarra, in Almería, Andalucía.

The outcrops of the marble in this valley show banks of different qualities and colours. The white version was and is of the highest quality and artistic value. Nevertheless, there are very few of pure white units, the stone usually shows grey foliation of more or less intensity (fig. 3.1) (Sáez Pérez, 2003).

Fig. 3.1. The Macael marble is a pure white marble with slightly darker layers of foliation.

Probably the Arabic peoples occupying this territory during the 8th – 15th centuries were the first ones to discover the quarries of this marble, if not already the Romans before them. The Arab masters of stone masonry intensively quarried and processed the Macael marble. All the white marble that can be found in the Alhambra (Granada, Spain), which is the most beautiful example of the Islamic architecture in Europe, proceeds from Macael. Elements constructed or carved of this marble are the Court of the Lions with its columns, galleries and bays; the Fountain of the Lions of dodecagonal base and the twelve lions around it (fig. 3.2); several other fountains of smaller size in the interior of the Palace together with different types of decorative elements.

Fig. 3.2. One of the most famous examples of the monumental use of the Macael marble: the columns and the lions of the Patio de los Leones of the Alhambra (Granada, Spain). Photo from Sáez Pérez 2003

The Court of the Lions is considered the apex of the art of the Nazarí or Nasrid dynasty in Granada; and it is a principle element of the Alhambra. It was constructed during the reign of Muhammá V (1354-59 and 1362-91). The court has a rectangular base of the size of 28,5 x 15,7 m. It is surrounded by galleries on the four sides, supported by 124 columns of Macael marble, which can be single, double or in groups of three or four on the corners of the court.

Another monument in the city of Granada of primary importance is the Cathedral, where the Macael marble is also present on a great number of sculptures and decorative elements. Among them, the statues and catafalques of the Royal Chapel from the year 1521 deserve special attention. The tombs in this chapel belongs to the so-called Reyes Católicos of Spain, Isabel I of Castile and Ferdinand II of Aragon, their daughter Joanna and her husband, Philippe I (fig. 3.3).

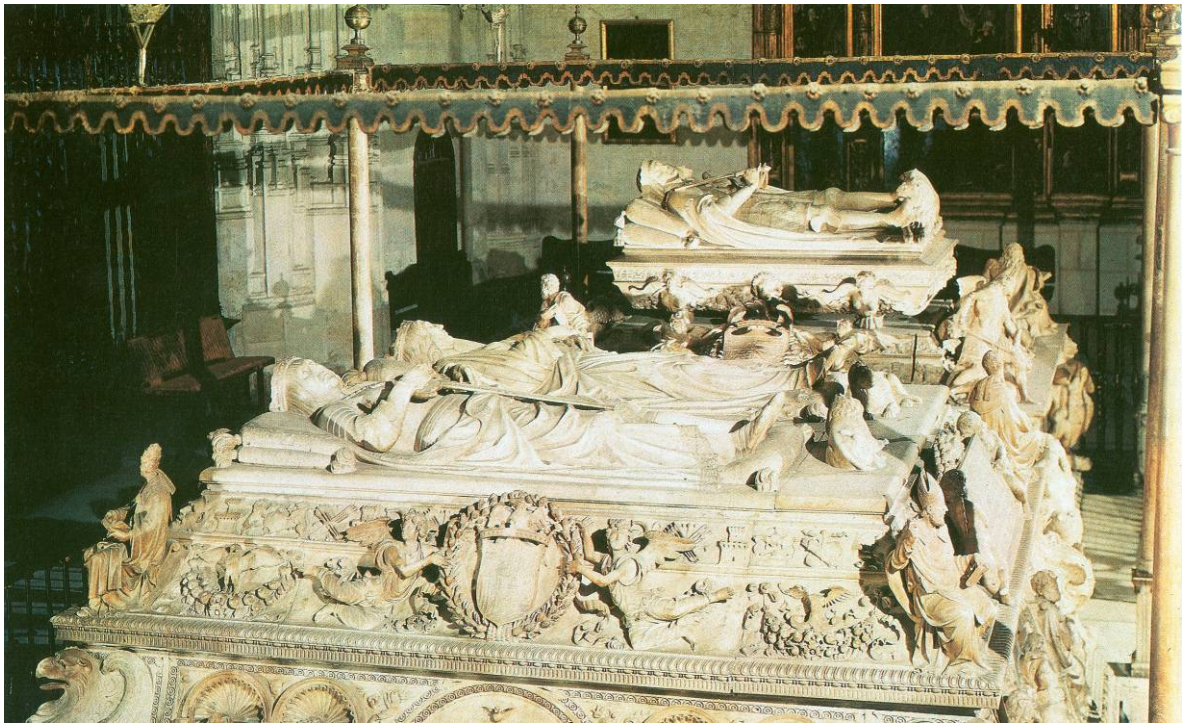

Fig. 3.3. The catafalques of the Royal Chapel of the Cathedral of Granada were also carved of Macael marble. Photo from Sarthou and Navascués, 1990

Besides of these geographically local monuments – not at all of local importance only – a great part of the marble that can be seen in the cathedrals of Spain, proceed from Macael (López Burgos, 2002). However, due to some special circumstances in the past, like differences in commercialization etc, in several cases the Italian Carrara marble was used also in Spain for the construction or ornamentation of monuments. Fortunately, since approximately three decades the Macael marble can cope with other more widely known marbles both in quality and commercialization, all over the world.

Marble in general is one of the most important and most well-studied monumental stones worldwide. Because of the significance of the monuments where it was applied, the Macael marble also has been subject to several scientific researches (e.g. Bello et al., 1992; Zezza and Sebastián Pardo, 1992; Barbin et al., 1995; Sáez Pérez, 2003; Rodríguez-Gordillo and Sáez-Pérez, 2006; Sebastián Pardo et al., 2006; Rodríguez-Gordillo and Sáez-Pérez, 2009 etc.).

Geological background and stone extraction

The Macael marble is a Late-Triassic carbonate rock that suffered poli-methamorphosis during the Alpine orogeny. It belongs to the Nevado-Filabride Complex in the Betic Internal Zone in Southern-Spain. Within the Macael group the commercial name of the studied stone is Blanco Macael.

The District of Macael is situated in the Northern part of Almería province, on the North-Eastern side of the Filabres Mountains.

The geographical and geological situation of the formation and the quarry are presented on figure 3.4.

From the geological point of view this area belongs to the Filabres Mountains, in the central-eastern part of the Betic Cordillera, in the Internal Zones of the Cordillera. This consists of three nappe complexes of variable metamorphic grade, which are, from bottom to top, the Nevado-Filabride, the Alpujárride ad the Maláguide complexes. The Macael marble formations belong to the first one of these. Although the Nevado-Filábride complex is the lowermost metamorphic structure, today its rocks are exposed at the highest elevations due to a folding and uplift event occurring since the Late-Miocene. The complex crops out mainly within large antiformal structures that form the Sierra Nevada, the Sierra de los Filabres and the Sierra Alhamilla (Azañón et al. 2002).

The Nevado-Filábride rocks can be divided into a lower Paleozoic and a higher Permian-Mesosoic sequence. The Macael marbles belong to the Upper-Triassic Las Casas Formation within the higher sequence. This formation, which has approximately 800m thickness, contains carbonate rocks, different types of micaschists and metabasites. The carbonate rocks, which are of white, blue, yellow and dark brown colours, are found mostly in the uppermost and lowermost parts of the formation, with frequent pellitic layers in the central part (Rodríguez-Gordillo and Sáez-Pérez 2006). The white and yellow ones are composed almost exclusively of carbonate minerals with some white mica, albite, quartz and sometimes pyrite (IGME 1975). These rocks are intensively folded due to the Alpine tectonism. Their metamorphic study reveals a high-pressure overprint reaching up to 14-16 kbar and 600-650°C, which evolved to an intermediate grade metamorphism of approximately 7 kbar and 550-600°C. The age of the first phase is about 48,4 ± 2,2 m.y and of the second is 24,6 ± 3,6 m.y (Azañón et al. 2002).

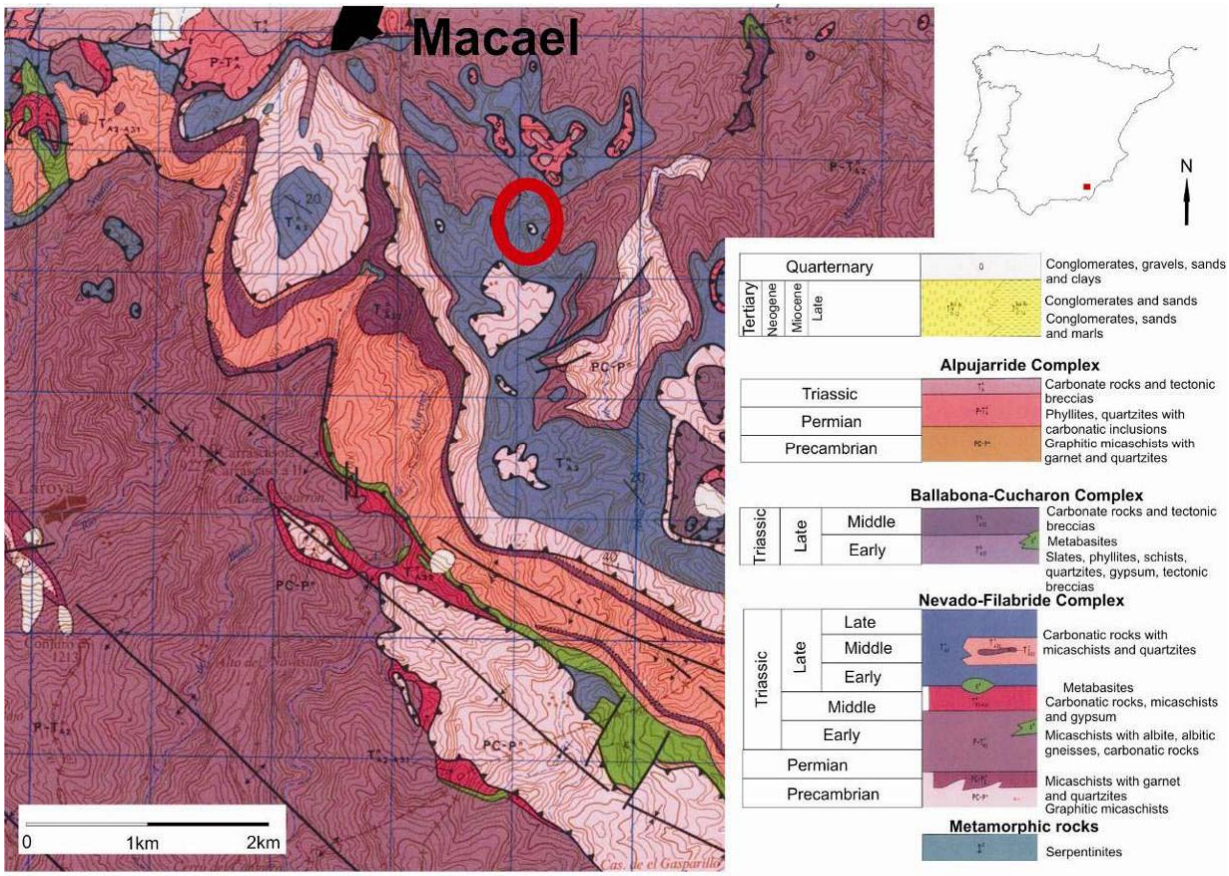

Fig. 3.4 The situation and the geological environment of the quarry of the Macael marble.

3.2.2. Silvestre Vilachán granite

Fig. 3.5. The Silvestre Vilachán is a slightly altered, greyish leukogranite.

The second selected stone is the Silvestre Vilachán granite from Galicia, NW Spain. Granite is the most frequently used igneous rock because of its abundance and great variety of colour and textures; and it is a major construction material of European historical buildings and monuments (Vicente et al., 1996). In Spain there are many types of granitoid rocks especially of Variscan age in Galicia and in the central-western part of the country, many of which were used for monumental purposes (Esbert 2007). In Galicia the different granite types are used since Neolithic times in religious and civil as well as in public and private works (Esbert, 2004; Mateos and Esbert, in press), so the deterioration and conservation of these materials is of fundamental importance. The selected greyish leukogranite (fig. 3.5) is very similar to the one used for the construction of the Cathedral of Santiago de Compostela. This magnificent cathedral (fig. 3.6) is the destination of the famous route of pilgrimage, the Way of St. James,

so it is not only a well-known monument of Spain but also has a great importance for the whole Christian world.

Fig. 3.6. The selected granite is very similar to the one used for the construction of the Cathedral of Santiago de Compostela (Galicia, Spain)

Fig. 3.7. The Pórtico de la Gloria is one of the most remarkable stone works of the medieval age in the Western world. Photo from Sarthou and Navascués, 1990

The actual Cathedral of Santiago replaces a temple from the 10th century, which was first destroyed by Almanzor and later restored. However, due to the large number of pilgrims visiting this sacred place, the temple proved to be too small and so had to be replaced. The objective of the pilgrimage was the sepulchre of the apostle, Santiago (James) situated in this primitive construction. Today the sepulchre is situated under the apse of the actual Basilica. The Construction of the mentioned Basilica – of Roman style and of impressive dimensions – started in 1075. In 1128, it was consecrated to the religious service although the works continued during the 12th and partly the 13th centuries. In 1168, when Matthew was the building master, started the construction of the Pórtico de la Gloria (Gate of the Glory) – the lintels of which were only placed 20 years later – and it continued during the 13th century. It is situated behind the main façade (el Obradoiro) on the top of a stairway and it is the main entrance. It has beautifully carved sculptures of the apostles, prophets and the 24 Elders of the Apocalypse lead by the figure of Christ in the tympanum and at the main place, at the mullion the apostle Santiago himself (fig. 3.7). It is one of the most remarkable stone works of the medieval age in the Western world. The stone of the entire gate is granite except for a small decorated marble column, on which the apostle leans. The cathedral of the shape of Latin cross occupies an area of 8000 square meters. It has three naves with 25 chapels altogether. The actual cupola is of Gothic style (15th century) and it substitutes the original Roman

element. The main façades are: the already mentioned "el Obradoiro", facing West, of Baroque style, which has an height of 68 meters and four parts of statues and mouldings (fig. 3.6); the "de las Platerias" facing South, of Roman style, which has statues originating from different parts of the Cathedral; and the "de la Azabachería" facing North, which was reconstructed in the 18th century. The gate called "de La Quintana" or "Pórtico Real" was built in 1666 and is one of the first Baroque motives of the city of Compostela. The gate "Santa" is from 1611 and it shows elements of maestro Matthew, which belonged to the now disappeared choir of the Cathedral. In the main façade, two magnificent towers are situated of 76 meters height and there is one more similar over the façade of the gate "Santa". Finally, the quadratic cloister of 40 m length of each side is also constructed of granite (16th century) (fig. 3.8.)

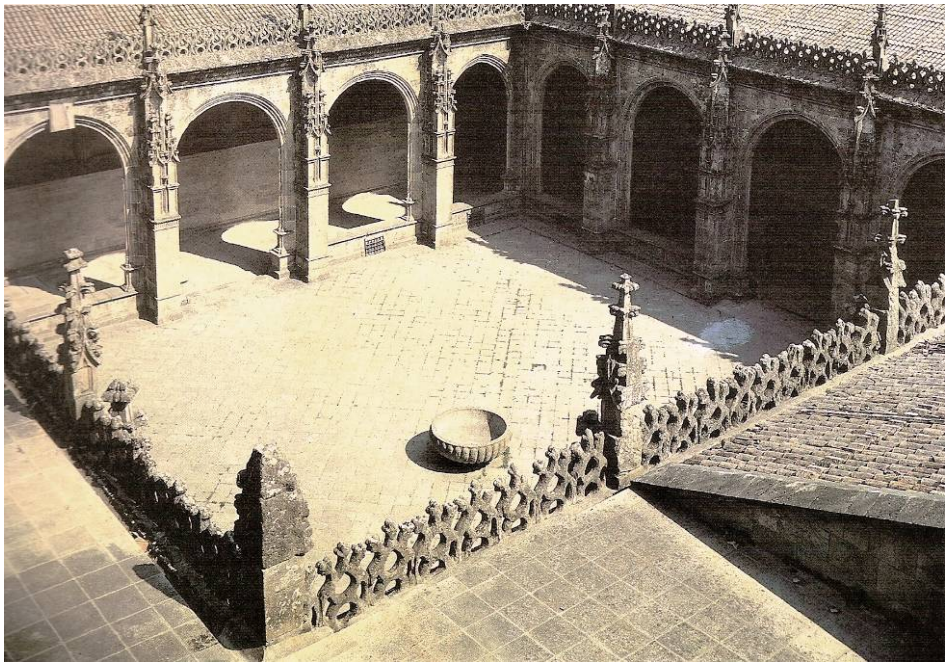

Fig. 3.8. The cloister of the Cathedral of Santiago is also constructed of granite. Photo from Sarthou and Navascués, 1990

Geological background and stone extraction

The Silvestre Vilachán granite belongs to a Variscan granite batolite in the Galicia-Tras-os-Montes zone within the Central Iberian Zone in North-Western Spain (Bustillo-Revuelta, 1996).

The outcrops of this granite are situated in the district of Pontevedra in the southern part of Galicia (NW Spain) (fig.3.9).

From the geological point of view this area belongs to the Galicia-Tras-os-Monte zone within the Central Iberian Zone (CIZ) (Bustillo-Revuelta 1996), which is a rather heterogeneous zone that comprises areas of high-grade metamorphism with abundant granitoids, as well as areas affected by very low-grade metamorphism during the Hercynian orogeny. Within the CIZ the Tras-os-Monte zone is distinguished as an allochthonous or para-autochthonous unit over the autochthonous parts. It is a thick wedge of Paleozoic siliciclastic rocks with abundant volcanoclastic inclusions (Ábalos et al. 2002), which was deformed and metamorphosed

during the Hercynian orogeny and which was intruded by several granitoids before and during the orogeny.

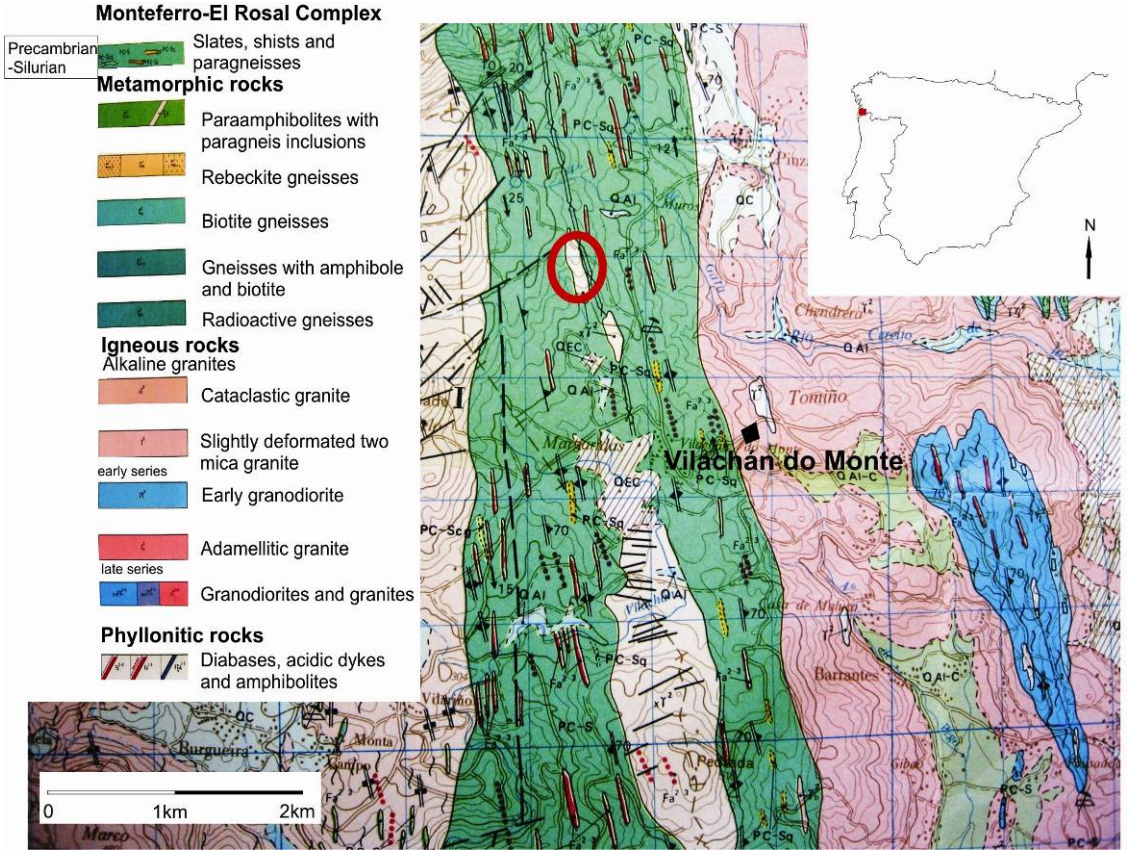

Fig. 3.9. The Silvestre Vilachán granite belongs to a Variscan granite batolite in the district of Pontevedra in the Southern part of Galicia.

In the vicinity of the Silvestre Vilachán granite the so called Monteferro – El Rosal unit represents the pre-Variscan metamorphic rocks. It is a wide band of slates, micaschists, paragneisses and quartzites of possibly Ordovician-Silurian age and N-S orientation. On both sides, as well as inside of this band, igneous rocks of different ages – from different phases of the orogeny – are situated. The most abundant types in this area are the so called clataclastic granites of Bayona granites, to which the Silvestre Vilachán belongs, and the so called low deformation two mica granites. All these intrusive rocks are two mica granites with differences in the grain size and the intensity of deformation and alteration. The common mineralogical composition is quartz, microcline, plagioclase (albite-oligoclase), muscovite and biotite as main components and apatite, zircon, and opaque minerals as accessory minerals.

The granites intruded after the first phase of Hercynian deformations and before the second one, because they are strongly affected by the second one (F_2). They show the signs of an intensive cataclastic deformation having a foliation which belongs to the F_2 phase, although the radiometric measurements gave 318 ± 21 m.y., which corresponds to the interval between the F_1 and the F_2 phase (IGME 1981). The Bayona granites are mostly situated westwards from the Monteferro – El Rosal metamorphic complex but due to the sinform structure of

this complex there are some small outcrops of the granite in its axis, as well. The quarry of the Silvestre Vilachán belongs to one of these (see map, fig.3.9).

3.2.3. Szob andesite

The third stone type was decided to be chosen from Hungary. In Hungary one of the most abundant igneous rocks is the andesite. The andesite and dacite variations have significant importance in the building history of the country. They were and are used as cobblestones in the roads of the capital as well as of the countryside cities, for hydraulic and railway structural constructions and, as some types are suitable for the carving of dimensional stone, for engineering, mostly bridge construction (Schafarzik, 1904).

Quarried andesite together with andesite tuff and agglomerate are common in historical buildings, as well. One of the very first buildings of the Christian kingdom of Hungary was the castle of the Esztergom hill, the construction of which was started by Prince Géza and finished by King Stephen I (beginning of 11th century). The oldest building elements were, besides the local sandstone, the andesite pyroclastics found also in the neighbourhood or coming from the quarry of Hideglelőskereszt (Kertész, 1985).

Fig. 3.10 The ruins of the royal palace of Visegrád. Photo from http://jupiter.elte.hu

The Gothic-Renaissance palace of Visegrád is situated on the top of a volcanic hill composed mostly of andesite agglomerate close to the river Danube (fig. 3.10). The castle was built around 1250-1260 by King Béla and Queen Mária Lascaric using local stone. King Károly Róbert expanded further the castle and moved the royal court and the capital here in 1323 and until 1526 this castle was the residence of the Hungarian kings. Its most flourishing period was during the era of the Anjou kings (14th century) and the following century; Matthias I. (1458-1490) reconstructed the whole palace in Renaissance style. Then during the Ottoman invasion, the castle was occupied and re-occupied several times by the Turkish and Hungarian troops and suffered severe damage. The remaining parts of the ruined castle were destroyed in 1702 by the Austrian Emperor Leopold. The re-construction was started at the beginning of the 19th century and was mostly carried out after the II. World War. In the walls of the castle and the palace, seven different types of andesite and andesite tuff were identified during a recent investigation by Török et al. (2008). For the reconstruction an eighth type of andesite was used. These varieties of andesitic rocks differ mostly in their colour, mineral content (e.g. amphibole, pyroxene and biotite), lithic clast content and type of cementation.

Besides these monuments of primary historical and cultural importance in Hungary, the different andesite types were used for the construction of local monuments in mountainous areas, like the Catholic church of Nagybörzsöny (fig.3.11) situated very close to the quarry of the selected stone, which was build of trachit at the beginning of the 13th century; and for the chain of fortresses-castles built or rebuilt from the 13th till the 17th century. The first systematic stone-castle building plan in the country is connected to King Sigismund of Luxemburg (1368-1437), which was completed finally during the Ottoman occupation in order to construct a continuous defence line against the hostile Turkish armies. These fortresses of regional or only local importance were mostly constructed of local building material, and thus many of them situated in the Northern volcanic chain were built partly or completely of andesite. Just one example is the castle of Hollókő presented on figure 3.12.

Fig. 3.11 The church of Nagybörzsöny constructed of trachite in the 13th century. Photo from http://wiki.utikonyvem.hu/

Fig. 3.12 The castle of Hollókő is one member of the defence chain built in the 13th-17th centuries using local stone material, mainly andesite

The selected stone for this research is the Szob andesite, a dark grey microporphyritic quartz andesite (fig.3.13), which is one type of the andesite variations of Northern-Hungary. It was chosen from among the several variations because it has a working quarry today and because it has been used very recently for the reconstruction of the caste of Ónod, North-Hungary, where a dark grey pyroxene andesite was one of the main original construction materials especially in the Medieval palace (Kovács, 2006).

3.13 The Szob andesite is a dark grey microporphyritic quartz-andesite, one of the many similar stone types of Northern-Hungary.

Andesite, generally, is not as common a monumental stone as granite or marble, but because of its good durability characteristics it is a popular construction material in the areas where it is easily available such as the volcanic areas of Central- and South America, India, Turkey, Japan, Indonesia etc. In these areas the deterioration and conservation of this stone type also have been of great interest for the scientific and engineering communities (e.g. Nishiura 1986; Karpuz and Paşamehmetoğlu 1992; Anom and Samidi 1993; Moropoulou et al. 2002; Tuğrul 2004; Török et al. 2008; Zedef et al. 2007 etc).

Geological background and stone extraction

The Szob andesite belongs to the volcanic complex of the Börzsöny and Visegrád Mountains of North-Hungary. It was formed during the calc-alkaline volcanism of the Carpathian volcanic arc taking place from the Miocene to the Quarternary (Harangi et al., 2001).

The Szob-Malomhegy quarry is situated on the Csákhegy (Csák-hill), which is in the southern part of the Börzsöny Mountain approximately 3 km northwards from the river Danube. Administratively it is in Pest county and belongs to the city of Szob and the village of Márianosztra (fig.3.14).

The volcanic complex of the Börzsöny Mountain is a member of the Miocene-Quarternary volcanic arc situated on the north-eastern - eastern edge of the Pannonian basin. The middle Miocene volcanic rocks of the mountain are mainly of andesitic composition and can be divided into 2 groups according to their facies: the rocks of the strato-volcano (which has two phases: 15,2 – 14,8 m.y and 14,8 – 14,5 m.y) and the subvolcanic and extrusive facies (which belongs to the older volcanic phase) (Korpás et al 1998). To this later one belongs the Szob andesite.

In the case of the Csákhegy the volcanic activity started with the deposition of tuffs continued with an amphiboleandesite formation and terminated with biotite amphiboleandesite. Finally the whole series was penetrated by dacite. The postvolcanic tectonism induced some more dacite intrusions. Around the hill on the SW and NE part there are Oligocene and early Miocene sediments, which were penetrated by the volcanites, the volcanic series is overlaid by an upper Miocene shallow marine limestone; and the uppermost member of the geological coloumn is the Quarternary loess (Papp 1950) (fig.3.14).

The quarry on the Csákhegy – the former name was Sághegy – is active since 1832. On the western and southern side of the hill 10 different stone-pits can be found. Most of these started to work at the beginning of the 19th century. In the 19th century it was one of the largest quarries of the country. The stone was used for setts, kerbs, pavement stones, ashlars and construction stone for foundations, superstructures and bridgework (Zelenka and Földessy, 2005). In the present quarry there are three varieties of andesite: a dark-grey garnet bearing coarse grained amphibolandesite; a light-grey garnet bearing finer grained amphibolandesite and a so called "dotted" andesite, in which the feldspar aggregates form dots in the texture; and the light grey, biotitic hypersthene amphiboldacite.

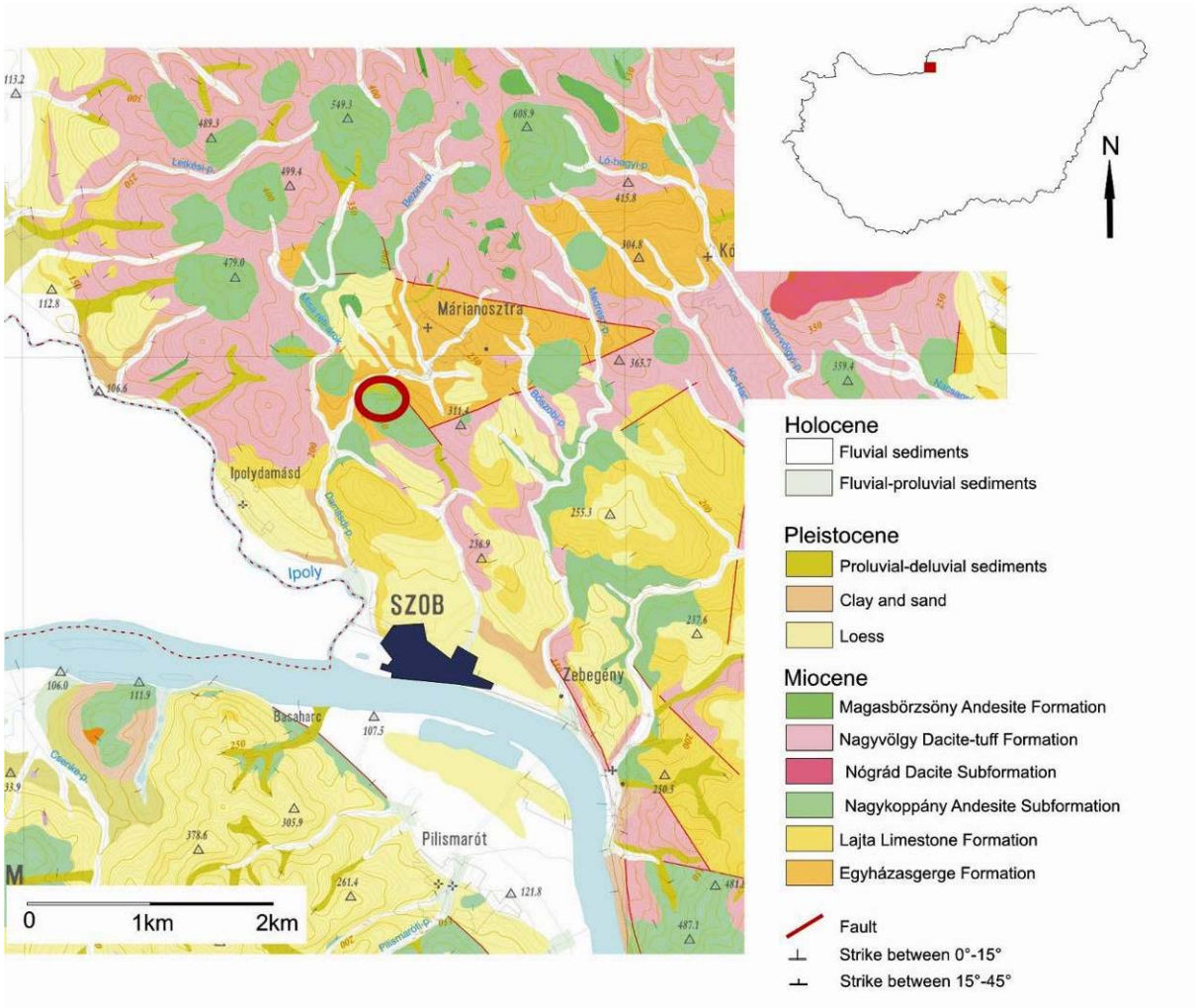

Fig. 3.14 The situation and the geological environment of the quarry of the Szob andesite.

4. Methods

4. Methods

To understand the degradation processes of a given material, we need a thorough knowledge of its properties. For the characterization of the sound stone we used "fresh" stone material from active quarries. The way of the sample collection and preparation is explained in the following chapter.

The most important characteristics of a stone material are: its mineralogical and chemical composition, its texture, anisotropy, homogeneity, its physical properties, the features of its void space, which is strongly connected to its hydraulic properties, and finally its surface characteristics. The methodologies applied for the characterization of these properties are described in the second part of this chapter (4.2.).

4.1. Sampling and sample preparation

The samples of the three stone types were purchased from working quarries. The way of extraction is different in the case of the two Spanish quarries (Macael and Vilachán) and in the Hungarian one (Szob). The Macael marble and the Silvestre Vilachán granite are mainly used as dimension stones so their extraction happens in blocks cut by wire saws. This way the orientation of the blocks is always clear and known. In these two cases oriented blocks of given dimensions were purchased from the quarries. The Szob andesite on the other hand, is mostly used as aggregate of different sizes, so the extraction (except for some special orders) happens by drilling and blasting. In the Szob quarry the block selection and cutting happened personally, so that the exact orientation of the samples can be known.

In all the cases the same scheme was followed: the plane parallel to the floor of the quarry was named 'T' plane, the one parallel to the face of the quarry is the 'M' plane and the third one, perpendicular to those is the 'N'. All the specimens for further investigation were prepared keeping this orientation (fig. 4.1).

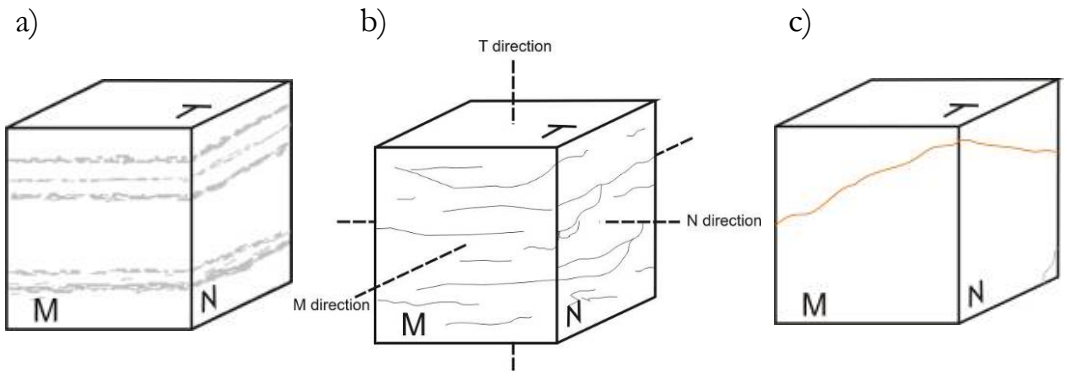

Fig. 4.1. Orientation of the sample specimens of the (a) Macael marble, (b) Silvestre Vilachán granite and (c) Szob andesite.

During the tests and analysis these directions are always referred to as T, M or N planes; or as directions, which are normal to the planes (e.g. the 'T' direction is normal to the 'T' planes of the specimen (see fig.4.1./b)). As the petrological investigation proved (see chapter 5.), these directions coincide with the directions of anisotropy for the Macael marble and the Silvestre Vilachán granite, while Szob andesite in an isotropic stone, so in this case the orientation has no real importance.

4.2. Techniques applied for the material characterization

4.2.1. Methods for the petrological characterization

The most important internal factors that determine the deterioration of a material are the mineralogical, chemical composition or the features of the texture like porosity, grain size, orientation of grains etc. These petrographic properties must be characterized as exactly and thoroughly as possible for the understanding of the responses of the material for different effects.

The petrographical investigation was based on thin section analysis using a NIKON polarizing microscope. The thin sections have a thickness of 30 μm. The quantitative measurement of the mineral phases happened with the point counting method based on 6 thin sections of each stone type. For further specification of the mineralogical composition we used X-ray powder diffraction (XRD); and the chemical composition was determined by X-ray florescence analysis (XRF). For the XRD analysis a "PHILIPS X' PERT PRO " diffractometer was used with a copper anode tube and a Bragg-Brentano alignment; and for the XRF analysis a "PHILIPS PW2404" spectrometer with a Rh anode tube of 4 kW potential and 5 analyser crystals (Fli 200, Fli 220, Pe, Ge and Px1).

Further details of the texture and petrographical features were investigated by a JEOL-6100 Scanning Electron Microscope with electron microprobe analysis (SEM-EDX) equipped with a wolfram filament. Before the measurement the surface of the samples has to be made electronically conductive; for this purpose gold coating was used, the coating was carried out in a BALZERS SCD400 equipment for 150 sec on 20 mA.

4.2.2. Methods for the characterization of the void space

As most of the deterioration processes are connected – directly or indirectly – to water, the knowledge of the water paths ways in the materials is crucial. The different features of the void space have a great influence on the mechanical, hydraulic, thermal etc. properties of the materials, as well. (Norton and Kapp, 1977; Poschold and Grimm, 1988; Nicholson, 2001; Sousa et al., 2005; Cultrone et al., 2008.etc.)

The expression 'void space' is used to summarize all the characteristics of the voids – empty spaces – in a solid material: the quantity of voids, their size, the size distribution, the morphological features: the geometry, connectivity and tortuosity of the voids and the specific surface of the material. Various methods exist for the examination and characterization of these properties, working based on a great variety of principles and technical achievements. A basic classification of these methods is the differentiation between direct and indirect ones. The first group includes the microscopic techniques, which allow the direct examination of the voids of a solid by means of observation, and completed with stereological or digital image processing methods, the quantification of the features is also possible. The indirect methods are usually based on the investigation of a fluid – water, mercury, inert gases etc. – in connection with the material, and the quantification happens by the measurement of the fluid properties and by the interpretation of those conclusions concerning the solid material can be withdrawn.

The efficacy of these methods highly depends on the material properties and the investigated parameters – so these must be taken into consideration at the moment of the selection of the technique and the parallel use of more methods is advisable.

The density and the porosity are strongly connected parameters. By using the classical water imbibition under vacuum method, the apparent density and the open porosity can be measured. Completing this with measurement by He pycnometry, we can determine the real density and the total porosity values. Besides, we chose three complementary methods for the detailed investigation of the void space characteristics, which together – based on different principles and detecting different void size ranges – give detailed and reliable information. These methods are the mercury intrusion porosimetry, the nitrogen absorption and the confocal laser scanning microscopy complemented with digital image processing.

Apparent and real density, open and total porosity

The density of a material by definition is its ratio of mass to volume. In the case of porous solids we can talk about real density, which is the density of the solid fraction excluding its voids; and about apparent density, where the pores are included in the measurement. The difference between the real and the apparent density evidently depends on the porosity of the material. The apparent density is usually measured according to the Archimedes' principle and the real density by some kind of (water or helium) pycnometry method.

Apparent density and open porosity

We determined the apparent density and the open porosity following the EN 1936 European standard. The measurements were made on 7 marble, 8 andesite and 8 granite cubes of 5x5x5 cm.

The procedure according to the standard was the following. The cubes were dried till constant weight (which means that the change in weight should be less than 0,1% within 24 hours) then this dry weight was determined with a precision of 0,001 g. The specimens were placed into a

vacuum chamber and were kept at a pressure of 2,0 ± 0,7 kPa for 24 hours. Then slowly (through 15 minutes) the chamber was filled up with distilled water and the cubes stayed there still at the above mentioned pressure for another 24 hours. After this, atmospheric pressure was re-established and the specimens were kept under water for 24 hours once again.

After the saturation the weight of the samples was measured again first under water then out of water but still saturated.

From these measurements we gained the following parameters:

- m_d: the dry weight of the sample, pores included (in grams)
- m_h: the weight of the sample under water, which can be used for the calculation of the volume of the specimen according to the law of Archimedes (in grams)
- m_s: the weight of the saturated sample, which means the dry weight and the weight of the water filling the pores (in grams)

From the measured parameters, using the above mentioned relations and the following equations we can calculate the volume of the open pores (V_o cm^3 (eq. 1)), the apparent volume (V_b in cm^3 (eq. 2)), the apparent density (ϱ_b in kg/m^3 (eq. 3)) and the open porosity (p_o in percentage (eq. 4)).

$$V_o = \frac{m_s - m_d}{\rho_{water}} \times 1000 \quad (1) \qquad V_b = \frac{m_s - m_h}{\rho_{water}} \times 1000 \quad (2)$$

$$\rho_b = \frac{m_d}{m_s - m_h} \times \rho_{water} \quad (3) \qquad p_o = \frac{m_s - m_d}{m_s - m_h} \times 100 \quad (4)$$

(ϱ_{water} = 998 kg/m^3)

Helium density

For the measurement of the He density a Micromeritics AccuPyc 1340 gas pycnometer was used. This gas displacement method measures the volume of solid objects. It works with a two chamber system, where one of the chambers is the sample holder and the other one is a reference chamber, both with known volume (V_{CELL} and V_{EXP}, respectively). Increasing the pressure in the closed sample holder chamber to a given value (P_1) and then opening a valve between the two chambers so that the pressure will equilibrate, we will get an intermediate pressure (P_2). Using the known original pressure (P_a) the volume of the sample (V_{SAMP}) can be calculated according to the Ideal Gas Law (equation 5).

$$V_{SAMP} = V_{CELL} - \frac{V_{EXP}}{\frac{(P_1 - P_a)}{(P_2 - P_a)} - 1} \tag{5}$$

Since the He penetrates into the smallest cracks and pores, the density calculated from the measured volume and the weight of the sample will be approximately the true density.

Total porosity

Based on the apparent density measured by water adsorption on atmospheric pressure and the He density, the total porosity of the materials can be calculated according to the following equation:

$$\phi_{total} = (1 - \frac{\rho_b}{\rho_{He}}) \times 100 \tag{6}$$

Mercury intrusion porosimetry

The mercury intrusion porosimetry has been one of the most commonly used, simple and rapid methods for the characterisation of porous media both in academic research and in the industry for many decades by now (Bousquie, 1979; Van Brakel et al., 1981; Nieminen and Uusinoka, 1988; Poschold and Grimm, 1988; Namorado Rosa, 1996; Nicholson, 2001; Montoto, 2003; Rigby et al., 2004; Kate and Gokhale, 2006). Besides the open porosity value in a quite wide range (appx. 3nm - 350μm), it gives information about the apparent and skeletal density, the specific surface and the pore throat size distribution.

The principle of this method is to measure the volume of mercury, which penetrates a dehydrated and degassed sample under increasing pressure – as the Hg – being a non-wetting fluid – must be pressurized in order to enter to the pores of a material. The pores are considered as cylinders, so from the Washburn equation the pore radius can be calculated from the applied pressure:

$$D = \frac{-4\gamma \cos\theta}{P} \tag{7}$$

Where D is the diameter of the pore, γ is the superficial tension of mercury (generally 485 x 10^{-3} N/m is used), Θ is the contact angle (generally 140°) and P is the applied pressure (Dubois et al. 1998; Beck et al. 2003; Parra Soto, 2007).

For the Hg intrusion porosimetry a Micromeritics AuroPore III. type porosimeter was used. 4 cylindrical samples of 2,5 cm height and approximately 2 cm diameter were used for this measurement of each stone. The samples were dried till constant weight on 60°C before the test.

The measurement itself consists of introducing the sample into a penetrometer and then into the porosimeter chamber. After creating vacuum of 50 μmHg in the chamber, the low pressure injection starts up to 30 psi (207 kPa) pressure. In the high pressure phase the pressure goes up to 33 000 psi (230 MPa).

Although, indeed nowadays Hg intrusion porosimetry is one of the most basic techniques to characterise the void space of solids, it also has provoked many discussions in the scientific world, especially when fissured materials are concerned. The supposition of cylindrical voids, the so called ink-bottle effect, the risk that the high pressure may cause damage in the material and the questionable values of the input parameters (γ, Θ) are all disputable points of this method (Good and Mikhail, 1981; Dubois et al., 1998; Beck et al., 2003; Roels et al., 2001). Nevertheless, we found that keeping in mind the drawbacks of the method and using it together with other techniques, it provides reliable and useful information, even in the case of low permeability, fissured rocks (Kovács et al., 2008).

Nitrogen adsorption

The gas adsorption techniques are based on the interpretation of isotherms of adsorption and desorption of gases on the surface of solids and they are mostly used for the characterisation of meso- and microporous materials. The basic idea is that when a gas comes into contact with a solid surface, molecules of the gas will adsorb to the surface in quantities that are a function of their partial pressure in the bulk. The measurement of the amount of gas adsorbed over a range of partial pressures at a single temperature results in a graph known as an adsorption isotherm. The interpretation of these isotherms may happen according to different methods, but the most commonly used one is the so called BET theory, which was originally elaborated by Brunauer et al. (1938). This method determines the specific surface of solid materials based on the principle of the monocapa - the number of gas molecules that are necessary and sufficient to cover all the surface of the material in one layer (BET surface). The technique also allows determining the total pore volume, median pore size and pore volume distribution, predominant pore shapes and the inception point and magnitude of hysteresis in case of mesoporous materials (Gruszkiewicz et al., 2001; Beck et al., 2003; Parra Soto, 2007; Guil Pinto, 2007) on the 1 – 100nm pore interval.

The nitrogen is the most typically used adsorbate gas and in this case the measurement happens on -196°C, which is the boiling point of nitrogen.

This technique is the most approrpriate one for the investigatin of the smallest pore size range of stone materials. The pores smaller then 1 μm play an important role in the dagradation

processes such as haloclasty and gelifraction (Camuffo, 1996; Winkler, 1997; Iñigo et al., 2000); and they determine the reactive surface area of the material, having an important influence on the chemical weathering rate (Pacheco and Alencoão, 2006).

The N_2 adsorption test at 77.3 K was performed on a Micromeritics ASAP 2420 apparatus. Approximately 5-7g of sample - cut to small pieces by a low deformation sawing machine – was used for the measurement. The samples were degassed at 100°C for 48 h and then at 120°C for another 16h.

Confocal Laser Scanning Microscopy

The confocal laser scanning microscopy (CLSM) has the great advantage compared to other microscopy techniques that it provides the possibility of three dimensional observations by means of serial optical sections (Montoto et al., 1995) and in the past two decades it has become more and more popular in geoscience researches. It has been used to investigate the void space of porous rocks (Friedrich et al., 1995; Friedrich, 1999; Martínez-Nistal et al., 1999; Petford et al., 1999; Menéndez et al., 2001) as well as the fractographic network of fractured rocks (Menéndez et al., 1999; Cwajna and Roskosz, 2001; Chae et al., 2003; Liu et al., 2006; Montoto and Mateos, 2006; Mauko et al., 2009).

The original concept of the confocal microscopy was first developed by Marvin Minsky in the middle of the 1950s, but - due to the lack of intense light sources, necessary for the imaging and high capacity computers, necessary to handle the large amount of data – it did not become a practically used method until the 1980s. Its common application started first in biological sciences.

The most important difference between the confocal and the traditional microscopies is the way of illumination and detection. Only a unique point of the sample is illuminated at a time by coherent light emitted by a laser system; and by inserting a pinhole – a confocal – in the way of the excited secondary fluorescence light only the signal of that point in the focal plain is detected by the photomultiplier; light from planes above and below that point is eliminated. The surface of the sample is scanned sequentially in the XY plane and, by means of a motorized stage, the vertical position of the sample can be controlled so two dimensional optical sections can be obtained in different depths. (Friedrich, 1999; Menéndez et al., 2001; Claxton et al., 2008)

The point to point detection manner and the use of laser light source both enhance the resolution of the CLSM, compared to other microscopy techniques, up to the degree that the lateral resolution exceeds the theoretical limit of the Raileigh criterion and can be calculated as:

$$F_{xy} = 0{,}4\lambda / NA \tag{8}$$

Where λ is the wavelength and NA the numerical aperture of the objective.

The vertical resolution is given by the half-width value in the z-direction as:

$$F_z = 1{,}28n\lambda / NA^2 \tag{9}$$

The n value is the refractive index of the matrix, which can be air or immersion oil (Onishi et al., 2005).

For the quantification of petrographic parameters digital image analysis was used.

The quantified parameters were the followings:

- the porosity (Φ (%)), which is the volume of voids versus the total volume:

$$\phi = \frac{\sum \text{pixel}_{\text{fissure}}}{\sum \text{pixel}_{\text{total}}} \tag{10}$$

- the specific surface of the fissures, which is calculated as the relation between the perimeter length of the fissures and the area of the reference surface (Martínez-Nistal, 1993):

$$S_v = \left(\frac{4}{\Pi}\right) \times \frac{\sum B_{i\_\text{fissures}}}{\sum A_{j\_\text{ref}}} \tag{11}$$

S_v: specific surface

B_{i_fissure}: perimeter length of fissures

A_{j_ref}: area of reference surface (the area of the image)

- fissure aperture: the average and the maximal aperture was measured supposing that the crack walls are parallel.

- linear crack density: the number of microfissures by length unit. The intersections of the fissures and an imaginary line of one millimeter length are counted.

The instrument used in this study was a Leica TCS-SP2-AOBS type microscope equipped with a multilaser configuration, of which we used a Diode Laser (405 nm) for the marble and the andesite; and a Helium-Neon Laser (543 nm) for the granite. The detected wavelength was within the range of 419-513 nm in the first case and in the 560-635 nm in the second. The used objectives were a PL APO 10X/0.40, a PL APO 20X/0.70 multi-immersion, a PL APO 40X/1.25-0.75 oil immersion and a PL APO 63X/1.40 oil immersion objective. The images have 1024x1024 pixel size. From each point of measurement a series of images were taken in different depths. The thickness of this optical sectioning depends mostly on the absorption spectrum of the rock forming minerals (Menéndez et al., 2001). In our case the average depth of penetration was around 60 μm for the granite, around 25 μm for the marble and around 15

μm for the andesite. The number of sections in the series depended on the thickness, usually keeping a 1-3 μm disctance between the images.

For the digital image processing the Leica QWIN software was used on a Leica Q550 QUANTIMET system with a Intel Pentium III (800 MHz) processor, 768 MB RAM memory, 40 Gb hard disk and a Matrox Milenium 32 MB graphic card. The software is complemented with some extra functions to suite the special purposes we needed (Martínez-Nistal, 1993).

During the image capturing the quality of the image can be improved by changing the offset and the gain settings. The first one can be used to decrease the background noise by adding a positive or negative voltage to the signal; and the second multiplies the output voltage by a constant factor so increasing the intensity without creating new grey levels (Claxton et al., 2008). We found that both the gain and offset settings and the numerical aperture of the objective have a large influence on the results of the measurements (Kovács, 2008), so we settled constant measurement conditions for all the stones. We decided to use the 40x objective, which gives the highest quantity information for all the materials; and a relatively low (330V) and constant gain setting to avoid the mistakes of the imaging. Evidently the gain and offset settings largely depend on the material: we aimed at getting the highest amount of information without changing the actual values in all the cases.

In the case of quantification by digital image processing the pixel resolution, which is usually smaller than the optical one, will determine the final resolution of the method.

The sample preparation starts with the impregnation of the specimens with a resin containing fluorescein dye. We used Rhodamine D, which is frequently used for this purpose. Its emitted light wavelength is λ=514 nm. The impregnation happens under vacuum first, and then under hydrostatic pressure of 10MPa. For the cutting of the samples a low deformation cutting machine is used to avoid the creation of artefacts during the preparation. Finally polished thin sections of 150-200 μm thickness are prepared with a surface of approximately 6 cm^2. For each stone two samples were taken for the characterization. From each sample 3 thin sections were prepared in the x, y and z directions in respect to the original position in the quarry and the directions of anisotropy, when there is any.

4.2.3. Hydraulic properties

The ways in which water can enter into the materials and its behaviour afterwards have a crucial importance on the deterioration processes. Understanding the mechanisms of moisture transport is vital when developing design, care and preservation strategies of building materials (Pender, 2004). These mechanisms are extremely complex but the most important steps are the water uptake, the diffusion of water within the material in liquid and in vapour phase and finally the drying process by evaporation. To experimentally investigate these processes in given materials we can use standardized tests of water absorption at atmospheric pressure

(EN-13755), water desorption (ICR-CNR NORMAL 29/88), capillarity uptake (EN-1925), water vapour permeability (ICR-CNR NORMAL 21/85), swelling (RILEM II.7). The water permeability is also an important issue although no standardized method exists for its measurement. The conditions of our measurement are also described in this chapter.

These usually simple, non-expensive and reliable tests provide preliminary information about the void space structure (Montoto, 2003); they help understanding the degradation mechanisms, the durability of the material and its mechanical properties (Esbert et al., 1997) in general and they also have their own proper practical importance:

- the water adsorption at atmospheric pressure is determined by the interconnected porosity. There are more different methods to measure this capacity of solids such as the one described in the mentioned standard or the free porosity (N48 RILEM II.1) or the Hirschwald or saturation coefficient, which are all based on the same process. More authors consider these parameters as important weathering indexes (Bell and Dearman, 1988; Begonha and Braga, 2002; Tuğrul, 2004) and it also plays an important role on the stone treatment methods (Pinto and Rodrigues, 2008).

- water desorption is a more complex process influenced by the evaporation rate from the surface and by the liquid and vapour transport rate in the material (Torraca, 1982; Pender, 2004). It plays an important role in the salt crystallisation damage (Dessandier, 2000; Ruedrich and Siegesmund, 2006) but also in the cleaning and conservation interventions. It mostly depends on the pore space structure of the material, on the environmental conditions (T, RH) and on the possible presence of pollutants like hygroscopic salts (Benavente et al. 2003b)

- capillarity uptake is the way of liquids entering into the solid in the first place and moving inside the material due to the capillary suction. It is responsible for the penetration of water into the bulk of the material but also determines the efficacy of water repellent treatments etc. (Peruzzi et al., 2003)

Water absorption

This test was performed according to the EN-13755 (2002) European standard.

The target of the test is to determine the quantity of water that the stone is able to absorb by complete immersion under atmospheric pressure.

Four 5x5x5 cm cube were used for the test for each stone. During the procedure the dried samples are gradually covered by distilled water: at t_0 time till the half of their height, at t_0+ 60 minutes till the 2/3 of their height and finally at t_0+ 120 minutes completely. The increase of the weight is monitored constantly and measured in given time intervals. When the weight becomes constant the sample reached the state of the complete saturation.

The change of weight plotted as a function of time gives the water absorption curve, which gives information of the kinetics of the process. Besides the water absorption coefficient (A_b) can be calculated according to the following equation:

$$A_b = \frac{(m_s - m_d)}{m_d} \times 100 \quad (12)$$

m_d: weight of dry sample

m_s: weight of saturated sample

The saturation coefficient (S), published first by Hirschwald (1908), can be calculated from the ratio of the open porosity (measured under vacuum (see eq. 4)) and the accessible porosity, which is that part of the open pores that become saturated in the first 48 hours of the water absorption test (w_{48h}/w_{total}).

Water desorption

The water desorption was determined following the Italian standard ICR-CNR NORMAL 29/88. The saturated cubic samples are placed under constant laboratory conditions (temperature and relative humidity) and their weight is detected in given time intervals with a precision of ±0,01g. The water content and the degree of saturation are plotted as a function of time.

Besides this graphical representation and important parameter, the so-called critical moisture content can be determined, as well. It is evaluated from the drying curve, which usually consists of two parts. The first one is linear, representing the period when sufficient moisture is transported to the surface by capillarity to keep up a continuous evaporation; and the second one, which has an asymptotic trend, describes the last stage of drying, which is controlled by the water vapour transport within the stone (Ruedrich and Siegesmund, 2006). The critical moisture content is given by the changing point of the curve. The ratio between the critical moisture content (moisture content ratio (R_{mc} (%)) and the moisture content in total saturation (w_{crit}/w_{total}) gives information about the velocity of the drying process.

Capillarity uptake

The determination of the water absorption by capillarity is described by the EN-1925 (1999) European standard.

The procedure of the test is the following: dried 5x5x5 cm cubes are placed in water of 3 (±1) mm height. In this case the orientation of the cubes is very important so for the 2 anisotropic stones (the Macael marble and the Silvestre Porrisal granite) the number of the samples was double so that the test could be performed in the 2 different directions. The weight increase was measured continuously. This increase in weight by surface unit plotted as a function of time results in a curve with usually two linear sections with different gradations. The coefficient of capillary uptake (C) is calculated from the first section:

$$C = \frac{m_i - m_d}{A \cdot \sqrt{t_i}} \quad (13)$$

m_i: weight of sample in i moment (g)

m_d: weight of dry sample (g)

A: the surface of the sample in the water (m^2)

t: time (s)

Water vapour permeability

The diffusivity or permeability of water vapour means the quantity of water that may cross through a stone piece of a given thickness when a pressure gradient is created between its 2 parallel surfaces. Clearly the precise result of this test largely depends on the ambiental conditions because they are responsible for the velocity of the vapour flux but the results will give information of the porosity and the connectivity of the pores, as well.

The procedure – according to the Norma ICR-CNR: NORMAL 21/85 - is the following: 5x5x1 cm slabs are used; they are sealed to the mouth of a specific test dish, which contains distilled water, then they are placed in a closed plastic tank that contains silica gel to absorb the water vapour penetrating through the sample. This setting creates the vapour flux. The whole test is produced under controlled and constant temperature and relative humidity conditions. The loss of water within each test dish is monitored by the measurement of weight.

The result of the test is the coefficient of permeability, which is calculated with the following equation:

$$Kv = \frac{-(\Delta M / S)}{t} \quad (14)$$

Kv: coefficient of permeability [g/m^2*24h]

ΔM: change of weight [g]

S: surface [m^2]

Swelling

Some stone materials, especially the ones with clay mineral content, may be susceptible to swelling when exposed to water, which may cause structural damages (Ordaz et al., 1985). In our case, it was the Szob andesite that we suspected of having such problems, as it is the most altered and it contains some clay minerals belonging to the montmorillonite group; however the test was carried out on all the three stones.

We followed the RILEM II.7 (1980) standard (Dilatation linéaire par absorption d'eau) procedure. The samples of 5x5x5 cm were dried on 60 °C till constant weight and their dimensions were measured with a accuracy of 0,01 mm. A special apparatus, which consists of a cylindrical sample holder and three micrometer dial gauges in the three directions of space, was used for the measurement. The samples are placed in the sample holder and are covered with water, and the swelling displacement is recorded as a function of time.

The linear dilatation (ε) is expressed as:

$$\varepsilon = \frac{L_1 - L_0}{L_0} \tag{15}$$

L_1: the maximal measured length or the measured length at 72 hours

L_0: original length of the sample

Liquid water permeability

The liquid permeability of materials has significant importance in many industrial and scientific field starting from the petroleum industry to hydrogeology, soil physics, building industry, etc. In monument conservation, it plays an important role not only in the circulation of water and pollutants in the stone materials but also in the conservation treatment application etc. Nevertheless, no standard procedure exists for its measurement, and there are a great number of applied techniques based on very different methods and properties in accordance with the material or fluid properties investigated.

The liquid water permeability in this research was determined in a permeameter 22.0030 at the University of Alicante. The technique was described in Benavente et al. (2007) and in Cueto et al. (2009). The system consists of a triaxial Hoek cell of 250 cm^3 capacity with a urethane sample holder that provides a barrier between the sample and the outer wall of the cell; three pressure controllers; and a computer system with a MecaSoft 1.2.1. software for controlling the measurement and detecting the data. One of the three pressure controllers maintains the pre-defined confining pressure in the cell along the measurement; the second one controls the inflow-pressure and the third one the outflow-pressure with accuracy below 1%.

The measurement is based on Darcy's law, according to which the water permeability (k) can be calculated as:

$$k = \frac{\eta Q L}{A \Delta p} \tag{16}$$

where, η: water viscosity

Q: volumetric flow rate of water

L: length of the sample

A: cross-sectional area of sample

Δp: pressure gradient

The inflow and outflow pressures are defined previously, based on the porosity and the capillarity uptake of the sample; and are determined in order to reach the steady-state flow as soon as possible but without causing any damage to the porous system of the material (rupture). The Q values are detected continuously and are plotted as a function of time. Once the steady-state flow is reached in the system under the defined differential pressure, meaning that the inflow and outflow rates are equal and the Q(t) curve becomes a straight line, the permeability of the sample of known dimensions can be calculated. The used samples were cylindrical of 3 cm diameter and 6 cm length. They were dried till constant weight and then vacuum saturated by distilled water previous to the measurement.

4.2.4. Surface properties

The surface properties of construction materials are of utmost importance influencing their aesthetical and so their economical value. The most evident of these properties is the colour but the light reflection, the gloss and the surface roughness – which are all connected to each other – and the durability of these properties must be considered also (Erdogan, 2000). The contact with atmospheric pollutants, the formation of crusts, dissolution of material, mechanical damages and then the cleaning interventions etc. have a direct effect on these properties, so their stability is an essential parameter that must be monitored and understood (Benavente et al., 2003a). The detection of the chemical changes of the surface provides fundamental information about the weathering processes that take place.

Colour

The colour is one of the most important properties of the ornamental or monumental stones. Its change during the degradation seriously influences the aesthetical value of the stone. The degree of this change must be detected during the ageing tests too. As colour is a very subjective phenomenon, we need to quantify it in order to avoid the mistakes of the human eye (MacAdam, 1985; Prasad et al., 1996). For this purpose there are colour charts like that of Munsell, which permit a semi-quantitative colour analysis or instrumental techniques (colorimeters or spectrophotometers) for quantitative analysis (Esbert et al., 1997; Grossi et al., 2007a).

Our measurements were performed with a Minolta CR-200 type colorimeter completed with a SpectraMagic NX software.

This method is based on the so called CIELAB colour system, which was recommended by the CIE (Comission Internacional de L'Eclairage) Colorimetry Committee. It is an approximately uniform colour system, of three values: the L, the metric lightness function representing lightness of luminance; the a, chromacity coordinate of red-green scale; and the b, chromacity coordinate of blue yellow scale (fig. 4.2) (Viscarra Rossel et al., 2006).

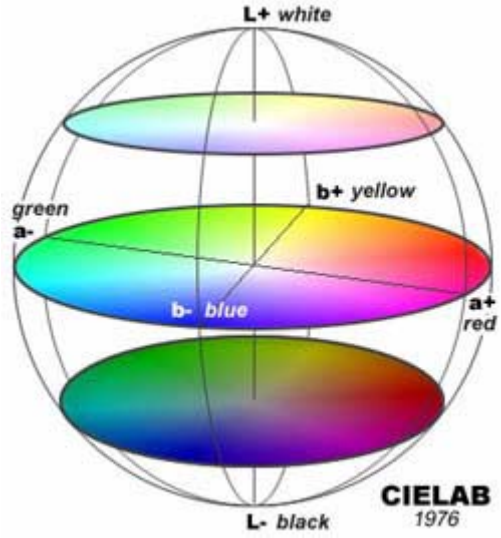

Fig. 4.2. The CIELab colour space.

The total colour difference (ΔE* CIE La*b*) between two colours can be calculated (Prasad et al., 1996):

$$\Delta E^* \text{ CIE } La^*b^* = [(\Delta L)^2+(\Delta a^*)^2+ (\Delta b^*)^2] \quad (17)$$

The number of measurements necessary for statistically representative results was decided based on the standard deviation of the values. As the colour of the marble and the andesite is quite homogeneous less than 50 measurements are sufficient for them, and the granite – including larger grains of minerals with different colour – needs 100 measurements.

Surface roughness

The surface roughness influences the colour of the material (Benavente et al., 2003a) and it also plays an important role in the surface degradation e.g. exposed specific surface etc. It is determined by the surface finish of the stone, its texture, grain size, porosity; and during the degradation it can be modified by the dissolution of the rock forming minerals, the precipitation of new minerals, formation of surface cracks etc.

A common method to quantify the roughness is the registration of linear surface profiles by means of a profilometer or rugosimeter (Rivera and Melo, 2001; Mateos, 2005). In this research we used a contact type Mitutoyo Surftest SV2000N2 profilometer. In this technique a diamond stylus is moved vertically in contact with a sample and then moved laterally across the sample for a specified distance. A constant load is applied to the stylus assuring that it never loses contact with the surface. Its height position generates an analog signal, which is converted into a digital signal stored, analyzed and displayed. The stylus used is of conical shape (60°) and has a 2 μm radius. The measuring force was 0,75 mN and the speed 1mm/s. The z-axis resolution was 800 μm/0,01 μm and the x-axis resolution 1 μm.

The measured and/or calculated surface parameters were the followings (see also fig. 4.3):

Ra: Arithmetical mean deviation of the profile (μm)

It is the arithmetical mean of the absolute values of the profile deviations (Yi) from the mean line.

$$Ra = \frac{1}{n}\sum_{i=1}^{n}|Yi| \tag{18}$$

Rq: Root-mean-square deviation of the profile (μm)

$$Rq = \left(\frac{1}{n}\sum_{i=1}^{n}Yi^2\right)^{\frac{1}{2}} \tag{19}$$

Sk: Skewness of the profile

Represents the degree of bias either in the upward or downward direction of an amplitude distribution curve.

$$Sk = \frac{1}{Rq^3}\cdot\frac{1}{n}\sum_{i=1}^{n}Yi^3 \tag{20}$$

Ku: Kurtosis of the profile

Represents the degree of concentration around the mean line of an amplitude distribution curve.

$$Ku = \frac{1}{Rq^4}\cdot\frac{1}{n}\sum_{i=1}^{n}Yi^4 \tag{21}$$

Rp: Maximum profile peak height (μm)

The maximum value of the profile deviations (Yi) from the mean line: the height of the highest point.

Rv: Maximum profile valley depth (μm)

The absolute value of the minimum value of the profile deviations: the depth of the lowest point of the profile from the mean line.

Ry: Maximum height of the profile (μm)

The sum of the height of the highest point and the depth of the lowest one both calculated from the mean line.

Sm: Mean spacing of the profile irregularities (mm)

On the profile provide two lines parallel to the mean line and located above and under the mean line at an equal distance (called "count level"). A peak projecting above the upper count level is called a "peak for peak count", and a valley dropping below the lower count level is called a 'valley for peak count". The arithmetical mean of the length of this peak and valley pair is called Sm.

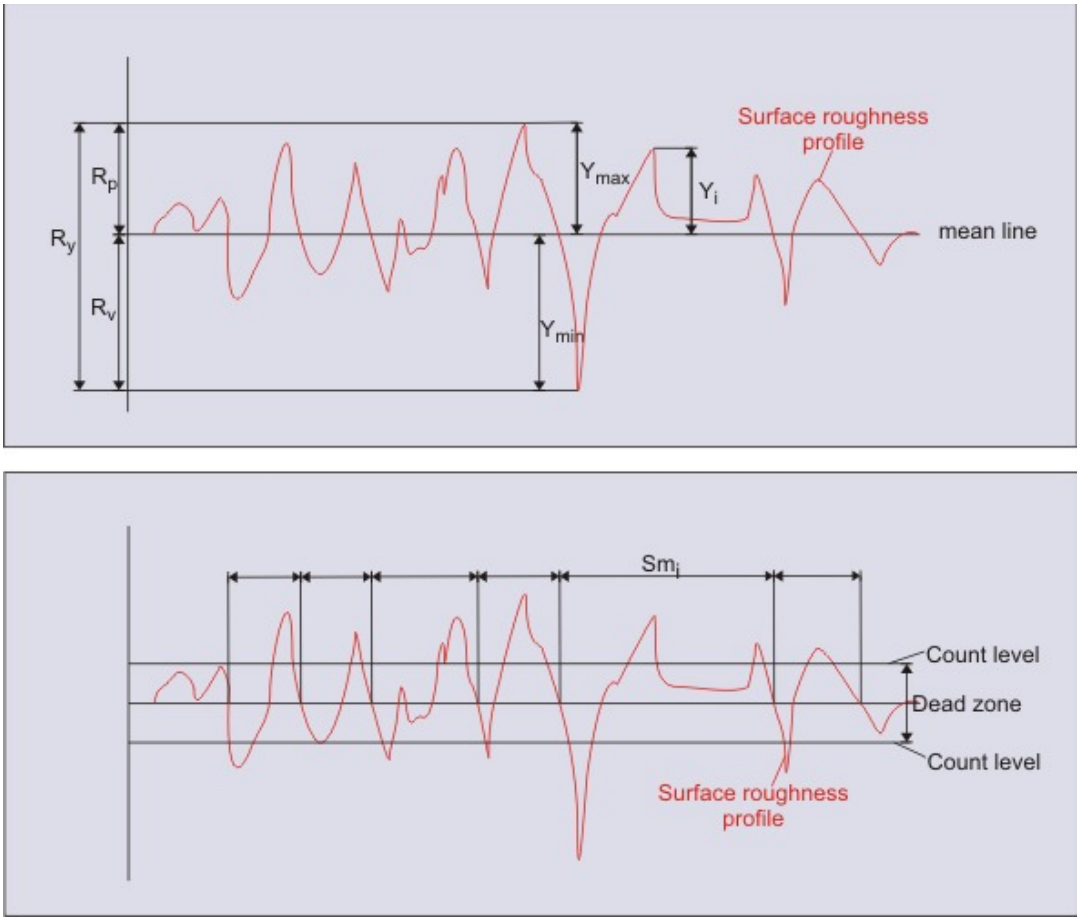

Fig. 4.3 The measured surface roughness parameters

All the parameters were calculated in the „mean type" mode, which means that they were performed on each sampling length included in the evaluation length, and then the calculation result is averaged to yield a final parameter value.

Surface chemistry – X-ray photoelectron spectroscopy

The X-ray photoelectron spectroscopy (XPS) is a technique especially adequate for the detection of the transformation of the outermost atomic layers of a stone material, occurring due to adsorption and/or desorption of atmospheric pollutants (Maravelaki-Kalaitzaki et al., 2002).

It has been extensively used for mineralogical studies (Raeburn et al., 1997a, 1997b; Stipp, 1999; Mattila et al., 2004 etc.) but its usefulness was recognized also in the field cultural

heritage conservation (Wilson-Yang and Burns, 1986; López-Arce et al., 2003; Ip et al., 2008; Aranda et al., 2008 etc).

Photoelectron spectroscopy utilizes photo-ionization and analysis of the kinetic energy distribution of the emitted photoelectrons to study the composition and electronic state of the surface region of a sample. The XPS technique uses X-rays to eject electrons from inner-shell orbitals. The kinetic energy of these photoelectrons is determined by the energy of the X-ray radiation and the electron binding energy. This energy is detected during the measurement in the form of a spectrum with a series of photoelectron peaks. It is characteristic of each element but it can be slightly altered by the chemical state of the emitting atom changing the situation and/or shape of the peaks. (Wagner et al., 1979)

The XPS measurements were carried out on a SPECS system equipped with a hemispherical electron analyzer, a Mg anode of 15 kV and 300W (1253,6 eV energy) and a low energy electrone source for the charge compensation. The general spectras, which include all the elements present in the sample, were made at a pass energy of 90 eV with an increment of 1 eV. And the individual ones, which contain the peaks of one element only, with a pass energy of 30 eV and an increment of 0,1 eV. All spectra were calibrated to the C 1s peak fixed at 284,6 eV. The detailed scans of single elements were determined according to the material in question and they will be described together with the results.

A Shirley type background substraction was applied and than the spectra were fitted with a non-linear fitting program adopting Gaussian-Lorentzian peak shapes with a 30% Lorentzian component.

4.2.5. Mechanical and thermal properties

Indirect mechanical characterization (homogeneity, anisotropy, pore shape) – Ultrasonic measurements

Anisotropy of physical properties of rocks may originate from more possible factors: the aligned grain fabric, crystallographically preferred orientation within the grains or the geometry of the void space (Tourenq et al., 1971; Sousa et al., 2002; Benson et al., 2005). To identify the directions of anisotropy and to determine its degree, the velocity of the ultrasound propagation is a useful tool as it is a non-destructive technique, which may be used in the laboratory and in situ, as well (Montoto, 2003; Benavente et al., 2006; Sáez-Pérez and Rodríguez-Gordillo, 2009). Moreover, this method gives information about many of the properties of the material; for example about the porosity, the degree of alteration, the geometry of the pores, the homogeneity of the material, the presence of discontinuities (joints, fractures), any changes of the material, grain or clast size, as well as about artificial changes like penetration of treatments etc. (Alonso and Suárez del Río, 1985; Al-Harthi, 1997; Esbert et al., 1997; Valdeón et al., 1997; Kahraman, 2002; Grinzato et al., 2004; Benson et al., 2005; Sousa

et al., 2005; Bourgès, 2006; Mateos et al., 2006; Martínez-Martínez et al., 2007). Besides, as it was proved by many researchers (Kahraman 2001; Yasar and Erdoğan 2004; Vasconcelos et al., 2008), there is a good correlation between the ultrasonic pulse velocity and the compressive strength and modulus of elasticity, and so, the method is a reliable tool of assessing mechanical characteristics of stone.

There are several different parameters to measure, such as the velocity of the P-waves (Vp), the velocity of the S-waves (Vs), the velocity ratio (Vp/Vs), the waveform energy, the attenuation, etc., which may give complementary information (Valdeón et al., 1996; Benavente et al., 2006). In this study we used the Vp only, as the P-waves are more stable and reproducible as the S-waves. This parameter is largely influenced by the measurement conditions (temperature, water content, etc), so the conditions were kept constant during the measurements (room temperature: 21°C and samples dried on 60°C till constant weight).

We used the transmission method, which consists of placing two piezoelectric transducers (a pulser and a receiver) on two opposite, parallel sides of the sample. The travel time is measured, and by knowing the exact distance between the transducers the wave propagation velocity can be calculated. Honey was used to achieve good coupling between the transducers and the sample surface. A PUNDIT Plus tester was used to carry out the test with transducers of 1 MHz frequency (fig. 4.4). By measuring the velocity of ultrasound propagation of the sound material and then after the different ageing tests, we can follow the degradation processes of the samples quite accurately and in a non-destructive way.

Fig. 4.4. Measurement of ultrasonic propagation.

Measuring the same sample in dried and in water saturated state provides extra information about the material (Kahraman, 2007); especially about the shape of the voids. There are two main types of voids in solids: pores, which have a more or less equidimensional shape, and cracks, which have extensions significantly larger in two directions of the space than in the

third one (Delgado Rodrigues, 1983). Certain physical properties of rocks are affected very differently by pores and by cracks and even though pores are usually present in larges quantities, cracks play a greater role in determining bulk properties of a rock (Walsh and Brace, 1966). Therefore, knowing the quantity of pores versus cracks is an important detail. The water saturation of materials characterized by fissure porosity cause an important increase in their Vp compared to the same property in dry state; while in the case of pore type porosity there is no significant difference. This phenomenon maybe due to the surface tension that the water evolves on the walls of cracks, which are situated close to each other (Tourenq et al., 1971); or to the simple fact that the elastic wave has to cross the thin but long fissures in order to progress through the specimen and cannot by-pass them as it does with the equidimensional pores (Delgado-Rodriguez, 2000). Bourgès (2006) found that by calculating a pore shape factor (Psf) from the ratio of the Vp in dry (Vpd) and in the saturated (Vps) sample (eq. 22) we can get an estimation about the relative quantity of pores and cracks:

$$Psf = \frac{(Vps - Vpd)}{Vps} \tag{22}$$

0 < Psf < 0,05	Porosity of pore
0,05 < Psf < 0,25	Porosity of pore and crack
Psf > 0,25	Porosity of crack

This measurement was also carried out before the ageing tests and at the different stages of the artificial ageing.

Thermal properties

Thermal degradation is an important issue in the building and monumental degradation field because of the significant temperature differences that can build up in the materials (Gómez Heras, 2005) and the thermal fatigue effect caused by cyclic temperature changes (Koch and Siegesmund, 2004).

Among the several properties that characterize the thermal behaviour of a material (such as specific heat capacity, thermal conductivity etc.) the thermal dilatation and the residual strain after thermal treatment are the most important from the thermal degradation point of view (Leiss and Weiss, 2000).

In this research, the thermal characterization of the materials happened by the measurement of the coefficient of the thermal expansion (CTE) and of the residual stress.

The CTE was determined from the lineal thermal dilatation according to the following equation (Martinez-Martinez, 2008):

$$\alpha = \frac{\Delta l}{l \times \Delta T} \tag{23}$$

α: thermal dilatation coefficient in 10^{-6} K^{-1}
Δl: length change of the sample
l: original length of the sample
ΔT: temperature interval.

The residual strain is the length change of the sample due to the thermal treatment after cooling back to room temperature as a function of the original length. It is calculated according to the following equation:

$$\varepsilon_{rs} = \frac{\Delta l_{rt}}{l} \tag{24}$$

ε_{rs}: residual strain in mm/m
Δl_{rt}: length change after cooling back to room temperature

The measurement of these parameters was carried out at the Technical Service of the University of Alicante on a TMA Q400 Thermo-Mechanical Analyser. 1x1x1 cm cubic samples were subjected to two heating-cooling cycles on the 35°C – 90°C range. A 0,05N force was applied on the sample surfaces and the measurement happened in nitrogen atmosphere. The velocity of heating and cooling was 0,5°C/min.

5. Stone characterization

5. Stone characterization

5.1. Petrographical description

The petrographical description includes the textural and compositional (both mineralogical and chemical) characteristics of the materials, which play an important role in the determination of their susceptibility to degradation processes. The diagrams of the ultrasonic propagation of each stone type are shown in appendix 1.

Macael marble

The Macael marble is a white heterogranular marble (L*:77,8; a*:-2,4; b*:-1,1) with an average grain size of 700-500 μm. Light grey layers with a thickness varying from 2 – 10 mm can be observed in one distinct direction (fig.5.1).

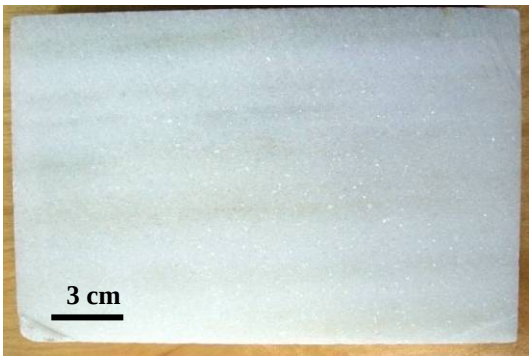

Fig. 5.1 The Macael marble is a white marble with slightly visible greyish layers in one direction

Approximately 90% of its grains is calcite with undulating grain boundaries and without textural orientation (fig.5.2).

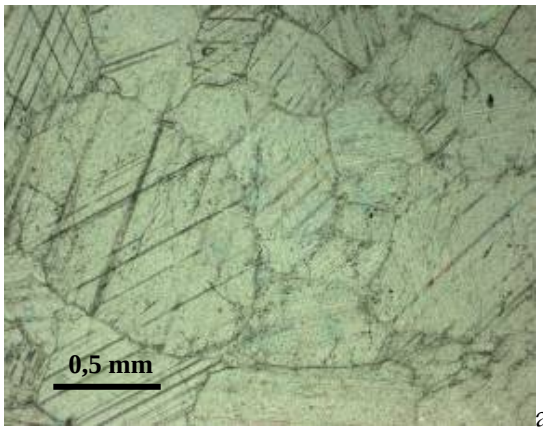

a)

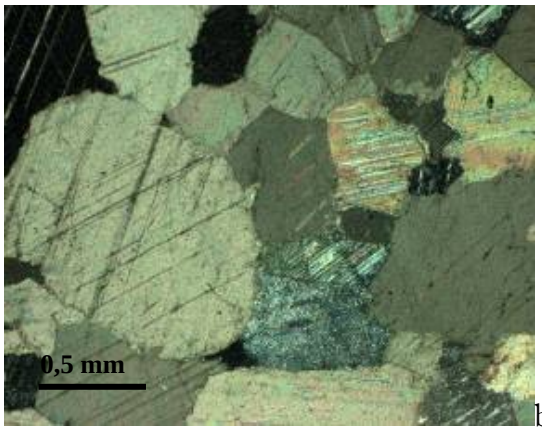

b)

Fig. 5.2 The Macael marble has a heterogranular texture with an average grain size of 700-500 μm. Microphotpgraph of POL with parallel (a) and with crossed (b) nicols.

The most usual accessory mineral is muscovite, which is usually present in the form of 125-250 μm long plates sometimes larger (~500 μm) elongated aggregates. Feldspar and quartz grains of approximately 100 μm size can be observed, as well. Very rarely some <100 μm large epidote and chlorite grains are present. The macroscopically observed grey layers are

intercalations rich in mica, pyrite, quartz and feldspar grains. Here textural orientation also can be observed; the orientation of the elongated grains is parallel to the plain of the layer (fig.5.3)

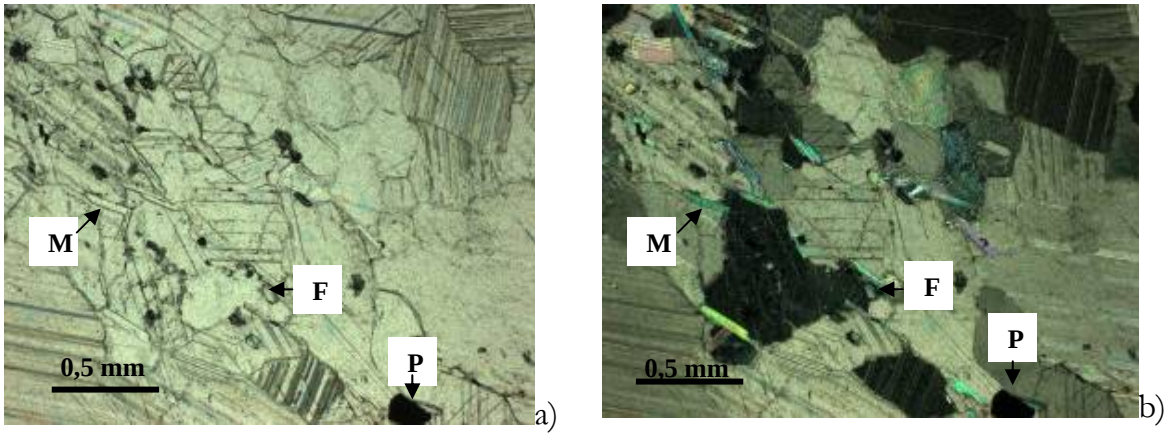

Fig. 5.3. The marble contains intercalations rich in mica (M), pyrite (P), quartz and feldspar (F), where textural orientation can be observed. Microphotpgraph with parallel (a) and with crossed (b) nicols.

The marble does not show any sign of chemical alteration.

By means of polarizing microscope no pores or fissures can be observed, only the high magnification of the scanning electron microscope makes it possible the find some cracks of extremely small size: the average aperture size is less than 1 μm and the average length is around 10-20 μm (fig.5.4). The fissures usually follow the grain boundaries or the foliation planes of the calcite crystals and their tortuosity is low.

This marble is a highly homogeneous material, but due to the above mentioned intercalations it has a slight anisotropy (coefficient of anisotropy: 1,1). This fact was proved by the ultrasonic measurements, which showed that the velocity of the propagation of the ultrasonic waves is a lot slower perpendicular to the foliation ('T' direction; average value: 4400m/s) than paralell to it ('M' and 'N' directions; average value: 5100m/s). This anisotropy is also due to the preferential orientation of the c-axis of the calcite crystals proved by other researches (Sebastián Pardo et al., 2006; Sáez-Pérez and Rodríguez-Gordillo, 2009).

The according to the comparison of the Vp in dry and saturated conditions, the voids are dominantly cracks as the pore shape factor (Psf) (after Bourgès, 2006) is 0,32 in the T direction and 0,25 both in the M and N directions. This also proves that the majority of the cracks are parallel to the T plain.

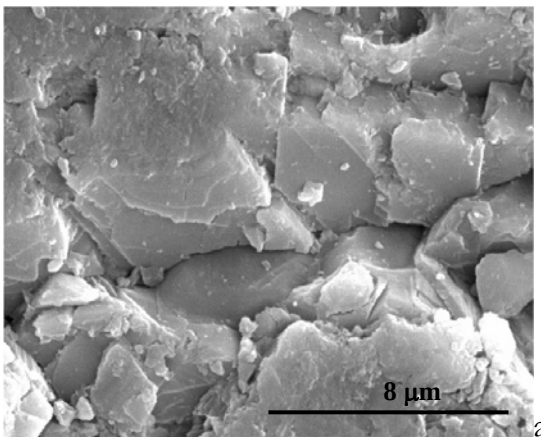

a)

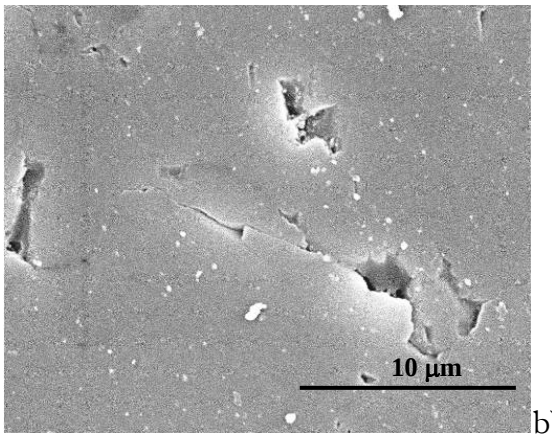

b)

Fig. 5.4 The micro-fractures of the marble, which are observable by SEM, are of very small aperture and length: a) fractured surface; b) polished surface.

Silvestre Vilachán granite

The Silvestre Vilachán is a light grey (L*:74,8; a*:-1,1; b*:5,5), medium-fine grained, two-mica leucogranite.

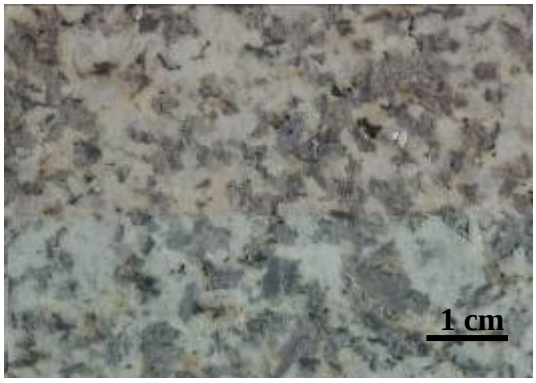

Fig. 5.5 The Silvestre Vilachán is a light grey medium-fine grained two-mica leucogranite with a slight alteration

The main rock forming minerals that can be distinguished by the naked eye are the feldspar, quartz, biotite and muscovite (fig.5.5). Its average grain size is about 1 mm but the grain size distribution is very wide varying from the centimetre to the sub-millimetre scale.

Quartz is the most common rock forming mineral (~40v/v%). 1-2 mm is the most frequent grain size but as it was mentioned above very different sizes can be observed in the thin sections.

The quartz grains have an undulating extinction, they started to be converted into sub-grains of smaller sizes, and very often their boundaries are sutured. These all suggest a slight metamorphism caused by stress.

There are two different types of feldspars in the granite, plagioclase (oligoclase) (~35v/v%) and microcline (~10v/v%). Both have a slight alteration, sericite and muscovite flakes can be observed (fig.5.7). Their grain size is a little bit finer than that of the quartz. The microcline shows signs of higher pressure as well, as in some grains the typical grid-patterned twin laminae partly or totally disappears.

The stone is rich in micas. The amount of muscovite (~10v/v%) is higher than that of the biotite (~5v/v%). It's probable that the muscovite had more phases of crystallisation as some of its grains are completely sound and often superimposed on other minerals. The biotite

grains are partly or totally altered to chlorite (figure 5.6) and the rutile phase – also created by this alteration – can be observed as shapeless nodules or as needle-like grains, called sagenite.

Zircon and apatite are the most common accessory minerals. Some small and very weathered grains of andalusite can be observed as well.

The granite has a hypidiomorphic heterogranular texture. No textural orientation can be observed (shape or orientation of the grains) in any direction.

The very high, fissure-type porosity can be well observed already by means of polarizing microscope due to the large apertures (fig.5.8.). As thin sections were prepared in the three directions of the space, it can be determined that most of the fractures are parallel to the 'T' side, which means the floor of the quarry. Inter-, intra- and transgranular fractures (the first in quartz and feldspar) were observed by means of SEM, as well (fig.5.9 - 5.10). The length of the fissures is often above 1 mm and their aperture frequently surpasses 50 μm. Usually, their tortuosity is low.

Because of the orientation of its fractures, this granite has a significant anisotropy: the average value of the ultrasonic wave propagation is about 2000m/s in the 'T' direction; and about 3000m/s in the two other directions ('M', 'N'). The coefficient of anisotropy is 1,4. The stone is homogeneous.

According to the comparison of the Vp in dry and saturated conditions the voids are dominantly cracks as the pore shape factor (Psf) is 0,35 in the T direction and 0,31 in the M and 0,32 in the N directions. This also proves that larger part of the cracks is parallel to the T plain.

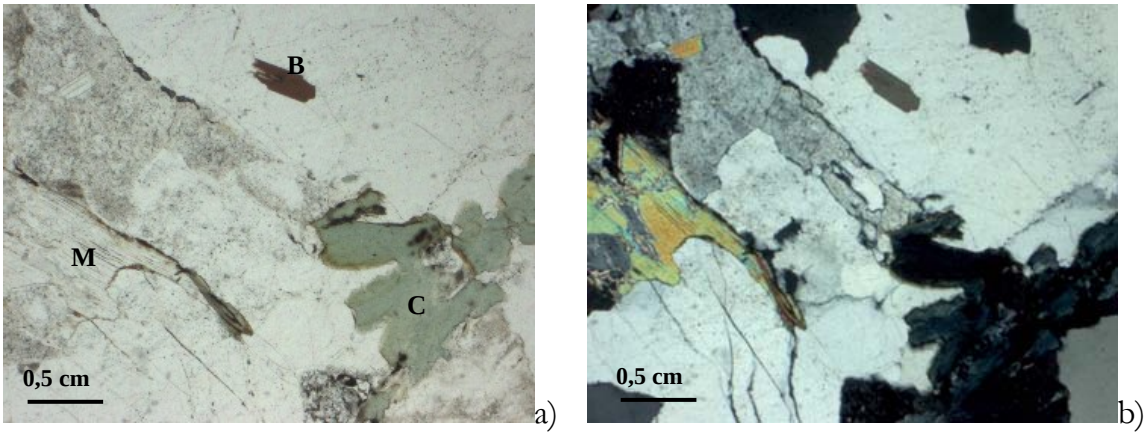

a) b)

Fig. 5.6. The Vilachán granite is a two mica granite, containing muscovite (M) and biotite (B), as well. The biotite grains in some cases are altered into chlorite (C). Microphotgraph with parallel nicols (PN) (a) and with crossed nicols (CN) (b).

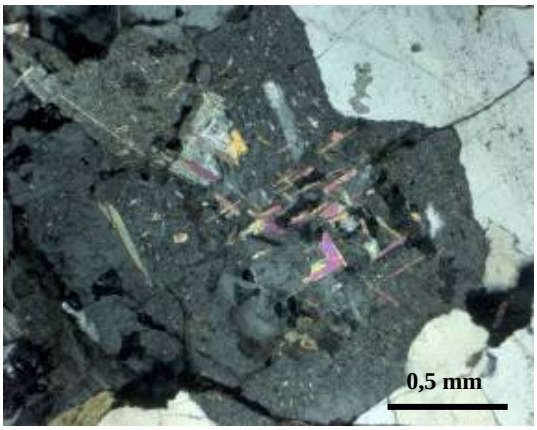

Fig. 5.7. The feldspar phases of the granite have a slight alteration and contain mica intercalations. Microphotograph PN.

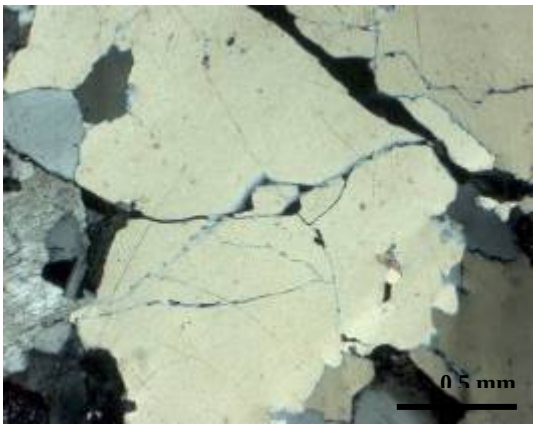

Fig. 5.8. Opened fractures in quartz grains of Silvestre Vilachán granite by POL PN.

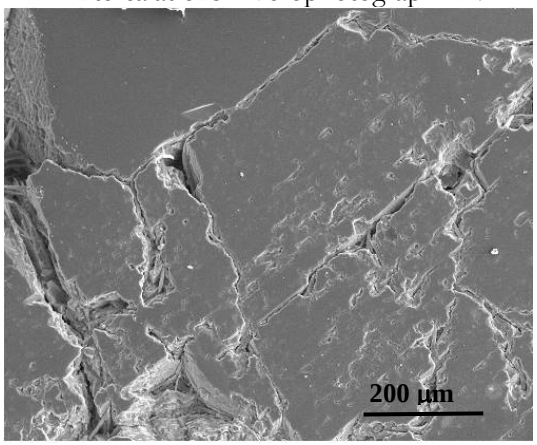

Fig. 5.9. The feldspar grains have a high intergranular porosity due to alteration. SEM

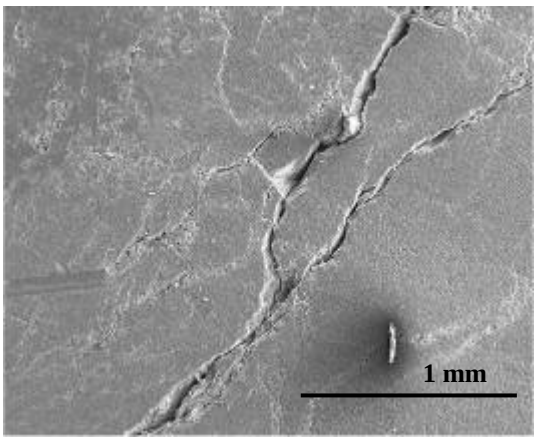

Fig. Figure 5.10. Inter- and intragranular fissures are usually connected to the quartz (Q) and feldspar (F) grains. SEM

Szob andesite

The rock is a fine grained quartz-andesite (L*:48,3; a*:-3,8; b*:2,8). In the light grey matrix some 2-3 mm long black amphibole, approximately 1 mm large biotite and some light, yellowish-grey feldspar phenoclasts can be observed by the naked eye (fig.5.11.).

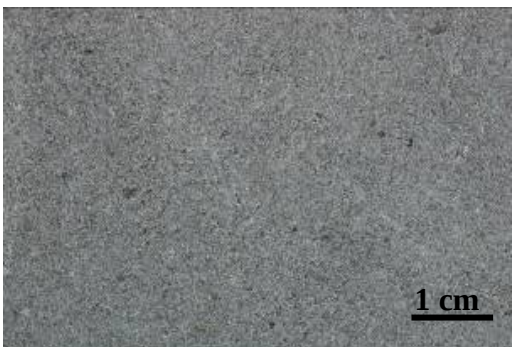

Fig. 5.11. The Szob andesite has a microporphiritic texture. In the light grey matrix blackish phenocrysts of biotite and amphibole can be observed.

The matrix/ phenoclast ratio is approximately ½ (fig.5.12.). The most abundant phenoclast is the plagioclase (andesine) (30v/v%). The plagioclase crystals are usually idiomorphic or

hipidiomorphic. Their average grain size is 1-2 mm. Very often they are constructed by more than one zones and generally the outermost zone is less altered than the core, or not altered at all (fig.5.13).

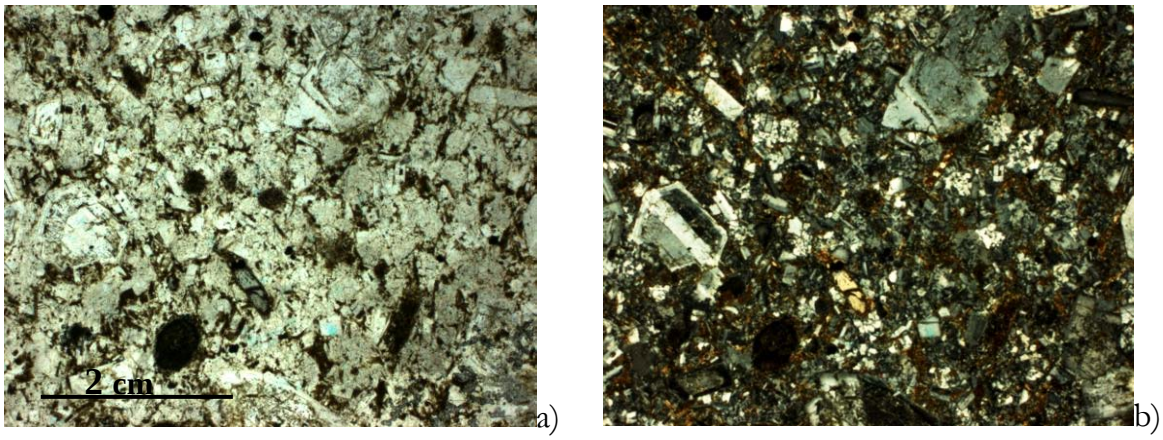

a) b)

Fig. 5.12. The andesite has a microporphyritic texture, the matrix/ phenoclast ratio is approximately ½. Microphotograph by POL a) parallel nicols b) crossed nicols

This means that the outer zones were formed later. There are some perfectly sound plagioclase crystals as well; probably they were formed at the same time when the outer zone of the older plagioclases. Sometimes the plagioclase grains form aggregates of the size of 2-5 mm or more. The alteration of the plagioclase – as it was mentioned above – is the most significant in the inner core of the older plagioclase generation but even there it is not too significant. On the other hand, these cores contain quite a lot of glass inclusions, which are not present in the younger plagioclase phase. These glass inclusions may be a weak point of the rock, as the glass is very easily altered and a high volume of microporosity may evolve in their places.

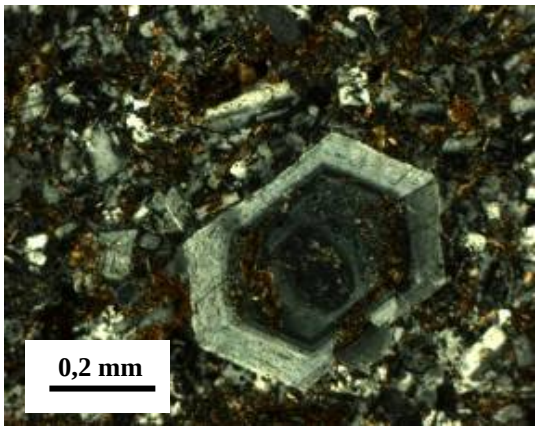

Fig. 5.13. The feldspar phenoclasts usually contain several zones, the inner ones often with glass inclusions, which are more sensitive for alteration. Microphotograph by POL, CN.

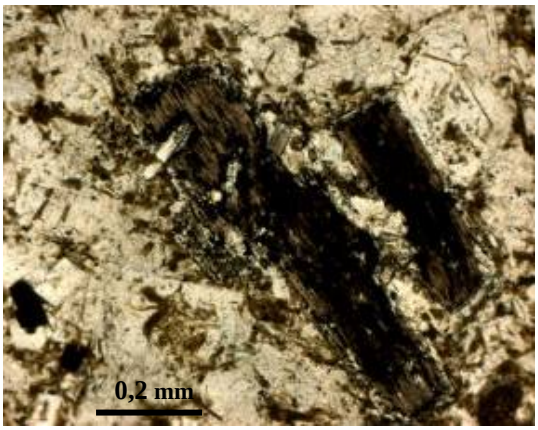

Fig. 5.14. The ferromagnesian minerals have a high degree of alteration and are partly or completely replaced by biotite and opaque minerals. Microphotograph by POL, PN.

The ferromagnesian minerals of the stone are all altered to a high level. The amphibole was partly replaced by aggregates of magnetite, biotite and plagioclase. In some cases there is only

a rim of the opaque phase and the core is more or less sound, in other cases the whole area is filled with very small opaque grains. The size of the amphibole-relics is around 0,8-1,5 mm. The pyroxene grains have suffered the same alterations as the amphiboles. In some cores small fragments of the original mineral phase remained, so it can be identified as a hyperstene. Biotite is the second more abundant mineral of the rock (~10v/v%) and it is present in two phases. The first one is the big (1-2 mm long) phenoclasts, which are more or less altered into magnetite (fig.5.14.). And the other one is the above mentioned alteration products in the amphiboles, pyroxenes and in the matrix. The rock contains opaque mineral grains as alteration products of the ferromagnesian minerals as well as individually in the matrix. The matrix is composed of very small (50-75 μm) grains of plagioclase, biotite and some quartz grains.

The texture of the rock is micro-porphiritic; orientation cannot be observed.

Some fractures with a thickness of a few mm-s filled by quartz, calcedon or limonite can be seen by the naked eye. Open fractures cannot be observed in the thin sections but in some cases sections of carbonate veins can be found. By means of SEM we can see the typical features of the fissures of the andesite: the small apertures (average ≤1 μm) and lengths (10-50 μm) and the very high tortuosity (fig.5.15).

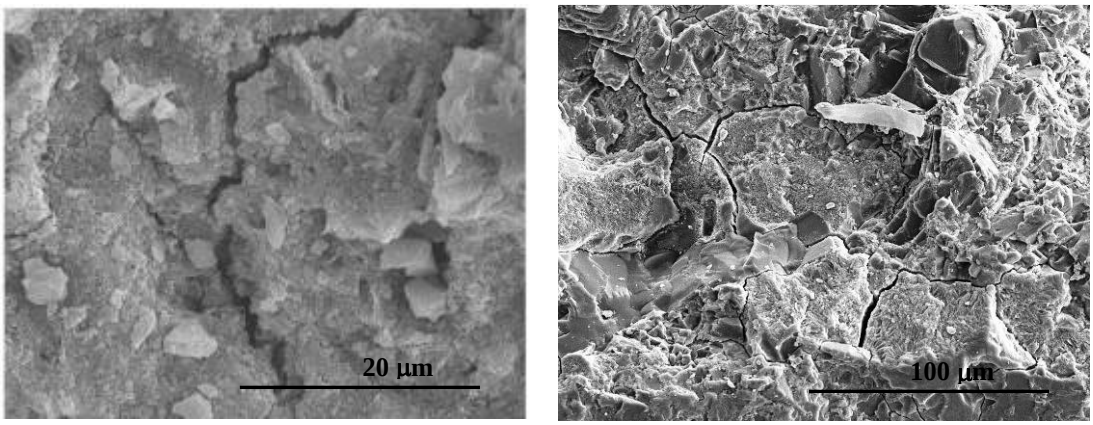

Fig. 5.15. The fissures in the matrix of the Szob andesite have small apertures and high tortuosity. Microphotograph by SEM.

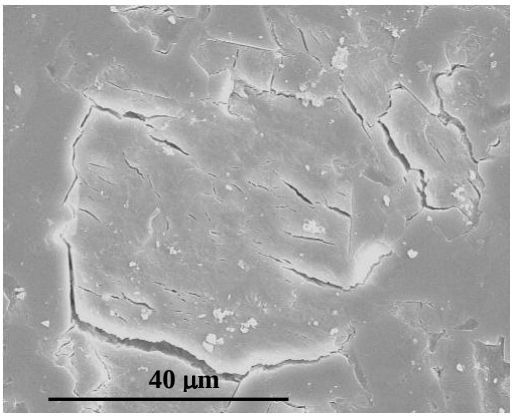

Fig. 5.16. Inter- and intragranular cracks in biotite grain. Microphotograph by SEM.

The fractures are mainly situated in the fine-grained matrix. Intragranular fractures are quite rare but sometimes they can be detected within the large feldspar grains or between the layers of the micas (fig.5.16). The porosity connected to the mineral alteration – both in the matrix and the phenoclasts – consists of spherical pores of micrometer – sub-micrometer dimensions.

According to the ultrasonic measurements the andesite is isotropic; the average velocity of ultrasound propagation is 5300m/s in all the directions. Due to the few macrofractures that are present in the stone, it is sometimes less homogeneous than the other two stones.

The according to the comparison of the Vp in dry and saturated conditions the voids are dominantly spherical pores as the pore shape factor (Psf) is 0,03 in all directions. This also can be explained by the very small size of the voids (both pores and cracks), which decreases the influence of the void shape in the saturated Vp velocity.

As a summary of the petroghraphic properties, the semi-quantitative mineralogical composition, the open porosity values and the texture of each stone is shown in table 5.1 and the chemical composition in table 5.2.

Table 5.1

	Mineralogical composition (%)								**texture**
	calc	musc	bio	Q	plg	mic	magn +pyr	matrix (%)	
Macael marble	90	tr	-	tr	tr	-	-	-	Medium grained heterogranular
Vilachán granite	-	10	5	40	35	10	-	-	Hypidiomorphic granular
Szob andesite	-	-	10	tr	30	-	7	50	Micro-porphiritic

Table 5.1. The semi-quantitative mineralogical composition and the texture of the Macael marble, Silvestre Vilachán granite and Szob andesite (calc=calcite; musc=muscovite; bio=biotite; Q=quartz; plg=plagioclase; mic=microcline; magn+Pyr=magnetite and pyrite; tr=trace minerals).

Table 5.2

	SiO_2	**Al_2O_3**	**Fe_2O_3**	**MnO**	**MgO**	**CaO**	**Na_2O**	**K_2O**	**TiO_2**	**P_2O_5**	**L.O.I**
Macael marble	0,05	0,02	0,02	0,01	0,51	55,34	0,02	0,02	0,02	0,01	43,10
Vilachán granite	70,60	16,06	1,10	0,02	0,33	0,57	3,80	5,60	0,15	0,41	1,45
Szob andesite	60,45	16,91	5,52	0,10	1,84	5,41	3,11	2,44	0,59	0,22	2,96

Table 5.2. The chemical composition of the Macael marble, Silvestre Vilachán granite and Szob andesite expressed in oxides. L.O.I. = loss of ignition

5.2 Other petrophysical properties

5.2.1 Void space

The typical features of the void space of the materials were observed and described by means of the microscopy techniques, mainly by CLSM, while for the quantification of its parameters the values gained by different methods (Hg porosimetry, N_2 absorption with BET analysis and digital image analysis of microphotographs) were used together, as they detect different pore size ranges.

Macael marble

The porosity – both the open and total – of the marble is very low: below 1 %. It mostly contains intergranular fissures of small aperture between calcite grains (fig.5.17.), and some intragranular pores can be observed, as well, connected to the mica and feldspar inclusions. The pores connected to feldspar and muscovite crystals are usually observed as spherical pores but due to their small size more detailed observations are not possible by the confocal microscopy. The average aperture of the observable cracks is smaller than 1 μm. Their tortuosity is usually low, as they follow the grain boundaries or the foliation planes of the calcite crystals. They are connected often in the triple points, where more calcite grains meet, but several intersections are not typical.

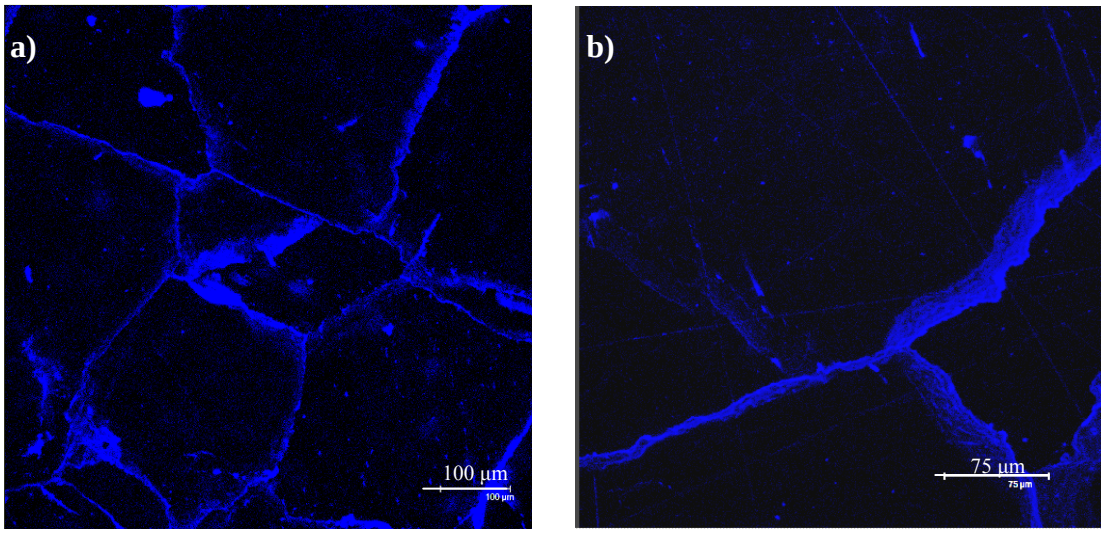

Fig. 5.17. The fissures of the Macael Marble are typically connected to the grain boundaries (a); they are of small aperture and low tortuosity (b) Microphotograph by CLSM.

The open porosity of the marble according to the Hg porosimetry is around 0,9% (±0,1%). All the apertures were detected within the interval: 0,005-10 μm in diameter. The size distribution within this interval is more or less even with a slight peak around 0,01 μm (fig.5.18). The N_2 absorption method could not be used in this case because the specific

surface (around 0,5±0,03 m^2/g based on Hg porosimetry) of the material is below the detection limit.

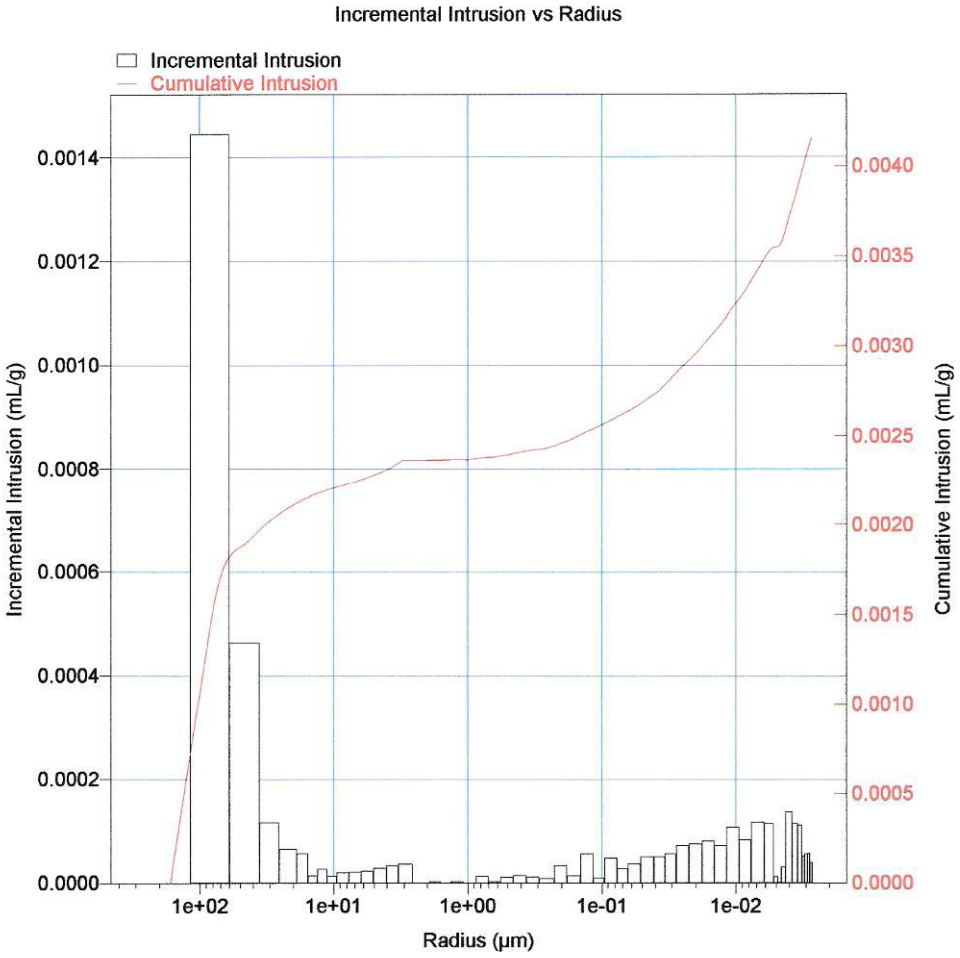

Fig. 5.18. The pore access size distribution of the Macael marble by Hg-porosimetry.

Silvestre Vilachán granite

Of the three stones investigated in this study the granite has the second highest porosity. Its void space is composed of trans- and intergranular macro fissures and intragranular voids (both fissures and pores) mostly in the feldspar grains (fig.5.19). The macro fissures are well connected, are usually not tortuous and have a preferential orientation parallel to the 'T' plane, which is the horizontal plane of the quarry; but there are more than one fissure groups. The ramifications and junctions of the fractures in different depths can be observed very well (fig.5.20). The other type of porosity due to feldspar weathering has significantly smaller aperture. These voids sometimes follow the crystalline structure of the feldspars or are disoriented.

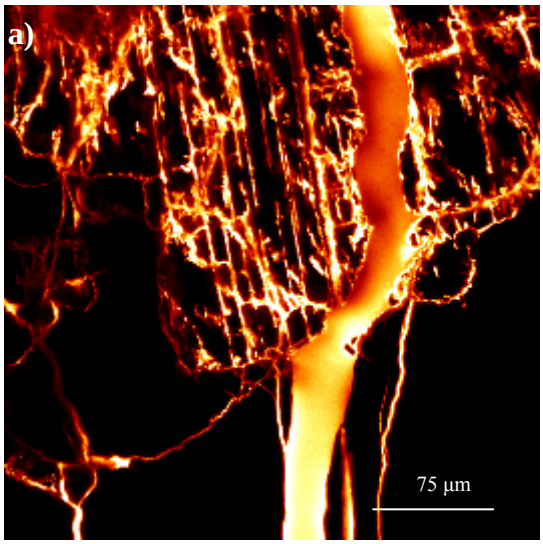

Fig. 5.19. The void space of the Vilachán granite is composed of trans- and intergranular macro fissures and intragranular voids mostly in the feldspar grains. Microphotograph by CLSM.

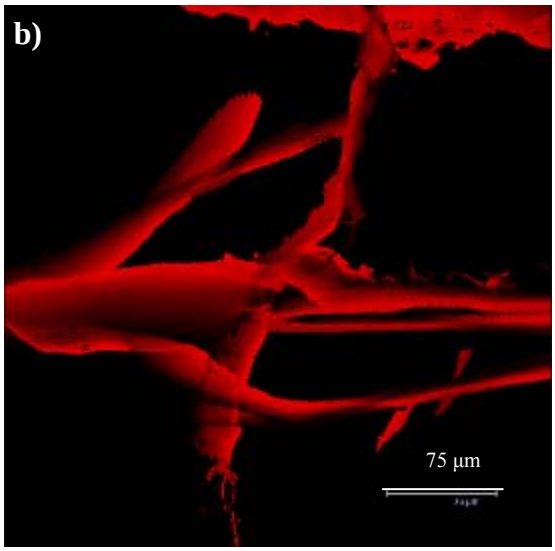

Fig. 5.20. The fractures of the granite are well connected and have low tortuosity. Fractures in quartz grain composed 3D image by CLSM.

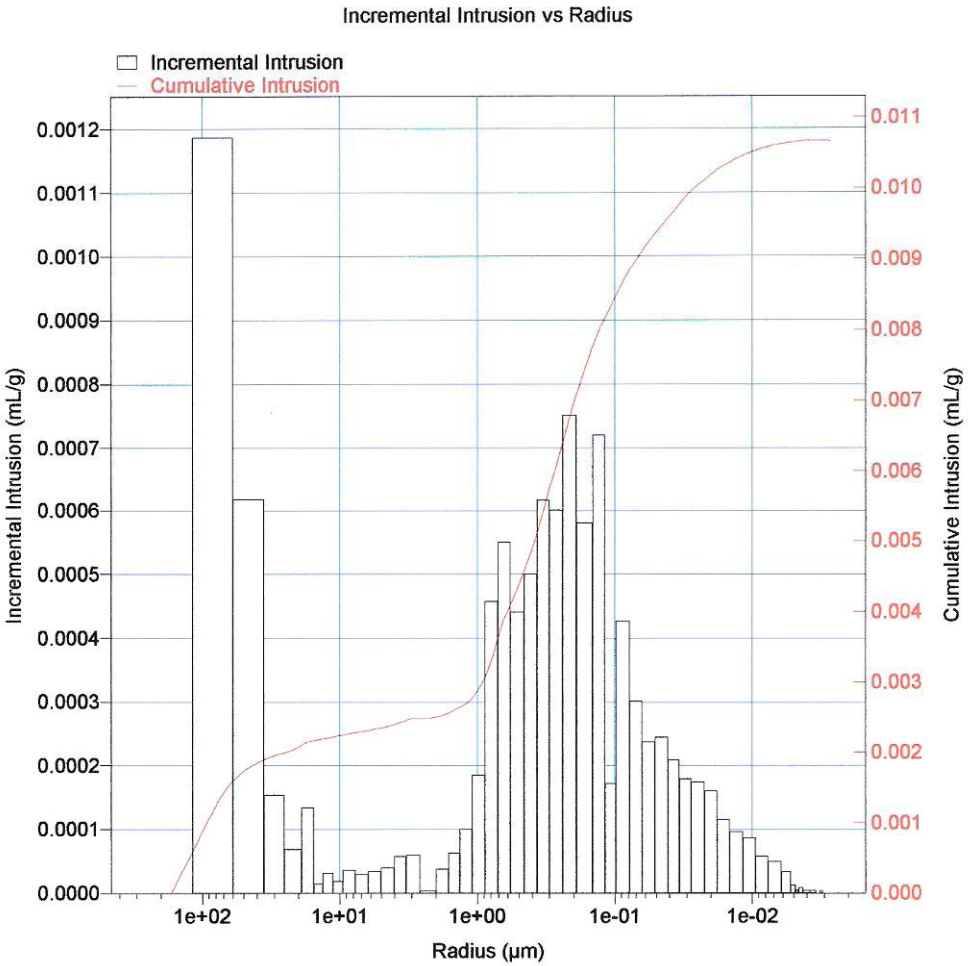

Fig. 5.21. The pore access size distribution of the Vilachán granite by Hg-porosimetry.

The open porosity of the Silvestre Vilachán granite based on Hg porosimetry is 3,3±0,1%. The apertures were detected in the 0,001-100 μm interval and have an uneven distribution. The majority (60-70%) of the apertures are within 1 and 0,1 μm, but the fact, that the N_2 adsorption test - which detects the pores between 1-100 nm - measured the double of the specific surface (1,9m^2/g) than the Hg porosimetry, proves that there is a large percentage of micropores, as well (fig. 5.21). According to the microscopic observations these are the intragranular pores, mostly situated in the feldspars.

Szob andesite

The andesite has a very different void space compared to the two other stones. Here, although the porosity is high, most of the voids have so small apertures that even with the highest magnification of the CLSM (63x objective) they appear like small spherical pores but no closer observation can be carried out (fig.5.22.). Most of these voids are situated in the fine grained matrix but the biotite and feldspar phenoclasts also show the signs of weathering. The few larger fissures are either connected to the phenoclasts, like the one on fig.5.23, which is a grain boundary fissure around a feldspar grain, or they are in the matrix, in which case their tortuosity is extremely high, usually they are of small aperture (average ≤1 μm) and length (10-50 μm).

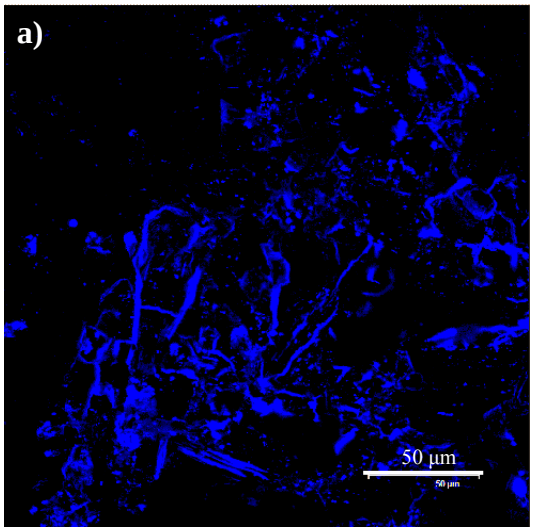

Fig. 5.22. Most of the voids of the Szob andesite are situated in the fine grained matrix, and are of sub-μm dimensions.

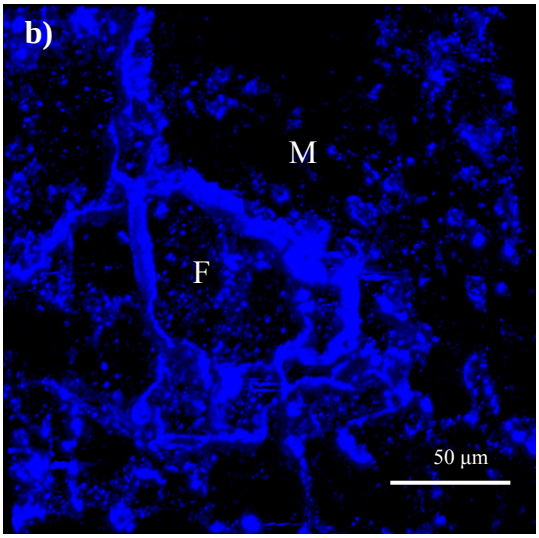

Fig. 5.23. Grain boundary fissure around a feldspar grain (F) of the Szob andesite, which continues in the matrix (M).

According to the Hg porosimetry measurement the open porosity of the andesite is 3,5±0,01%. The apertures were detected in the 0,001-100 μm interval again, but in this case the size distribution is clearly unimodal and is shifted towards the small sizes (fig. 5.24). Approximately 80% of the pores are smaller than 0,1 μm in diameter and the majority

between 1 nm and 100 nm, proved by the specific surface values: 3,3±0,1 m^2/g by Hg porosimetry and 3,9 m^2/g by N_2 adsorption.

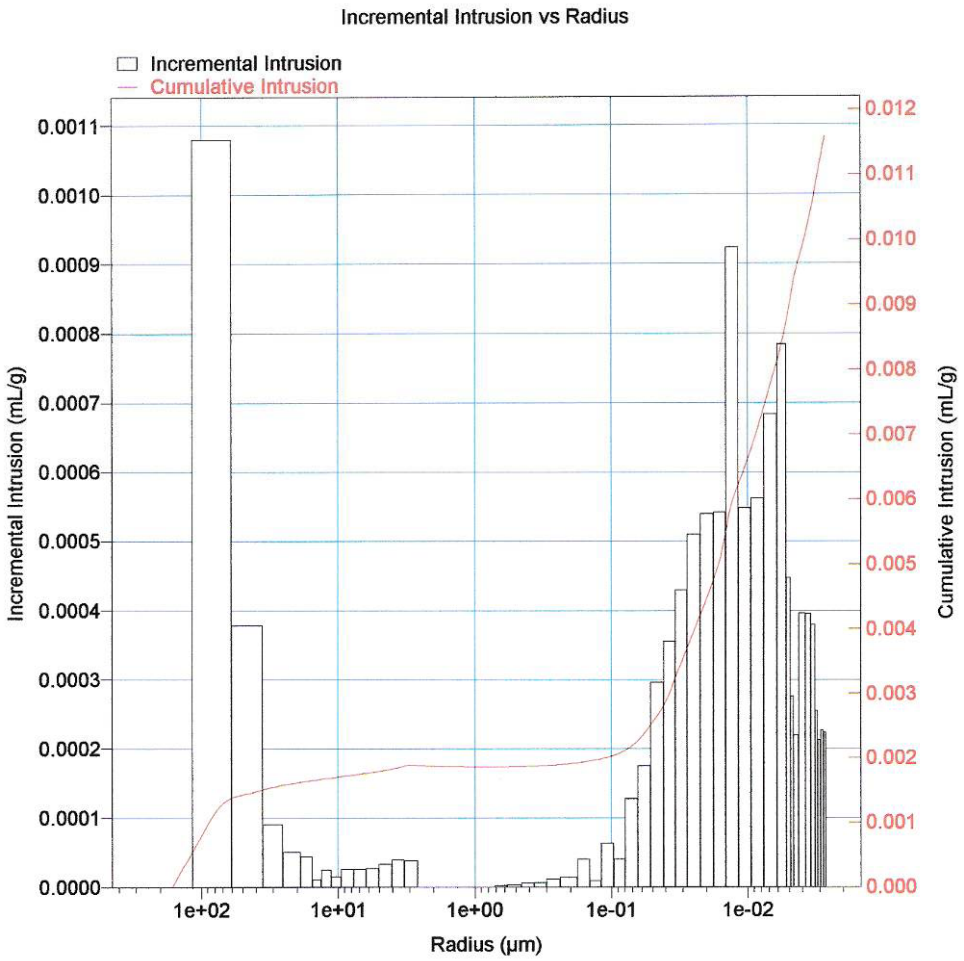

Fig. 5.24. The pore access size distribution of the Szob andesite by Hg-porosimetry.

Based on the observations during this research, the parameters of the void space, that play the most crucial part in the degradation processes, are the open porosity and the size distribution. Also, these are the parameters that suffer most of the changes. This was the reason to establish a uniform and summarizing diagram for their graphical presentation.

This diagram can be seen in figure 5.25 with the values of the fresh stones. The void size range is divided into 4 sections: smaller than 0,01µm, between 0,01µm and 0,1µm, between 0,1µm and 1µm and larger than 1µm. The columns represent the quantity (V%) of open voids in the given size interval, while the lines represent the cumulative values of the same, reaching the total open porosity value at the end.

The first three intervals are the values gained by Hg porosimetry, as this method seems to be the most reliable for these stones in this size range. The Hg porosimetry sometimes over-estimates the quantity of the largest voids due to the inaccuracy introduced by the superficial roughness of the samples and the compressibility of the mercury, as it can be observed on figures 5.18 and 5.24 for the marble and andesite, respectively. So this range was excluded from the measurement and the smaller values were proportionally correlated. The CLSM-DIP method on the other hand is reliable on the >1µm range, so that technique was used for the quantification of the open voids in this interval.

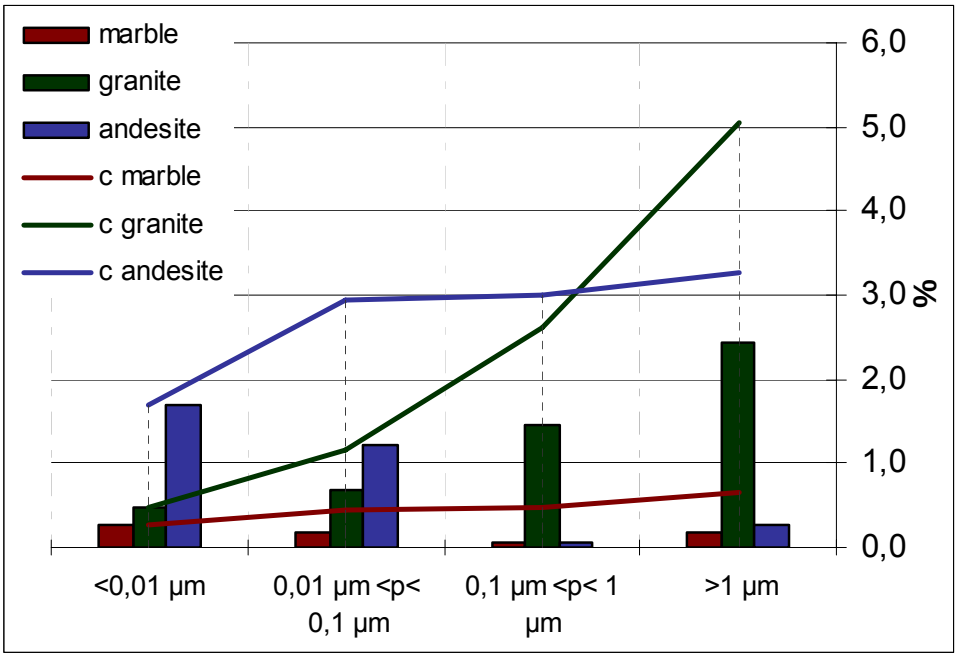

Fig. 5.25 The void size distribution of the three stones based on Hg porosimetry and CLSM-DIP measurements. Coloumns: absolute values; Lines: cumulative values.

There is a large difference in the working principles of the two techniques. The Hg porosimetry detects the void throats, while with the microscopy an average void diameter is measured. Nevertheless, in the case of fissured materials, such as the ones in concerned in this research, the definition of "pore throat" becomes unclear. The apertures of cracks and fissures can be considered relatively constant along the whole length or expansion of the feature. Consequently, the values measured by the two techniques are regarded as complementary and coherent on the different void size ranges.

5.2.2. Density

The density was determined by means of water absorption under vacuum and He pycnometry. The results are shown in table 5.3.

The Macael marble shows the highest apparent density followed by the Szob andesite and the lowest value corresponds to the Silvestre Vilachán granite. The helium can enter to all the voids that are wider than 0,1-0,2 nm so the density measured by this method is often considered as the real density of the material.

Based on these two values (the apparent density and the He density) the total and the open porosity of the stones can be calculated. The values are presented in table 5.3.

5.2.3. Hydraulic properties

The hydraulic properties, such as water absorption, evaporation, capillarity uptake, water vapour permeability, and liquid water permeability give information about the water movement kinetics within the material.

The determined coefficients are summarized in table 5.3, and the corresponding curves are shown on figures 5.25-27.

Water absorption

The water absorption value in case of total saturation depends on the open porosity of the material and the shape of the water adsorption curve, which gives information about the velocity of the process, depends on the connectivity of the porous network. The Macael marble has the lowest water absorption value, 0,22±0,01 %; while the values of the Silvestre Vilachán granite and the Szob andesite are very similar, 1,90±0,04 % and 1,92±0,12 %, respectively. On the other hand the velocity of the water uptake process (fig.5.25.) is more similar in the case of the marble and the granite. The marble reaches the total saturation within 24 hours, while the granite reaches 90% within the same time, and then the micropores continue to be slowly filled during another 10 days. On the other hand, the Szob andesite reaches only approximately 40% saturation in 24 hours and needs approximately 21 days for the total saturation. This is due to the very small average void size of the andesite and the high tortuosity of its fissures, which slow down the water movement in the material. The values of the saturation coefficient (S) presented in table 5.3 express this velocity numerically.

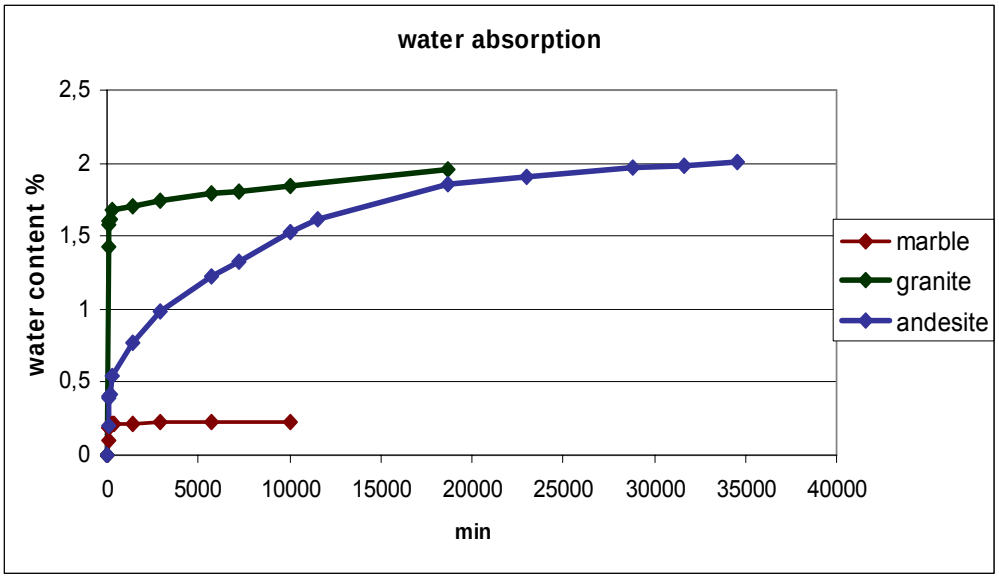

Fig. 5.25. Water absorption curves of the Macael marble, Silvestre Vilachán granite and Szob andesite.

Water desorption

As drying incorporates several different processes (vapour flow, liquid flow, vapour-liquid phase changes etc.) it is a lot harder to interpret the results of the drying curves. In general the first part of the curve describes the evaporation process from the surface of the stone, when the capillary transport is fast enough to provide liquid water on the surface for the continuous evaporation; and the second part is controlled by the water transport velocity within the stone both in liquid and vapour phase.

An example of the water desorption curves (saturation as a function of time in minutes) of the three materials are presented in fig.5.26. As it can be seen all the three curves start with a steep phase, which is the evaporation of the water from the surface, but the length of these phases and the relative water amounts lost are very different for the different materials.

Within 20 minutes the Macael marble loses 50% of its water content only by the evaporation process. While the 20 minutes saturation of the Szob andesite and the Silvestre Vilachán granite is still about 90-95%. This first phase finishes at about 90 minutes for the Macael marble, by which time its saturation is about 40%. The second drying phase of the marble is a lot slower, within approximately one week it reaches a constant value with a saturation of 20-25%.

The Silvestre Vilachán granite after the evaporation of the water from its surface still keeps a pretty fast drying rate: within one day it loses 80% of its water content, which proves the very good connectivity of its porous network again. After this point there is an abrupt change in its drying rate: in one week it arrives to constant 10-15% saturation.

The first evaporation phase of the Szob andesite lasts approximately 30 minutes and results in a saturation of approximately 95%. After this the drying process continues very slowly and with a more or less constant velocity. After one week the saturation is still about 75%.

This drying velocity rate can be expressed numerically by the moisture content ratio, shown in table 5.3.

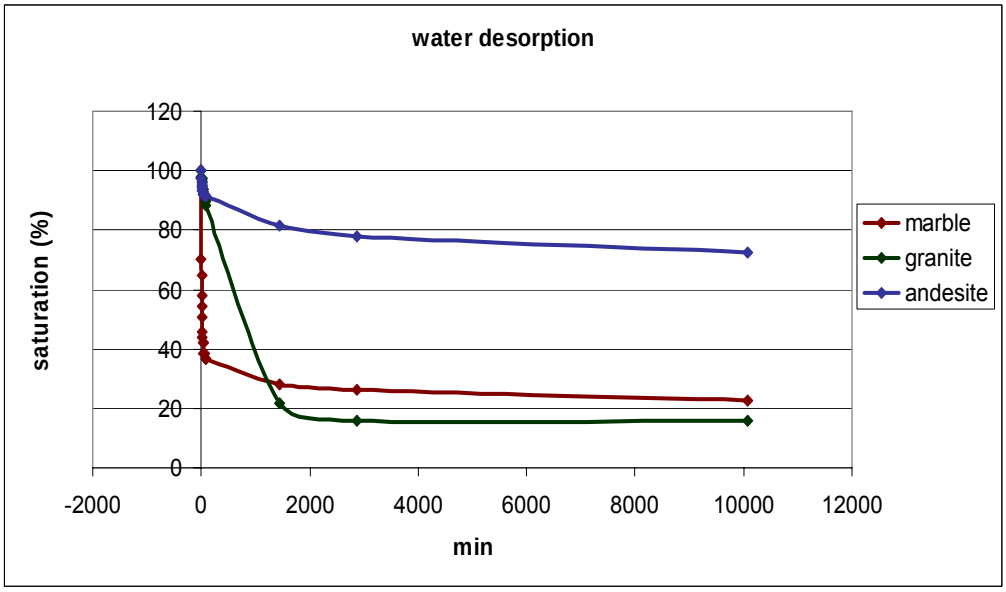

Fig. 5.26. Water desorption curves of the Macael marble, Silvestre Vilachán granite and Szob andesite.

Capillarity uptake

The investigation of the capillarity uptake process provides information about the velocity of the water uptake. The capillary coefficient is calculated from the slope of the first part of the capillarity uptake curve.

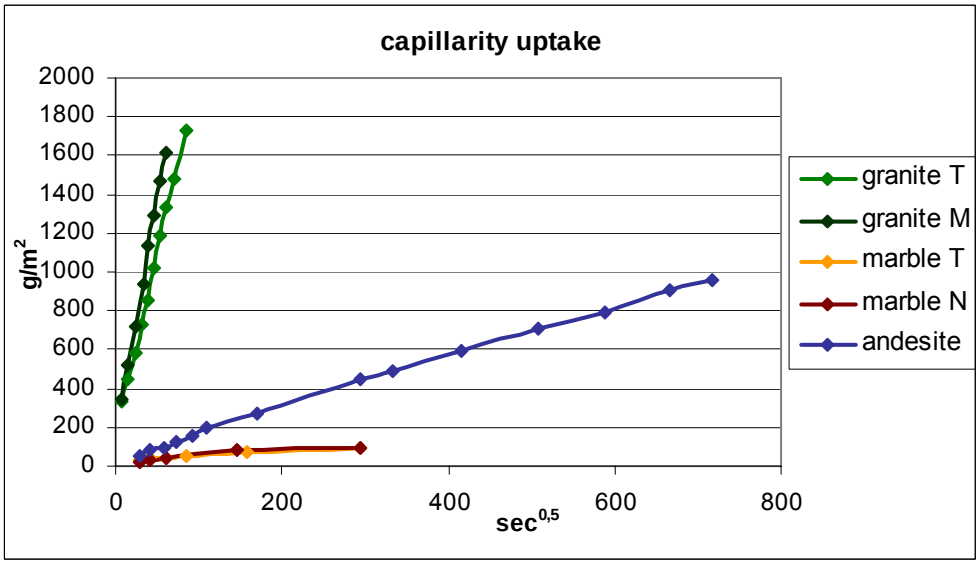

Fig. 5.27. Capillarity uptake curves of the Macael marble, Silvestre Vilachán granite and Szob andesite. In the case of the anisotropic marble and granite the capillarity was measure in two directions (T and M/N).

The lowest values belongs to the Macael marble (average: 0,30±0,03 in the T and 0,33±0,1 in the M direction), which suggests that the capillary pores of the marble are either too few or not well connected. The values in the two investigated directions are very similar, meaning that the existing capillary pores do not have any special orientation. The second lowest value is that of the Szob andesite (1,4±0,2), which, similarly to the water absorption, may be due to the high tortuosity of the pores or their low connectivity. Finally the Silvestre Vilachán granite shows a fast and effective capillarity uptake, its coefficients being an order of magnitude larger that that of the andesite. In this case the difference of the coefficient in the two different directions (18±0,7 and 22±1,2 in the T and M/N directions, respectively) shows the orientation of the fractographic network of this stone; in the M direction the capillarity pores are better connected.

Water vapour permeability

The water vapour permeability is another property that may give us information about the structure of the void space of solid materials (especially of the connectivity) and may be especially important in the case of building materials.The coefficients of permeability at 20°C are shown in table 5.3, in the case of the granite and the marble in two directions (T and M/N). The highest is the permeability in the Vilachán granite showing again that this material has the most well connected void space out of the three; and that its fissure network is mostly parallel to the T direction, as the permeability in the M/N direction is higher, although the differences are not too significant. The second highest values belong to the Szob andesite although the large standard deviation does not allow withdrawing further conclusions from this observation. Finally, the lowest is the permeability of the Macael marble, which does not show significant anisotropy in this property, as the difference between the T and M/N directions is within the range of the standard deviation.

Swelling

The swelling was also investigated following the RILEM 1980 standard, but none of the three stones shows swelling properties.

Water permeability

The liquid water permeability values were measured in two directions for the Macael marble and the Vilachán granite and in one direction for the Szob andesite. The value are presented in table 5.3. The measurement was only possible in the case of the Vilachán granite. The water permeability of the marble (in both directions) and the andesite are so low that they are under the detection limit of the instrument, which is 0,001mD. The granite gave a relatively high value (1,01 mD) in the M direction, parallel to its fracture network, where the connectivity of the pores is the highest; while perpendicular to it the measured value is more than an order of magnitude lower, around 0,06mD.

Table 5.3

	Macael marble		Szob andesite		Silvestre Vilachán granite		Standard
	average	st.dev.	average	st.dev.	average	st.dev.	
Apparent density by water (g/cm^3)	2,70	0,002	2,56	0,004	2,53	0,002	EN 1936
He-density (g/cm^3)	2,71	0,0005	2,71	0,0004	2,63	0,0005	-
Total porosity (%)	0,42	0,07	5,4	0,2	4,88	0,07	-
Open porosity (%)	0,36	0,08	4,6	0,2	4,42	0,05	EN 1936
Water absorption coefficient (%)	0,10	0,01	0,95	0,08	1,59	0,04	EN-13755
Saturation coefficient (%)	1	-	0,46	-	0,91	-	-
Moisture content ratio (%)	0,08	-	0,8	-	0,4	-	-
Water vapour permeability in T direction ($g/m^2 24h$)	59,2	15,4	63,0	30,6	66,9	13,4	NORMAL 21/85
Water vapour permeability in M/N direction ($g/m^2 24h$)	47,6	11,4			87,8	8,4	
Water permeability in T direction (mD)	<0,001	-	<0,001	-	0,06	-	-
Water permeability in M/N direction (mD)	<0,001	-			1,0113	-	
Capillarity in T direction ($g/m^2 s^{0,5}$)	0,20	0,02	1,41	0,20	18,03	0,70	
Capillarity in M/N direction ($g/m^2 s^{0,5}$)	0,13	0,04			22,00	1,20	EN-1925

Table 5.3 The density and hydraulic property values of the Macael marble, Szob andesite and Silvestre Vilachán granite.

5.2.4. Surface properties

Colour

The colorimetric parameters were measured according to the CIE Lab system. The values are shown in table 5.4. They will be important for comparison with the values after the different ageing tests.

Table 5.4

	L*		a*		b*		c*		h	
	avg.	**st.dev.**	**avg.**	**st.dev.**	**avg.**	**st.dev.**	**avg.**	**st.dev.**	**avg.**	**st.dev.**
Macael marble	77,8	0,1	-2,4	0,2	-1,1	0,1	2,7	0,1	205	4
Szob andesite	48,3	0,6	-3,8	0,1	2,8	0,1	4,9	0,1	321	2
Vilachán granite	74,8	0,8	-1,1	0,1	5,5	0,3	5,7	0,3	301	10

Table 5.4. Colorimetric parameters of the Macael marble, Szob andesite and Silvestre Vilachán granite.

Surface roughness

The surface roughness properties are summarized in the table 5.5.

The first thing that requires some consideration is the very high standard deviation experienced in all the measured parameters. The deviations, especially in the case of the Sm values and in all the parameters of the Silvestre Vilachán granite, are in the order of magnitude of the measured value. This probably is due to the fact that the contact type profilometers, such as the one used for this measurement, are more suitable for polished surfaces. In the case of the cut surfaces of the samples of the investigation, the irregularities created by the cutting disk give a very high background noise to the measurement, which may be responsible for the observed standard deviations.

As the values are not intended to be used for an absolute characterization but for the comparison of the surface properties of the samples before and after the ageing tests, the measurement can be useful even with these high standard deviations.

What can be concluded already from the measurements is that the parameters that describe the irregularity of the surface in more general terms, such as the Ra, Rq and Ry, are far the highest for the Silvestre Vilachán granite, and are lower and similar for the other two stones. This is due to the high fissure density on the surface of the granite, which can be clearly detected by this method. The very low porosity of the marble and the small pore size of the andesite provide a fairly smooth surface.

Also the height of the peaks and the depth of the valleys are significantly higher for the granite, and in all the cases the depth of the valleys detects higher values than the peaks. On the other hand the skewness is negative for all the three stones, pointing out the dominant

role of the peaks in the profiles. The kurtosis and the mean spacing values are of similar magnitude and of very high standard deviation in all cases, which suggests that these values may not be suitable for the characterization of these materials under these circumstances.

Table 5.5

	Ra (μm)		**Rq** (μm)		**Sk**		**Ku**	
	average	**st.dev.**	**average**	**st.dev.**	**average**	**st.dev.**	**average**	**st.dev.**
Vilachán granite	15,26	8,29	25,50	14,46	-3,00	0,54	14,00	4,35
Szob andesite	3,64	0,21	5,05	0,36	-1,95	0,42	9,47	3,25
Macael marble	2,68	0,29	3,84	0,61	-2,18	0,87	13,33	8,43
	Rp (μm)		**Rv** (μm)		**Ry** (μm)		**Sm** (mm)	
	average	**st.dev.**	**average**	**st.dev.**	**average**	**st.dev.**	**average**	**st.dev.**
Vilachán granite	25,95	15,47	151,27	79,67	177,22	91,86	4,34	3,00
Szob andesite	8,28	1,19	33,60	7,57	41,88	7,49	1,04	0,60
Macael marble	6,62	0,62	29,90	10,72	36,52	11,02	1,90	1,70

Table 5.5. Surface roughness parameters of the Macael marble, Szob andesite and Silvestre Vilachán granite

5.2.5. Thermal properties

Two important thermal properties were measured in this research: the linear thermal expansion and the residual thermal deformation. Both of them in two directions (T and M/N) for the Macael marble and Vilachán granite and one direction for the Szob andesite.

On figure 5.28, the deformation (mm/m) of each stone is presented as a function temperature (°C). The coefficient of thermal expansion (CTE [K^{-1}]) is defined by the gradient of the slope of the first curve of heating and the residual thermal deformation (ε [mm/m]) from the difference between the first point and the last point of the curves. The values can be found in table 5.6.

Both from the curves and the numerical values, we can observe that the highest thermal dilatation belongs to the Macael marble. There is a very pronounced anisotropy in the thermal properties of this stone, the CTE being more than the double in the T direction than in the M/N direction. This phenomenon is due to the anisotropic thermal expansion of the calcite and proves once again the orientation of this mineral in the marble. Some residual strain can also be observed but these values are similar and quite low in both directions.

a)

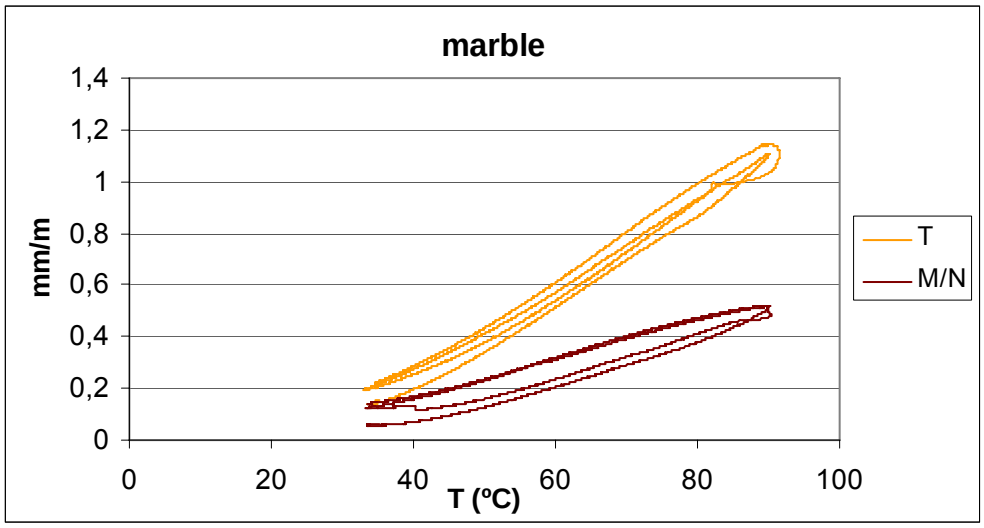

b)

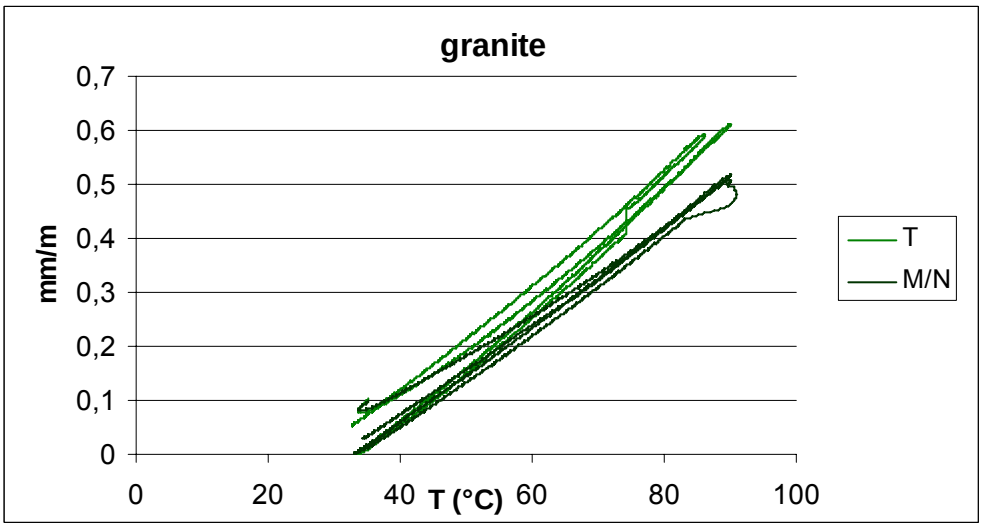

c)

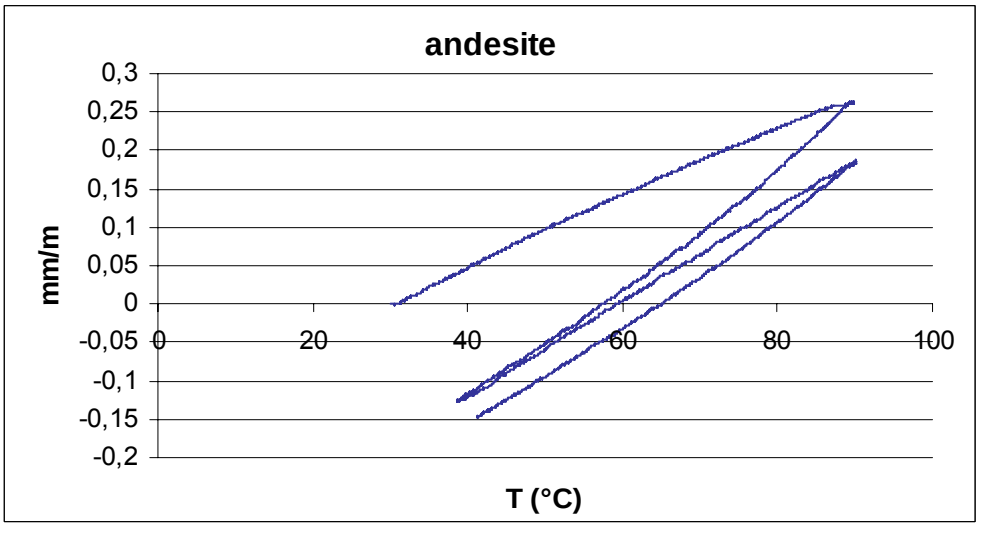

Fig. 5.28 The thermal expansion curves of the Macael marble (a), Vilachán granite (b) and Szob andesite (c)

The CTE of the Vilachán granite is similar to the lower value of the Macael marble in both directions. This stone also shows a slight thermal anisotropy – both the CTE and the ε values

are somewhat higher in the T direction – but the differences are not very significant. The residual deformation is even lower in this case than that of the marble.

Table 5.6

		CTE (10^{-06} K^{-1})	ε (mm/m)
Macael marble	T	17,5	0,056
	M/N	8,17	0,067
Vilachán granite	T	9,80	0,052
	M/N	7,84	0,027
Szob andesite	1st cycle	4,51	-0,126
	2nd cycle		-0,022

Table 5.6 The thermal expansion coefficient and the residual thermal deformation values.

The Szob andesite has the lowest thermal expansion value of all the stones; it can be considered thermally stable. Nevertheless, a very curious phenomenon was observed: the andesite shows negative residual deformation, which would mean that, the stone contracts under heating. The "contraction" is especially strong during the first cycle of heating but continues even in the second one. Very few solids are known to behave in this way and none of the rock forming minerals of this stone. The most probable explanation is that due to the very slow drying kinetics, the samples still contained some water at the moment of beginning the test and by loosing it gradually during the heating, the volume of the samples decreased a little. This on the other hand means that no or very small positive residual strain evolves in this material as an effect of high temperature.

5.3. Summary of the stone properties

Based on all the observations of the petrographical and physical, we can summarize the followings:

- In the case of the Macael marble, the mineralogical composition predicts the susceptibility of the stone in front of weathering. The calcite is easily soluble by acids and the presence of pyrite in the material further emphasizes the probability of chemical degradation. The anisotropic thermal expansion of the calcite minerals favours the thermal degradation also. The open porosity of the stone is very low. It consists of small fractures connected to the grain boundaries of calcite. The very low water absorption and capillarity uptake suggests a good durability in front of weathering processes connected to water. Due to the textural orientation its properties show a slight anisotropy.

- The Silvestre Vilachán granite is slightly susceptible chemically because of the already present alteration of the biotite grains to chlorite and of the feldspars. Of the three stones it has the second highest open porosity, but its water absorption and capillarity uptake is far the highest due to the high connectivity of its porous network. Its void space mostly consists of two-dimensional cracks of low tortuosity, which belong to two subgroups: macro-fissures mostly situated in an inter- or transgranular position connected to quartz and feldspar grains; and the micro-voids (both cracks and pores) which are intragranular in the feldspar grains. The network of the macro-fissures is orientated (parallel to the T direction), which gives a high anisotropy to the mechanical and hydraulic properties. The mechanical resistance of the stone is lower than the others because of the high open porosity and large void sizes. Thermally the stone does not show high susceptibility and the anisotropy is also less pronounced. Its surface roughness is far the highest of the three stones because of the high fissure density on the surface.

- The Szob andesite has unfavourable mineralogical composition due to the high amount of ferromagnesian minerals and the already high level of alteration. This makes it susceptible to chemical processes. On the other hand, although it has the highest porosity of the three stones, the very bad connectivity of its porous network and the very small void sizes impedes the water movement in the material. This was shown by the low water absorption, water permeability and the extremely slow capillarity uptake values. Its void space mostly consists of pores of dimensions smaller than 0,1 μm, which are situated either in the fine grained matrix or within the phenoclasts in an intracrystalline position due to weathering. Thanks to the small void sizes its mechanical resistance is not weakened by the high porosity, it has the highest Vp values of the three stones. Thermally the andesite can be considered stable.

6. Ageing tests

6. Ageing tests

For the experimental testing of the performance of materials in front of different weathering agents, artificial ageing under controlled laboratory conditions were used. The so-called ageing tests are relatively simple standardized or non-standardized procedures that aim at the acceleration of natural weathering by exposing the samples to fast cycling of extremely varying conditions.

In this thesis, the testing of six deteriorating agents was carried out on the three stone types. The agents are: the salt crystallization, the thermal cycles, the effects of freeze-thaw in pure water and in the presence of soluble salts, the salt mist and the action of SO_2 in the presence of humidity.

All of the selected deterioration types are common and serious weathering processes, which are present at all or some of the monuments, the stone types of which are investigated in this research. We aimed at the testing of both bulk and superficial processes by the aid of both standardized and non-standardized methods.

In chapter 6.1 a literature survey and the theoretical background for each of the ageing tests carried out in this research can be found.

The results of the ageing tests are discussed in chapters 6.2-6.6. Additional data about the evolution of the hydraulic and pore space properties during the tests are presented in appendix 2 – 3.

6.1 Theoretical background – State of the art

6.1.1 Salt weathering

It is a generally accepted fact that salt crystallization is the most damaging weathering agent affecting building materials and one of the primary agents in the loss of our architectural heritage (Amoroso and Fassina, 1983; Winkler, 1996). Therefore, the research concerning this topic was started very early – the first salt crystallization test to evaluate the durability of construction materials was carried out in 1828 (Rodriguez-Navarro and Doehne, 1999) - and till today there is a very intensive investigation. An extensive and diverse literature can be found on the topic, which was summarized in some excellent books and review papers, like that of Pühringer (1983), Grossi and Esbert (1994), Goudie and Viles (1997), Rodriguez-Navarro and Doehne (1999), Charola (2000), Doehne (2002) etc.

The research mainly deals with the following topics:

- types and sources of salts
- mechanisms of salt crystallization
- mechanisms of stone deterioration
- material properties determining the damage
- conservation and prevention methods

All the above mentioned issues are based on or connected to case studies concerning historical and modern constructions or laboratory experiments.

The main reasons for the soluble salts being such a serious weathering agent are that (i) they are present in almost all the environments, in desert, urban, coastal and polar regions (Goudie and Viles, 1997; Smith et al., 2005); (ii) that the damaging processes occur due to changes of the relative humidity and temperature within ranges common in many environments (Pühringer, 1983); and that (iii) the forces that are induced during these processes can easily overcome the tensile strength of the average construction materials (stone, brick, concrete etc) (Tsui et al., 2003).

The most frequent salts are the sulfates, chlorides, carbonates and nitrates of different cations, mainly of Na^+, K^+, Mg^{2+}, Ca^{2+} and NH^+, of which the Na_2SO_4 (in different phases), the $CaSO_4$ and the NaCl are considered the most damaging and the most common. But other less frequent ones, such as alums, nitrites, oxalates etc, must be taken into account, as well, because all the water soluble salts are able to cause damage (Arnold and Kueng, 1985). In real situations there are always more than one salt present (Cardell et al 2008,), which may even have synergetic effect on each other. This means that we have to take into consideration a complex system, the processes of which are hard to predict (Arnold, 1981; Robinson and Williams, 2000).

The main sources of the salts are the ground water, the sea water, the atmosphere, de-icing treatments and the building materials themselves (Cardell et al. 2003b; Vallet et al. 2006). The most common way for the salts to get into the stone material is by capillary uptake from the ground or by wet or dry deposition on their surface, typically by sea-spray (Chabas and Jeannette 2001). These two mechanisms may act at the same time (Chabas and Jeannette, 2001; Lubelli et al., 2004), although the effect of the marine spray is evidently limited to areas in the vicinity of coastlines, while the uptake from the groundwater is a more general process. According to Silva et al. (2007) marine influence in the composition of bulk deposition of aerosols on buildings is important until a distance of 20km from the coastline (at least in the examined area); and there it was found to accelerate the weathering by a factor of 1,59 (Mottershead et al. 2003).

Marine aerosol is one of the major particulate types in the atmosphere; its quantity is about 10^9 and 10^{10} t/y (Eriksson, 1960). It is formed by small seawater drops that originate from the bursting of bubbles, mostly in the area of wave whitecaps (Blanchard and Woodcock, 1957). Thus, the original composition of the drops is equal to that of the seawater, more than 85% of which is sodium chloride (Zezza and Macri, 1995). Depending on its size and the relative

humidity of the air, the droplet will start to evaporate and at the moment of deposition it may be in the form of a drop of sea water, a drop of saline solution more concentrated than sea water or a solid salt particle (Silva et al., 2003).

The main ions originating from the marine mist are the Na^{+}, Mg^{2+} and the S^{4-} and Cl^{-} (Chan et al., 2000; Stefanis et al., 2009) but not exclusively; and usually they act together with other polluting agents, such as SO_4^{2-}, NO_3^{1-} etc (Torfs and Van Grieken, 1997). The typical weathering form associated with the marine spray action is the salt disintegration, an extreme form of which is the alveolization (Moropoulou et al., 1995; Cardell et al. 2003a; Silva et al., 2003). The damage occurs by wet and dry cycles (changes in RH), which will cause the repeated crystallization of the salts. The factors determining its degree are the geomorphological and environmental conditions, the distance from the sea and the height above sea level (Zezza and Macri, 1995; Birginie, 2000; Mottershead et al., 2003).

Under continental conditions – if we exclude the atmospheric pollutants causing gypsum formation – the most damaging salt without doubt is the sodium sulphate (Arnold, 1975; Charola and Weber, 1992; Rodriguez-Navarro et al., 2000; Tsui et al., 2003).

At room temperature the Na_2SO_4-H_2O system has two stabile phases: the thenardite, which is the anhydrous phase (Na_2SO_4) and the mirabilite, which contains 10 water molecules in its crystalline structure ($Na_2SO_4 \bullet 10H_2O$). Besides, a metastable phase, a heptahydrate ($Na_2SO_4 \bullet 7H_2O$) is also known, but it has not been identified under natural conditions (Flatt, 2002). The thenardite precipitates directly from solution above 32,4°C, while mirabilite under this temperature. The two phases have a strong dependence of relative humidity also; mirabilite dehydrates to thenardite under 75% RH (Ruiz-Agudo et al., 2007).

The high damaging capacity of these salts has been subject to scientific discussion for a long time. The original idea was that the hydration of thenardite to mirabilite happens in solid phase and includes a significant volume increase, so thus exerting high pressure ("hydration pressure") on the wall of the pore where the process takes place (Mortensen, 1933; Winkler and Wilhelm, 1970; Goudie, 1977). Later on however, independently, more researchers found this statement to be untrue, and it was proved that the thenardite to mirabilite transformation happens in solution via the dissolution of thenardite and the precipitation of mirabilite (Charola and Weber, 1992; Rodriguez-Navarro and Doehne, 1999). Nevertheless, the phase transitions play an important part in the damaging process. Charola and Weber (1992) stated that the increased deterioration can only be attributed to the multiple crystallizations taking place during the dehydration of the hydrated salt. However, other researchers, like Chaterji and Jensen (1989), Tsui et al. (2003) or Steiger and Asmussen (2008) affirm the opposite process, the hydration of the dehydrated phase, as the most damaging step. According to them, below 32°C if a material contains thenardite and becomes into contact with water, the thenardite will dissolve resulting in solutions highly super-saturated to mirabilite, therefore mirabilite will precipitate. This situation is repeated several times during a standard salt crystallization test, when the wetting phase starts. The tensile stresses due to mirabilite

crystallization are larger than the tensile strength of most stone and concrete, which means that mirabilite precipitation alone is sufficient to cause damage during rewetting.

Additionally, the outstandingly fast crystallization and phase transformation kinetics of sodium sulphate and the fact that it prefers to crystallize in the solution (and not on the air solution interface as the halite), preferably forming sub-fluorescence, were also found to be reasons for the higher damage (Rodriguez-Navarro and Doehne, 1999; Benavente et al., 2004; Cardell et al., 2008).

Based on the above literature survey, the standardized salt mist test (EN 14147:2004) with NaCl and the also standardized salt crystallization test (EN 12370:1999) with sodium sulphate were decided to be carried out in this investigation.

Apart from the nature and the origin of the salts, the mechanisms of the salt's entering into the stone, of the crystallization and of the final damage are basically similar.

Lewin (1982) was one of the first authors to propose an entire model of the salt weathering process, which model is still valid (Cardell et al., 2008). It considers that the salt solution enters into the solid and circulates inside by capillarity. The salt precipitation will take place wherever evaporation occurs. The site of this is determined by the dynamic balance between the rate of evaporation and the rate of solution supply to that place. The evaporation rate is a function of temperature and relative humidity, as well as of the specific permeability of the material, which is a function of pore size (Cardell et al., 2003a). On the other hand, the rate of solution supply depends on the capillarity flux, determined by the surface tension, the contact angle between the solution and the solid, the viscosity of the solution, the permeability of the solid, the pore radii, and the path length from the source to the site of evaporation (Scherer 2004). If the rate of the supply is equal or higher than the rate of evaporation, the salt crystallization will take place on the surface of the material causing an aesthetically negative but otherwise harmless efflorescence. In the opposite case, the salts will precipitate inside the porous network of the material (subflorescence) causing serious mechanical damage.

From the above model, we can conclude that the conditions of salt precipitation depend on the (i) environmental conditions (T, RH); (ii) on the material properties (pore size distribution, permeability, contact angle); and (iii) on the properties of the solution (viscosity, surface tension, density, concentration, vapour pressure) (Lewin, 1982; Ruedrich and Siegesmund, 2006; Cardell et al., 2008).

Once the salt entered to the porous material and under the adequate conditions subflorescence was formed, mechanical damage will take place. During the several decades of investigation, many theories explaining this damage were proposed. Some of them, as it was explained above about the "hydration pressure" theory, proved to be false; others are still under discussion. These days the most generally accepted theories are (i) the crystallization pressure; (ii) the differential thermal expansion among the salt and the rock forming minerals (Ruedrich and Siegesmund 2006); (iii) the osmotic (or hydraulic) pressure identically to the

frost damage (McMahon et al., 1992); and (iv) the chemical weathering due of the dissolution of some minerals (mostly calcite) because of the higher ionic strength of the salt solution compared to pure water (Cardell et al., 2003). All of these mechanisms may to some degree contribute to the overall damage (Ruiz-Agudo et al., 2007). However, without doubt the first one, the crystallization pressure is the most important of them all (Scherer, 1999, 2004; Flatt, 2002; Chatterji, 2005; Steiger 2005a, b; Coussy, 2006).

There are several models concerning the mechanism of the building up of crystallization pressure, also.

One of the first models was that of Correns (1949), which calculated the crystallization pressure as a function of concentration, meaning the degree of super-saturation (eq.25)

$$P = \frac{RT}{V_s} \ln \frac{C}{C_s} \tag{25}$$

where, P is the crystallization pressure, R is the gas constant; T is the absolute temperature, V_s is the molar volume of solid and C/C_s is the degree of supersaturation (C is the existing concentration and C_s is the saturation concentration). Later on, more scientists used the Correns equation as a basis for their calculations but substituting the concentration values with activities (Neugebauer, 1973) or with ion activity products (Xie and Beaudoin, 1992).

The other classical model is that of Everett (1961) thought originally for the water freezing process, but later applied to salt crystallization (Wellmann and Wilson 1965; Fitzner and Snethlage, 1982), which is based on the properties of curved interfaces between the solution and the crystal, meaning the size and shape of the crystal (eq 26).

$$P = \gamma_{cl} \frac{dA}{dV} \tag{26}$$

where, γ_{cl} is the interfacial free energy, A and V are the surface and the volume of the crystal. In theoretical calculations concerning porous materials the simplest model of the pores is the spherical geometry, which gives the following form of the Everett equation (27):

$$P = 2\gamma_{cl}\left(\frac{1}{r_1} - \frac{1}{r_2}\right) \tag{27}$$

where, r_1 is the radius of the larger pore, where the crystallization takes place and r_2 is the radius of an adjacent smaller pore. For the crystal it is thermodynamically more favourable to grow in the large pore so the crystallization will start there. Once the crystal fills that pore completely but there is still solution present (supplied by the surrounding smaller voids) the crystal will have to grow towards the smaller neighbors and will have to change its curvature (Steiger, 2005b). This is the moment when the highest pressures evolve and when the material rupture usually happens.

The equation 27 has been especially popular in stone degradation research because it seems to give the possibility to calculate the pressure that will appear in a stone material based on its pore size distribution; and by comparing the calculated stress to the tensile strength of the material, its susceptibility can be assessed directly, as it was done by more than one authors (Rossi-Manaresi and Tucci, 1991; La Iglesia et al., 1997; Theoulakis and Moropoulou, 1997; Moropoulou et al. 2002b). However, the supposition of spherical pores only is an oversimplification, especially, considering that according to the original equation of Everett (26), the crystal shape has dominant effect in the process (Benavente et al., 2007).

However, the above models seem to be the correct way to the understanding of the crystallization pressure, as the two classical equations of Correns and of Everett follow identical approaches only expressed by different properties (only that using the concentration values to express the degree of super-saturation is not correct in the Correns' model, it is better to use the activity or activity product (Steiger, 2005a)), as it was pointed out by Scherer (1999), Flatt (2002) or Steiger (2005a, b). The later author also derived an equation that includes all the before used properties.

These theoretical calculations once again drew attention to the importance of the material properties in the degradation process, mostly to the pore size distribution and the pore shape. These parameters were found to be fundamental by experimental results also (Ordoñez et al., 1997; Nicholson, 2001; Benavente et al., 2004; Ruiz-Agudo et al., 2006 etc). But these are not the only parameters that must be taken into account when assessing the susceptibility of a stone material to salt damage. Already Arnold and Kueng (1985) pointed out that "… substrate properties which must strongly affect crystallization are the porosity and its structure (permeability), the surface activity and wet-ability (both on the surface of the substrate and on the pore surfaces)". Besides, the tensile strength (Dessandier, 2000; Tsui et al., 2003); the capillary coefficient (Hammecker, 1995); the saturation coefficient (Goudie, 1999); the water absorption (Dessandier 2000); the critical water content (Ruedrich and Siegesmund, 2006); the connectivity (Nicholson, 2001); and the fluid transport properties in general (Birginie, 2000) are basic aspects to consider.

The properties to monitor the changes and deterioration taking place in the material during the damage have also been discussed. Parameters generally found useful for this purpose are the pore size distribution (usually by Hg porosimetry) (Ordoñez et al., 1997; Přikrly et al., 2003); the effective porosity (Yavuz and Topal 2007); the water absorption (Dessandier 2000); the fracture density (Nicholson, 2001, 2002; Cueto et al. 2009) and the ultrasound velocity (Nicholson, 2001, 2002; Sousa et al., 2005; Ceryan et al., 2007; Alonso et al., 2008), the compressive strength (Dessandier 2000; Benavente et al., 2006) and the classical but sometimes discussed weight loss (Zedef et al., 2007 etc.).

6.1.2 Frost weathering

Frost damage – due to alternating freeze and thaw events - is one of the major causes of building material decay. Its importance evidently depends on the climate but in the majority of European countries it is an important issue. In Central Europe the number of freeze-taw cycles can reach 30 per year (Ruedrich and Siegesmund, 2006) and although with the global climate change this number may decrease in some parts of the Continent, in the northern regions it will affect archaeological sites that have been preserved in the permafrost so far (Grossi et al., 2007b).

The importance of the effects of freezing was soon discovered and the scientific research started as early as the beginning of the 19th century. Then, especially after the fundamental work of Hirschwald (1908), it has been continuing with never ceasing significance till today.

During all these decades of investigation several aspects of the ice formation and of the damaging mechanisms have been discovered, although there are still questionable points.

Experimental results showed that the ice forming in the voids of a porous body has the same physical characteristics as ordinary ice, the so called Ih type with a hexagonal crystal lattice. The melting point is also the same, 0°C, but inside the pores freezing does not always occur at this temperature. The freezing point – among other parameters – is determined by the pore size as, from thermodynamic considerations, water and ice can be in equilibrium depending on the temperature and the pressure with a given curvature of the interface between the two, as it is shown by equation (28) (Pigeon et al., 2003)

$$R_{eq} = \frac{2 \cdot \gamma_{ls}}{\int_{T_0}^{T} \frac{\Delta s^{ls}}{v^{l}}} \qquad (28)$$

Where:
R_{eq}: radius of curvature of the interface between ice and water on the equilibrium T
γ_{ls}: superficial tension between solid and liquid
Δs^{ls}: entropy of ice formation
v^{l}: molar volume of liquid water
T_0: equilibrium temperature for the flat interface (0°C in this case).

This means that the ice will only be able to penetrate a given void size when the temperature is lower than the equilibrium temperature. Consequently, the water in a porous body will crystallize progressively with the decreasing temperature starting in the largest pores. The degree of freezing point depression can be derived from equation (28) or from the Kelvin equation, which is based on the same principles (Camuffo, 1996).

The rate of cooling, the duration of the freezing period and the contact angle between the water and the solid (Scherer, 1999) will also have an influence on the crystallization process.

Once the ice is formed or has started to form inside the porous material, the next question is the way the damage is caused. There are also many theories concerning this issue, which probably all take their part of the real process.

The first and most evident cause of damaging – already considered by Hirschwald (1908) – is the 9 per cent volume change suffered by the water as it solidifies. If the void space is completely (or at least to 91%) filled with water, this volume expansion will exert pressure on the walls of the voids. The explanation seems straightforward enough, but the fact that building materials hardly ever reach such degree of saturation in reality, requires other solutions.

A second theory, strongly connected to the first one, is that when the expansion in some of the pores takes place it causes the drainage of the still liquid water towards other pores inducing a hydraulic pressure in the material (Powers, 1945) For saturated materials the generation of hydraulic pressures is commonly considered to be the most important cause of frost deterioration (Pigeon et al., 2003).

A third theory is that of the frost heave, which was introduced to explain the swelling of frozen soil. As it was explained by Torraca (1982), this model is based on the notion that ice crystals, or ice lenses, grow in relatively large voids (fractures or large pores) but are unable to develop in the small pores, unless under pressure. Water present in the small pores is fed to the growing crystals by diffusion instead of freezing on the spot. If water is still available in the small pores when all the large spaces are occupied, a pressure is developed which should allow ice crystals to grow also in the small pores. It is interesting to note that the frost heave pressure does not depend upon the fact that water increases in volume when it freeze.

The actual formation of the ice crystals and the generation of crystallization pressure based on thermodynamic approach have also been discussed by many authors (Everett, 1961; Scherer, 1999; Coussy, 2005; Coussy and Monteiro, 2007, 2008 etc.) and they are fundamentally identical to the crystallization of salts from solutions (discussed more in details there).

Other works focusing on the materials rather than the ice crystals revealed some basic material properties influencing the frost degradation.

The first and definitely most important issue is the degree of saturation. This is not a material property but a consequence of several intrinsic and extrinsic characteristics. The intrinsic properties determining the saturation are the effective porosity, the permeability, and capillarity uptake etc., thus the void space structure. Materials with high saturation degrees are a lot more susceptible to frost weathering (Hirschwald, 1908; Chen et al., 2004; Ingham, 2005; Takarli et al., 2008 etc.)

As a consequence of the above point and considering the mechanisms of ice formation, the pore size and the pore size distribution are also fundamental parameters. The experimental observations proved that pore sizes in the range of 0,1 – 1 μm give rise to the highest stresses in stone materials during freezing (Torraca 1982). Other researches pointed out the <2 μm

(D'Have and Motteu 1968) or the 1-5 μm range (Bourgès, 2006). The joint set of these intervals are the pores that are small enough to become quickly saturated under natural conditions and that actively participate in the ice formation, either as pores where ice crystals form or as pores that provide the water supply to ice formation in neighbouring larger pores.

Another general observation is that ice damage usually concentrates at areas with pre-existing flaws, such as discontinuities or abrupt changes in porosity or other textural features (Ruiz de Argandoña et al., 1999; Nicholson and Nicholson, 2000; Ruedrich and Siegesmund, 2007).

The compressive and/or tensile strength was also found to be an important property in frost resistance (Matsuoka, 1990; Benavente et al., 2004) as those will determine the capacity of the stone to resist the evolving stresses.

These are also the properties that are usually monitored in order to evaluate or trace the effects of the damage. Besides, the weight loss, the P-wave velocity, the dynamic modulus of elasticity, the fracture density, the length change of the samples, the capillarity and drying have been observed, more or less effectively.

Based on these observations many authors presumed to suggest index properties for the evaluation of stone materials in terms of frost resistance.

The first of them was Hirschwald's (1908) well famous saturation coefficient based on the ratio of the 24 hour water absorption to the total water absorption. If this value exceeded 0,8, he considered the material as not resistant to frost damage.

Fagerlund (1975) developed the critical degree of saturation concept for concretes, which later was generalized to other materials. This implies that a critical degree of saturation exists for a solid such that frost damage will inevitably occur if its saturation is higher than that. This critical degree varies from material to material because it is related to its properties such as pore size distribution, pore connectivity and porosity (Chen et al., 2004).

A former national Belgian standard had an indirect test to assess frost resistance based on Hg-porosimetry. The determined a parameter called d_{10}, which is defined as the mean pore diameter at which the test sample exhibits 10% saturation under an applied force of Hg. They found empirically that if $d_{10} > 2{,}5$ μm the risk of frost damage is negligible (Ingham, 2005).

6.1.3 Frost weathering in the presence of soluble salts

The most common supposition of freezing experiments is that the freezable fluid is pure water. On one hand, this is a simplification of the experimental setup in order to decrease the number of unknown parameters. On the other hand, although in natural conditions the fluids are usually more or less concentrated saline solutions, in the freezing process only the water molecules participate, the forming ice does not incorporate any salt ions in its lattice

(Wessman, 1997). Nevertheless, experimental evidence both from field and laboratory observations proved that the presence of soluble salts during the freezing results in more serious damages than when they are not present (Sun et al., 2002; Pigeon et al., 2003), suggesting that the salts play some kind of synergetic part in the process. This was mostly observed in coastal areas with a high frequency of freeze events or in cold climates (Williams and Robinson, 1991), where the frequent and heavy freezes require the abundant use of de-icing salts.

The most evident signs of this amplified damage in the presence of salts are observed on concrete constructions. The so-called frost salt scaling (FSS) of concrete was first described through laboratory tests in the 1950s (Verbeck and Klieger, 1957). The phenomenon, by definition, consists of a superficial damage caused by freezing a saline solution on the surface of a concrete body by the loss of chips or small flakes (Valenza and Scherer, 2007a). This, being a superficial damage, does not cause the complete breakdown of concrete but opening up the surface it exposes the coarse aggregates, increases the saturation and makes the material more susceptible to other damaging agents (Pigeon, 2003; Valenza and Scherer, 2007a, b). Probably this is the reason why the most extensive research on the effect of frost and salt together can be found in the concrete research and industry field. Several standard methods exist for its testing such as the ASTM C672; the Swedish Standard SS 13 72 44 or the German CDF method (1996). Besides, independent standards for the frost resistance of loose aggregates in the presence of salt (generally of NaCl) also have been developed (NT BUILD 485; Pétursson, 2005). The negative effect of salts during freezing of soils was also described and investigated (Bing et al., 2007; Darrow et al., 2009). And finally, some investigation of the "frost and salt" weathering on natural stone can be found, also.

Goudie (1974) and Williams and Robinson (1981) were among the first ones to conclude that the presence of salts enhance the damage caused by frost on natural stone also. Although McGreevy (1982) presented exactly contrary results, the ongoing research (Hall, 1988; Williams and Robinson, 1991; 2001; Wessmann, 1997; Lindqvist, 2007b) proved that some salts, mostly the halite, have negative effect on frost weathering of stone.

The exact mechanism of the damage is still under discussion due to the fact that the complexity of the system makes it complicated to describe the ongoing processes. The interaction of the three components (water, salt and solid) results in some deviations from the basic laws of thermodynamics, such as the decreased vapour tension or the freezing point depression of a salt solution (Camuffo, 1996).

The freezing temperature of a solution depends on its concentration according to the following equation (eq. 29):

$$\Delta T_f = K_f m \tag{29}$$

where, ΔT_f is the freezing point depression; K_f is the freezing point depression constant (for water K_f=1,86 K/mole); and m is the molality of the solute (Camuffo, 1996). In the case of

NaCl, ΔT_f = -20°C for a 23w% solution (Weast, 1985). This means that highly concentrated solutions will not freeze in the pores of the stone material within natural or the artificial tests' temperature range.

Another specific feature of the freeze-salt damage is the existence of the so-called pessimum concentration. Arnfelt (1943) was the first scientist to demonstrate that at a given concentration of salt solution, the damage will be more intensive than at any other – higher or lower concentrations. This value is about 1-3% by weight for most of the salts (Wessman, 1997). This is why the standard tests require the use of 3% solutions in the case of concrete; and 1% solutions in the case of aggregates.

Probably these very specific properties led to the numerous and often contradictory theories of the damage mechanisms that have been published so far.

Williams and Robinson presented a review on the topic in 1991, in which they collected 10 different theories from former investigations to explain why the salt frost degradation is more damaging than the simple frost weathering, without accepting any of them as a correct and/or complete explanation.

Based on this and further publications (Valenza and Scherer, 2006; Lindqvist et al., 2007) the possible mechanisms taking place during the salt frost damage are the followings.

The internal crystallization of ice and the connected hydraulic pressure act, just like during the frost damage, although due to the lower freezing point they probably have a smaller effect. The fact, that given stones show very different durability to frost damage with or without salts, proves that the mechanisms must be at least partly different. On the other hand, the reduction of the water vapour means that the same material under the same relative humidity can reach higher saturation degree in the presence of a salt solution than with pure water only. As saturation is a basic parameter to determine the damage of frost, this may act as an enhancing factor in the salt and frost damage.

The crystallization of salts is not probable, because it would only happen from highly concentrated solutions, which are usually not present; or together with the crystallization of ice under the eutectic temperature, which is usually not reached.

Another probable explanation for the amplified damage is the osmotic pressure. As during the freezing only the water molecules go into the lattice of the ice, the remaining solution will have higher salt concentration than the surrounding smaller pores where freezing has not taken place yet. This will result in an osmotic pressure because of the solution transport from the sites of lower concentration towards those with higher, additionally to the hydraulic pressure because of the transport of water towards the forming ice.

The chemical interaction between the salt solution and the rock forming minerals cannot be excluded from the reaction either. Besides the fact that the higher ionic strength of the solution increases the solubility of calcite, the reaction of chloride with some of the

components of concrete (mostly the C_3A and C_4AF) has been described in the literature, also (e.g. Yuan et al., 2009). This kind of interactions must be considered in the case of natural stones, as well.

Finally, the last model explaining the frost salt scaling of concrete is the so-called glue spalling model. It was first published by Valenza (2005), later confirmed by others (Çopuroğlu and Schlangen, 2008). The theory is based on an industrial procedure producing a given type of glass surface finish. According to it, if there is a pool of low concentration salt solution on the surface of the concrete and the temperature is deceased gradually, the freezing solution will suffer a contraction that is 5 times higher than the contraction of the concrete. This will cause the breaking of the ice layer into small "islands", and the fractures will propagate into the concrete causing the loss of small flakes of the material. According to the authors this is the only model that completely explains the process of the salt frost damage, at least in the case of concrete.

Based on these theoretical models, the material parameters controlling the degree of the caused damage are on one hand the same as in the case of the simple frost weathering, meaning the saturation and the pore size distribution (Pigeon, 2003); besides, the surface strength of the material (Pigeon, 2003; Valenza and Scherer, 2006; 2007a, b); and the quantity of micro- and nanno-pores (Lindqvist et al., 2007).

6.1.4 Thermal degradation – The effects of heating-cooling cycles

Thermal degradation is an important issue in the building and monumental material field and not only under extreme climate conditions. Even in temperate climates the thermal stresses resulting from temperature changes can be large enough to produce microfractures in and among mineral grains of rocks (Robertson, 1982).

The most important way of temperature transfer is the solar radiation, which heats the outer side of the building elements, while the inner side remains cooler, resulting in significant temperature differences within the material (Gómez Heras, 2005). Rock surface temperatures can reach 60°C depending on the albedo of the surface, the maximum temperature and the thermal conductivity (Winkler, 1997). In cold climates the variation of the wind speed also has a controlling effect on the sub-surface rock temperatures (Hall and André, 2001).

The most important bulk thermal properties are the specific heat capacity (the amount of heat (energy) required to raise the temperature of 1 kg of a substance by 1°K); the thermal conductivity (the rate at which heat is conducted per unit of time through a given area of surface down a temperature gradient of 1°K over a unit of length) and the thermal expansion (the rate of expansion of a natural stone when it is exposed to a defined rise in temperature).

From the thermal degradation point of view the most important of these properties is the thermal dilatation and the residual strain after thermal treatment (Leiss and Weiss, 2000).

Thermal expansion of solids results from the increasing atomic motions as heating adds more kinetic energy to the system and the lattice structure expands. It is measured by the lineal thermal dilatation (see eq. 23 in chapter 4). The residual strain is the length change of the sample due to the thermal treatment after cooling back to the initial temperature as a function of the original length (eq. 24).

The thermal expansion is a specific property of each mineral phase and as such, there are two groups of rocks according to their mineralogical composition, where it can cause serious damage: the polymineralic rocks and the carbonate rocks. In the first case, the different thermal expansion values of the rock forming minerals may generate tensions on the intercrystalline interfaces (Esbert et al., 1997) and drive to breakdown by means of granular disintegration. A higher variety of mineral phases – with possibly different thermal properties – enhances to probability of thermal degradation (Benavente et al., 2008). Different surface temperatures between minerals magnify the thermal expansion differences (Gómez Heras et al., 2006). In the second case, it is the peculiar thermal behaviour of the calcite that causes the problems: calcite is known to expand on heating much more in the direction of its optical axis than perpendicular to it. The grains' shapes change with temperature and as the anisotropy directions of individual grains are oriented randomly the result is a springing apart of contiguous grains, giving rise to a non-zero residual stress state inside the material (Royer-Carfagni, 1999).

The so-called thermal shock, due to high temperature changes, is a well known effect in the stone deterioration field even standardized methods exist for its investigation (EN 14066:2003). It occurs if the thermally-induced stress is of so high magnitude that the material is unable to adjust fast enough to accommodate the required deformation so it fails (Hall, 1999). On the other hand, low but repeatedly occurring temperature changes also can cause material damage through thermal fatigue. In this case the cause of the breakdown is a series of thermally-induced stress events. Because of the spectacular and rather disastrous marble-bowing phenomenon this effect has been increasingly investigated lately. The thermal degradation of marbles – as low porosity carbonate rocks – is especially well studied in the literature, due to the serious deformations experienced both on monuments and on modern constructions (Logan et al. 1993; Winkler, 1996; Royer-Carfagni, 1999; Siegesmund et al., 2000; Leiss and Weiss, 2000; Weiss et al., 2003; Koch and Siegesmund, 2004; Mahmutoğlu, 2006; Yavuz and Topal, 2007; etc). The Macael marble itself was also investigated from this point of view by Rodríguez-Gordillo and Sáez-Pérez (2006).

It was found that a temperature increase of only 20-30°C may cause the partial decohesion of calcite grains (Battaglia et al., 1993) and that repeated heating can lead to permanent damage (Koch and Siegesmund, 2004). The same authors also found that the heating experiment in the presence of moisture leads to an unlimited residual expansion. This later observation proves the importance of the water in the thermal degradation, object of scientific discussion for many years (e.g. Winkler, 1996), although the explanation of the phenomena still remains unclear (Koch and Siegesmund, 2004). The most susceptible stone type is the marble, because of the specific thermal properties of calcite and because of the low porosity, but

granite was also found to suffer micro-cracking due to a cyclic thermal change from -20°C to 20°C due to the differential thermal expansion among the rock forming minerals (Takarli et al., 2008). By research in cold regions it was shown that the effect of the temperature change is independent from absolute temperature, it can cause the same damage on low or on high temperatures (Hall and André, 2001).

Besides the mineralogical composition, other material properties that have influence on the thermal susceptibility of the stones are (i) the colour, because of the afore mentioned insolation heating, (ii) the porosity, as the thermal dilatation may be buffered by pre-existing cracks up to a given level (Leiss and Weiss, 2000), and (iii) the microstructure, especially the shape of grain boundaries (Cantisanit et al., 2009).

6.1.5 Sulphation weathering

Deterioration of historic and modern building stones by different agents originating from atmospheric pollution is maybe the most common and most well-studied of all the weathering forms. The spectacular decay patterns and the obvious increase in the decay rate in the last two centuries called the attention of scientists, architects and users, as well. The development of the industrial activities and the corresponding increase in air pollution accelerated the deterioration of stone by several times, especially in urban environment (Winkler, 1994). The most typical signs the weathering are different types of crusts ("white" and "black" crusts) appearing on the stone surface and so-called washed-out areas with evident loss of material (Camuffo et al., 1983; Moropoulou et al., 1998). The decay in all the cases is a consequence of acidic attack of the stone. These crusts or patinas are usually composed of a framework of gypsum crystals, in which particulate and gaseous inorganic/organic pollutants are deposited and fragments of the stone substrate are embedded (Schiavon et al., 1995). The abundant presence of gypsum ($CaSO_4 \cdot 2H_2O$) very soon brought the attention to the role of the sulphur compounds of the air in the process (Burdick and Barkley, 1939). Already Camerman (1945) described the correlation of the atmospheric sulphur and the gypsum present on the stone surfaces. Since that time, wide and vivid scientific research is aimed at the understanding of the mechanisms of sulphation, the sources of pollutants, the weathering rates and weathering susceptibilities of different building materials, etc. (e.g. Ausset et al., 1996; Moropoulou et al., 1998; Chiriga and Oyama, 1999; Malage-Starzec et al., 2003; Maravelaki-Kalaitzaki, 2005 etc.).

The main source of SO_2 in the atmosphere is the combustion of fossil fuels, coal, oil and gas, which all contain more or less amount of sulphur that oxidizes during the burning (Winkler, 1994). This SO_2 then can be deposited on the surface of materials in the gaseous phase by dry deposition; or it can convert to sulphurous acid (H_2SO_3) in the presence of atmospheric humidity and deposit in the form of acid rain, cloud (Lindberg and Lovett, 1992) or fog water (Del Monte and Rossi, 1997). Field and laboratory studies usually calculate with dry deposition of gases or wet deposition of ions, although most exposed structures experience

both processes (Johnson et al., 1996; Ausset et al., 1996). However, water plays a key role in the reaction, because in the absence of moisture or in low relative humidity conditions SO_2 and calcite, which is the most susceptible mineral phase in this context, do not react (Böke et al., 1999). Besides, humidity determines the rate of dry deposition. Spiker et al. (1992) observed that SO_2 deposition on marble increases exponentially with relative humidity; and even the gypsum crystal growth and morphology is governed by the moisture on the substrate (Zehnder and Arnold, 1989). Moreover, the dry deposition rate will be determined by the specific surface of the stone, which depends on the surface finish, roughness, morphology; the insolation, and the presence of hygroscopic contamination (Spiker et al., 1992; Dolske, 1995).

After the deposition in the gaseous phase, the SO_2 will be dissolved in the liquid film on the surface of the substrate (eq. 30) forming the relatively weak sulphurous acid (eq. 31) which by oxidation converts into strong sulphuric acid (eq. 32) (Böke et al., 1999)

$$H_2O + SO_2\,(g) \leftrightarrow SO_2 \cdot H_2O\,(aq) \tag{30}$$

$$SO_2 \cdot H_2O\,(aq) \leftrightarrow H^+ + HSO^{3-} \tag{31}$$

$$HSO^{3-} + \tfrac{1}{2}\,O_2 \rightarrow SO_4^{2-} + H^+ \tag{32}$$

The oxidation reaction resulting in the formation of sulphuric acid has received a lot of attention lately. It is assisted by atmospheric oxidants, ozone and hydrogen peroxide, and can be catalysed by the presence of several substances (Bai et al., 2006). The two most important of these are the NOx gases and the particulate pollutants.

Nitrogen oxides, which mostly originate from automobile exhaust, can also deposit on the stone surface in the gaseous phase. It has been observed, that in the presence of humidity, NO_2 can promote the oxidation of SO_2 (Johannsson et al., 1988; Grossi and Murray, 1999); for example under laboratory conditions the maximum thickness of gypsum crust on a sandstone decreased according to the gas phases used in the order of: $SO_2 + NO_2 + O_3 > SO_2 + NO_2 > SO_2$ (Bai et al., 2006).

Carbonaceous particles emitted by the incomplete combustion of fossil fuels from diesel-powered vehicles, power plants, domestic heating systems etc. also act as a catalytic support to the sulphation process (Tittarelli et al., 2007). Non-carbonate carbon of anthropogenic origin was found to be the second most important component present in the damage layers (Zappia et al., 1993; Sabbioni, 1995). This particulate matter, besides the C, contains transition and heavy metals, such as Fe, V, Zn and Ni. The particles have a very high specific surface, and thus they may provide efficient sinks for pollutants, especially in urban environment (Simão et al. 2006; McAlister et al., 2008).

Once the oxidation of SO_2 has taken place in the presence of humidity, the forming H_2SO_4 will cause acid-base reactions with the mineral phases of the substrate. Practically all materials used in construction are susceptible to the acidic attack from metals to brick and mortar. The response of each stone type towards sulphation is related to the stability of their constituent mineral phases towards acidic attack (Simão et al., 2006). This is the reason why stones with carbonate content (limestones, marbles, carbonate sandstones, etc) suffer the highest damage. Calcite has the highest solubility in high pH values of all the common rock forming minerals. The presence of acid will cause the dissolution of calcite (eq. 33) and the formation of sulphite hemihydrate (eq. 34) or after the oxidation, of calcium sulphate bihydrate (gypsum) (eq. 35).

$$CaCO_3\,(s) + H^+ \rightarrow Ca^{2+} + HCO^{3-} \quad (33)$$

$$SO_3^{2-} + Ca^{2+} + \tfrac{1}{2}\,H_2O \leftrightarrow CaSO_3 \cdot 0{,}5\,H_2O \quad (34)$$

$$SO_4^{2-} + Ca^{2+} + 2\,H_2O \leftrightarrow CaSO_4 \cdot 2H_2O \quad (35)$$

Under laboratory conditions the sulphite phase was found to be the main product of the reaction (Böke et al., 1999) but in the field usually only gypsum is present (Grossi and Murray, 1999). The gypsum forms a porous crust on the surface of the substrate, which permits the further diffusion of pollutants towards the calcite underneath where new gypsum layers form (Moropoulou et al., 1998; Bugini et al., 2000).

The acidic degradation of carbonate rocks is a well-documented and well-understood process. On the other hand, the same effect on siliceous minerals still remains unclear. The soiling phenomena and the black crust formation have been observed on siliceous rock, as well (Schiavon et al., 1995; Moropoulou et al., 2003; Turkington et al., 2003; Alonso and Martínez, 2003; Prieto et al., 2007 etc.). The general assumption is that these stone types are not affected by acid deposition because silicates are far less soluble at acidic pH than carbonates (Simão et al. 2006); and because the Ca-rich minerals necessary for the gypsum formation are less abundant in them. Nevertheless, the few detailed study dealing with silicate rocks proved that this approach is an oversimplification of reality. The stability towards chemical weathering of silicate minerals decreases in the order of muscovite - alkali feldspar – biotite – pyroxene - Ca feldspar – nepheline – olivine (Franke and Teschner-Steinhardt, 1994). The higher susceptibility of mafic rocks – containing more minerals from the end of the former list – was proved by Simão et al. (2006). But dissolution of feldspars (mostly plagioclase but not only) and even of quartz has been documented by several authors (Schiavon et al., 1995; Turkington et al., 2003; Xie et al., 2004; Lee et al., 2007). Others suggest that significant gypsum formation will only occur on granite if there is an extra source of Ca, for example mortars used for the construction (Delgado Rodrigues, 2000; Prieto et al., 2007).

In conclusion, the mineralogical composition of the material and the environmental conditions are the two most important factors determining the sulphation processes. Besides,

the microstructural properties of the material, such as grain shape, size, mineral defects (Malaga-Starzec et al., 2003; Metaxa et al., 2008) and above all the porosity have fundamental importance. Porosity plays a key role in controlling the surface moisture (Spiker et al., 1992), the condensation (Moropoulou et al., 1998), the absorption, evaporation and permeability both in the liquid and gaseous phase and the specific surface (Grossi and Murray, 1999). Additional influencing factors are the presence of hygroscopic salts, other chemicals (e.g. treatments or paint layers) (Maravelaki-Kalaitzaki, 2005) and biological colonisation (Turkington et al., 2003).

6.2 Salt crystallization

6.2.1 Procedure

The determination of the resistance to salt crystallization was carried out based on the European standard EN 12370:1999. 6 cubic samples of 5x5x5 cm and 8 slabs of 2,5x2,5x1 cm for the andesite and 16 of the same samples for the marble and granite (all orientated) were used for the test.

Before the test the samples were cleaned and dried till constant weight at 60°C; their original dry weight (w_0) was recorded. Each cycle consisted of 4 hours of total immersion in a 14% $Na_2SO_4 \bullet 10H_2O$ solution and 18 hours of drying in the oven on 60°C (instead of 105°C). After the drying phase, the samples were left to cool down to room temperature during 2 hours by the end of which their weight was recorded. The velocity of the ultrasound propagation was measured after every 3 cycles and 1 of the 2,5x2,5x1 cm samples was taken for microscopic investigation after every 5 cycles. Three times 15 cycles were carried out. After every 15 cycles the samples were cleaned and dried so that the dry, clean weight loss (eq.36) and US velocity and the hydraulic properties (water absorption, desorption and capillarity uptake) could be measured.

$$\Delta M\% = \frac{M_0 - M_n}{M_0} \times 100 \qquad (36)$$

M_n: dry mass of sample after n number of cycles in grams

The pore space properties were measured by means of Hg intrusion porosimetry after the 45th cycle.

6.2.2 Results of the salt crystallization test – Evaluation of the changes

The changes of the material properties were continuously monitored during the test. The methods of this evaluation were: visual observation, detection of weight loss and the velocity of ultrasound propagation and the monitoring of the void space properties by means of Hg porosimetry and CLSM and the hydraulic properties.

Visual observations

During every drying phase of the test an evident efflorescence could be observed on the surface of the specimens, on the lower part in the case of the marble and the andesite and on

almost all the surface in the case of the granite (fig. 6.1). The situation of the efflorescence is determined by the drying rate (evaporation) of each material.

Fig. 6.1. The salt efflorescence appears on the lower part of the marble (a) and andesite (b) samples and on the entire surface of the granite samples (c).

The three stone types show different behaviour in front of this test. The disintegration of the granite, especially on the corners of the samples started already after the 15th cycle (fig.6.2/a) and continues all along the test, resulting in a quite significant loss of material by the end of the 45 cycles mostly on the corners and edges of the cubes, but there are also some pits forming on the surface of the samples (fig 6.2/b).

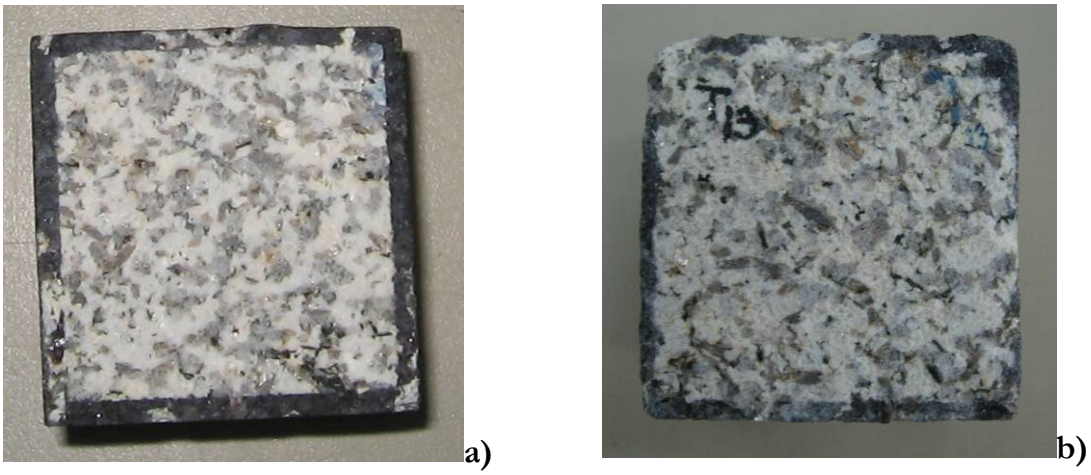

Fig. 6.2. The first signs of disintegration of the granite were observable after 15 cycles of salt crystallization (a) and it suffers an important loss of weight after 45 cycles (b).

On the marble the first losses of flakes could be observed after the 30th cycle on the edges of the specimens and after 45 cycles small pits appear on the surface (fig.6.3).

The andesite does not show any visual changes, not even after 45 cycles (fig.6.4).

Fig. 6.3 The marble suffered a slight loss of material during the 45 cycles of salt crystallization.

Fig. 6.4 The andesite did not show any visual changes after 45 cycles of salt crystallization.

Weight loss

The weight loss was monitored continuously during the test without cleaning the samples. The weight change values are presented on figure 6.5. The marble and granite samples shows similar tendencies as far as their weight variation is concerned, although all the changes are more significant in the granite than in the marble; while the andesite samples differ in their evolution. The marble and granite samples first show increase of weight because of the salt deposition inside. The difference in the magnitude of this increase is due to the difference of the open porosity of the two materials. This phase is followed by a continuous decrease in weight due to the starting material damage. This tendency could be observed after every 15 cycles, when the samples were cleaned. Another typical feature is that the deviation of the weight of the single specimens compared to the average of each group got higher at each phase (meaning each 15 cycles) of the test.

The andesite behaved quite differently; it showed a continuous decrease of weight during the first 15 cycles, and only started to uptake salts from the 16th cycle, showing now the same tendency as the other 2 stones

Both the granite and the marble lose weight gradually, while the andesite detected the highest weight loss value after the 30th cycle and then the weight increased again. This proves again the importance of drying in the case of the andesite.

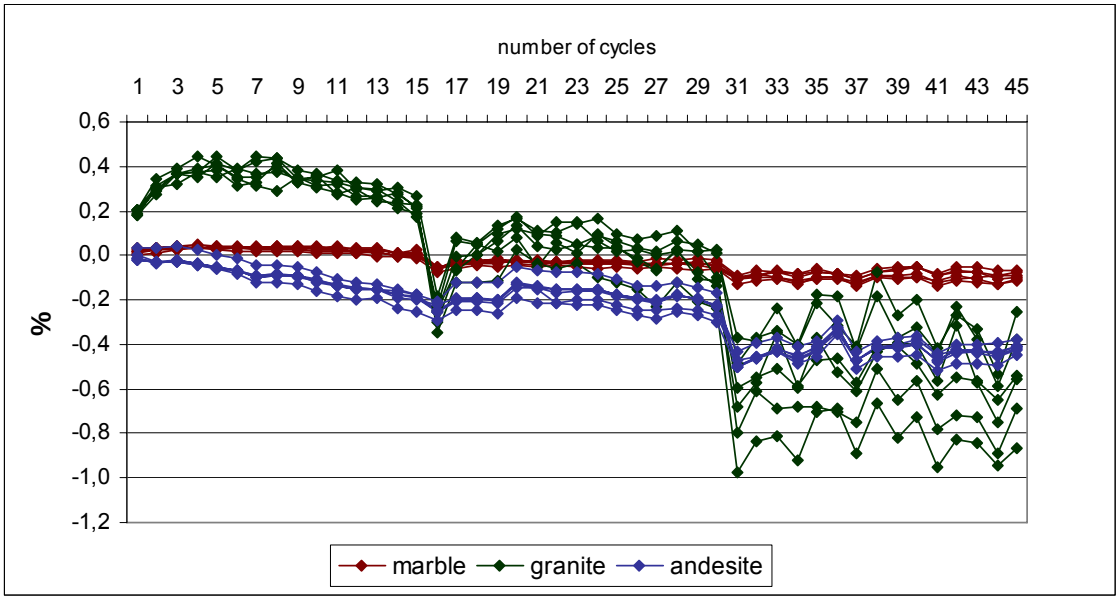

Fig. 6.5 The changes of weight during the 45 cycles of salt crystallization represents the different behaviour of the three stone types in front of this test.

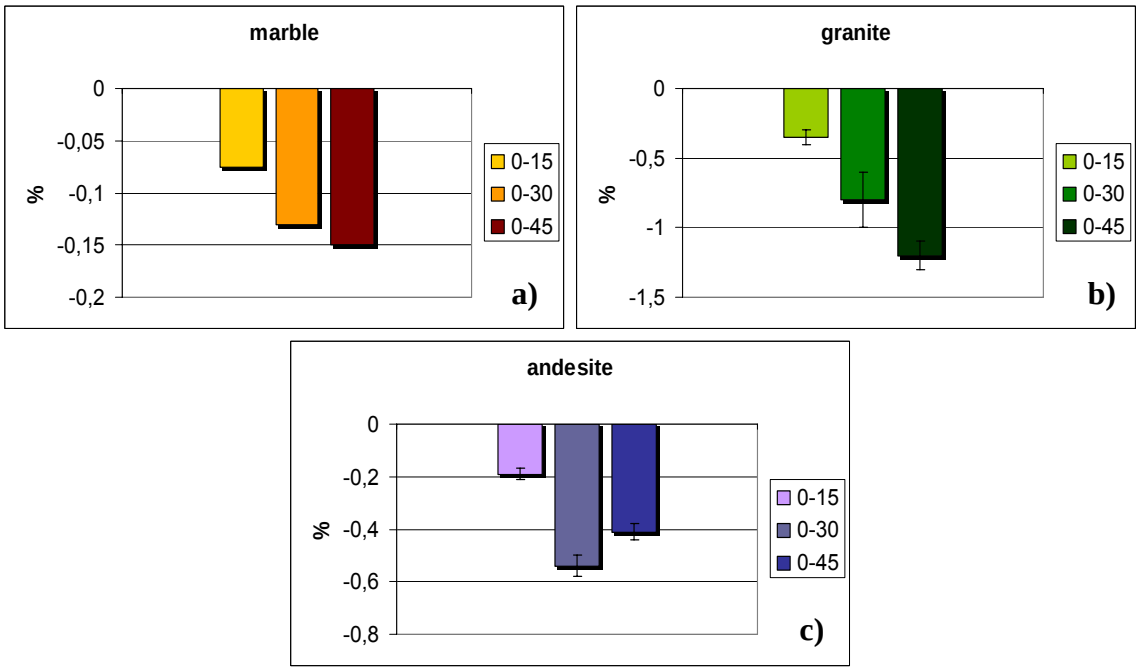

Fig. 6.6. The highest final weight loss corresponds to the Vilachán granite (b), followed by the Szob andesite (c) and finally the Macael marble (a).

Velocity of ultrasonic propagation

The ultrasonic propagation was measured after every three cycles on the samples without cleaning, but the velocity values did not show any significant or consistent changes. On the other hand on the cleaned and dry samples the velocity of the ultrasound propagation has an important decrease in all the cases. Figure 6.7 presents the Vp values of the three stones during the cycles. The values were measured in the three directions of space, called T, M and N directions, although only the Macael marble and the Vilachán granite shows anisotropy.

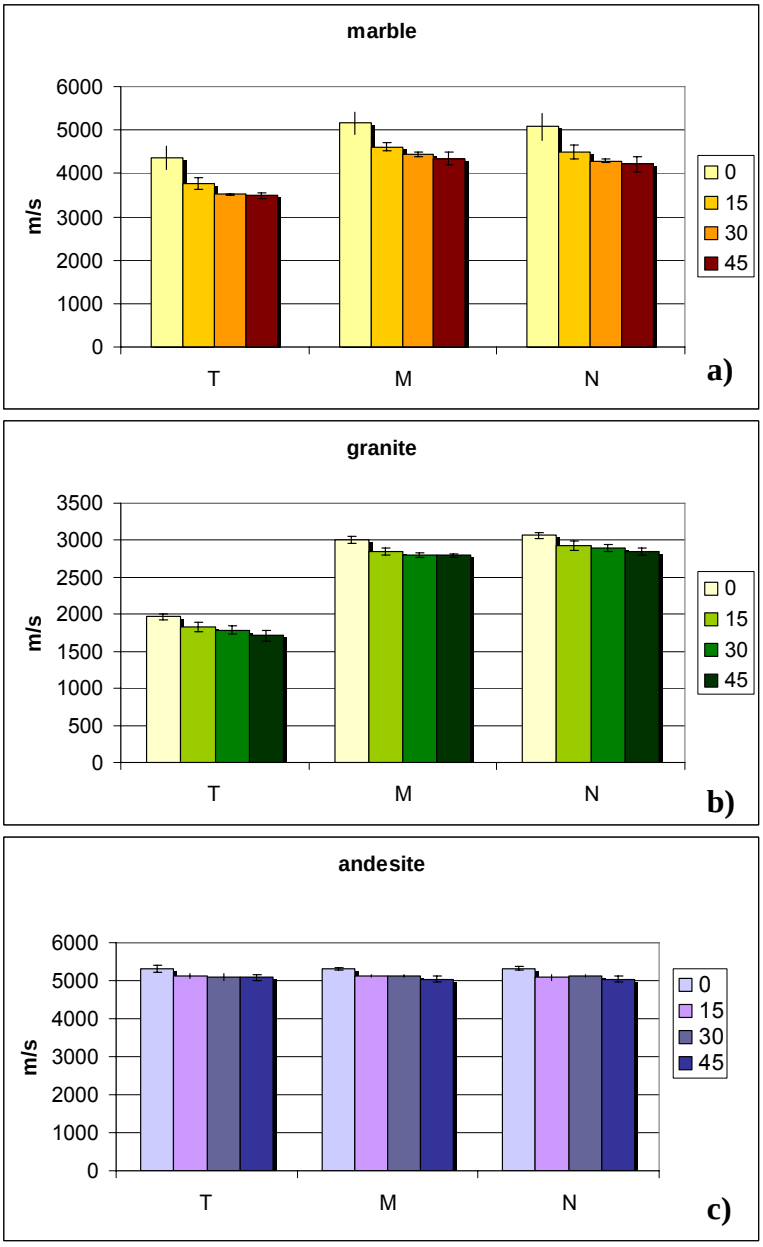

Fig. 6.7 All the examined stones show a continuous decrease in the P wave velocity during the salt crystallization test. T, M, N: three directions of space. Macael marble: a; Vilachán granite: b; Szob andesite: c.

The highest decrease in this case belongs to the marble, the Vp of which has a -20% of change in the T direction and -16,5% in the other two directions after the 45th cycle. The changes of the granite are also significant: -13% and -7% in the two directions, respectively; and finally for the andesite the ultrasound velocity decreases with approximately 5% in all the directions. In all the cases the highest is detected after the first 15 cycles; afterwards the changes are less significant but still continuous.

The pore shape factor (Psf) practically did not change for the Macael marble (0,33; 0,25 and 0,25 in the T, M and N directions, respectively); the Vilachán granite shows slightly higher

values in all the directions (0,38; 0,32 and 0,33 in the T, M and N directions, respectively); while the Psf decreased in the Szob andesite (the average of the three directions is 0,008).

Void space properties

The properties of the void space were investigated after every 10 cycles by means of CLSM and after the 45 cycles by means of Hg porosimetry and N_2 adsorption.

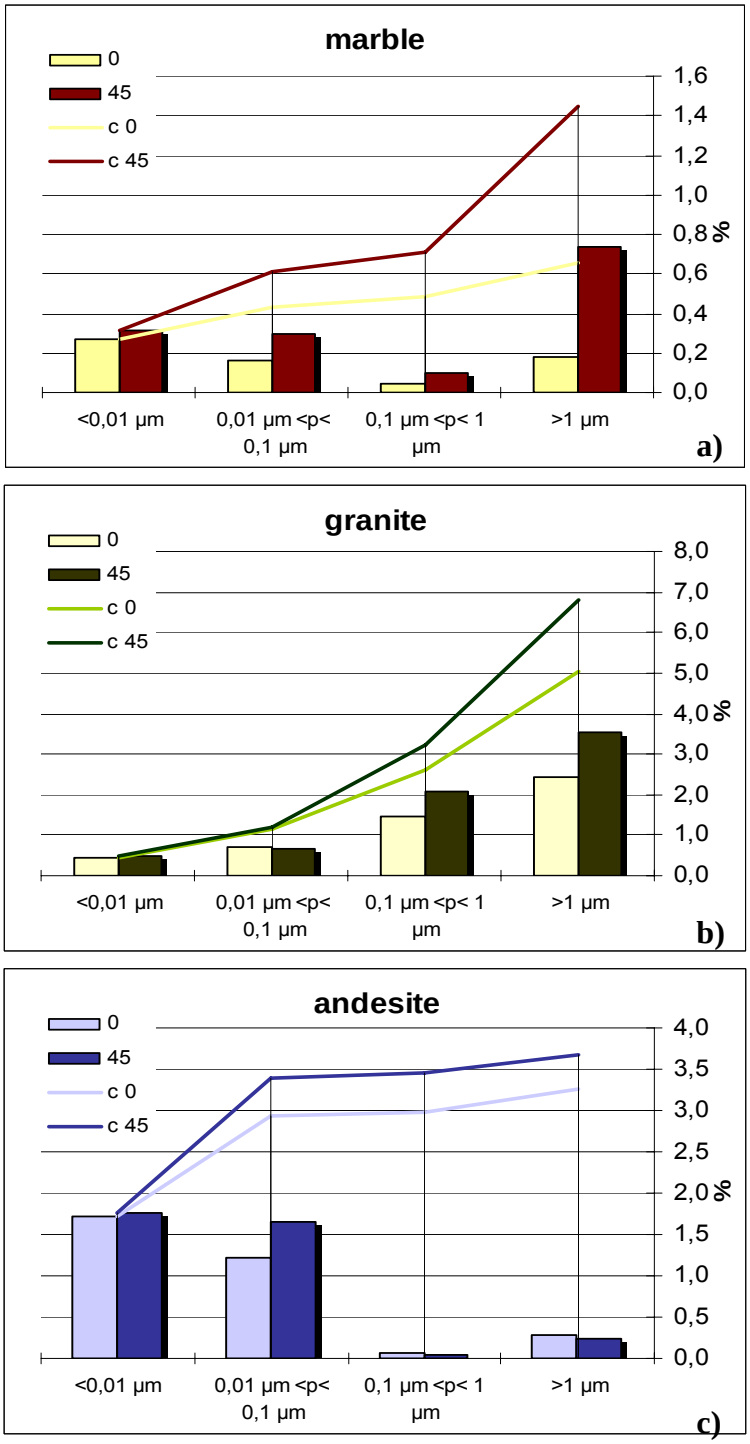

Fig.6.8 The evolution of the void space of the Maceal marble (a) , Vilachán granite (b) and the Szob andesite (c) during the 45 cycles of salt crystallization test. Columns: absolute values; Lines: cumulative values.

In figure 6.8 the changes of the open porosity by different void size ranges are presented after 45 cycles of salt crystallization. No significant variations of the specific surface and the linear crack density were observed.

As it can be observed on figure 6.8, the open porosity increased for all the three stone types. The highest is the relative increase in the case of the Macael marble, where the open porosity reaches the 1,3%. The absolute increase is the highest for the Vilachán granite, where the open porosity of the samples is about 7% after the test. And the last one is the Szob andesite, where this value is still around 3,7% after the test.

On the other hand, the change of the distribution of the voids shows a different pattern in all cases. In the Macael marble the most significant increase can be observed in the largest void size range (>1μm), although the high standard deviations in this case makes this value less reliable. The second largest in the 0,01< p < 0,1 μm interval, which seems to play an important part in this process. In the Vilachán granite it is evidently the larges size ranges that suffered the highest increases, while in the andesite the two smaller intervals were affected by the test.

Hydraulic properties

The water absorption and the capillarity uptake were measured before the test, after the 30th cycle and after the 45th cycle. The results are summarized in table 6.1.

Table 6.1

		original		after 30 cycles		after 45 cycles	
		average	st.dev.	average	st.dev.	average	st.dev.
water absorption (5 day water content (%))	**marble**	0,10	0,01	0,14	0,01	0,18	0,02
	granite	1,59	0,04	1,70	0,03	1,74	0,03
	andesite	0,95	0,08	0,97	0,08	0,96	0,16
capillarity coefficient ($g/m^2s^{0,5}$)	**marble T**	0,20	0,02	1,01	0,08	1,25	0,05
	marble N	0,13	0,04	0,89	0,05	1,18	0,13
	granite T	18,03	0,71	20,05	0,49	21,11	0,80
	granite N	22,00	1,20	25,24	1,10	25,27	3,38
	andesite	1,41	0,19	1,42	0,09	1,41	0,08

Table 6.1 Changes in the hydraulic properties during the salt crystallization test.

The changes in the water absorption capacity were evaluated based on the comparison of the 5 day water content. The highest relative increase of this value was observed in the case of the marble, where the original 0,1±0,01% value increased to 0,14±0,01% after 30 cycles and to

0,18±0,01% after 45, which finally means a 80% increase. In the case of the granite the changes are not that significant (from 1,6±0,01% to 1,7±0,03% after 45 cycles); while for the andesite the water absorption practically did not change.

The results of the capillarity uptake are similar to those of the water absorption. The highest change belongs to the marble, where this value increased by an order of magnitude in both the T and the NM directions. The changes in the case of the granite are still significant: an approximately 17% increase in the T direction and 15% in the N and M directions after 45 cycles. The andesite did not show any significant change.

6.2.3 Wetting-drying – heating-cooling cycles

During the salt crystallization test, some doubts arose concerning the role of the temperature changes during the tests. Low but repeatedly occurring temperature changes can cause material damage through thermal fatigue. This effect has been increasingly investigated lately, mostly on marbles (Logan et al. 1993; Weiss et al., 2003; Koch and Siegesmund 2004 etc). It was found that a temperature increase of only 20-30°C may cause the partial decohesion of calcite grains (Battaglia et al 1993) and that repeated heating can lead to permanent damage (Koch and Siegesmund 2004). The same authors also found that the heating experiment in the presence of moisture leads to even more severe damage. Others (e.g. Winkler 1996) also emphasised the role of moisture in the process. The most susceptible stone type is the marble, because of the specific thermal properties of calcite and because of the low porosity, but granite was also found to suffer micro-cracking due to a cyclic thermal change from -20°C to 20°C due to the differential thermal expansion among the rock forming minerals (Takarli et al. 2008).

The temperature changes during the salt crystallization test are 40°C, from 20°C to 60°C in the presence of moisture. This raises the issue of the thermal fatigue to take part of the degradation process, especially in the case of the Macael marble.

These were the reasons why a complementary test was decided to be carried out. With fresh samples 20 cycles of heating-cooling was carried out exactly the same way as during the salt crystallization test, only substituting the salt solution by distilled water. 6 cubic samples of 5x5x5cm of each stone type were immersed into water during 4 hours, then dried in the oven at 60°C during 18 hours and then let cool down to room temperature (20°C) during 2 hours before starting the next cycle.

The weight change was monitored continuously as well as the macroscopic aspect of the samples; the P-wave velocity was measured before the test, after 10 and after 20 cycles; and the capillary uptake before and after the test.

Results

Serious macroscopical changes did not happen during the 20 cycles, although the Vilachán granite shows the first signs of granular disintegration on the corners at the end of the test.

The evolution of the weight loss on the other hand, served with some unexpected results. The weight changes as a function of time are presented on figure 6.9. As it can be observed, the Macael marble suffers a very slight (maximum value 0,04%) but continuous weight loss. The Vilachán granite detects fluctuations in the weight of the sample, the maximum weight loss (after 20 cycles) is 0,07%. Contrarily, the Szob andesite shows a significant and tendentious loss of weight, reaching 0,5% by the end of the test. This value is in the same magnitude as the weight loss suffered during the 45 salt crystallization cycles. The two big steps in the weight loss curves of the andesite correspond with weekends, when the samples were left in the oven, which means longer drying phases.

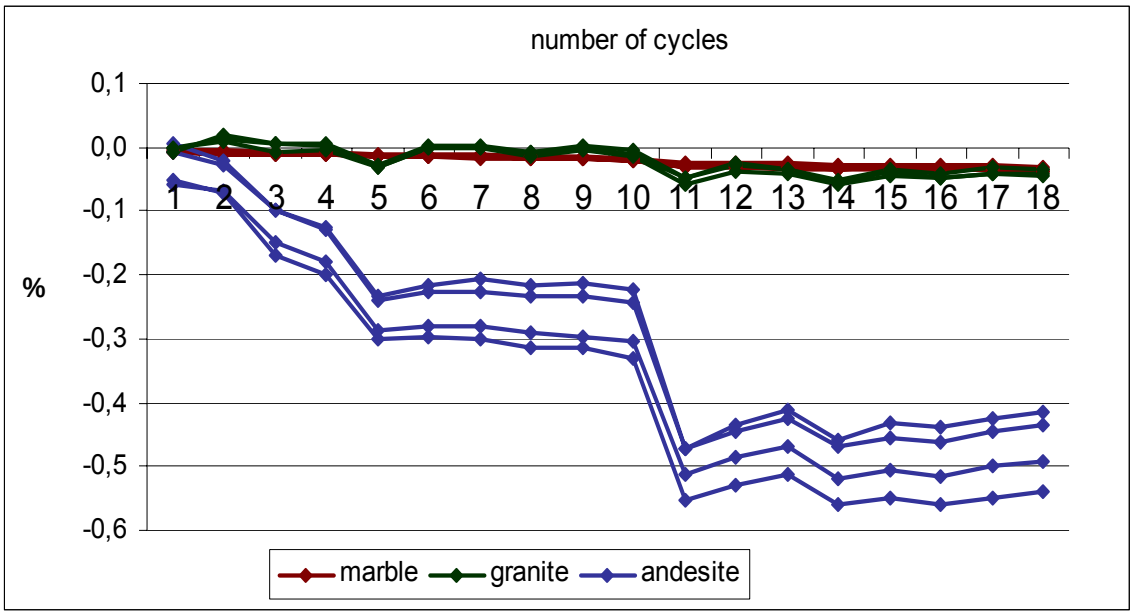

Fig. 6.9. Weight loss of the Macael marble, Vilachán granite and Szob andesite during the 20 cycles of heating-cooling.

The results of the P-wave measurement are presented on figure 6.10. The Macael marble suffers a continuous decrease in the ultrasonic velocity, which is around 6% at the end of the test. This is corresponds to the change after 10-15 salt crystallization cycles for the marble. The Vilachán granite shows an increase of Vp after the first 10 cycles and by the end of the test an approximately 1% decrease in all the directions. Finally, in the Szob andesite the velocity of P-waves is evidently increasing, the final value is a 4% increase.

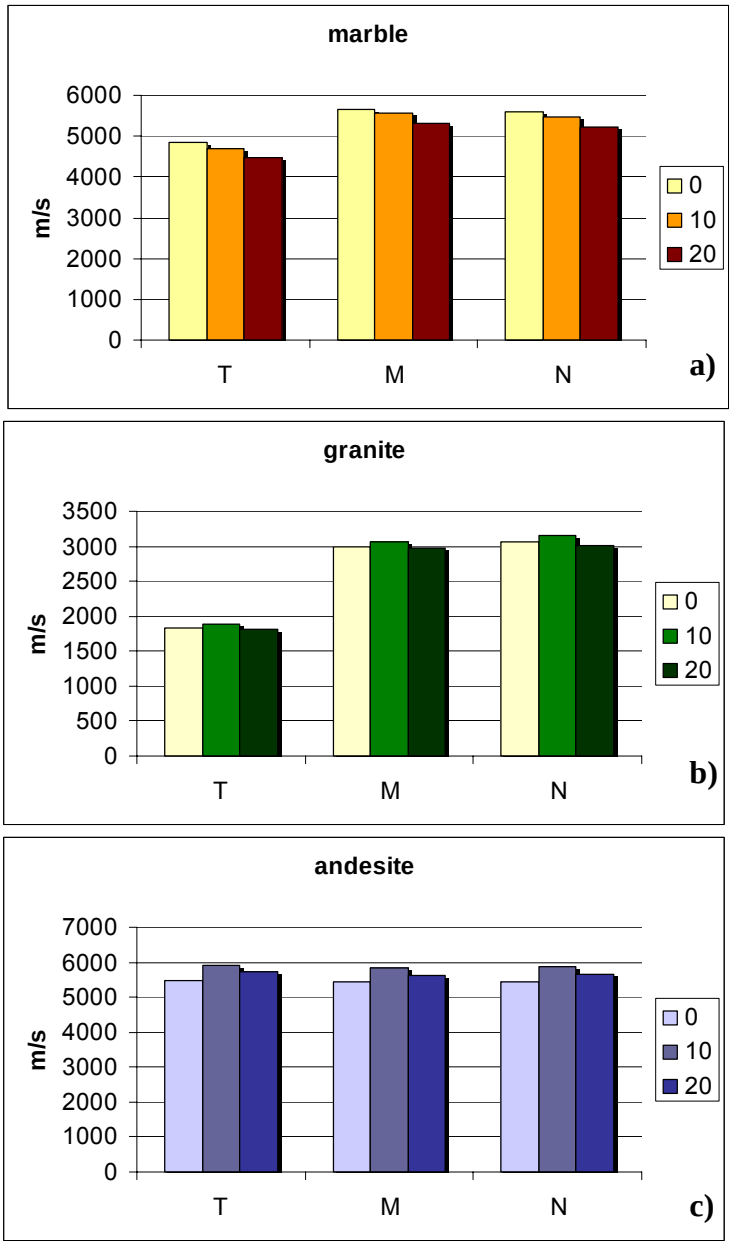

Fig. 6.10 The changes in the Vp of the Macael marble (a), Vilachán granite (b) and Szob andesite (c) after 10 and 20 cycles of heating-cooling

Table 6.2

		original		after 20 cycles	
		average	st.dev.	average	st.dev.
capillarity coefficient ($g/m^2s^{0,5}$)	**marble T**	0,1	0,07	1,0	0,07
	marble M/N	0,12	0,07	1,13	0,03
	granite T	19,7	-	21,7	-
	granite M/N	23,4	0,8	25,9	0,4
	andesite	1,6	0,1	1,7	0,1

Table 6.2 Capillary coefficient values before and after the heating-cooling test.

The capillarity coefficients before and after the test are shown in table 6.2. The Macael marble shows an order of magnitude increase in the capillarity in both directions, exactly as in the case of the salt crystallization test. The increase of Vilachán granite is lower than after 45 cycles of salt crystallization; while the Szob andesite does not show any changes in this parameter.

6.2.4 Discussion

The salt crystallization and the heating-cooling test were used as complementary tests here, so their results are discussed together.

The highest damage caused by the salt crystallization test was observed on the Vilachán granite. The material loss, which compared to the two other stones, is outstandingly high appears as sand disintegration, which is due to the loss of cohesion among the grains of the rock-forming minerals due to the appearance of new intergranular fractures or to the widening of the pre-existing ones. The observable material loss and the weight loss are the most classical ways to evaluate the damage of the materials, and if the damage is intensive, like in this case, they serve as good indicators. Nevertheless, they give no information about the hidden or internal breakdown, which may occur at the microscale (Nicholson, 2002). A reliable and fast evaluation of these is the measurement of the propagation of ultrasonic waves. The decrease of the ultrasonic velocity suggests the formation of new fractures also inside the samples of the Vilachán granite. The increase in the open porosity and the augmented water absorption and capillary uptake also proves the evolution of the porous network of the granite. According to the pore size distribution curve, the most intensive process was the widening of the pre-existing cracks (see the shift of the curve towards the macro-pores), which suggests that the damage was caused by processes taking place in the already existing voids. The increase of the anisotropy proved by the two oriented properties, the Vp and the capillarity coefficients, also shows that the damaging mechanism is connected to the fractures, as in the case of this granite, the anisotropy originates from the oriented crack network.

The heating-cooling test did not have such disastrous effect on the Silvestre Vilachán granite. The weight loss and the capillary coefficient increase are lower, while the P-wave velocity practically does not change. This once again proves that the most important damage during the salt crystallization test that occurs in the Vilachán granite is indeed due to the effect of the salts. However, the effect of the thermal cycling cannot be completely excluded, seeing the starting granular disintegration on the corners of the samples.

The high susceptibility of the Silvestre Vilachán granite is in accordance with the collective knowledge of the salt crystallization, detailed in chapter no 6.1. The relatively high porosity, the wide void size distribution, the abundant presence of meso- and macro-pores, due to the dual nature of its void space, the very well connected void network, which assures the fast

fluid movement kinetics, all point to the high probability of the formation of subflorescence within the stone and the development of high crystallization pressures. The mechanical resistance of the stone is also relatively low, which incapacitates its resistance to the evolving stresses. In conclusion, the Vilachán granite is a stone showing low durability during the salt crystallization test, and the damage occurring is due to the precipitating salts in the porous network of the material.

The fact that the effect of the salt crystallization test was due to the crystallization of salts should not be surprising or important, had not we seen the happenings on the other two stone types.

The Macael marble also suffered serious damage during the test. The properties showing the highest variations were the ultrasound velocity and the hydraulic properties. This is exactly the case mentioned before, when the weight loss only does not give sufficient information about the damage. Especially, because most of the weight loss in this case is due to the dissolution of calcite in the alkaline saline solution, as it can be observed on the surface of the samples. The chemical degradation is a well-known "side effect" of the salt crystallization test, which mostly affects the carbonate stones (Orkoula and Koutsoukos, 2001, etc.) and which can be considered a mostly superficial process. The weight loss during the heating-cooling cycles is practically zero, proving the truth of the above statement. The very significant decrease in the P-wave velocity, as before, is due to the formation of new discontinuities or to the opening of pre-existing ones. Comparing the change in Vp in the salt crystallization and in the heating-cooling test, we can see that during the 20 cycles of heating-cooling the change is more than 50% of the change during 20 cycles of salt crystallization. The results of the capillary coefficient are even more striking, showing exactly the same change after 20 cycles of heating-cooling than after 45 cycles of salt crystallization. All these observations suggest, that a significant part of the damage suffered by the Macael marble during the salt crystallization test in reality behoves to the thermal changes during the test. The sensibility of carbonate stones to thermal cycles, especially in the presence of moisture is a known fact (Koch and Siegesmund, 2004). Nevertheless, the temperature range and the number of cycles to cause damage are usually considered significantly higher. In this test, it was proved that only 20 cycles of 40°C change are sufficient to open up the intergranular connections of a sound marble, which then facilitates the attack of the other deteriorating agents. It must be mentioned here, that the European standard requires the drying of the samples on 105°C, which means an even more drastic temperature cycling.

The final damage of the Macael marble – the increase of open porosity, the increase of the number of macropores, the starting granular disintegration etc. – are due to the effect of the salt crystallization (and maybe to the chemical dissolution that now can take place in the voids as well). But this stone, which originally has practically zero water absorption, would be maximally resistant to the salt attack without the thermal effect because the solution could not enter inside the stone.

Under real life conditions the salt crystallization process does not necessarily includes such temperature changes, as it can be caused by changes of relative humidity only. In this view, the reliability of the standardized method to assess the resistance of a material to the salt crystallization becomes questionable.

The last stone type is the Szob andesite. This stone shows no signs of damage at all. The decrease in the ultrasonic velocity is minimal, the changes in the hydraulic properties are practically zero, and the increase in the open porosity is low and only occurs in the smallest pore size ranges. The only property that seems to be affected by the salt crystallization test is the weight. The andesite shows a higher weight loss than the marble, even if no material loss could be observed on the samples. This is a somewhat surprising result. The surprise is even greater considering the results of the heating-cooling cycles. The Vp of the andesite increases during the heating-cooling, the capillarity coefficient does not change at all, but once again there is a significant decrease in the weight of the samples. The weight loss curves of the two tests has a similar pattern (figures 6.5 and 6.9), meaning that the weight starts to decrease from the first cycle, the decrease continues constantly during the first couple of cycles, suffers drastic drops whenever a longer drying phase takes place and then keeps more or less constant. The only difference between the two curves is the slight weight increase during the second series of salt crystallization test due to the salt uptake.

The comparison of the two tests and of the different parameters proves that, once again, the weight change is not a reliable parameter to evaluate the damage. As it was seen during the stone characterization, the Szob andesite has outstandingly slow water movement kinetics, the drying process included. The fact that the weight-drops are linked to longer drying periods suggests that the mass changes are simply due to the water evaporation from the samples, which happens very slowly and which – at least during the first few cycles - is not balanced by the water uptake during the 4 hours of immersion, hence the continuous decrease.

This means that, in spite of the registered weight loss, no damage whatsoever took place in the andesite. The European standard requires the weight loss only for the evaluation and quantification of the deterioration. Following this requirement the Szob andesite would be judged to have a slightly low resistance (only slightly because the weight loss was low); while it is maximally resistant to the salt crystallization.

A stone material having almost 5% porosity and an outstandingly high number of micro- and meso-pores is supposed to be exceedingly susceptible to salt crystallization damage, according to the theoretical calculations (referred to above); especially, because in the case of the andesite, the pores fulfil the assumption of having spherical shapes; not like in the case of the Vilachán granite. The calculated crystallization pressure according to the Fitzner and Snethlage (1982) model would highly overpass the tensile strength of the andesite.

In table 6.3 the results of the calculation are presented according to the method used in Rossi-Manaresi and Tucci (1991). The pore space (the values of the Hg porosimetry were used) was divided to four categories according to the pore size distribution: larger than 1μm; between 1

and 0,1 μm; between 0,1 and 0,01 μm and smaller than 0,01 μm. The crystallization was supposed to take place in the largest range, so the pressures are calculated in the three smaller intervals. Equation 27 was used for the calculation of the theoretical pressure of each interval, where the $1/r_1$ (the radius of the larger pore) was neglected being an insignificantly small number in the equation. Following the afore mentioned authors, the surface tension was taken 8Pa. Then these pressure values were multiplied by the ratio of the volume of pores in the given interval to the total volume of pores (V_r/V_R) to get the real pressure in each interval of pores (p_i); and finally these partial pressures were summarized to get the total value.

Table 6.3

pore size interval	**>1 μm**		**1>x>0,1 μm**		**0,1>x>0,01 μm**		**0,01 μm>**		**Hg-porosity (%)**
	pore volume (%)	**% of total porosity**	**pore volume (%)**	**% of total porosity**	**pore volume (%)**	**% of total porosity**	**pore volume (%)**	**% of total porosity**	
Szob andesite	0,3	8,6	0,1	1,6	1,3	41,2	1,6	48,7	3,2
Vilachán granite	2,5	47,6	1,9	36,8	0,7	14,3	0,1	1,3	5,2
Macael marble	0,2	15,4	0,1	8,3	0,3	29,2	0,5	47,1	1,1
p theore-tical (MPa)	0		0,3		3,2		32,0		**total pressure (MPa)**
mean radius	5		0,5		0,05		0,005		
	V_r/V_R	**p_i**	**V_r/V_R**	**p_i**	**V_r/V_R**	**p_i**	**V_r/V_R**	**p_i**	
Szob andesite	-	-	0,18	0,06	4,80	15,36	5,68	181,72	197,14
Vilachán granite	-	-	0,77	0,25	0,30	0,96	0,03	0,87	2,08
Macael marble	-	-	0,54	0,17	1,89	6,06	3,06	97,93	104,16

Table 6.3 Theoretical calculation of crystallization pressure (after Rossi-Manaresi and Tucci, 1991). The stresses highly overpass the tensile strength of the Szob andesite and Macael marble and slightly that of the Vilachán granite.

Almost 200 MPa theoretical crystallization pressure was calculated for the Szob andesite and about 100 MPa for the Macael marble. Both of these values are approximately an order of magnitude higher than the tensile strength of the two materials, respectively. On the other hand, the calculated value for the Vilachán granite (2 MPa) hardly surpasses its tensile strength. The calculations suggest exactly opposite results than the experimental observations, which means that this kind of theoretical approach is not valid for the materials examined in this research.

This conclusion is in harmony with Cardell's and others' (2003b) opinion, saying "… anomalies limit the extent to which generalisations can be made". In the special case of the

Szob andesite, the other properties, such as the badly connected porous network, the very slow water movement kinetics, meaning very low capillary uptake and slow drying process (which can be expressed by Hirschwald's coefficient (1908) or the critical water content (Ruedrich and Siegesmund, 2006), respectively), will be the ones that determine the resistance of the material to salt damage.

6.2.5 Correlation among parameters - Conclusions

The discussed results can be summarized in the following points

- The Vilachán granite shows the highest susceptibility of the three stone types to salt weathering
- The properties that make the granite especially susceptible to the salt weathering are the high open porosity and the very good connectivity of the porous network. The importance of the pore size distribution was neither proved nor disproved
- The dense and low-porosity Macael marble is not susceptible to the damage caused by salt crystallization
- The damage suffered by the Macael marble was due to the thermal changes and the chemical dissolution. The thermal changes are not necessarily involved in the natural process, which means that the test gives false results about the performance of the marble in front of salt weathering
- Only 20 cycles of 40°C change were sufficient to open up the intergranular connections of this sound marble
- Once the intergranular cohesion of the marble is weakened (by the thermal or chemical degradation) is becomes more susceptible to the salt weathering
- The material loss, in the cases when it was observable, appears in the form of granular disintegration, therefore the damage is caused in the intergranular space both for the Macael marble and the Vilachán granite
- The Szob andesite is not susceptible to the salt weathering. The supposed negative effect of the high open porosity and small average pore size was effaced by the extremely slow water kinetics due to the very bad connectivity of its porous network
- The detected weight loss of the andesite was not due to the deterioration but to the very slow drying

- The properties that best described the occurring damage were the Vp and the hydraulic properties for the Macael marble; the weight loss, Vp and the open porosity of the Vilachán granite

- The weight loss is only reliable when the damage is severe enough to cause significant material loss. In the case of the Macael marble is under-estimated, in the Szob andesite it over-estimated the damage

6.3 Frost resistance

6.3.1 Procedure

The basis of the determination of frost resistance was the Europen standard EN 12371:2001, although some changes were implemented in order to achieve the highest effectiveness possible. The changes concerned on one hand the temperature range, which was broadened in our test because of the high proportion of micropores in the materials, which cause the depression of the freezing point temperature of the water. On the other hand, the samples were kept in total immersion during the entire test (in the freezing as well as in the thawing phase) in order to keep the level of saturation as high as possible.

Taking into account the above mentioned changes the procedure of the freeze-thaw test was the following.

5 cubes of 5x5x5 cm dimensions of each stone type, and 8 slabs of 2,5x2,5x1 cm for the andesite and 16 of the same samples for the marble and granite (all orientated) were used. The samples were dried till constant weight on 60°C before the test and after recording their dry weight (w_0) they were saturated by water. One cycle consisted of two parts: 6 hours of freezing on -15°C and 6 hours of thawing on 20°C. The velocity of heating and cooling was 0,5°C/min. 250 cycles were carried out. The evaluation of the changes happened by continuous visual inspection, by the measurement of weight loss and the measurement of the US propagation every 50 cycles, the measurement of the hydraulic properties (water absorption, desorption and capillary uptake) at the 100^{th}, 200^{th} and 250^{th} cycle. Samples of 2,5x2,5x1 cm were taken every 50 cycles for microscopic investigation, and the pore space properties were also measured by Hg intrusion porosimetry after the 200^{th} and the 250^{th} cycles.

6.3.2 Results - Evaluation of changes

Visual observation

The visual observation of the cubic samples was carried out continuously during the 250 cycles of freeze-thaw test in order to detect the macro scale superficial changes such as the loss of material, the possible colour changes etc..

The three stone types give different responses to the freeze-thaw process; although the differences and in general the visual changes are not as pronounced as during the salt crystallization test.

The most significant material loss, observable by the naked eye, again corresponds to the Silvestre Vilachán granite. The loss of grains – granular disintegration – could be observed

from the 100th cycle on, and was getting gradually more severe resulting in a slight material loss on the corners and the edges of the cubes (fig.6.11).

Fig. 6.11. Slight granular disintegration can be observed on the Vilachán granite after 250 freeze-thaw cycles.

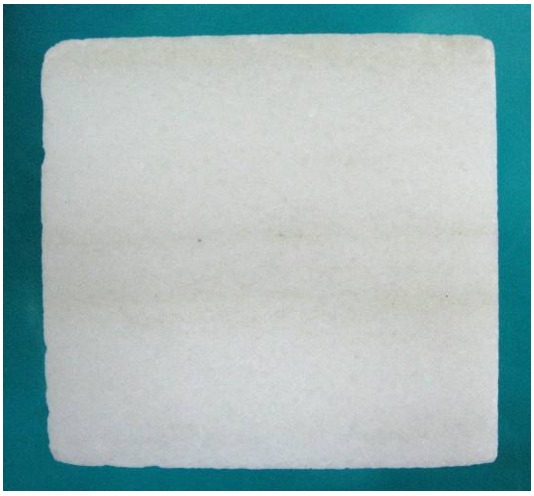

Fig. 6.12 The material loss of the Macael marble mostly occurs on the corners and edges of the samples.

Fig. 6.13. The Szob andesite does not show any visual changes after 250 freeze-thaw cycles

The same effect can be observed on the Macael marble samples, although due to the finer grain size, the material loss is less spectacular in this case (fig.6.12). The superficial pitting, which was observable as a result of the salt crystallization test, does not occur this time. The first signs of material loss appear around the 150th cycle. And finally, the Szob andesite, as before, does not show any visual changes all through the test (fig.6.13).

Weight loss

The weight loss gives further information about the material loss, as by this method the loss not observable by the naked eye can also be detected.

On figure 6.14 the weight loss – expressed in percentage – is shown after 100 cycles, which means more or less the middle of the test, after 200 cycles and at the end of the test, after 250 cycles.

As it can be seen on this figure, all the three stone types suffer a gradually increasing weight loss during the test. Far the highest value is that of the granite – in harmony with the visual observations – which by the end of the 250 cycles reaches the -0,27%. However, this value is still a lot lower than the loss of weight provoked by 45 cycles of salt crystallization test, which exceeded 1%. The second highest weight loss corresponds to the marble – -0,12% after 250 cycles – which is quite similar to the material loss of this stone during the salt crystallization test. And finally, on the andesite samples hardly any loss of weight can be detected (-0,05%), while during the salt crystallization test the same value was around -0,5%.

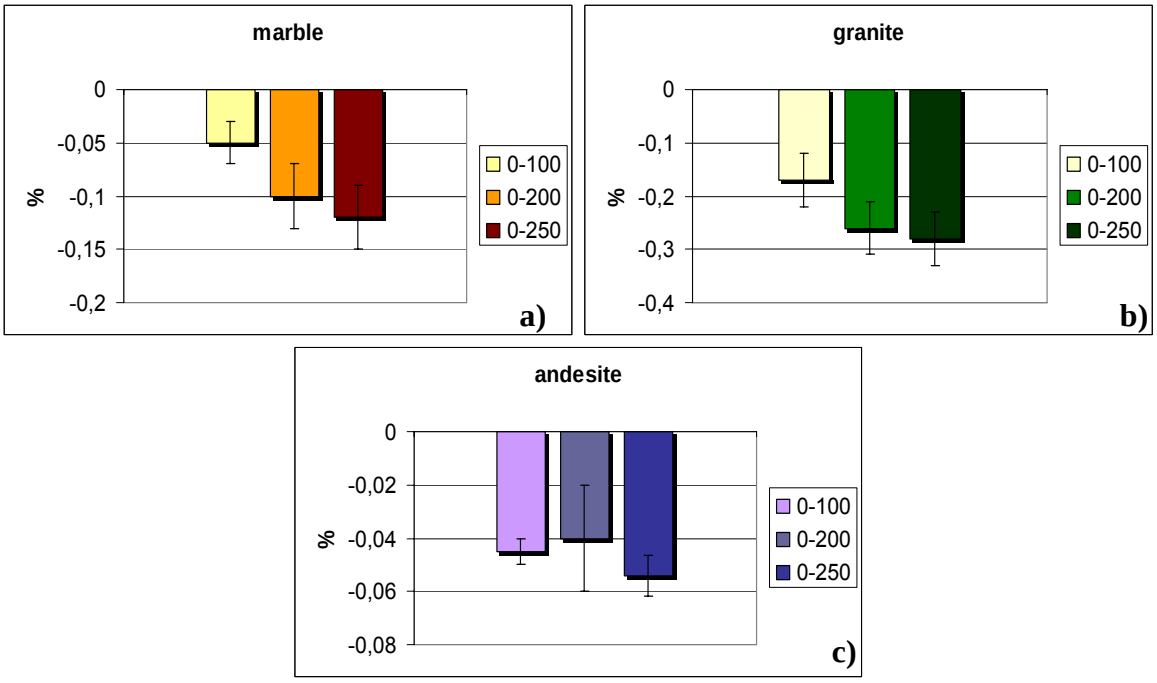

Fig. 6.14 Weight loss of the materials along the freeze-thaw test. The Silvestre Vilachán granite (b) suffers the highest weight loss due to the freeze-thaw cycles followed by the Macael marble (a) and finally the Szob andesite (c).

US velocity

The velocity of P waves provides information about the changes inside the material. It was measured on the dry samples after 100, 200 and 250 cycles. The velocities are shown on figure 6.15 in three directions of space.

In this case the highest decrease occurs for the Macael marble. The change of the Vp by the end of the test is about 30%, of which 25% corresponds to the first 100 cycles. The decrease is somewhat higher in the T direction, in which the Vp values are lower originally as well, which means that the anisotropy increases.

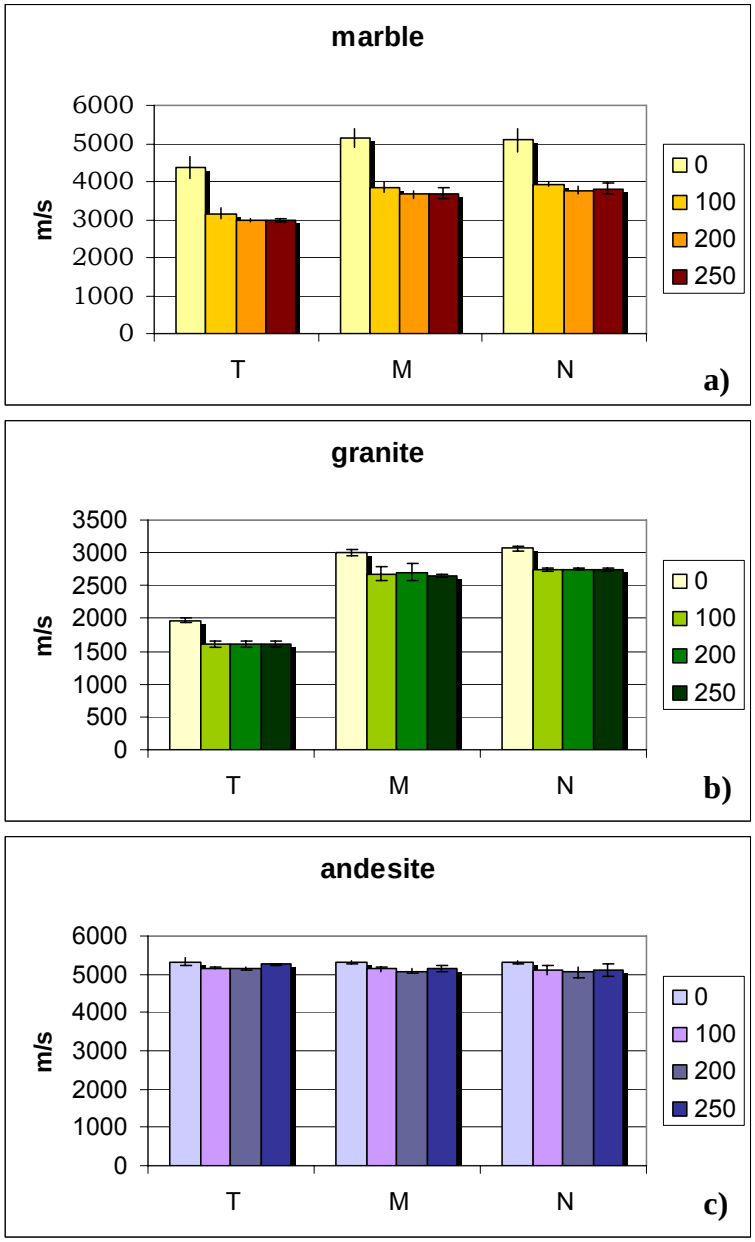

Fig. 6.15 The evolution of the Vp along the freeze-thaw test. The Macael marble (a) shows far the highest decrease in Vp due to the freeze-thaw cycles followed by the Vilachán granite (b) and the Szob andesite (c).

The second highest change is of the granite, occurring almost exclusively during the first 100 cycles. Afterwards, the Vp values are more or less constant. Again in the direction where the values were originally lower (T direction), the decrease is higher, increasing the anisotropy of the stone.

The maximum decrease of the andesite is around 4%, presenting similar values in all the directions, proving the isotropy of the stone once again.

By the comparison of the Vp in dry and in saturated samples the pore shape factor was calculated at the different phases of the test also. The Psf shows a very similar tendency in the Macael marble and the Vilachán granite. In both cases the values increase gradually after 100, 200 and 250 cycles. The final values of the marble are 0,50; 0,41 and 0,39 in the T, M and N directions, respectively; and of the granite 0,52; 0,39 and 0,40 in the T, M and N directions, respectively. The Szob andesite does not show any tendentious changes in this sense, the Psf values vary continuously, sometimes even taking negative values. This suggests that there are no new cracks induced during the test.

Void space structure

The evolution of the void space was monitored during the test by means of CLSM and by Hg porosimetry after 200 and 250 cycles. In figure 6.16 the changes in the open porosity at different size ranges are presented. No significant variations of the specific surface and the linear crack density were observed.

An increase of the open porosity was observed in all the three stones during the test but the magnitude of increase and the pattern of the void size distribution differ.

In the Macael marble the effect of the first 200 and the last 50 cycles shows significant differences, although it is mostly due to the change of the largest pore size range, where the high standard deviations requires the cautious interpretation. During the first 200 cycles the open porosity grew up to 1,2% and the most significant changes can be observed in the intermediate void size range: between 0,01μm and 1μm. In the last 50 cycles there is a sudden leap in the largest void size range, which infers a drastic change of the cumulative value also. The result of the first 200 cycles seems to be the more realistic.

The Vilachán granite also suffers an increase in the open porosity value, although it is somewhat lower than was the effect of the 45 salt crystallization cycles. Also we can observe that the increase takes place almost exclusively during the first 200 cycles. Except for the smallest interval, here all the void size range is almost uniformly affected by the process.

A significant increase of the open porosity of the Szob andesite occurs during the test. The value reaches 4,5-5% and seems to be continuously increasing after 200 and after 250 cycles. All the void size intervals play an important role in the course, except for the $0,1 < p < 1\mu m$ range, which has a very inferior part of the void space.

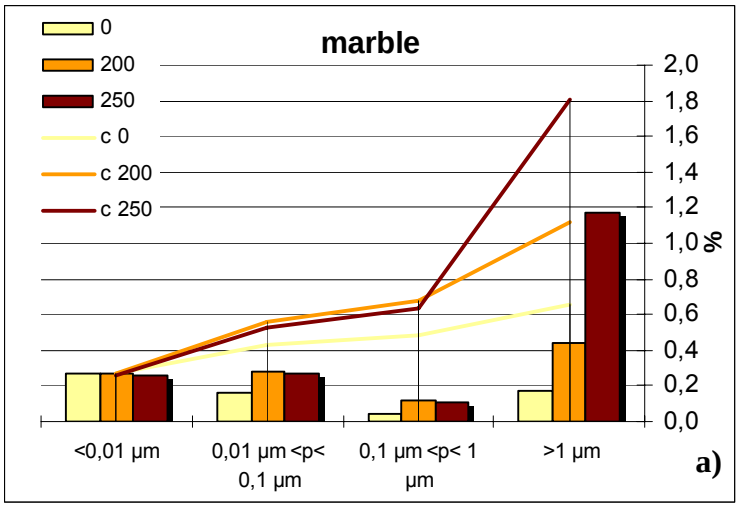

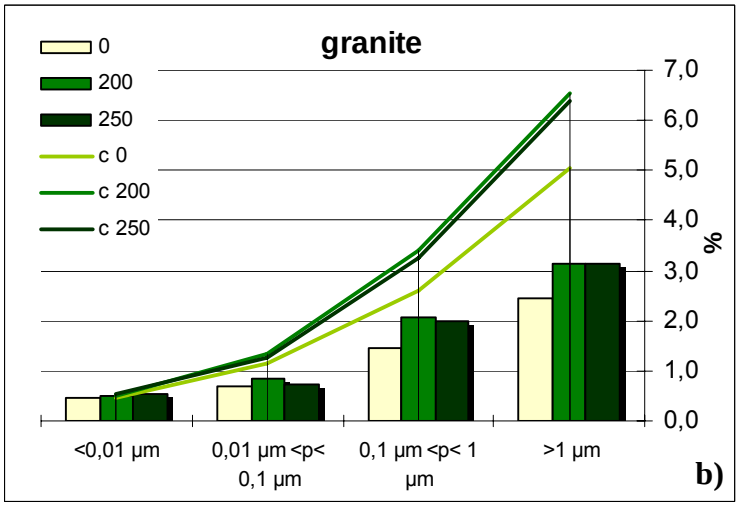

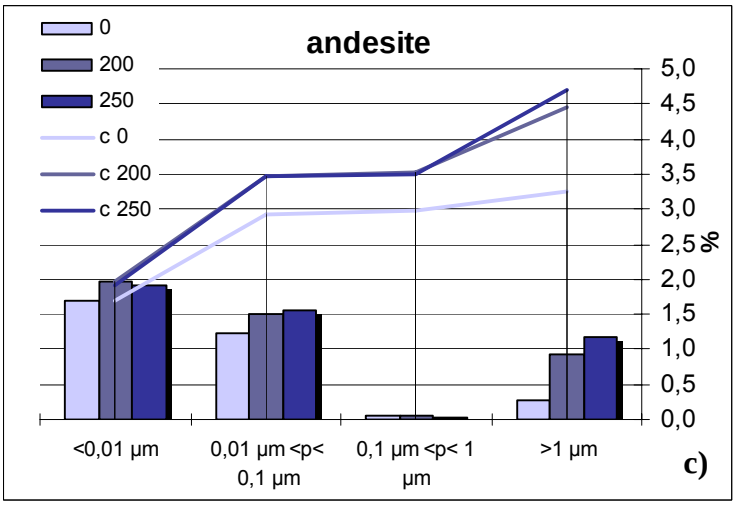

Fig. 6.16. The evolution of the void space of the Maceal marble (a) , Vilachán granite (b) and the Szob andesite (c) during the 250 cycles of freeze-thaw test. Columns: absolute values; Lines: cumulative values.

Hydraulic properties

The hydraulic properties were evaluated through two parameters: the water absorption and the capillary uptake. The water absorption curves are shown in the appendix 2, and the 5 day water content (%) was used as a single value for comparison. The capillary uptake was measured in two directions (T and M/N) in the two anisotropic stones, the marble and the granite; but only in one direction in the isotropic andesite; it is expressed as capillarity coefficient, according to the relating European standard (EN 1925:1999). The values before the test and after 100, 200 and 250 cycles are shown in table 6.4.

Table 6.4

		original		after 100 cycles		after 200 cycles		after 250 cycles	
		average	st.dev	average	st.dev	average	st.dev	average	st.dev
water absorption (5 day water content (%))	**marble**	0,1	0,01	0,21	0,01	0,23	0,01	0,24	0,01
	granite	1,59	0,04	1,73	0,03	1,78	0,03	1,90	0,02
	andesite	0,95	0,08	1,08	0,11	1,07	0,098	1,19	0,12
capillarity coefficient ($g/m^2s^{0,5}$)	**marble T**	0,19	0,02	0,77	0,02	0,77	0,05	0,95	0,07
	marble M/N	0,13	0,04	0,71	0,05	0,98	0,1	1	0,1
	granite T	18	0,7	26	1,7	21	-	20	-
	granite M/N	22	1	27,8	0,6	25,6	0,6	25,7	0,05
	andesite	1,4	0,2	1,7	0,2	1,7	0,3	1,6	0,3

Table 6.4 The change of hydraulic properties before and during the frost resistance test

The water absorption increases gradually in all the cases, although not to the same extent neither in the same rhythm. The highest increase is produced by the marble, where the 5 day water content reaches the double of the original value already after the 100th cycle. During the following cycles a slower increase can be observed. The marble is followed by the andesite, which suffers an approximately 25% increase of the water absorption, but the 50% of this increase happens in the last 50 cycles. Finally, the total increase of the granite is around 20%, which is reached gradually along the 250 cycles.

The capillary uptake also increases in all the stone types. The Macael marble shows an outstandingly high increase, the final values being an order of magnitude larger than the original ones. The major part of this change occurs during the first 100 cycles. The increase is of similar magnitude in the two measured directions, although somewhat higher parallel to the foliation of the rock.

The increases in the capillary coefficients are similar in the case of the granite and the andesite; around 20%. It is interesting to observe that in both cases the highest values were

measured in the 100th cycle and during the second part of the test the values decrease, although at the end of the 250 cycles they are still higher than the original values.

6.3.3 Discussion

The Macael marble suffered the highest damage out of the three stone types if all the monitored parameters are taken into consideration. The weight loss, although it may seem insignificant (-0,12%), has the same magnitude as the weight loss during the salt crystallization test, but here it cannot be ascribed to the calcite dissolution.

The two parameters that show far the highest changes are the ultrasound velocity and the capillarity uptake. The P-wave velocity – among other parameters – depends on the number of discontinuities in the material that impede the undisturbed propagation of the wave. This effect is more pronounced if the discontinuities are elongated (cracks), because the elastic wave has to cross the thin but long fissures in order to progress through the specimen and cannot by-pass them as it does with the equidimensional pores (Delgado-Rodriguez, 2000). So the decreasing Vp suggests the increasing number of cracks in the material.

The decreasing capillarity coefficient proves the improving connectivity of the capillary pore network of the material. This improvement can happen in two ways; either by the increasing number of capillary voids or by the increasing radius of the capillary voids. The capillary coefficient describes the velocity of the capillary uptake, and although the length of the fluid penetration is in inverse proportion with the radius, the velocity of the process is directly proportional to it (Cerepi at al. 2002). The measurement of the pore size distribution suggests the truth of this second option. As it can be seen on figure 6.16/a, the void size distribution shifts towards the larger ranges, while the smallest interval remains more or less the constant.

Taking into consideration all the three above mentioned parameters – the Vp, the capillarity coefficient and the void size distribution – we can summarize that due to the freeze—thaw cycles two effects took place in the marble: the appearance of new cracks and the growing of the existing ones. The appearance of new discontinuities may be due to the internal stress among the calcite grains due to the anisotropic expansion of this mineral phase during the thermal cycles (Weiss et al., 2003). The pre-existing and the new cracks then facilitated the penetration of water into the material giving place to the effect of the ice formation, which causes the growing of the voids. As a final effect, the increased open porosity and improved connectivity of the porous network resulted in higher water absorption.

In both of the orientated parameters – the Vp and the capillary coefficient – an increase of anisotropy can be observed. This means that the new cracks are parallel to the foliation of the marble, as it was observed in other works, as well (Martínez-Martínez, 2008).

The observed grain disintegration and weight loss is a product of the same process, as the outside parts of the samples are more exposed. It can be considered a consequence of the

ongoing damage but none of these two parameters give real information about the processes that take place inside the material.

Another interesting point to consider is the obvious difference in the magnitude and type of damage between the first and the second hundred cycles. In all the above discussed parameters that concern the void space – except for the total porosity – the major part of the changes took place during the first part of the test, while in the second part the tendencies continue but significantly more slowly. The material and weight loss on the other hand, intensifies with the increasing number of cycles getting more significant in the second half of the test. This suggests a kind of equilibration of the texture, the changes of which were connected to the calcite expansion and new crack forming. This process with time gives place to the physical damaging effect of the ice formation, which results in the material loss starting in the outer parts – edges and corners – of the samples.

The Silvestre Vilachán granite is the one of the three stones that suffered the highest visual damage during the test. Also it has the highest weight loss value due to the material loss. Again, as in the case of the Macael marble we can observe that as the material and weight loss are intensifying with the increasing number of cycles, the other parameters reach a kind of stabile state after the first 100 cycles. There is a big negative leap in the P-wave velocity from the 0 to the 100th cycles, although the relative change is not as high as in the case of the marble. This suggests the appearance of new cracks in the samples, which is also proved by the significant increase in the capillary uptake. Again an increase in the anisotropy can be noted, which means that the new crack appear parallel to the direction of the original fracture network. Also, as the pre-existing cracks suffer growth in length and/or aperture, the capillarity will be faster in the direction where their number is higher.

The new fractures may be due to the crystallization pressure of ice already during the first 100 cycles, as the original open porosity and water absorption of the granite is large enough to facilitate the ice formation inside the material. On the other hand, from the 100^{th} cycle on there is no more significant change in the capillary coefficient, nor in the Vp. Actually, the capillarity detected lower uptake values in the 200^{th} and 250^{th} cycle than before. Also the porosity in the intermediate void ranges decreases from the 200^{th} to the 250^{th} cycle.

The water uptake and the open porosity values increase continuously during the test such as the weight loss. All this suggests that after the initial part of the damage, when some new cracks appear – far less than in the case of the Macael marble – the process continues with the widening of the already existing fissures. This course in the end will lead to material loss, which starts at the edges and corners of the specimens in the form of granular disintegration. This form of weathering points out the importance of the intergranular fissures in the degradation.

The Szob andesite, like in the salt crystallization test, does not show any visual changes of damage. The weight loss, such as the ultrasonic velocity decrease, or the changes in the

hydraulic properties, is very low showing that the damages that take place in the andesite are of small significance.

The weight loss in the former tests was proved to be the effect of a very long and slow drying process. As there is no drying phase during the freeze-thaw test (only when the test is interrupted for the measurements), this process has no importance here. The almost constant hydraulic properties show, that even if there is slight decrease in the open porosity, the connectivity and communication of the void network did not improve due to the damage.

The only properties, where somewhat higher changes were detected, were the open porosity and the pore size distribution, because the ratio of the macro pore size range (>1μm) increased.

The slow water kinetics of the Szob andesite was the main reason for the modification of the standard frost resistance procedure during this research. As during the salt crystallization test, the lack of damage could mostly be attributed to the fact that the salt solution did not reach the inner pores, we decided to carry out the freeze-thaw test under constant immersion. This way the higher saturation value of the andesite was assured, which is a basic criteria for the ice to cause damage (Hirschwald 1908; Chen et al., 2004; Ingham, 2005; Takarli et al., 2008 etc.). Nevertheless, significant damage did not occur.

The next important property of a stone material that determines its susceptibility to frost damage is its pore size distribution (Torraca, 1982; Chen et al., 2004; Bourgès, 2006). The high proportion of micropores in the andesite acts against the freezing process because of the freezing point depression. This means that in small pores the water can exist in supercooled state due to the higher pressure in small pores and larger crystal-water interface curvature (Camuffo, 1992; Coussy 2005), so thus, in part of the pores of the andesite the freezing did not even happen during the test. However, lowering the temperature below -15°C did not seem a realistic approach.

Exactly because of the freezing point depression phenomenon, the most dangerous pore size range for the frost damage is considered to be between 0,1 and 1-2 μm (Torraca, 1982; D'Have and Motteu 1968) or 1-5 μm by others (Bourgès, 2006) because these are the pores where the freezing will surely happen, but which are still small enough to become easily saturated. If we take a look at the pore size distribution of the Szob andesite, the 0,1 and 1μm interval is almost completely missing from its pore structure. In the pores smaller than 0,1μm, the freezing point depression will inhibit the ice formation, so it is only the >1μm class, where any damage can be expected. Probably this is the reason why the only detected change is linked to the increase of this pore size range.

Still, due to the small original amount of this pore size, the damage that took place during the 250 cycles of freeze-thaw can be considered minimal, meaning that the Szob andesite is highly resistant to frost damage.

6.3.4 Correlation among parameters - Conclusions

The discussed results can be summarized in the following points

- The Macael marble is the most susceptible to frost weathering of the three investigated stone types
- The thermal effect is damaging on low temperature ranges, as well
- The thermal cycles caused the opening of the porosity of the marble, which allowed the damaging effect of the ice formation. The process finally resulted in the formation of macropores.
- The Vilachán granite is also susceptible to frost weathering due to its high open porosity
- The frost weathering is less damaging to the granite than the salt crystallization
- The Szob andesite has low susceptibility to frost weathering. The high degree of saturation was guaranteed by the constant saturation so the lack of damage is not due to the badly connected porous network but to the small average pore size
- The importance of the void size distribution and the fundamental role of the 0,1 – 10 μm range in the frost weathering was proved
- The parameters that best described the damage were the Vp, the capillary coefficient and the open porosity for the marble, and the Vp for the granite

6.4 Frost resistance with salt solution (SFT)

6.4.1 Procedure

There is no European standard for this test for natural stone, although its serious effects were observed on natural stone as well as on other types of construction materials (concrete, aggregates) (Wessman, 1997, Pétursson, 2005; Lidnqvist, 2007b, etc). To establish the process of this test the NT BUILD 485 (frost resistance of aggregates), the RILEM TC 117 FDC (frost resistance for concrete) and the above described freeze-thaw test were taking into account.

6 cubes of 5x5x5 cm and 8 slabs of 2,5x2,5x1 cm for the andesite and 16 of the same samples for the marble and granite (all orientated) were used. The samples were dried till constant weight at 60°C before the test and after recording their dry weight (w_0) they were saturated by a 1% NaCl solution. The cycles consisted of a 12 hour freezing phase at -20°C and a 12 hour thawing phase at 20°C. The temperature and the time range were widened compared to the freeze-thaw test because of the lower freezing point of the salt solution. The samples were kept in total immersion all through the test. The total number of cycles was 50. The loss of weight was detected after every 12 cycles and samples for microscopic investigation were taken by the same intervals. After the 25^{th} and the 50^{th} cycles the samples were cleaned and dried and the dry weight loss, the US propagation and the hydraulic properties (water absorption, desorption and capillary uptake) were measured. Hg intrusion measurement was carried out after the test.

6.4.2 Results – Evaluation of changes

Visual observation

The visual observation of the cubic samples was carried out continuously. In contrast to the former tests, here the Silvestre Vilachán granite was the only one that showed any visible signs of alteration, in the form of granular disintegration (fig. 6.17a). On the Macael marble no changes could be observed, while on the Szob andesite the pre-existing macro-fissures widened a little bit (fig. 6.17.) but otherwise there were no observable sings of degradation.

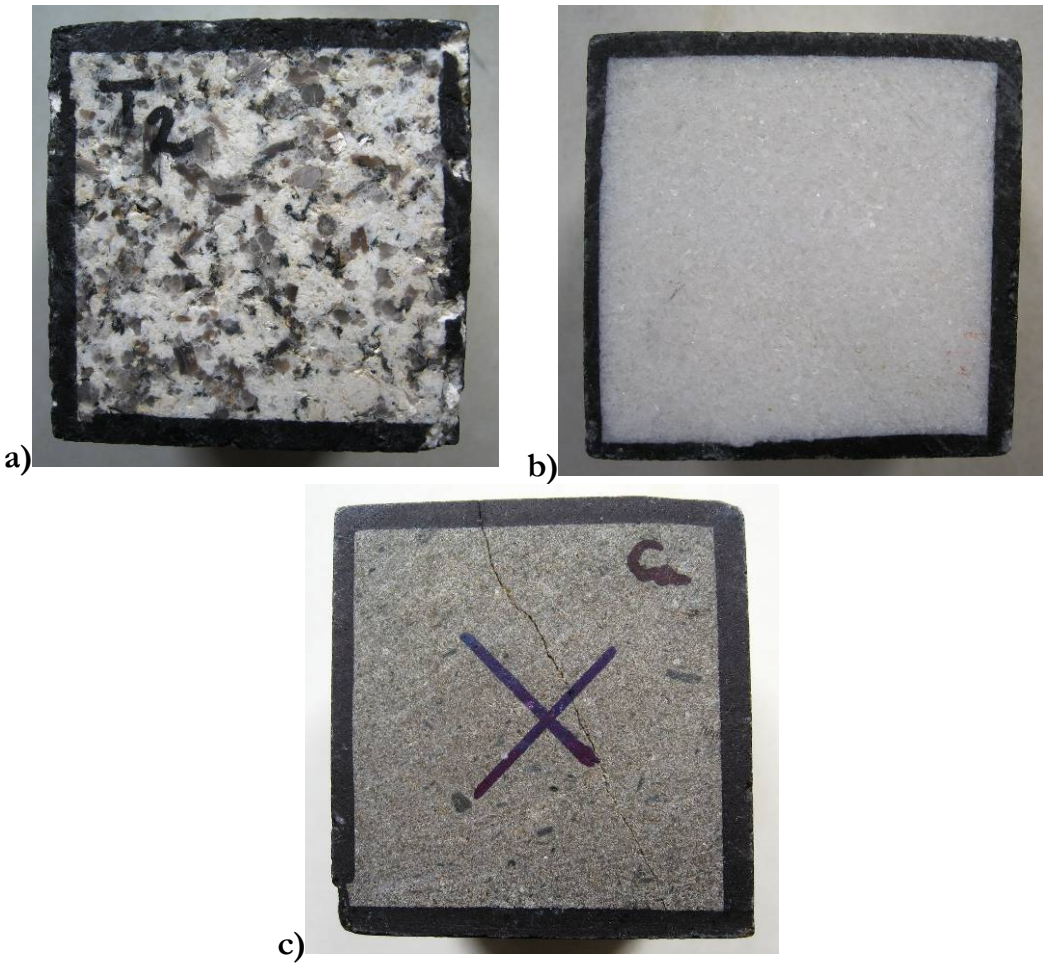

Fig. 6.17 The Silvestre Vilachán granite (a) is the only one of the three stones that shows macroscopical deterioration after the SFT cycles. The Macael marble (b) and the Szob andesite (c) did not suffer visual changes.

Weight loss

The weight loss was measured after 25 cycles (the middle of the test) and at the end of the 50 cycles. In both cases the samples were washed in order to remove the salts form the void space and dried till constant weight. The values are shown on figure 6.18.

As in the formal tests, the granite suffers the highest weight loss, although the value is lower than both in the case of salt crystallization and freeze-thaw test. The second highest weight loss is that of the marble, about -0,2% by the end of the test, which is higher than the same value in the two former tests. The andesite detects a weight gain of +0,15% after the 25th cycle, due to the salt accumulation in the micropores, from where they were impossible to remove. However, by the end of the 50 cycles the loss of weight of the andesite is around -0,09%, which is higher than the loss after 250 cycles of freeze-thaw. This means that the weight loss due to the damage overcomes the possible weight gain of salt accumulation.

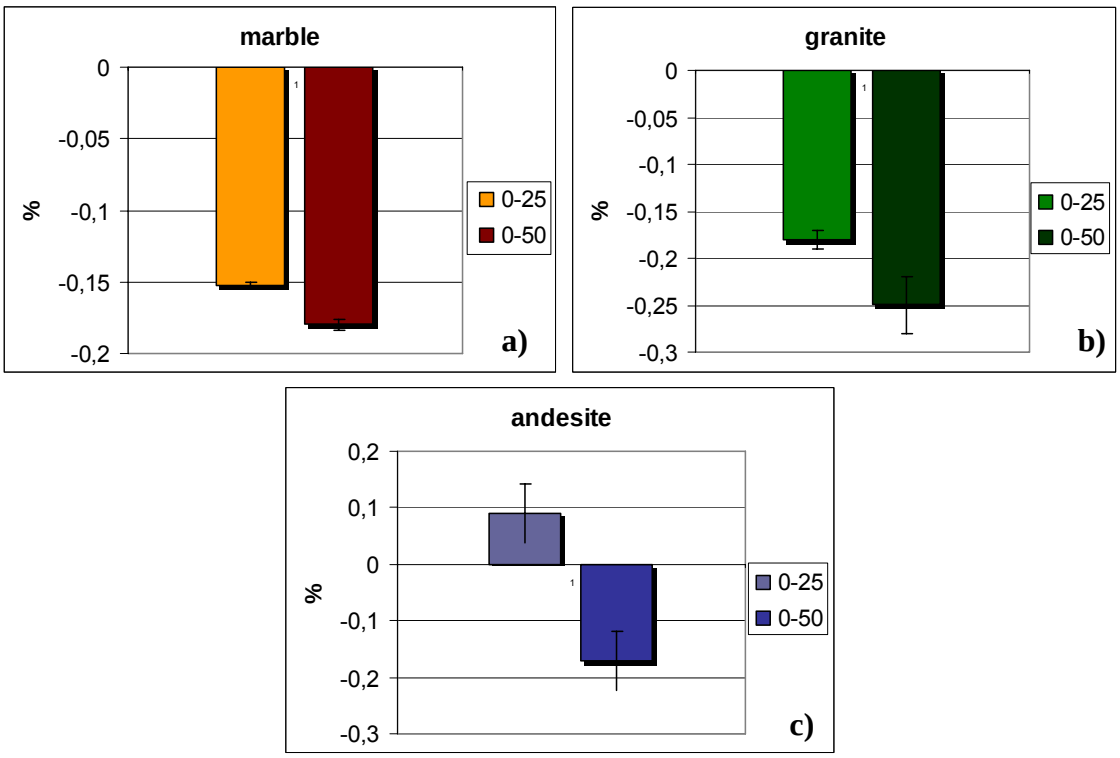

Fig. 6.18. The weight loss of the Macael marble (a), Vilachán granite (b) and Szob andesite (c) after 25 and 50 cycles of STF

US velocity

The velocity of the ultrasonic propagation was measured at 25 and at 50 cycles on cleaned and dried samples. The P wave velocities values are shown in figure 6.19.

The marble suffers the highest decrease, about -25%, mostly during the first half of the test. The average Vp change of the granite is around -12%, similar to the freeze-thaw test. While the andesite, in accordance with the weight loss measurements, increases its Vp during the first 25 cycles, and the decrease only starts in the second half of the test, although the final value is still higher than the original one.

The evolution of the pore shape factor of the marble and the granite are very similar to that during the frost resistance test. The values increase gradually proving the appearance of new cracks in the materials. The final values of the marble are 0,50; 0,41 and 0,41 in the T, M and N directions, respectively; and of the granite 0,47; 0,39 and 0,39 in the T, M and N directions, respectively. The response of the Szob andesite is somewhat different in this case than in the former tests. The Psf values increase gradually after the first and the second 25 cycles of this test, although the final value (an average 0,042) still proves the dominance of pores among the voids.

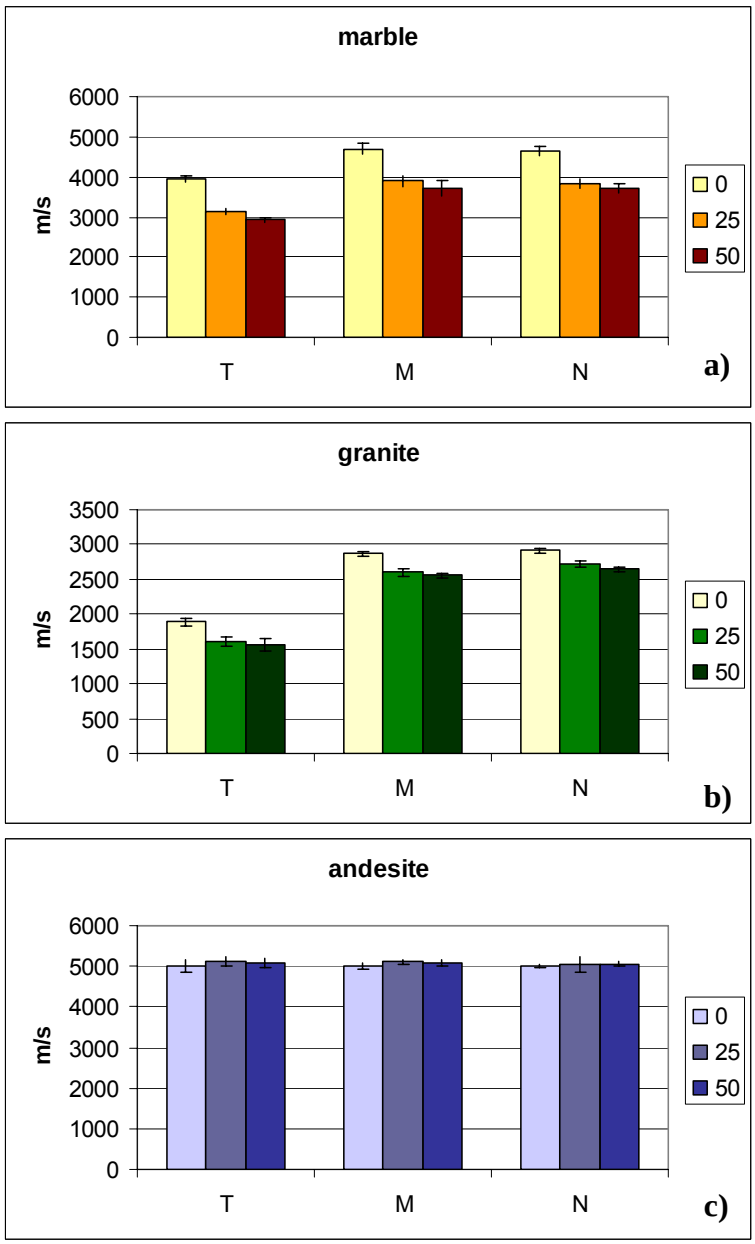

Fig. 6.19. The changes in the Vp of the Macael marble (a), Vilachán granite (b) and Szob andesite (c) after 25 and 50 cycles of STF

Void space

The evolution of the void space was monitored during the test by means of CLSM and by Hg porosimetry after 25 and 50 cycles. In figure 6.20 the changes in the open porosity at different size ranges are presented. No significant variations of the specific surface and the linear crack density were observed.

A significant increase of the open porosity can be observed in all the three stones after the test. The void size distribution patterns are similar to the former tests with one exception: in this test the largest void size range (>1μm) seems to play the most important in all the materials. The Macael marble gains an approximately 1,4% open porosity and besides the largest interval, its again the intermediate range that increase the most. The open porosity of

the Vilachán granite is around 8-9% after the 50 cycles, which is far the highest value compared to the other tests. The largest size ranges are the most affected. The Szob andesite also suffers a higher increase than in the former tests but the size distribution is similar as before.

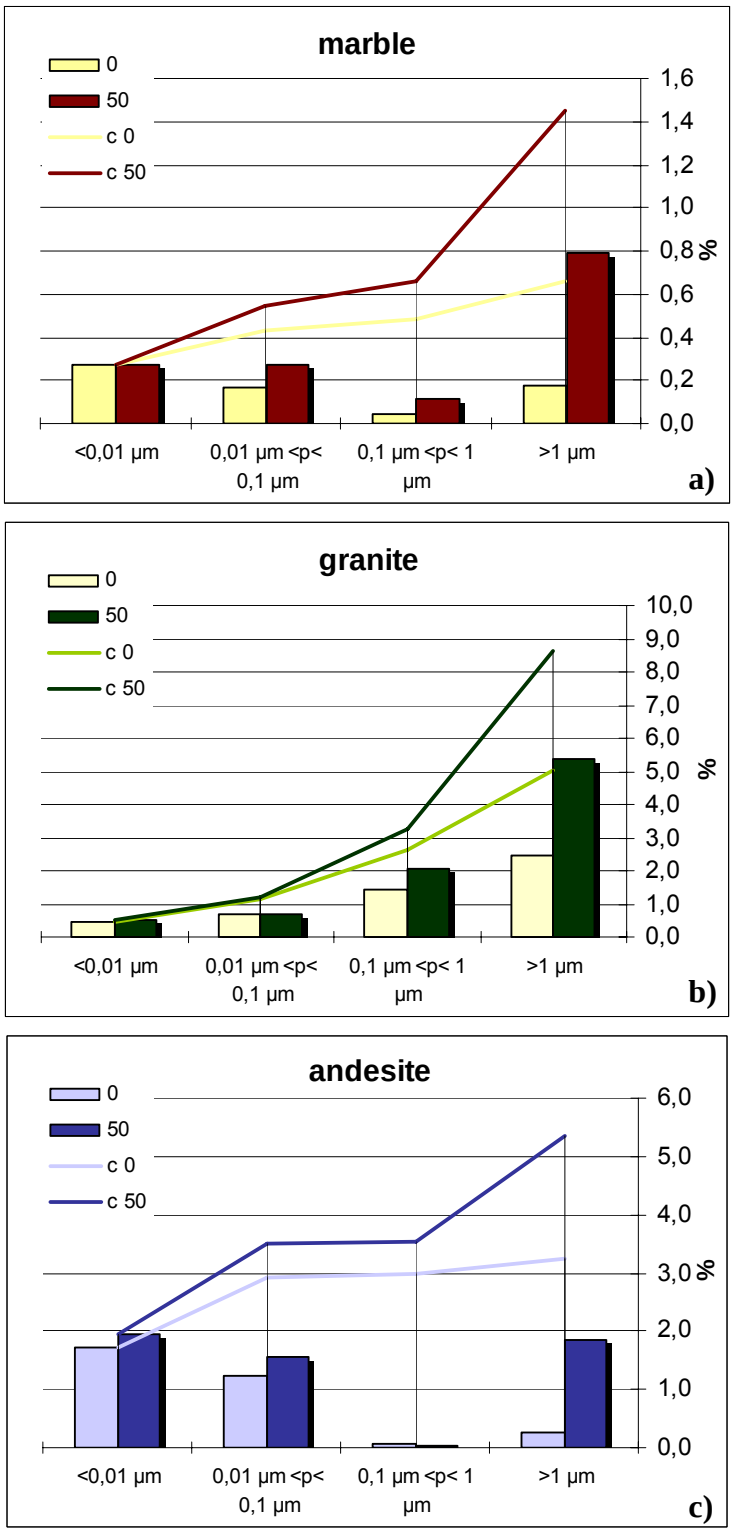

6.20. The evolution of the void space of the Maceal marble (a) , Vilachán granite (b) and the Szob andesite (c) during the 50 cycles of SFT test. Columns: absolute values; Lines: cumulative values.

Hydraulic properties

The water absorption and the capillary uptake were measured on cleaned samples before the test, after the 25th cycle and after the 50th cycle. The values are shown in the table 6.5.

Table 6.5

		original		after 25 cycles		after 50 cycles	
		average	st.dev.	average	st.dev.	average	st.dev.
water absorption (5 day water content (%))	**marble**	0,17	0,004	0,23	0,009	0,18	0,00
	granite	1,65	0,05	1,55	0,04	1,78	0,07
	andesite	1,02	0,03	1,01	0,03	1,0	0,20
capillarity coefficient ($g/m^2s^{0,5}$)	**marble T**	0,58	0,02	0,7	0,2	1,4	0,4
	marble M/N	0,8	-	0,8	-	1,4	-
	granite T	19	0,8	21	1	22	0,4
	granite M/N	19	1	25	-	28	-
	andesite	1,8	0,3	1,5	0,4	1,9	0,3

6.5 The changes of the water absorption and capillarity uptake values due to the SFT test.

There are no significant or tendentious changes in the water absorption in neither of the stone types. The final values of the marble and the granite are somewhat higher than the original ones, but the changes are very low, they may be within the detection error of the measurement. The values of the andesite are practically constant.

On the other hand there is a significant increase in the capillarity uptake of the marble in both directions, but the changes only occur during the second half of the test. During the first 25 cycles there are no noticeable changes. It is interesting to notice that in this case, it is the T direction that suffers the larger damage.

The granite shows a lower but continuous increase of capillarity, somewhat higher in the M/N direction. While the andesite, in accordance with the other parameters, decreases its capillarity uptake during the first half of the test due to the blocking of the pores by the salt, and shows a very slight increase in the second 25 cycles.

6.4.3 Discussion

There are differences and similarities in the results of the SFT test compared to the former ones.

The Macael marble suffered the highest damage so far. It has a more severe weight loss than during the other two bulk ageing tests and the same decrease in the ultrasound velocity as in the freeze-thaw test, although the number of cycles was significantly lower. On the other

hand, no material loss can be observed by the naked eye, which is somewhat surprising considering the high weight loss. The capillary coefficient increases significantly, but not the water absorption. All these results suggest that the effect of the thermal cycles produced the same effect, meaning the micro-cracking or loss of cohesion among the calcite grains (proved by the P-wave velocity) but the other mechanisms may be different from the processes observed in the former tests. According to the literature (Valenza, 2005; Valenza and Scherer, 2007b etc), the salt frost damage has an important superficial component. Nevertheless, no signs proving the presence of this scaling effect were observed on the Macael marble. The significant increase in the larges void size range on the other hand, shows that the coarser voids have some importance in the process, but the constant water absorption suggests that these newly formed coarse voids do not evolve in all the sample but probably only close to the surface, enhancing the velocity of the capillarity uptake. The chemical effect due to the higher ionic strength of the salt solution cannot be excluded from the process (Orkuola and Koutsoukos, 2001).

The Vilachán granite presents a more evident material loss after the test. The detachment of grains, which mostly appears on the edges and corners but also on the surface of the sample, is a lot more significant after these 50 cycles than it was after even 100 cycles of freeze-thaw. This proves that there must be other mechanisms taking place in this test than the only crystallization and hydraulic pressure due to the ice formation. The higher surface roughness of the granite ensures a stronger interaction between the surface of the sample and the ice layer outside of it (Valenza and Scherer, 2006), which may enhance the scaling effect. On the other hand, the improving hydraulic properties and the increase in the total porosity show that this superficial process is not the only one present. The decrease in the ultrasound velocity also proves that internal damage took place during the test resulting in the formation of new micro-cracks. The increasing anisotropy also points out the role of the crack-network of the granite in the damage. The augmenting ratio of the coarser pores can be observed here again, just like in the Macael marble.

The Szob andesite shows quite a different behaviour during the test compared to the other two stones. The most important process in this case, especially during the first 25 cycles, is the uptake of salts into its porous space. This results in the increase of weight, increase of P-wave velocity and decrease of hydraulic properties, as the salts block the path-ways of the fluids impeding their circulation. This is a somewhat unexpected observation, as during this test the crystallization of salts has a very low probability due to the low concentration of the solution (Williams and Robinson, 1991). However, the behaviour of the andesite suggests that due to the ice crystallization the concentration of the solution reaches the saturated level and salt crystallization also occurs, at least in some of the pores. The other possible explanation is that the salt crystallization takes place when the test is interrupted and the samples are cleaned and dried for the measurements. As it was learnt in other tests, the complete removal of the salts from the porous space of the andesite is almost impossible due to the very low connectivity. However, by the end of the 50 cycles, the weight loss due to the damage overcomes the weight gain due to the salt uptake proving that the deteriorating processes

affect the andesite, as well. Superficial material loss cannot be observed at all, but the pre-existing cracks started to open up. This evidently points out the importance of the (ice) crystallization pressure, which takes place inside the material. The increase in the highest pore size range – just like in the Macael marble, and the Vilachán granite – was detected in this material, also.

In summary, we can state that the effect of the frost in the presence of the salt solution was somewhat higher than in pure water. For all of the stone types, the weight loss is equal or higher after 50 cycles of SFT than after 250 cycles of freeze-thaw; and the other measured parameters also move in a very similar range.

The most outstanding observation is the increase of the quantity of the largest pore size range, in all the stones. This infers the increase of the open porosity but not the increase of the water absorption, which suggests that it may be rather a superficial effect. On the other hand, the intense superficial mechanical degradation (see frost salt scaling effect) was not observed on the samples. On the contrary of the opinion of Valenza and Scherer (2006; 2007 a, b) these results prove that the ice formation inside the porous space of the stones play an important part in the damage. The amplified damage proves the presence of other mechanisms also, which may be the osmotic pressure due to the change of the solution concentration at the pores, where freezing takes place (Lindquist et al., 2007). The importance of the higher saturation degree due to the decreased vapour pressure of the solution (Camuffo, 1996) was not proved, as the constant immersion maintains a high saturation degree all along the test.

Due to the freezing point depression of the salt solution, the freezing probably takes place in the largest pores only and in the parts closer to the surface, which are the first one to reach the lowest temperatures. This would explain the increase in the proportion of the largest pore size range in all the stones, which not necessary results in higher water absorption.

6.4.4 Correlation among parameters – Conclusions

- The Macael marble is the most susceptible to the effect of frost in the presence of soluble salts of the three stone types
- The damage of the marble caused by the SFT cycles is higher than the frost in pure water or the salt damage
- The thermal degradation has the same importance on the marble during this process than in the former tests
- The possible chemical effect between the salt solution and the calcite may enhance the degradation of the marble

- The Silvestre Vilachán granite is also susceptible to the effects of the SFT test
- The frost damage suffered by the granite is more severe in the presence of salts than in pure water
- The Szob andesite shows low susceptibility to the SFT test but it suffers higher damage than in the freeze-thaw test
- The >1μm void size range is the most affected by the process, which is probably due to the freezing point depression of the salt solution, which impedes the freezing in the smaller voids
- The freezing in general proved to be more damaging in the presence of soluble salts than in pure water
- Severe surface scaling (so typical on concrete) was not observed on the stone samples. The enhanced damage may be due to other additional mechanisms, such as the osmotic pressure.

6.5 Salt mist

6.5.1 Procedure

The determination of resistance to ageing by salt mist was carried out based on the European standard EN 14147:2003. Again some small changes of the standard were included in the procedure. On one hand, the concentration of the NaCl salt solution was decreased from 10% to 5%, as this concentration was found to be sufficient to cause serious damage on stone materials and is closer to an average natural value. On the other hand, the duration of the drying phase was increased from 8 hours to 20 hours to emphasise the salt crystallization effect even more. And finally, 5x5x1 cm samples were used instead of 5 cm cubes, as the important dimension in this test is the surface exposed to the mist, which is the same. 6 of these 5x5x1 cm slabes were used of each stone type and also smaller samples (2x1x1 cm), which could be investigated by microscopy directly, without further sample preparation.

The samples were exposed to 4 hour salt mist with 5% NaCl solution and then left drying during 20 hours. The entire test (90 cycles in total) was carried out at room temperature. The samples were cleaned and dried at 60°C after every 30 cycles for the measurements.

6.5.2 Results – Evaluation of changes

The effects of the salt mist test were evaluated by the monitoring visual changes continuously. Besides, samples for microscopy were taken every 10 cycles; the clean, dry weight and the surface roughness were measured every 30 cycles; and the colour and the water vapour permeability were measured before and after the test. As this test provokes a superficial effect only, the surface properties are more probable to show changes but also a small loss of weight can be expected, if the crystallization of salt crystals provokes physical damage.

Visual observations

During the drying phases of the test the halite forms crystals of variable size on the surface of the samples. This could be observed on all the stone types, but the most evident was on the surface of the andesite because of the darker colour of this stone (fig.6.21). There were no visual signs of deterioration during the first 60 cycles on any of the stone types. During the last 30 cycles loss of grains could be observed on the surface of the granite samples (fig.6.22), while the marble and the andesite still remained intact.

Fig. 6.21. Halite crystals on the surface of the Szob andesite during the salt mist test.

Fig. 6.22. The Silvestre Vilachán granite suffers a slight loss of material during the 90 cycles of salt mist test.

Observations by SEM

By means of the scanning electron microscope the deterioration of the stones due to the superficial salt crystallization can be observed in details. Samples for this purpose were taken after every 10 cycles in order to follow the weathering processes continuously and they were examined without removing the salts. The first and most evident effect of the test is the crystallization of halite on the samples. Salt crystals of different habit and size can be observed on the surface of the samples at the different phases of the test. Sometimes the salt forms an almost homogeneous layer covering all the surface of the sample, which very often breaks exposing parts of the material surface to the further damage (fig.6.23-25.).

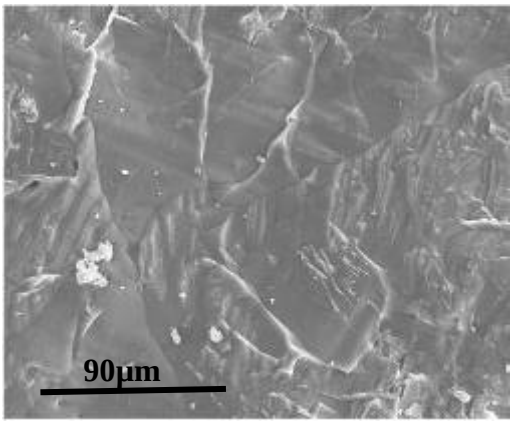

Fig. 6.23. Continuous salt layer covers the surface of the marble after 10 cycles of salt mist.

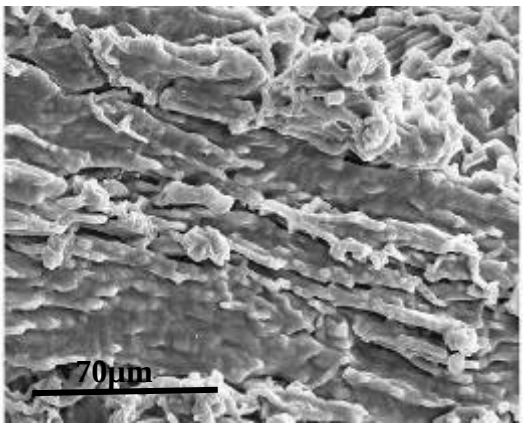

Fig. 6.24. The salt crystals cover the laminae of muscovite of the granite after 40 cycles of salt mist.

In other cases independent crystals are formed, which may be of rectangular shape (typical crystal form of the halite) or xenomorf (fig.6.26-27). Salt crysalts can be observed inside the pre-existing fractures of the granite, as well (fig. 6.28). The shapes and sizes of the salt crystals do not show any continuous tendency during the test.

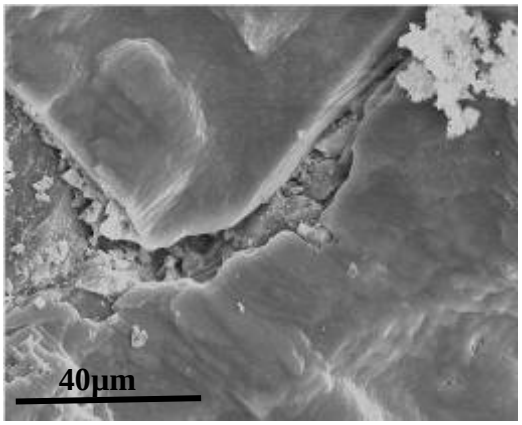

Fig. 6.25. The cracking of the salt layer on the surface of the andesite emphasises the exposure of some parts of the surface (40 cycles)

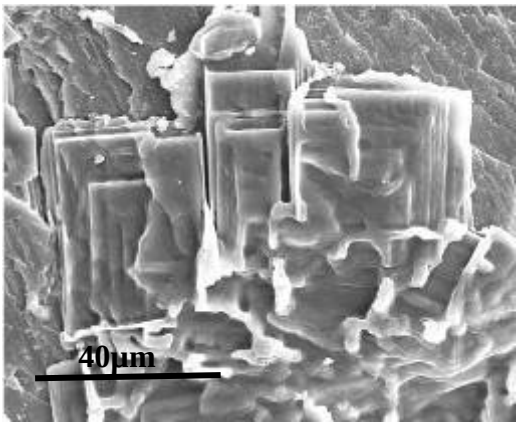

Fig. 6.26. Idiomorphic halite crystals on the surface of the marble after 60 cycles of salt mist.

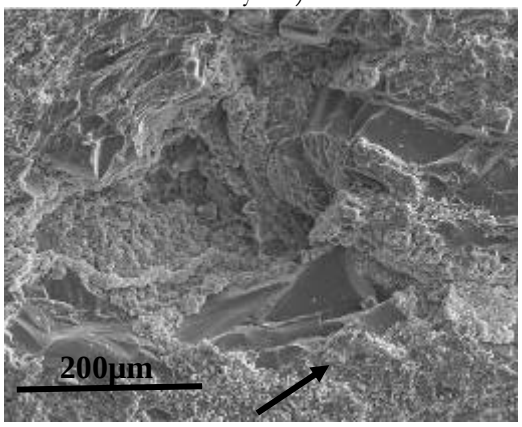

Fig. 6.27. The small halite crystals do not cover completely the surface of the granite.

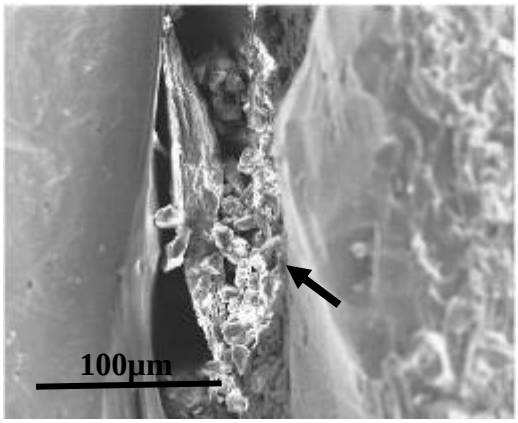

Fig. 6.28. The salt crystallizes inside a pre-existing crack of the granite.

The degradation forms observable by this technique are mostly connected either to pre-existing cracks or to mica crystals. The first type is most typical in the case of the granite, where the large number of fractures and their large apertures allow the easy penetration of the salt solution into the material. The crystallization pressure of the salt inside the cracks produces further rupture and finally loss of material (figures 6.29-30.). Similar features – the opening of larger cracks on the surface – can be observed on the andesite as well, although to a lesser degree (fig.6.31). Open fractures on the surface of the marble are not that typical, but sometimes can be observed.

The second type of damage, connected to the mica crystals, appear on all the three stone types. The salt crystallizes among the laminae of the mica, opening and finally breaking them. This type of damage could be observed already after the first few 10 cycles but with the ongoing test its effects become more and more serious. On figures 6.32-35 some photos show the effect of the salt mist test on the three stone types.

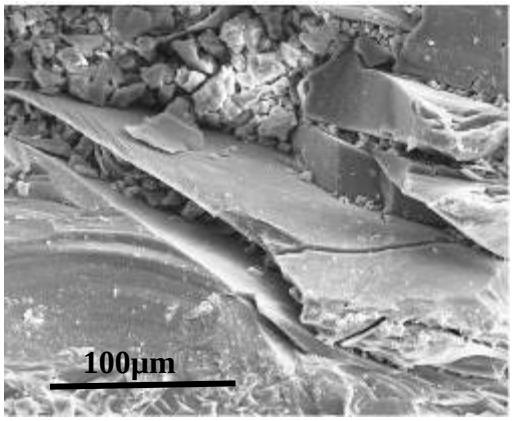

Fig. 6.29. The halite crystallizes in the pre-existing cracks of the granite causing further rupture of the material

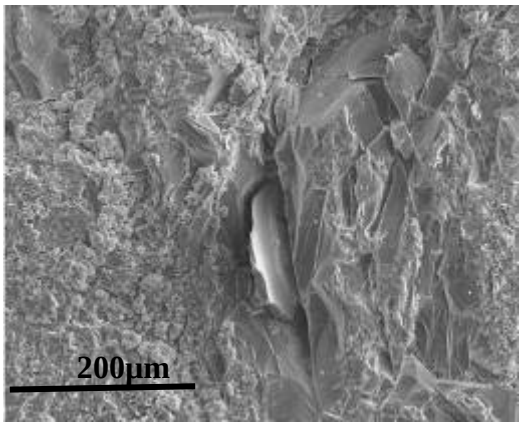

Fig. 6.30. The final effect of the salt crystallization inside the crack is the loss of material fragments.

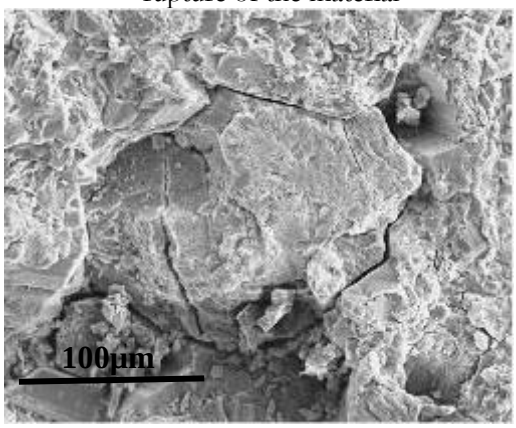

Fig. 6.31. Opening of cracks on the surface of the andesite due to the effect of salt crystallization pressure.

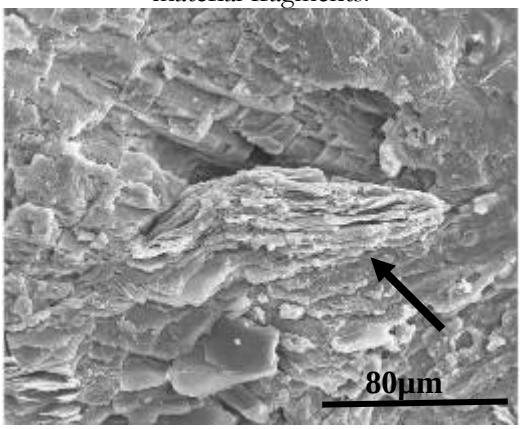

Fig. 6.32. The few muscovite crystals of the marble are the most susceptible points of this stone in front of salt mist.

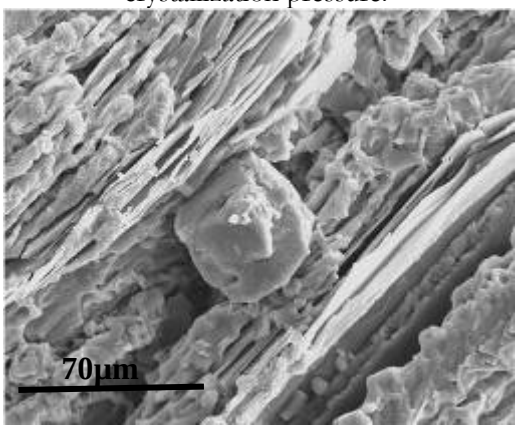

Fig. 6.33. Idiomorphic halite crystal in a muscovite crystal of the granite after 40 cycles of salt mist.

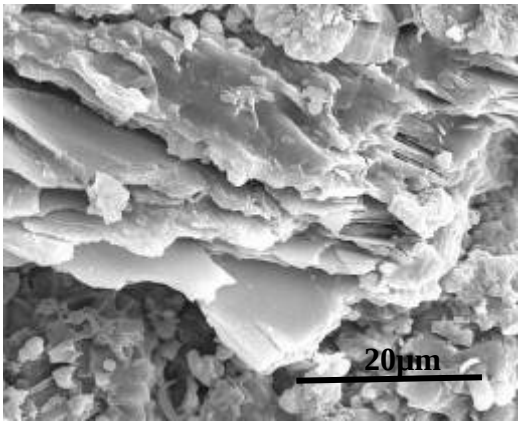

Fig. 6.34. The deterioration (opening of laminae) of biotite of the granite after 50 cycles of salt mist test.

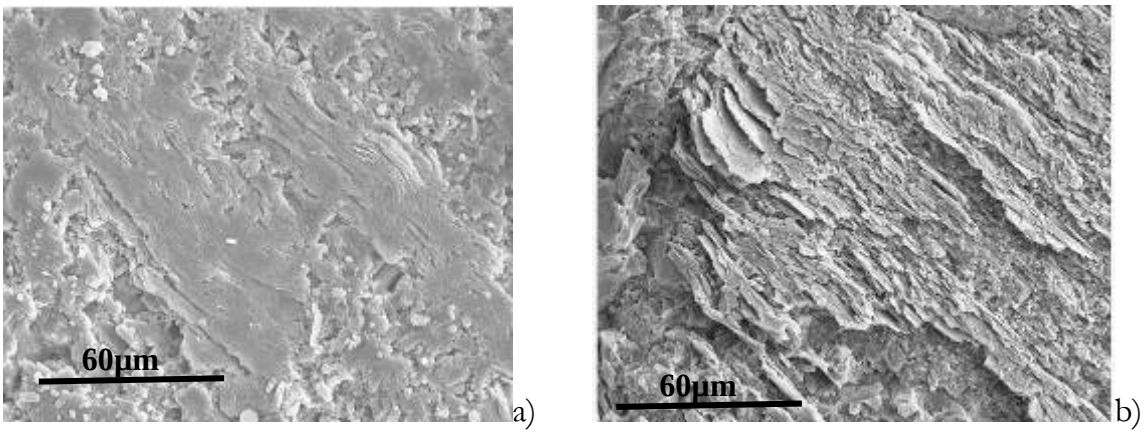

a) b)

Fig. 6.35. The ongoing deterioration of biotite crystals of the andesite after 10 (a) and after 60 (b) cycles of salt mist test.

Weight loss

The weight loss increases gradually with the increasing number of cycles for the granite and the marble. The highest value corresponds to the granite, followed by the marble. The andesite shows an increase of weight during the first 60 cycles, which is probably due to the accumulation of salts in the small voids of this material, which could not be removed by washing. Nevertheless, from the 60th cycle on the andesite suffers loss of weight, as well.

The weight loss (%) values are presented in figure 6.36.

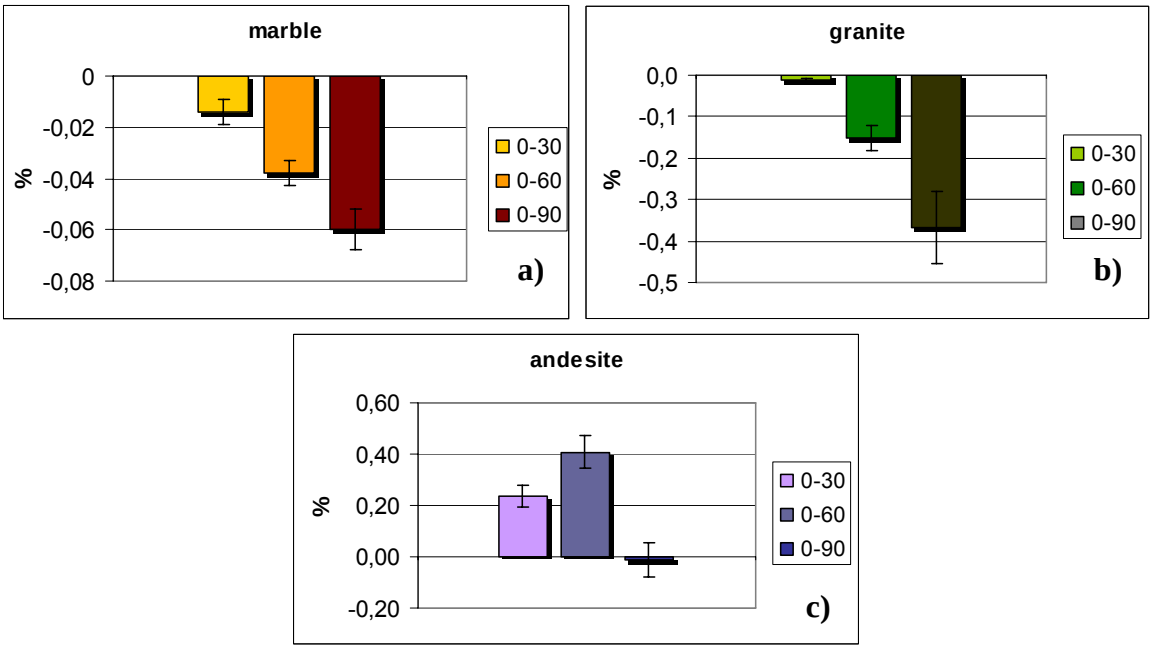

Fig. 6.36. Weight loss (%) of the materials at the different stages of the salt mist test: Macael marble (a), Vilachán granite (b) and Szob andesite (c).

Water vapour permeability

The water vapour permeability values before the test and after 90 cycles are shown in table 6.6. The highest increase was detected on the Vilachán granite, followed by the Macael marble, while the Szob andesite does not show any changes out of the range of the standard deviation of its values. It is interesting to observe that contrarily to the other tests, the anisotropy both in the marble and the granite seems to decrease, although this method did not demonstrate significant differences in the distinct directions of these stones in the original values either.

Table 6.6

		Macael marble		**Szob andesite**		**Silvestre Vilachán granite**	
		average	st.dev.	average	st.dev.	average	st.dev.
before	**T direction**	59,2	15,4	63,0	30,6	66,9	13,4
	M/N direction	47,6	11,4			87,8	8,4
after 90 cycles	**T direction**	68,6	14,0	51,2	19,3	98,1	18,0
	M/N direction	63,7	4,7			97,1	5,6

Table 6.6 The water vapour permeability values (g/m²24h) before the test and after 90 cycles. The permeability increased significantly for the Vilachán granite, slightly for the Macael marble, and did not change for the Szob andesite.

Surface roughness

The surface roughness parameters before the test, after the 60th and the 90th cycles are shown in table 6.7.

The graphical comparison of those parameters that were found representative (not the kurtosis neither the mean spacing) is presented on figure 6.37.

The responses of the three stones to the test are different in terms of surface roughness.

The mean deviation of the profile of the Macael marble increases due to the increase of the height of the peaks but the other parameters do not change significantly during the 90 cycles of salt mist test. The Silvestre Vilachán granite does not show practically any changes. Only the height of the peaks seems to increase gradually but the amount of increase does not exceed the range of the standard deviation. Finally, the Szob andesite is the one of the three stones that shows the highest changes in the surface properties; especially until the 60th cycle. The variation between the 60th and the 90th cycle measurement is lower. The increase of the mean deviation and of the maximum height of the profile in this case is due both to the

heightening of the peaks and the deepening of the valleys. Also the skewness becomes less negative showing the increasing importance of the valleys in the profile.

Table 6.7

		before		after 60 cycles		after 90 cycles	
		average	st.dev.	average	st.dev.	average	st.dev.
marble	**Ra**	2,68	0,32	3,20	0,29	3,29	0,36
	Rq	3,84	0,69	4,43	0,67	4,64	0,78
	Sk	-2,18	0,92	-1,82	0,80	-2,16	0,78
	Ku	13,3	8,6	9,5	6,8	12,4	7,6
	Rp	6,62	0,65	7,78	1,12	8,63	2,15
	Rv	29,9	11,2	29,1	10,3	34,2	10,7
	Ry	36,5	11,4	36,9	10,7	42,8	11,1
	Sm	1,90	1,92	0,45	0,21	0,79	0,73
granite	**Ra**	15,1	11,5	13,4	6,2	18,3	10,7
	Rq	25,2	20,3	19,9	9,0	27,6	16,0
	Sk	-3,00	0,55	-2,26	0,57	-2,25	0,63
	Ku	14,0	4,35	10,5	3,8	10,9	5,2
	Rp	25,6	20,8	36,0	17,6	52,3	29,9
	Rv	149	112	114	43	154	72
	Ry	175	130	150	58	206	100
	Sm	4,34	3,01	1,77	0,98	2,18	1,67
andesite	**Ra**	3,64	0,21	5,83	0,40	6,56	0,53
	Rq	5,05	0,35	7,69	0,68	8,68	0,93
	Sk	-1,95	0,41	-1,53	0,29	-1,52	0,51
	Ku	9,47	3,24	6,30	1,94	6,81	4,95
	Rp	8,28	1,64	12,77	2,00	16,25	6,86
	Rv	33,6	7,5	43,6	9,8	48,4	16,5
	Ry	41,9	7,6	56,4	11,0	64,6	18,9
	Sm	1,04	0,62	0,39	0,14	0,54	0,88

Table 6.7 The surface roughness parameters during the salt mist test

We always have to keep in mind that the lack of the tendentious numerical changes of the surface parameters may be due to the very high background noise mentioned in chapter 5, especially in the case of the granite.

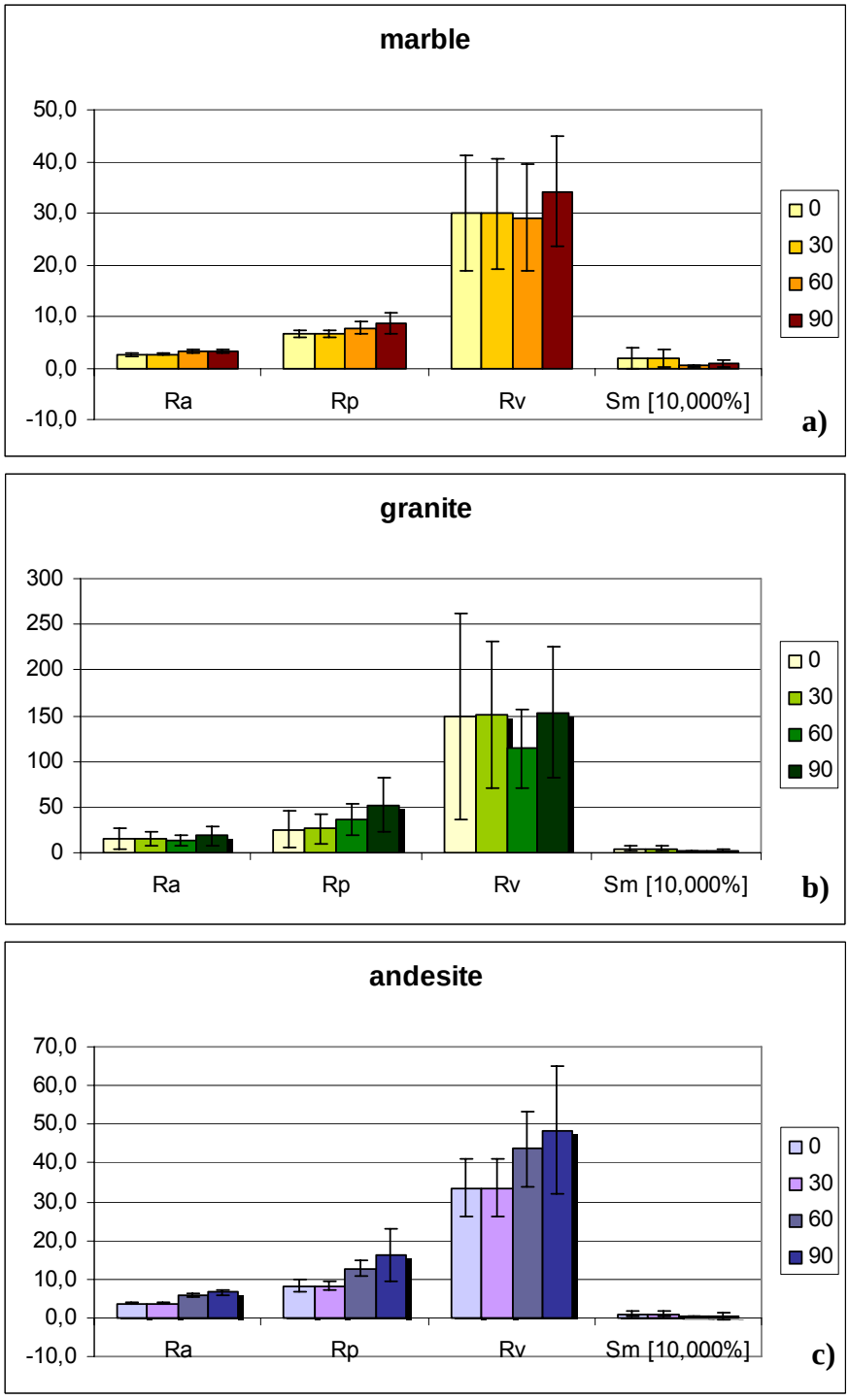

Fig. 6.37 Evolution of the surface roughness parameters during the salt mist test of the Macael marble (a), Vilachán granite (b) and Szob andesite (c).

Colour

The colour parameters were measured before and after the test on two specimens of each stone. The results are presented in table 6.8. and the changes in the a* and b* parameters can be observed on figure 6.38.

Table 6.8

			L*	a*	b*	C*	h	ΔE
andesite	before	average	43,1	-3,5	4,1	5,7	127,2	112,4
		st.dev.	1,1	2,0	0,7	1,2	18,0	
	after	average	34,6	-1,8	10,2	10,6	99,4	
		st.dev.	0,4	2,3	1,4	1,7	10,7	
granite	before	average	74,3	-1,1	5,0	5,2	101,9	8,8
		st.dev.	3,7	0,9	0,7	0,7	9,8	
	after	average	73,1	-1,3	6,8	7,0	100,8	
		st.dev.	3,9	0,9	0,6	0,7	7,0	
marble	before	average	83,2	-2,2	-0,7	2,4	196,5	5,1
		st.dev.	0,8	0,6	0,4	0,6	12,0	
	after	average	84,8	-2,5	0,8	2,6	161,5	
		st.dev.	0,5	0,7	0,4	0,7	9,8	

Table 6.8 The colorimetric parameters before and after the salt mist test

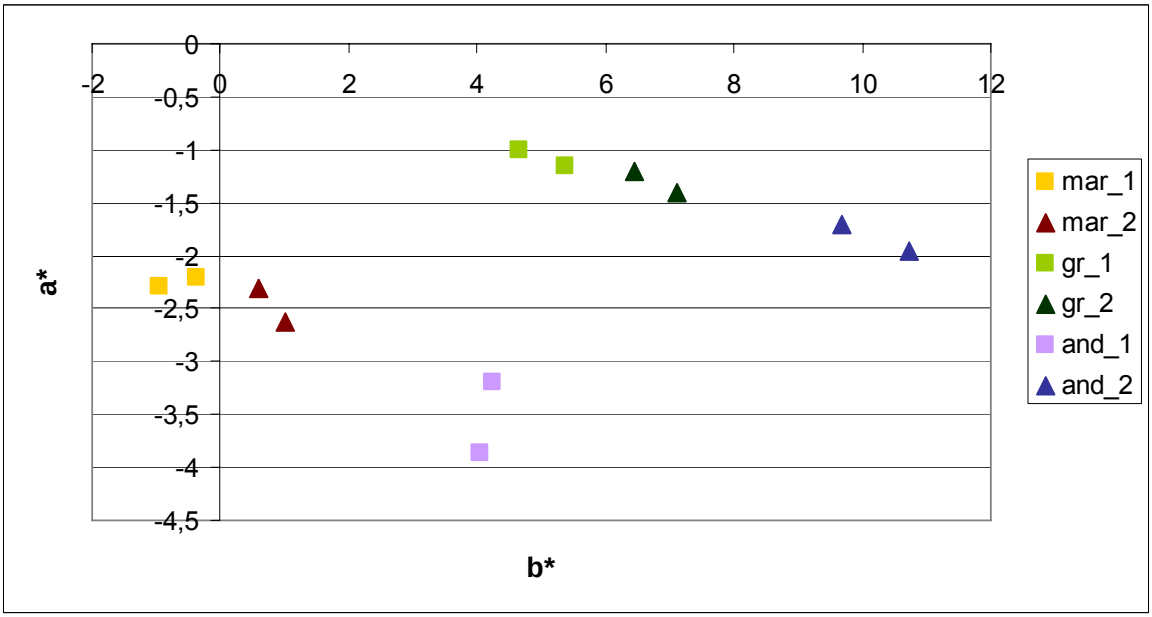

Fig. 6.38 Changes of the a* and b* colour parameters due to the salt mist test. mar: Macael marble; gr: Silvestre Vilachán granite; and: Szob andesite; 1: before the test; 2: after 90 cycles

As we can observe on figure 6.38 all the three stones show some changes in colour especially in the b* values, which means a slight yellowing of the materials. These changes are not really significant for the marble and the granite – they cannot be detected by the naked eye either – and their ΔE values, which expresses the total colour difference are quite low, 5,1 and 8,8 respectively. On the other hand the andesite presents quite an important discoloration (ΔE=112). In this case the highest change can be observed in the b* value again (yellowing), but also the a* (reddening) and the L* (darkening) values show changes. This change of colour is easily observable by the naked eye, as well (fig.6.39).

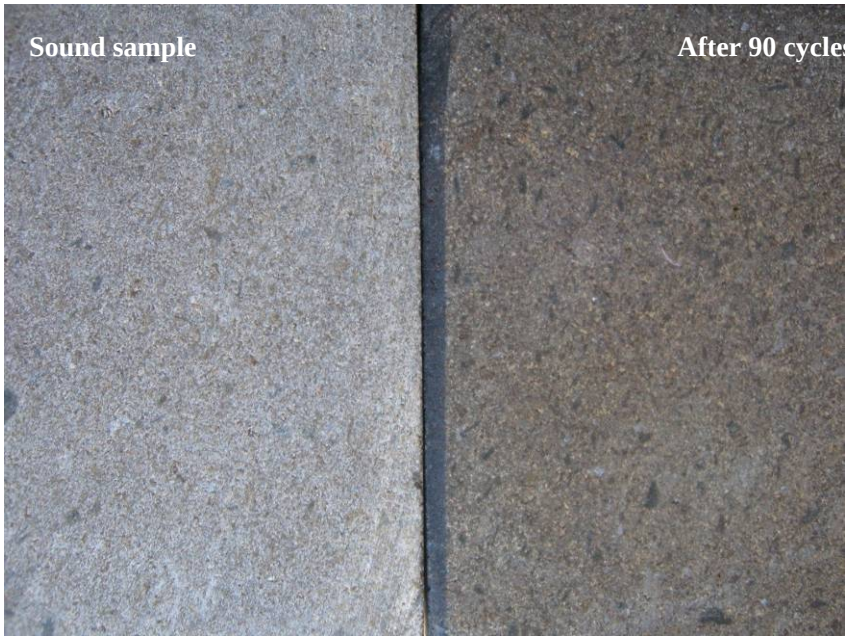

Fig. 6.39. The change of the colour of the Szob andesite after the salt mist test is observable by the naked eye.

6.5.3 Discussion

Out of the three stones, the highest damage was observed on the Silvestre Vilachán granite. This can be deduced as well from the highest weight loss, as from the damage observed by the naked eye and by means of SEM, and from the increase in water vapour permeability. The observable damage on the surface was linked to the pre-existing cracks and to the mica crystals, where the solution could enter with the greatest ease and the precipitating salts could cause damage due to the crystallization pressure. The granular disintegration is a typical weathering form of granite under these conditions (Silva et al. 2003; Chabas and Jeannette 2001). The above observations suggests, in accordance with other authors, that two important characteristics of the granite are (i) the high number of cracks (Silva et al 2003) and (ii) the high quantity of phillosilicates (Silva and Simão, 2009; Mateos and Esbert, in press), that make the granite especially susceptible to the weathering effect of salt mist.

The second highest weight loss was detected on the Macael marble. The physical damage observed by means of microscopy was again connected to the mica grains, although the amount of micas is almost insignificant in this material. Also, the low permeability of the material does not favour the entrance of the solution and the generation of high crystallization pressures. Moreover, due to the higher ionic strength of the saline solution compared to pure water, chemical degradation, namely the dissolution of calcite can be expected (Cardell et al., 2003a). However, no signs of dissolution were detected macroscopically on the marble. The samples that were examined by SEM were not cleaned samples and the salt precipitation on their surface may have disguised this kind of damage.

The slight increase of the surface roughness may suggest some superficial processes to take place. In summary, no calcite dissolution was noted during or after the test but taking into account the weight loss of the marble, we cannot completely exclude the occurrence of this weathering form.

The evolution of the weight of the Szob andesite samples suggests that at least during the first part of the test no significant damage occurred. The weight increased, showing the precipitation of salt inside the stone in the small pores, from where they could not be removed even by intensive washing. On the other hand, by means of SEM damage could be observed, similarly to the other two stones, connected to the mica grains. Here, again, the salt crystallization pressure among the laminae of the biotites encountered on the surface of the samples, results in rupture and material loss; also proved by the surface roughness increase. The weight evolution of the samples is a balance between the weight gain by the uptake of salts and the weight loss by the loose grains on the surface (Birginie, 2000). This balance only turns negative after the 90^{th} cycle for the andesite, showing the relatively large resistance of the stone in front of this weathering agent. The significant colour change, on the other hand, introduces a new aspect to the matter. Changes in colour are typically linked to chemical processes, such as oxidation etc. Nevertheless, although the chemical reaction of calcite is well-known and well-accepted in the literature (Zezza and Macri, 1995; Birginie, 2000; Cardell et al., 2003a), significant chemical degradation is not expected in the case of this andesite. Furthermore, no other signs suggesting any such degradation process were observed. Otherwise, the presence of the precipitated halite right under the surface may cause changes of the colour, which seems a more plausible explanation. This, anyway, does not diminish the importance of such change in the case of a monumental or ornamental stone, which may decrease its worth significantly.

The mechanism of the whole process, also observed in natural conditions (Chabas et al., 1999; Chabas and Jeannette, 2001 etc.), is that the halite deposited on the stone samples dissolves as the RH rises above 75% - in the laboratory test it means the next wetting phase – forming a brine on the surface. Then this solution enters into the stone by capillarity – to a depth determined by the permeability of the material – and in the drying phase it precipitates. The position of the precipitation compared to the surface will also be a function of the water kinetics; which is determined by the void space, the environmental conditions (RH, T) and the properties of the solution (concentration, viscosity etc.) (Ruedrich and Siegesmund, 2006; Cardell et al., 2008). During the laboratory test the environmental conditions and the solution properties are kept constant, so the determining factor will be the void space.

The damage is caused by the pressure that the growing crystals of the precipitating salt exert on the pore walls during the repeated wetting and drying phases (Birginie, 2000). The mechanism is the same as during the salt crystallization test, and following the same theoretical approach, some authors (e.g. Theoulakis and Moropoulou, 1997; Moropoulou et al., 2003) tend to explain the salt mist - susceptibility of a stone considering the pore size distribution only, based on the relation of the crystallization pressure and the pore dimensions (after Fitzner and Snethlage, 1982). However, this theoretical approach has proved to be

incorrect or incomplete in other studies (e.g. Cardell et al., 2003a, b); and it does not serve as an explanation to the results of this work either, as out of the three tested stones the one with the smallest average void size suffered the less damage and the one with the larges pores the most damage. This proves that we have to look for other stone properties that govern the degradation processes and so the susceptibility of the stones.

Besides the crystallization pressure, the position of the crystallization and the amount of salts in the material are crucial points of the process. Both of these factors are determined by the solution kinetics in the solid, as it was mentioned above (Chabas and Jeannette, 2001).

In this scenario, both the transport in liquid and in vapour phase plays an important part; the first one in the wetting, the second one in the drying phase. The transport of the liquid is governed by capillarity forces (Lewin, 1982; Cardell et al., 2008; etc), which requires a well-connected, well-communicating capillary network to be effective, otherwise the saline solution cannot enter into the material. According to the observations of Goudie and Viles (2007), the concentration of the salts inside the rock is affected by the ease with which the water enters. The vapour transport on the other hand, is determined by the specific permeability of the material, which is directly proportional to the square of the radius of the "tube" where the flow occurs (Cardell et al., 2003a), meaning the void size. This means that the large pores make possible the fast evaporation of the water and provide that the salts will crystallize deep under the surface of the stone causing damage.

Both of these considerations suggest that without a well-communicating void network the salts will not enter to the material and no subflorescence will occur. Once these conditions are satisfied, the theoretical calculations of the crystallization pressure according to the pore size distribution can be relevant, but without them, they do not describe sufficiently the damage process.

This is the reason why the damage caused by the salt mist test is insignificant for the Szob andesite, because its very low permeability and capillarity impedes the entrance of the salts to the interior of the stone. Consequently, the high permeability of the granite makes this material the most susceptible out of the three stones. The Macael marble exhibits good susceptibility as far as the physical process is concerned, but the dissolution of calcite increases its porosity and so with time the increasing permeability will expose it to the crystallization pressure also, as it is often observed under real conditions (Zezza and Macri, 1995; Torfs and Van Grieken, 1997; Chabas et al., 2000).

6.5.4 Correlation among parameters – Conclusions

- The Silvestre Vilachán granite is the most susceptible to the effects of salt mist of the three stone types

- The properties that make the granite especially susceptible are (i) the high open porosity and high surface crack density, which results in a high permeability and fast capillary uptake, and (ii) the high amount of phyllosilicates

- The Macael marble shows a relatively high resistivity to the salt mist due to its low porosity and capillary uptake and thanks to the lack of the thermal effect

- The dissolution of calcite was neither proved nor disproved by this test

- The Szob andesite has a low susceptibility to the physical damage caused by the salt mist but it suffers a significant visual change due to the salt uptake

- The most important properties that determine the degree of damage during this test are those characteristics of the material that control the uptake of the solution, as both the amount of solution and the time of exposure is significantly less than in a process via immersion. These properties are the capillary uptake and the permeability, which are controlled by the open porosity and the crack density

- The pore size distribution does not seem to have influence on the damaging process

- The phyllosilicates are the most susceptible material phase to the effect of salt mist, so their quantity in the stone influences its susceptibility

- The most useful parameter in the evaluation of damage was the weight change

- The highest colour change was detected on the andesite partly because of (i) the highest probability of salt uptake in this material, and because of (ii) its dark colour which makes it more sensitive to chromatic changes

- The surface roughness measurement by means of a contact profilometer did not prove to be useful on non-polished stone surfaces

6.6 Action of SO_2 in the presence of humidity

6.6.1 Procedure

The resistance to ageing by SO_2 action in the presence of humidity was determined following the European standard EN 13919:2002.

Again, as in the former tests, besides the samples required by the standard (12x6x1 cm), smaller samples (2x1x1 cm) were also used. Two types of solution of SO_2 were prepared of H_2SO_3 and distilled water; one with higher (3,85%) and another one with lower (1,15%) concentration. According to the standard procedure visual observation and the detection of weight loss were carried out after 21 days of exposure on the large samples. Besides, the surface roughness and the colour changes were also measured at the end of the test. Small samples were taken for SEM investigation after 7 and 21 days of exposure. The XPS measurement of the surface chemical composition was carried out after one week of exposure. In both of the later cases the stronger solution was used.

6.6.2 Results – Evaluation of changes

Visual observation

The visual changes are quite significant in all the three cases, although not to the same extent. On the figures 6.40 – 6.42 we can observe on the left hand side (a) the samples after 21 days of exposure to the high concentration solution without cleaning; and on the right hand side (b) the samples after cleaning with water and drying. The visual effects after treatment with the weak or the strong solution are similar, but they are more pronounced in the later case.

On the Macael marble, as it can be seen on figure 6.40/a, besides the white needle-shaped gypsum crystals covering large part of the surface, dark yellow stains appear. This discolouration occurs only on the lower part of the samples. Part of the discolouration can be removed by washing (fig. 6.40/b) but not completely.

The Silvestre Vilachán granite also shows a significant yellowing, this case homogeneously on the entire surface. Observed under a magnifier glass (fig. 6.41/a, magnified detail) the discolouration is evidently connected to the biotite grains, so the effect is due to the oxidation and mobilization of the iron of this mineral. The colour remains similar after cleaning, as it will be probed by the colorimetric measurements, although the bright yellow colour turns more brownish and rusty.

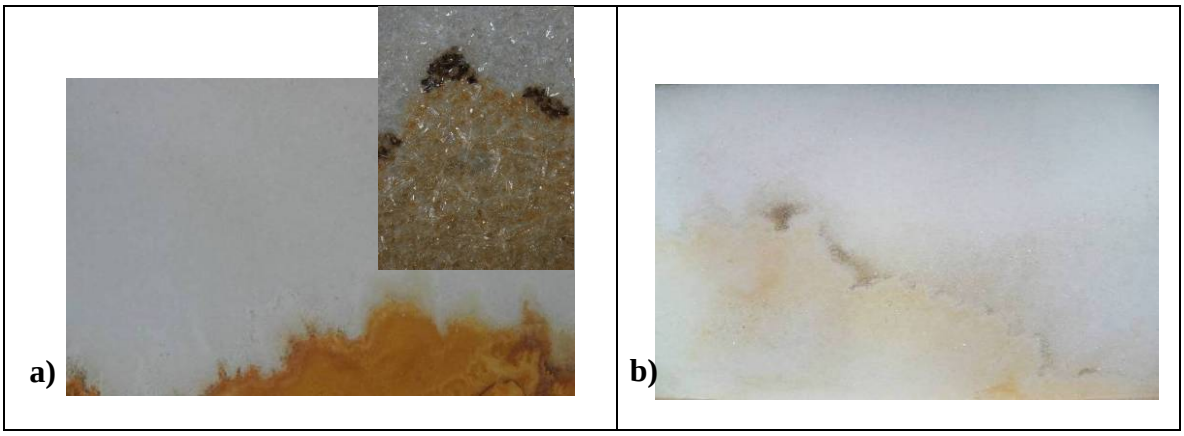

Fig. 6.40 The yellow stains that appear on the surface of the Macael marble due to the effect of SO_2 (a) can mostly be removed by cleaning (b)

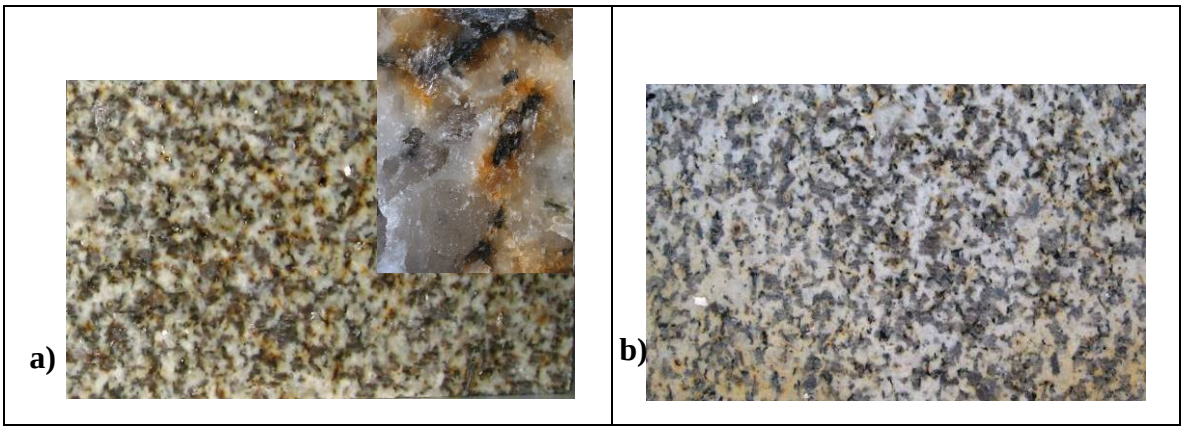

Fig 6.41 The yellow discoloration observable on the Vilachán granite is due to the oxidation of biotite

The most drastic colour change can be observed on the Szob andesite (fig. 6.42.). Here again, the effect is the appearance of yellow-orange stains on the surface of the samples, but in this case the stains appear completely randomly, or sometimes as vertical bands, following the possible path of the solution-flow during the test. The original dark grey colour of the stone on the other hand, turns lighter. With cleaning yellow colour becomes browner and somewhat less vivid but the discolouration cannot be removed.

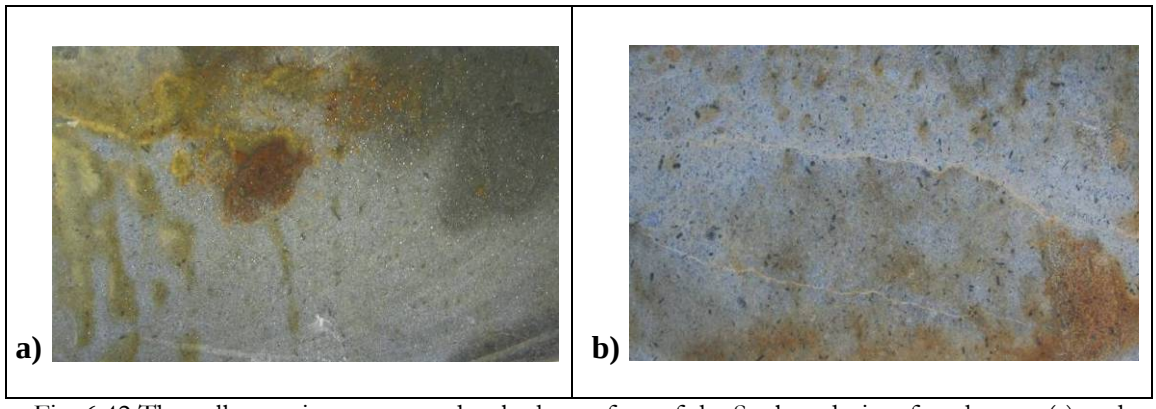

Fig. 6.42 The yellow stains cover randomly the surface of the Szob andesite after the test (a) and they cannot be removed by cleaning (b)

Observations by SEM

By means of Scanning Electron Microscopy the processes of the alteration can be observed more directly. Samples were investigated after one and three weeks of exposure

After one week already, a thick and continuous gypsum crust can be observed on the surface of the Macael marble (fig.6.43). On the Silvestre Vilachán granite very few gypsum crystals appear after one week of exposure. They are normally isolated from each other, have a size of approximately 100μm and tabular shapes sometimes cross-twins (fig. 6.44). The Szob andesite shows a surprisingly high number of gypsum crystals already after one week. The crystals are also of tabular shape and the approximate size of 100μm, like on the granite surface, but in this case they grow in groups of radial or chaotic structure (fig. 6.45). These areas of focused crystallisation are typically connected to feldspar grains.

After three weeks of exposure the amount of gypsum significantly increases on all the stone types. The crust on the surface of the marble becomes even more well-evolved and compact; on the figure 6.46/a, where there is a small discontinuity in the gypsum layer due to a muscovite grain, the several 10μm thickness can be seen. On 6.46/b the more general photo shows the continuity of the crust.

The number of gypsum crystals increased on the surface of the Silvestre Vilachán granite, forming now groups of radial structure (fig. 6.47/a), but these knots are still isolated from each other, no continuous crust can be seen. On figure 6.47/b the physical effect of the crystallization can be observed, as the crystals growing among the laminae of the mica cause the rupture of the material.

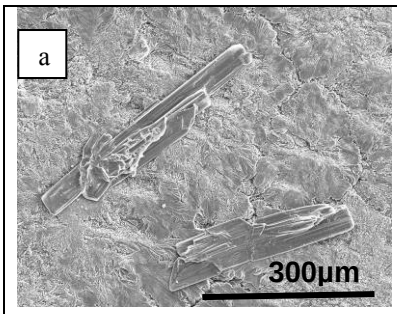

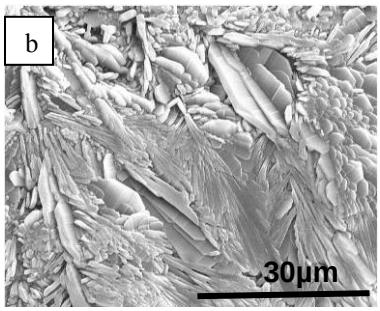

Fig. 6.43 Gypsum crust on the Macael marble after 1 week of exposure

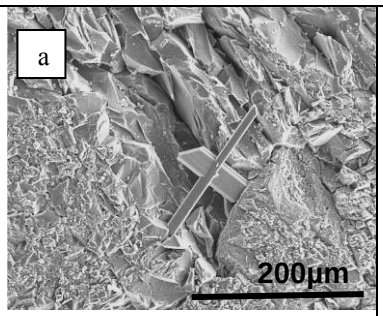

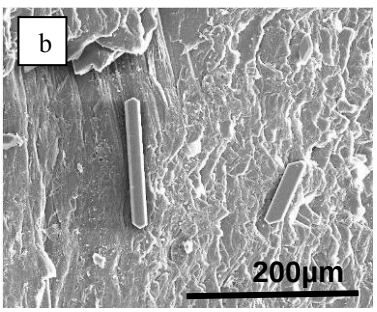

Fig. 6.44 Few gypsum crystals appear on the granite after 1 week of exposure

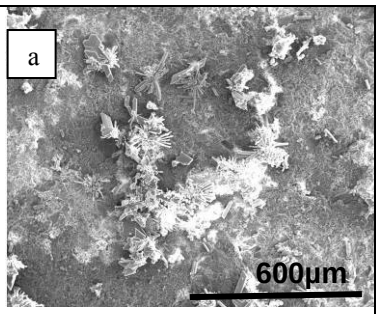

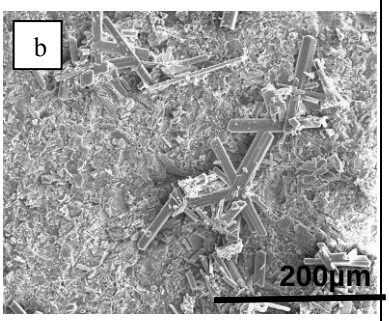

Fig. 6.45 The gypsum crystals on the andesite forms radial groups

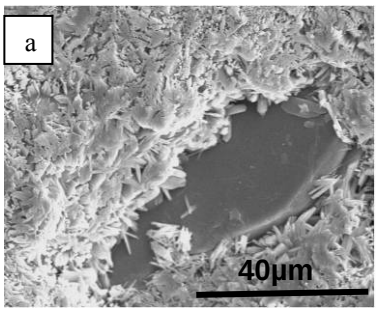

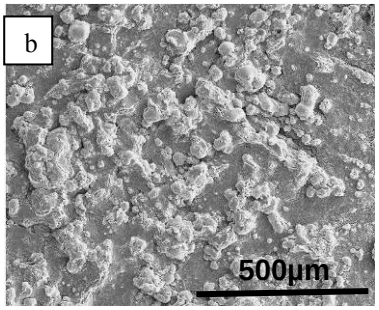

Fig. 6.46 The gypsum crust on the marble reaches more 10 µm thickness after 3 weeks

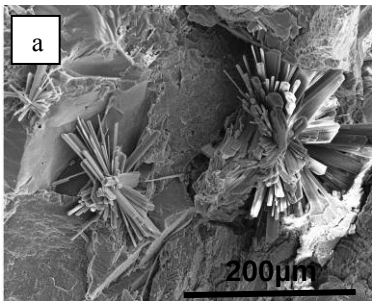

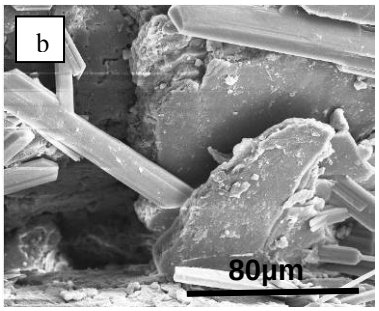

Fig. 6.47 The number of gypsum crystals grow on the granite after 3 weeks causing physical damage

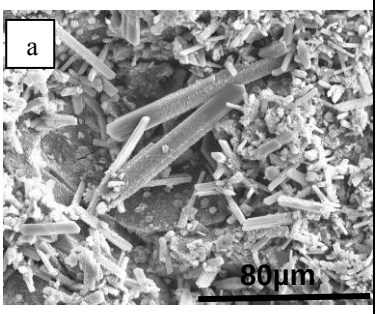

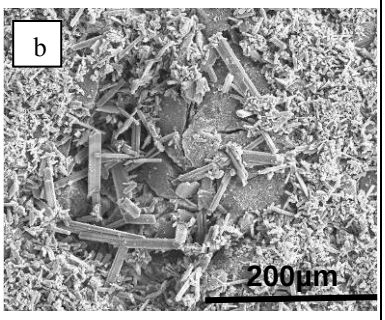

Fig. 6.48 A continuous crust forms on the surface of the andesite after 3 weeks of exposure

The evolution of the gypsum formation is the most surprising in the case of the Szob andesite. During the two further weeks of exposure an almost continuous salt crust was formed on the surface of the material. As it can be observed on figures 6.48/a and /b smaller crystals of approximately 10µm size cover the surface, while at some given places crystals of larger size form similar groups as observed after 1 week. The layer is not as thick, neither as continuous as that of the marble, but significantly more well-developed than the isolated crystal groups of the granite.

Weight loss

The weight loss due to the treatment with both the high and the low concentration solution was measured according to the standardized process and is shown in figure 6.49.

The result is quite different in the three cases. The Macael marble is the only one of the three stones that suffered loss of weight. The loss is relatively low, but taking into consideration that this is a superficial test, it is not insignificant. The effect of the strong solution is higher than the weak one, although the difference is not very important.

The Silvestre Vilachán granite and the Szob andesite present a gain of weight due to the salt formation on the materials, although the mass was measured on cleaned samples. The weight gain of the granite is significantly higher using the strong solution, than the weak one. On the other hand, the samples of the andesite exposed to the stronger solution show lower weight.

The explanation of this may be that the stronger solution besides of the formation of the salt (meaning the extra weight) already produces a more important damage of the material, causing weight loss also.

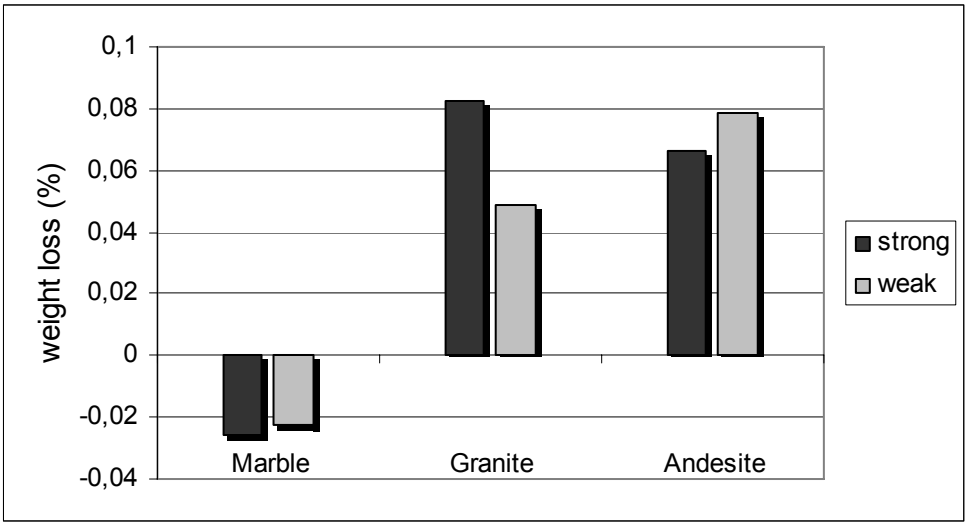

Fig. 6.49. Weight loss after 21 days of exposure to the action of SO_2. The strong solution means 3,85% concentration and the weak one 1,15%, according to the referring standard.

Surface roughness

The surface roughness parameters were measured before the test and after 21 days of exposure to the high concentration solution. The values before the test are shown in table 6.9.

The graphical comparison of those parameters that were found representative (not the kurtosis neither the mean spacing) is presented on figure 6.50.

The responses observed in the surface parameters of the three stones are similar to those after the salt mist test. The measurement was carried out on cleaned samples, so they detect the changes of the material and not that of the gypsum crust.

The Macael marble registers an increase in the parameters describing the general irregularity of the surface, such as the Ra, Rq and Ry, due to the increase of the height of the peaks. On the other hand, the depth of the valleys and the skewness do not seem to vary. The Silvestre Vilachán granite does not show significant variations in none of the parameters. The Szob andesite, similarly to the marble, has an increase in the average irregularity of the surface due to the heightening of the peaks. The depth of the valleys does not increase, but the skewness does, which means that the number of the valleys increases relatively.

Table 6.9

		before		after 21 days	
		average	st.dev.	average	st.dev.
marble	**Ra (µm)**	2,37	0,30	4,79	0,43
	Rq (µm)	3,62	0,71	7,06	0,92
	Sk	-2,90	0,92	-1,95	0,70
	Ku	18,3	9,5	11,0	4,0
	Rp (µm)	6,0	0,9	19,0	6,2
	Rv (µm)	30,9	10,4	46,6	10,8
	Ry (µm)	36,9	10,8	65,6	12,4
	Sm (mm)	2,01	1,57	2,13	0,77
granite	**Ra (µm)**	12,0	2,9	11,1	1,9
	Rq (µm)	18,1	6,0	16,0	3,1
	Sk	-2,65	0,85	-2,50	0,54
	Ku	13,1	7,1	12,3	4,7
	Rp (µm)	18,5	5,3	18,6	3,4
	Rv (µm)	118	51	111	31
	Ry (µm)	137	54	130	33
	Sm (mm)	2,25	3,76	1,59	0,54
andesite	**Ra (µm)**	3,28	0,21	4,49	0,36
	Rq (µm)	4,77	0,38	6,25	0,59
	Sk	-2,38	0,43	-1,53	0,33
	Ku	11,7	3,9	7,2	1,8
	Rp (µm)	7,14	0,58	14,19	2,57
	Rv (µm)	33,6	7,2	36,4	6,9
	Ry (µm)	40,7	7,3	50,6	7,7
	Sm (mm)	1,74	1,46	1,53	0,48

Table 6.9 Surface roughness values before and after the SO_2 test

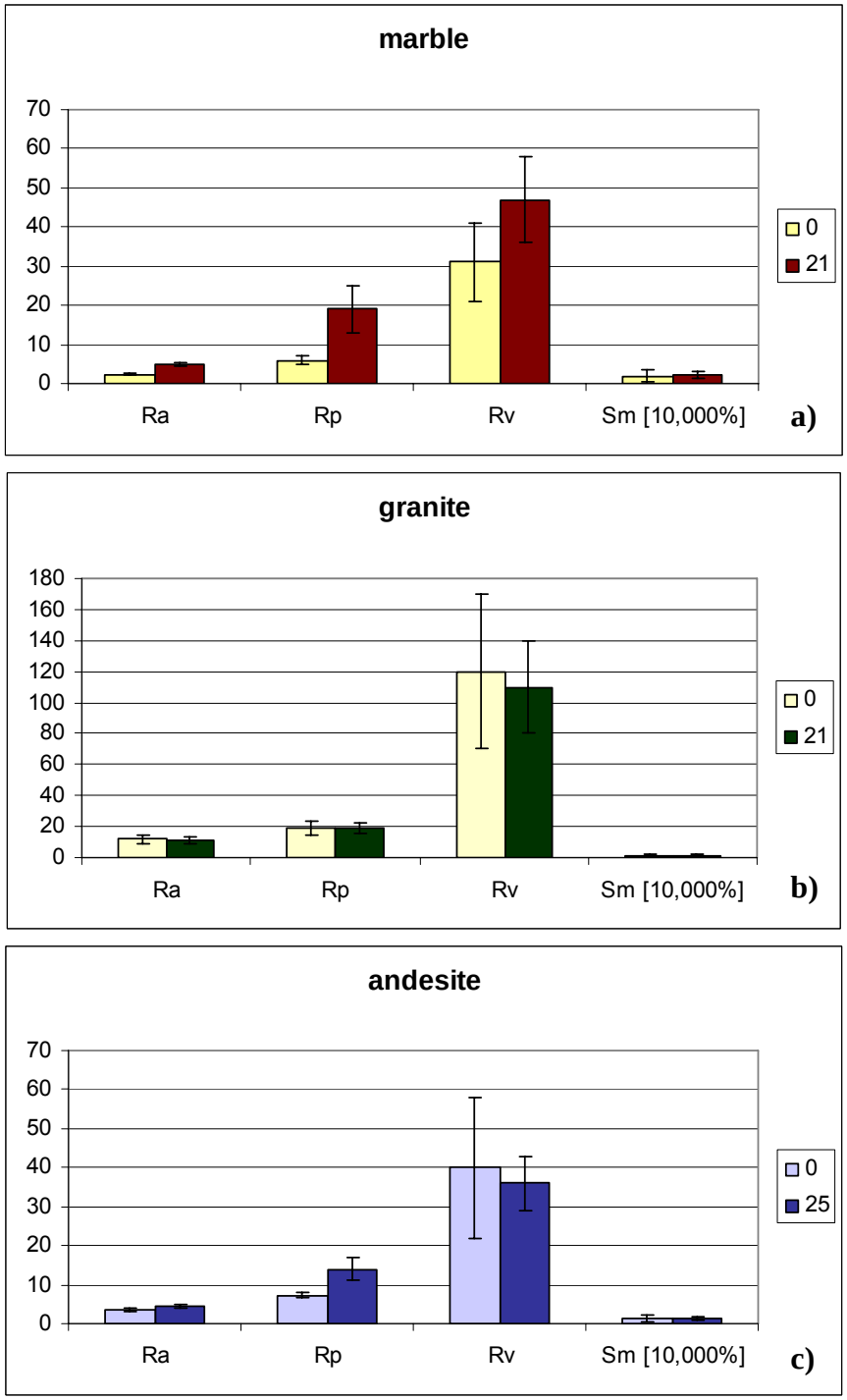

Fig. 6.50 Evolution of the surface roughness parameters during the SO_2 test of the Macael marble (a), Vilachán granite (b) and Szob andesite (c).

Colour

The colour of the samples was measured before the test, after the 21 days exposure without cleaning and after cleaning. The measured and calculated parameters can be found in table 6.10, and the changes of the a* and b* parameters are presented graphically on figure 6.51.

Table 6.10

			L*(C)	a*(C)	b*(C)	C*(C)	h(C)	ΔE
marble	before	average	82,5	-2,5	-0,3	2,5	188,1	
		st.dev.	0,7	0,7	0,5	0,7	11,4	
	after test	average	80,4	-1,8	7,9	9,1	127,6	72,4
		st.dev.	5,6	2,6	10,9	10,4	26,4	
	after cleaning	average	80,7	-2,8	7,0	7,9	122,7	56,1
		st.dev.	3,1	0,9	5,8	5,3	19,4	
granite	before	average	75,8	-0,8	5,5	5,6	98,5	
		st.dev.	3,3	0,8	0,8	0,8	8,3	
	after test	average	68,0	-1,1	10,1	10,2	96,7	81,6
		st.dev.	3,5	1,1	1,9	1,9	6,5	
	after cleaning	average	72,4	-1,2	10,4	10,5	97,3	35,2
		st.dev.	3,5	0,9	2,8	2,8	5,8	
andesite	before	average	44,5	-4,4	4,6	6,6	131,0	
		st.dev.	1,4	1,9	0,7	1,1	16,4	
	after test	average	60,2	-2,5	19,0	19,3	98,4	460,1
		st.dev.	1,9	1,7	4,0	3,8	5,7	
	after cleaning	average	56,4	-1,5	16,8	17,0	96,2	298,9
		st.dev.	3,7	1,9	4,1	4,1	6,3	

Table 6.10 The measured and calculated colour parameters before and after the SO_2 test and after cleaning.

The colour changes due to the SO_2 test are significantly higher in all the cases than those after the salt mist test.

The Macael marble shows a ΔE value of ~70, which decreases to ~55 after cleaning. This change mostly consists of a significant shift of the b* value towards yellow, and the shift of the a* value towards the red, which returns to the original value after cleaning. The difference between the cleaned and not cleaned samples is also important above all in the a* value.

The final colour change is the lowest in the case of the Silvestre Vilachán granite. Here, the most important change is evidently the shift of the b* value towards yellow, which remains constant after the cleaning. On the samples without cleaning a darkening effect (lower L* values) can also be observed, but this disappears after the cleaning and drying of the samples, and probably is mostly influenced by the state of dryness of the sample.

Finally, the highest changes, as it was expected after the visual observation, were measured on the Szob andesite. The ΔE values are an order of magnitude higher than for the other two stones; 460 and 300 respectively, without and with cleaning. In all the basic values, meaning the L*, the a* and the b*, high changes occur. The shift of the b* value towards yellow is the highest, although it moderates a bit after cleaning. The shift of the a* value towards red is getting even more pronounced after cleaning, because the yellow patches turn darker on the surface. And the darkening also decreases somewhat after the cleaning.

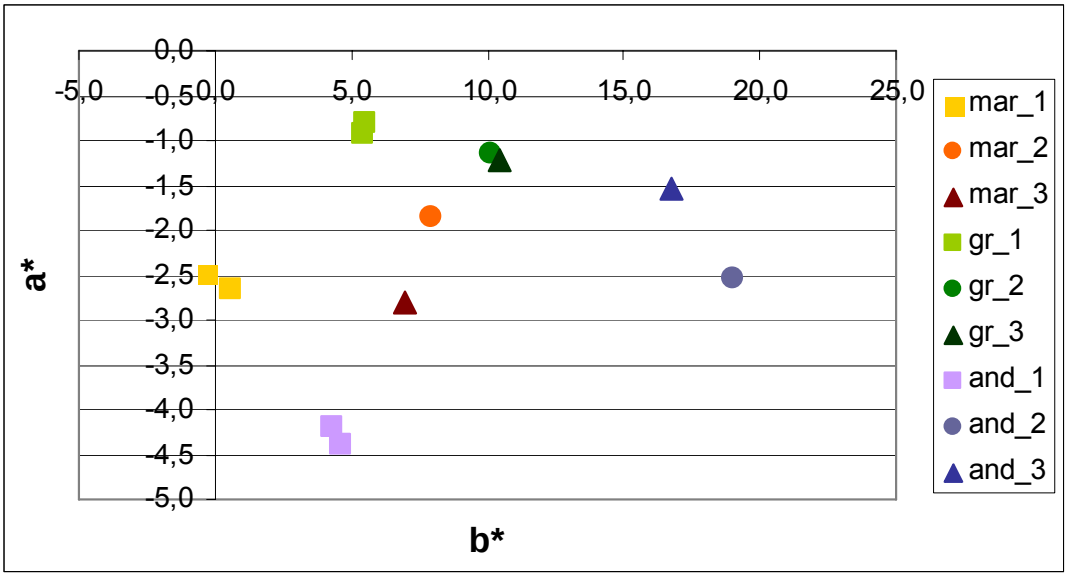

Fig. 6.51. Colour changes due to the SO_2 test. mar: Macael marble; gr: Silvestre Vilachán granite; and: Szob andesite; 1: before the test; 2: after the test without cleaning; 3: after the test cleaned

Surface chemical composition

The surface chemical composition was measured before the test and after one week of exposure by means of XPS. Besides the surface composition, this method gives information about the chemical state and/or environment of each element.

The quantitative and qualitative superficial compositions are shown in table 6.11. In the same table, the measured binding energies and the possible molecule configurations from literature for each element are also presented.

The measurement before the test revealed the presence of O, C and Ca on the surface of the Macael marble, which corresponds to the calcite (part of the C is of atmospheric origin) and traces of Fe, Si, Na and S. On the Vilachán granite the main elements are the O, the Si, the C and the Al with smaller quantities of Ca, Na, Mg, Fe and S. All these elements come from the different silicate phases of the rock expect for the C, which is of atmospheric origin (always present in the XPS measurements) and the S, which is probably contamination. The Szob andesite contains O, Si, Al, Mg, Ca, Fe, Na and K, and the atmospheric C and the S appears here, again.

After the test the most important change in the quantitative composition is the increase of the S, which caused a relative decrease in the concentration of all the other elements. The atmospheric carbon also appears in higher quantities. The appearance of Al and Mg on the surface of the marble comes from contamination from the other stones. The slight increase of the Mg and Fe on the granite may be due to errors because of the low concentration and

the high background noise of the spectra or simply due the higher quantity of biotite in the second measurement.

Besides the quantitative variations, the changes in the position and sometimes the shape of the peaks of determined elements also give information about the processes that took place during the test. For the examination of this, more detailed analysis was carried out about the Ca, S, C, O and Fe peaks of each stone. The most significant results are presented on the figure 6.52.

In the Macael marble, besides the appearance of the S, the most important changes were observed on the C, O and Ca peaks. The C peak, before (M0) and after the test (M1), is shown in figure 6.52/a. Before the test, the peak was a duplex with two subunits of equal importance; one at 289,0eV, the C of the carbonate, and another one at 284,5eV, which is C coming from the atmosphere. After the exposure, the carbonate-carbon peak disappears from the surface due to the gypsum layer that covers the sample completely. In both the O and the Ca peaks a shift of about 1eV can be observed. The shift in the O 1s peak shows the difference of the binding energy of this element in the carbonate phase (531,2ev) and in the sulphate phase (532,0eV). In the case of the Ca 2p3/2 the same change is from 346,7eV ($CaCO_3$) to 348eV ($CaSO_4$).

In the Vilachán granite, the only important changes were detected on the S and the O. The increase of the intensity of the sulphur peak and the decrease in its binding energy proves the formation of gypsum on the surface of the granite. The evolution of the oxygen 1s peak is shown on figure 6.52/b. After the test two subunits can be differentiated in the peak: the O in the silicon phases, which was already very strong in the spectra before the test; and a new phase, which has slightly higher binding energy. The two peaks overlap, as the binding energies of the oxygen in the silicate and in the sulphate are very close to each other, but the increasing amount of the new phase is due to the gypsum formation. The slight changes in the Mg2p, the K2s and the Na1s are probably only inaccuracies due to the very low concentrations of these elements on the surface of the granite.

In the Szob andesite, significant changes can be noted on the Ca and the Fe, besides the increasing quantity of sulphur. The Fe2p peaks, before and after the test, are shown on figure 6.52/c. The Fe(III)/Fe(II) ratio suffers a significant increase, which means the oxidation of the iron during the sulphation process. The Ca2p signal is a duplex of the 3/2 and 1/2 subshells (fig.6.52/d). Before the test two Ca phases can be differentiated, one of which disappears from the surface of the andesite after the exposure. As the binding energies of Ca in different silicate and sulphate phases are close to each other, and the amount of Ca is relatively low, it is difficult to say which were the two phases before the test. After the test the only remaining Ca phase is probably the gypsum.

Table 6.11

	Macael marble				Vilachán granite				Szob andesite				Literature BE (eV)
	before		after		before		after		before		after		
element and shell	BE (eV)	Conc (%)	BE (eV)	Conc (%)	BE (eV)	Conc (%)	BE (eV)	Conc (%)	BE (eV)	Conc (%)	BE (eV)	Conc (%)	
O 1s	531,0	52,5	532,2	57,6	531,9	56,2	532,2	49,5	531,8	53,9	532,3	49,4	532,0 $CaSO_4$(2); 531,2 $CaCO_3$ (2); 532,3 SiO_2(2)
C 1s	289,0	30,3 50%	284,6	10,9 65%	284,6	12,7 89%	284,6	26,8 50%	284,6	16,2 58%	284,6	22,5 46%	289,4 $CaCO_3$ (2); 284,8 hydrocarbon contaminants(1)
	284,5	50%	286,4	35%	287	11%	286	50%	286,7	42%	286	54%	
Ca 2p3/2	346,5	15,3	347,9	7,9	348,1	0,8	348,3	0,05	348,2	1,6	348,4	0,2	346,7 $CaCO_3$ (2); 348,0 $CaSO_4$ (2) 347,0 $CaSiO_3$ (1)
Ca 2p1/2	350		351,5		351,6		352		351,8		352,1		350 $CaCO_3$ (1); 351,5 $CaSO_4$ (1)
Fe 2p	711,1	0,1	711,8	0,2	712,6	0,1	711,9	0,2	711,4	0,9	711,8	0,2	709-710 Fe(II) oxide(2); 711-712 Fe(III) oxide(2)
Si 2p	102,2	0,9	102,7	8,2	102,4	20,4	103,0	10,3	102,4	17,9	102,7	14,5	102,2 SiO_2(1); 102,6 Si(IV) in silicon oxides (2)
Al 2s	-	0	119,3	1,4	119,0	6,3	119,9	3,6	118,9	4,7	119,9	2,1	119,0 Al_2O_3(2); 120,2 Al_2O_3/Al (2)
Mg 2p	-	0	56,5	0,8	55,2	0,4	57,1	1,7	56,0	2,8	56,8	2,7	
K 2s	-	0	-	0	378,0	1,4	372,1	0,03	377,5	0,3	374,8	0,04	
Na 1s	1071,4	0,5	1072,8	0,04	1072	0,7	1073,4	0,03	1072,1	0,7	1072,9	0,04	1072-1073 in silicate compounds(2)
S 2p	168,3	0,4	169,1	13,6	175,4	1,1	169,2	7,9	173,4	1	169,2	8,3	168,1 $CaSO_4.2H_2O$(2); 169-170 Ca sulphates (1,2)

Table 6.11 XPS analysis of the surface of the three stone types. The measured binding energies (BE); the relative concentrations (Conc); and the possible molecule configurations from the literature are presented. The literature references are taken from (1) Maravelaki-Kalaitzaki et al. 2002; or from (2) http://srdata.nist.gov/xps/Default.aspx, where all the values are futher referred.

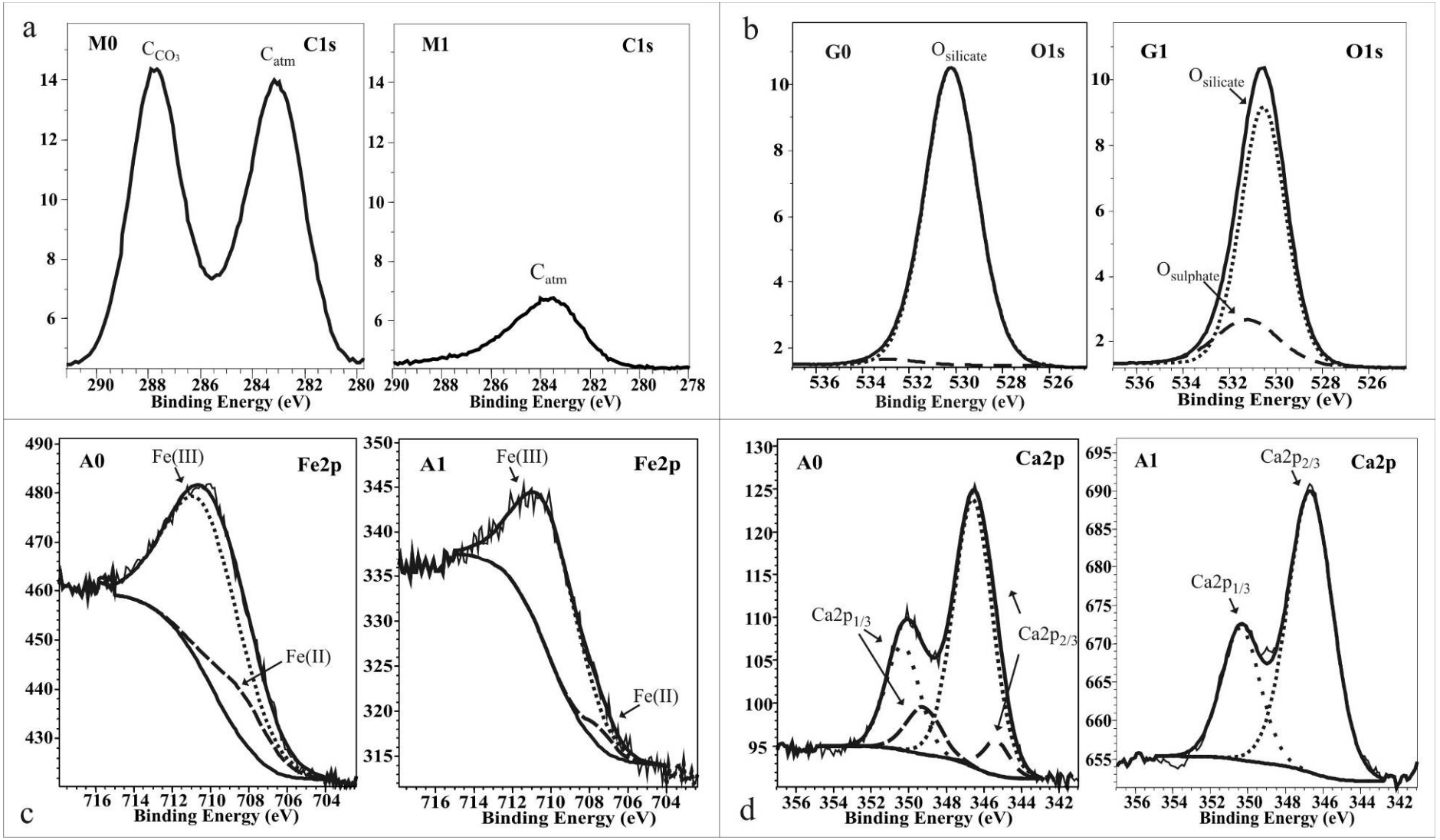

Fig. 6.52 XPS detailed scans of the (a) C1s of the Macael marble before (M0) and after (M1) the SO_2 test; (b) of the O1s of the Vilachán granite (G0 and G1); and (c) of the Fe2p and (d) Ca2p of the Szob andesite (A0, A1). The thin line is the original spectra, the thick continuous line is the fitted curve, and the dotted lines are the results of the peak desconvolution.

6.6.3 Discussion

The Macael marble suffered highest damage due to the action of SO_2. It was the only one of the three stones that detected a negative weight balance by the end of the test, which is due to the dissolution of the calcite in the acidic environment. The high solubility of calcite in low pH value conditions is well known. The reaction that takes place results in the formation of gypsum ($CaSO_4 \cdot 2H_2O$), which was observed by means of SEM and detected by XPS. The process is very fast and efficient even in the solution of relatively low concentration; a continuous crust was observed on the surface of the marble already after one week of exposure.

The change of colour is a specifically important issue in the ambient of ornamental and monumental stones. The typical appearance of black crust in the field is due to the deposition of organic or inorganic particulate matter on the surface of the buildings, which will be embedded in the forming crust (Bugini et al., 2000). This effect evidently does not take place under laboratory conditions in a climate chamber. In our case, the discolouration is of yellow colour, which is also commonly observed in real conditions. The yellowing of white marble may be due to three causes (Bams and Dewaele, 2007): (i) the oxidation of iron bearing minerals; (ii) the reaction of organic matter contained by the stone; or (iii) by external agents. The Macael marble contains pyrite as accessory mineral, the oxidation of which may cause this intensive yellowing. In this case, coloured spots are expected to be situated randomly on the specimens or connected to the greyish veins in the marble, where the quantity of pyrite increases. Nevertheless, the discolouration of the marble slabs is situated always in the lower part of the samples. The explanation for this phenomenon can be found in the conditions of the measurement. The samples during the test – in order to avoid the direct contact between the samples and the acid solution – are placed on supports inside the chamber. The supports in our case were made of granite. This suggests the possibility there may have been an interaction between the two stones at their contact. This, although being a mistake in the design of the experiment, provides us the information that the Macael marble is very susceptible to the third type of staining, namely the external agents; especially that the caused discolouration cannot be completely removed by cleaning.

The two other stones, the Vilachán granite and the Szob andesite, being silicate stones both, were expected to perform similar deterioration to this chemical attack. However, their responses differed significantly.

The Vilachán granite suffered the lowest grade of degradation of the three stones. As the silicate mineral phases have low solubility in acids and granites are poor in Ca, they are often considered highly resistant to sulphation weathering and the gypsum observed on granites in the field is attributed to external sources (Delgado Rodrigues, 2000; Prieto et al., 2007). However, under the controlled conditions of the laboratory test there are no external sources of calcium, so it must be taken from the plagioclase phase of the granite itself. The formation of gypsum was proved by the SEM observations and also by the XPS measurement, where the

changes of the binding energies in the oxygen prove the appearance of new phases on the surface. The variation of the Ca itself unfortunately was not possible to measure because of the relatively low concentration of this element in the granite. Some authors observed the replacement of silicate phases (feldspar and even quartz) by gypsum (Schiavon et al., 1995), however this strong chemical effect was no observed on the Vilachán granite. On the other hand, the physical effect of the forming gypsum crystals was proved to cause the rupture of the material, especially of the most vulnerable mica phases. The material loss due to the physical damage does not overpass the weight gain from the gypsum formation, but this degradation process cannot be left out of consideration when assessing the susceptibility of this granite. The observable colour change, due to the oxidation of biotite, also puts into danger the acceptability of this granite as ornamental or monumental stone under the possible effects of sulphation.

The most unexpected results, however, were experienced in the case of the Szob andesite. The degree of the damage suffered by the andesite can be situated between those of the Macael marble and of the Vilachán granite. An intense gypsum formation was observed, which started in connection with the plagioclase crystals but after three weeks of exposure, it covered all the surface of the samples. In the weight variation we can observe that the weak solution resulted in higher weight gain, which may be because the stronger solution already caused more damage to the material. The colour changes are probably the most striking on the andesite out of the three stones. All these observations proved that significant reactions took place in the andesite due to the acidic attack.

The main question was why there is such a great difference between the granite and the andesite in this test.

Mafic rocks were proved to be more susceptible to acidic attack due to the higher solubility of their mineral phases, such as pyroxenes or amphiboles (Simão et al., 2006). This may be one answer to the question. The second one is the difference in the composition of the plagioclase of the granite and the andesite. The plagioclase is the most important Ca-bearing mineral in magmatic rocks, so its properties are crucial in this question. The plagioclase of the granite is oligoclase ($Ab_{70}An_{30}$-$Ab_{90}An_{10}$) and that of the andesite is andesine ($Ab_{50}An_{50}$-$Ab_{70}An_{30}$). This on one hand means, that the andesite is richer in Ca and, on the other hand, that its plagioclase phase is less resistant to chemical processes. And finally, a third explanation may be found in connection with the iron-content of the two stones. The very strong yellow discoloration of the andesite brought the attention to the role of the iron in the sulphation process. The significant degree of oxidation of this element was also proved by the XPS measurement.

The iron-sulphur interaction in aquatic environment is part of several geochemical processes and so, has been investigated profoundly, revealing the formation of complexes of the two elements (Eggleston et al., 1998). Then the iron-sulphite and –sulphate complexes cause redox reactions in solution (Pérez Bernall and Bello López, 2004). The catalytic effect of iron oxides in the oxidation of SO_2 and the formation of H_2SO_4 was observed in connection with stone decay, as well (Simão et al. 2006; McAlister et al., 2008). Also the higher degradation of Fe-

bearing stones to non Fe-bearing stones was described (Alonso and Martinez, 2003; Müller, 2008). These suggests the possibility that the significantly higher iron content of the andesite (5,52% total Fe expressed in Fe_2O_3) is a third reason for the enhanced decay of this stone compared to the Vilachán granite (1,1% total Fe expressed in Fe_2O_3).

Although physical damage was not observed during the test on the Szob andesite, the strong chemical reaction with time leads to the overall decay of the material. For this reason, the susceptibility of the andesite to sulphation is very high.

6.6.4 Correlation of parameters – Conclusions

- The Macael marble was the most susceptible of the three stones due to the high solubility of calcite in acidic conditions
- The Szob andesite also has a very high susceptibility to the action of SO_2 due to the Ca-rich plagioclase phase, the low-resistance mafic minerals and the high iron content
- The iron acts as a catalyser in the sulphation process
- The susceptibility of the Vilachán granite is lower than that of the other two stone types but not zero. Gypsum forms with the Ca of the plagioclase and the growing crystals exert physical stresses resulting in material rupture
- The susceptibility of a stone to the action of SO_2 is determined by the chemical composition
- The colour changes were important in all the stone types due to the oxidation of iron, which came from the material itself in the case of the granite and andesite and form external source in the case of the marble
- The weight loss does not provide useful information about the damage in the materials
- The surface roughness measurement by means of a contact profilometer did not prove to be useful on non-polished stone surfaces in this test either
- No significant differences were observed between the effect of the stronger and weaker solutions required by the European standard. On the other hand, the monitoring of the evolution of the degradation process in time provides further information about the evolution and mechanism of the damaging process

7. Critical review of standardized and non-standardized methods

7. Critical review of standardized and non-standardized tests in the stone industry and the academic research

Standardization is a fundamental and necessary step in every industrial field, the natural stone sector included. Quarries, stone processors and every member of the production chain must follow equal regulations in order to keep a given level of quality and to give the security to the user or purchaser that the given product will fulfil the requirements. The European Union via the CEN, the European Committee for Standardization, has been making a lot of effort to unify the stone industrial procedures within its member countries and is aiming at the development of a harmonized stone industry market. The CE labels are obligatory on many of the stone products commercialized within the Union. These considerations are true as much within the range of modern constructions as of restoration and conservation works of monuments.

The "repeatability", "comparability" and "harmonization" are key-words in the necessity of standardization (Exadaktylos, 1998) as well in the academic research as in the industry. Although research will always need the liberty of modification of testing conditions for the development of knowledge, common guidelines for different laboratories all over the world could significantly improve scientific cooperation. They could facilitate to share the scientific results of different investigations and to avoid working parallel without communication.

Nevertheless, standardization has its disadvantages, as well. The qualification of natural products is incomparably more complicated than that of artificial ones due to their high inhomogeneity. Moreover, standards necessarily consider an "average" material and establish the testing or measurement conditions according to that. Within the natural stone field the variability of materials and their properties is so high that this approach inevitably leads to errors. Therefore, slight modifications of measurement procedures are necessary in accordance with the properties of the tested material. A second stage of the standardization should aim at the recommendations of these modifications both for the industrial and the academic sector.

In this chapter an attempt is made to consider possible modifications of this type, strictly focusing on the applied methods and the tested material types of this research. Two groups of test must be differentiated: the methods for the characterization of the stone properties and the methods for the assessment of its durability.

7.1. Stone characterization

There are several properties that must be included in the primary characterization of a stone material; the mineralogical and chemical composition, the texture, the grain size, the density, the characteristics of the void space, the mechanical properties such as compressive, flexural strength, etc., the hydraulic properties, the thermal properties, etc. Of all these, now only the characterization of the void space and the hydraulic properties will be discussed, because they were found to be fundamental in the durability and because they were the most thoroughly investigated in this research.

7.1.1. Void space

The only European standard dealing with the void space is the EN 1936, which specifies the measurement of the open and total porosity and the apparent and real density. As proved by the experiments, the value of open and/or total porosity, although a fundamental property, is not the most dominating in the deterioration processes. The void/aperture size distribution and the connectivity of the void space proved to be of primary importance. For the investigation of these parameters non-standardized instrumental techniques exist, which although may vary a little bit due to the different types of instruments, probably have a good repeatability and comparability. Nevertheless, the reliability and the punctuality of results obtained by these techniques largely depend on their working principles and their detection range.

In this research Hg intrusion porosimetry, nitrogen adsorption and Confocal Laser Scanning Microscopy with Digital Image Processing was used. The following observations were made when applying these techniques on crystalline stones:

- The Hg porosimetry gave the largest amount of information due to its widest range of detection. The open porosity value is reliable and firmly reproducible. Taking into consideration that the working principles of the method consider cylindrical pores for the calculation of the pore throat radius as a function of pressure, the size distribution diagrams must be handled with care in the case of rocks with a high fissure/pore ratio. Moreover, the dilemma of pore throat versus fissure aperture gives place to further erroneous interpretations. Nevertheless, at least in this research, the distribution diagrams calculated automatically by the software of the instrument gave a relatively good estimation of the real size distribution. Therefore, the application of this technique was considered recommendable.

- The nitrogen adsorption technique is especially adequate for micro- and mesoporous materials. A large part of natural stones belongs to the macroporous group, and so cannot be investigated by this technique or the results will be hardly informative. In this research the technique proved to be useful for the andesite, which is a stone of outstandingly high specific surface among the natural stones, but did not give any information about the Macael marble.

- The largest inconvenience of the CLSM-DIP method is its detection range, as the lower detection limit is about 1 μm. This, in stones with small average void size, is not sufficient for a detailed investigation. The quantification of the parameters also carries some uncertainty depending on the method (see the very high standard deviations). Therefore, this method is more suitable for the qualitative description of the void space than for its measurement, and that only in the >1 μm range. The use of other types of microscope, like SEM, completed with Digital Image Processing may overcome the problem of the detection range, although in that case the difficulty is in the differentiation of open and closed pores. Anyhow, these kind of detailed examinations are only possible in the academic field and not in the industry.

In summary, as much in the investigation as in the industry, more information is necessary about the void space of a stone material than the value of open and total porosity. The pore size distribution is a fundamental and very useful data, which can be relatively easily obtained by means of Hg porosimetry. The results of this method must be interpreted circumstantially in the case of crystalline stones, and it is recommendable to use more than one method in parallel.

7.1.2 Hydraulic properties

The most important ones of the hydraulic properties were found to be the water absorption (under vacuum and at atmospheric pressure), the capillary uptake and the evaporation or drying. While there are European standards concerning the first two properties, for the evaporation only national (like the Italian) standards exist. Here, the necessity of including the drying in the European standards must be emphasised.

Another issue concerning these standards is the way of measurement. The standard procedure is still "wiping the surface of the samples with a wet cloth" before detecting the weight. In the case of a stone of less than 1% open porosity (like the Macael marble), the quantity of water inside the material and on the surface are almost in the same range. The error resulting from this "wiping method" – see the degree of humidity of the cloth, the intensity of wiping etc – can be enormous. Automated measuring methods are used and have been described in the literature from more laboratories (like Benavente et al., 2007). The avoidance of the human factor from the measurement may improve significantly the reliability of these measurements on low porosity materials also.

7.2 Durability assessment

The durability of stone and stone-like materials is traditionally and relatively efficiently assessed by means of durability tests or ageing tests. The aim of these tests is to avoid the need of several years of testing – necessary in real exposure tests – and so they intend to artificially accelerate the damaging process. In order to reach this aim, the conditions of the

tests are usually extremely exaggerated. This in itself will lead to some deviations from real processes, but as far as these deviations are included in the interpretations, this approach may be correct. Nevertheless, during the testing of the three stone types of this project some possible sources of errors and some possible points of the improvement of the testing were revealed.

7.2.1. Salt crystallization test (EN 12370:1999)

The most outstanding problem in this test is the large temperature difference between the wetting and the drying phase. In thermally non-sensitive materials the cyclic temperature fluctuation of 80°C (from 20 to 105°C) may not cause large problems, but during this research the marble was proved to suffer thermal degradation due to changes in the range of 40°C, as the drying was carried out on 60°C. This extreme thermal fluctuation is not necessary part of the natural process of salt crystallization, as thus is alters both the mechanisms of the damage and the susceptibility of a given material. Carrying out the whole test on room temperature would lengthen the duration of the test but would give more realistic results.

Another problem experimented during the test was the length of the wetting phase, which was too short for the andesite to reach a significant saturation degree. In the case of materials of slow liquid uptake, 4 hours of immersion may not result in the uptake of sufficient quantity of salt to suffer damage. The duration of the wetting and drying phases therefore, should be determined as a function of the liquid uptake and evaporation properties of the material. For this a classification of the stone materials according to these properties could serve as a useful practical tool.

7.2.2 Frost resistance test (EN 12371:2001)

A few modifications were implemented in the freeze-thaw test of this research compared to the standard procedure. The temperature range was amplified in order to secure the freezing to take place in smaller pores also, as all the tested stones have an important proportion of pores <5 μm. Moreover, the whole test was carried out in immersion. This evidently is not a realistic approach, but in order to maintain a relatively high saturation degree in all the stones, it was found to be necessary.

7.2.3 Freeze-thaw in the presence of soluble salts

No European standard exists for the investigation of this weathering process for natural stone. In the concrete industry, the frost-salt weathering was found to be an important issue and this research also proved that the presence of salts enhance the degree of damage caused by frost. The introduction of this test in the natural stone sector may be recommendable.

7.2.4 Salt mist (EN 14147:2004)

The European standard orders four hours of salt spray and eight hours of drying. The length of the spraying phase will determine the quantity of salt that enters into the material. Other test types with cycles of 1 min of spray and 29 min of drying has been applied and described in the literature (Birginie et al., 2000; Cardell et al., 2003a), which seems to be a more realistic approach.

7.2.5 Action of SO_2 in the presence of humidity (EN 13919:2003)

The European standard specifies 21 days of exposure to two types of solution with different concentrations. In this research, the importance of the different concentrations was not proved. However, the examination after 7 and after 21 days of exposure proved useful information about the evolution of the damage.

7.2.6 Evaluation of damage

The evaluation of the damage that takes place during the tests is almost always specified as visual inspection and the measurement of weight loss. The freeze-thaw is the only European standard of the applied ones that requires the detection of the change in the modulus of elasticity. Both the visual inspection and the weight loss are useful measures of damage, if that damage results in significant material loss. But they do not give any information about the micro-fractures or other flaws in the interior of the samples, neither about the modified material properties.

The monitoring of the ultrasonic propagation and the investigation of the hydraulic properties, especially of the capillary uptake (in more than one direction is the material is anisotropic) proved to be very significant during this research.

Also, in academic research for the evaluation of possible chemical change of the surface, the XPS was found to be an adequate tool.

As ornamental or monumental stones are considered, the colour changes of the material due to any type of surface or chemical process is of fundamental importance. The instrumental detection of colour changes and the determination of the limit between acceptable and non-acceptable variations may be useful.

8. Final discussion - Conclusions

8. Final discussion - Conclusions

Three crystalline stones with different mineralogical composition and textural features were examined in this research; a marble, a granite and an andesite. Their petrophysical characteristics were determined and their durability was investigated by means of six different ageing tests.

The main objective was

1) to evaluate the overall durability of crystalline stones in correlation with their intrinsic properties, the petrophysical characteristics.

To reach this aim, further partial objectives were established. The conclusions are presented according to the proposed objectives.

2) To assess the durability of the three selected crystalline stones in terms of the performed ageing tests

The three selected stones showed very distinct behaviour in the different tests. Their durability, therefore, is discussed individually.

- Macael marble

The Macael marble proved to be susceptible to all the processes where cyclic changes of temperature were involved irrespectively of the absolute temperature. Moreover, because of the chemical characteristic of the calcite, it is sensitive to chemical processes, such as acidic attack or increasing solubility in saline solutions. Also the presence of accessory minerals, such as pyrite and muscovite, further increases its susceptibility to chemical processes, see oxidation of pyrite. Otherwise, due to its very low open and total porosity, to processes that consist of the movement of fluids or of crystallization in the void space – such as the crystallization of salts or of ice – it shows high durability. Nevertheless, if the intercrystalline bonds among the mineral grains are weakened by other processes, like thermal weathering, the fluid uptake of the marble increases and the afore mentioned actions (especially the crystallization pressure) cause damage to the material. Due to its anisotropic thermal properties, the orientation of the stone specimens may have an important role in the velocity or degree of thermal weathering.

Thermal cycles occur during outside application in almost all environments due to insolation. However, the thermal cycles included in the applied ageing tests are exaggerated both in temperature range and in the heating or cooling rate. In all the tests

40°C was the range, either from -20°C to 20°C or from 20°C to 60°C and the change occurred within 1-2 hours or less. An interesting question for future research could be to determine the smallest temperature range where the fluctuation still causes damage to the marble and the influence of the rate on the weathering. This could help in deciding in which environment this marble can be applied on outside structures. The high chemical susceptibility, however, requires circumspection in the outside application regardless from the temperature regime.

- Vilachán granite

The Vilachán granite can be considered highly susceptible to crystallization pressure. The highest damage was caused by the crystallization of $NaSO_4 \bullet xH_2O$ salts, followed by NaCl and finally ice. Due to the characteristics of the void space structure of this stone, both the saturation and the evaporation happens very quickly, therefore large quantity of salt can enter into the material and then during the drying subflorescence forms. The large pores allows the formation of ice on relatively low sub-zero temperatures, and thus the effect of the forming ice also causes damage even in the presence of soluble salts, although the crystallization pressure of the ice is not that high as that of the salts. The high amount of micas means another weak point of the stone in front of physical damage. The mechanical strength of the stone is also low, therefore it cannot resist to the stress exerted by the precipitating or growing crystals. Thermally and chemically the granite is not sensible, the action of SO_2 caused minimal damage on this stone. The application of this material under conditions, where it can be object to salt weathering is not recommendable.

- Szob andesite

The Szob andesite is highly durable to any kind of weathering where the damaging agent acts via fluids entering into the material, such as salt or frost damage. The fluid movement kinetics is so slow and the void space is so poorly connected that the circulation of fluids in this andesite is almost zero. The salt solution hardly reaches the void space during the tests and thus minimal crystallization takes place inside the material. The depression of freezing point due to the small average void size is another reason why it is highly resistant to the effect of frost. The high mechanical strength further improves its durability to physical damage. The only test where the Szob andesite suffered considerable weathering was the action of SO_2. Due to the mineralogical and chemical composition, it is susceptible to chemical processes, specifically to the attack of sulphuric acid. Moreover, the dark colour of the stone is especially sensitive to colour changes, which is a very important aspect in the field of monumental and/or ornamental stones. Therefore, this stone is especially suitable for structural constructions but its application for ornamental purposes is not recommendable.

3)-4) To understand the mechanisms of the different weathering processes and their effect on each stone

Unfortunately, the mechanism of a given weathering agent and the mechanisms that act during the ageing test, which is used for the investigation of this weathering agent, sometimes can differ significantly. This paradox is further discussed in the last point of the conclusions. Here the processes of the ageing tests are considered with a comparison to those of the real agent.

- Salt crystallization and salt mist

The mechanisms of the salt crystallization (using sodium sulphate) and the salt mist (using sodium chloride) are basically equal; therefore these two agents are discussed together. The difference in the two tests, besides the difference in salts, is in the way how the salt solution gets into contact with the stone, which will have an influence on the degree of weathering, as discussed below.

The most important mechanism that causes salt weathering is the pressure exerted by the precipitating salt, the so-called crystallization pressure. Besides, other mechanisms, such as the hydraulic pressure, may participate in the process but their contribution to the damage seems to be minor. The damage caused by the crystallization pressure depends on (i) the quantity of salt solution that enters into the material, as this controls the quantity of salts that will precipitate; (ii) the velocity of evaporation from the material during the drying phase, as this determines the place of the crystallization; and (iii) the size of the pores where the crystallization takes place, as this determines the crystallization pressure. Leaving out of consideration the material properties – they are discussed in the following point – these factors will be determined by the experimental conditions in the laboratory testing and the environmental conditions in the reality; such as the length of the wetting and drying phases and the temperature and relative humidity during both of them.

The conditions of the two tests, the salt crystallization and the salt mist, differ considerably, which gives us the possibility to further evaluate the importance of these extrinsic factors. Two important differences between the conditions of the two tests are the temperature regime – which is constant room temperature in one and cyclically changing from 20°C to 60°C in the other – and the phase of the salt solution – vapour in one and fluid in the other. This second factor seems to have very slight influence in the results of the laboratory experiment because in the salt mist test the mist condensates on the surface of the samples and enters in liquid form into the material. Under real conditions however, there may be significant difference between the two processes due to other factors, such as the effect of wind, the quantity of ground moisture etc. The temperature conditions on the other hand introduce significant errors in the laboratory salt crystallization test, as it was proved by the thermal degradation of the marble.

- Freeze-thaw cycles with or without soluble salts

The mechanisms of the freeze-thaw cycles with and without the presence of soluble salts do not seem to differ significantly. The main damaging mechanism is the crystallization pressure of the ice. Besides, the 9% volume change of the water as it turns into ice, the hydraulic pressure and, in the presence of soluble salts, the osmotic pressure also may contribute to the process. The fact that the cycles in the presence of salts cause more severe damage than without salts proves that the osmotic pressure may have an important role in the process. The degree of damage therefore depends on the quantity of ice that forms inside the material and the concentration of the freezing liquid.

The quantity of ice will be determined by the (i) quantity of water in the porous space, (ii) the temperature, (iii) the length of the freezing period, (iv) the pore sizes, because of the freezing point depression, and (v) the concentration because of the same reason, as highly concentrated solutions have lower freezing temperatures. All of these factors are determined by the experimental or environmental conditions; and the quantity of water in the porous space and the pore size also by the material characteristics. To reach the highest saturation degree, these tests were carried out in constant immersion, which evidently is an exaggeration of the realistic conditions. The temperature ranges and the rate of cooling and heating are also rather extreme. The aim of this is to accelerate the processes but the introduction of unrealistic processes (like the thermal degradation of marble once again) may result in the misinterpretation of the results.

The concentration of the salt solution influences more than one aspect of the process. Besides the above mentioned freezing point depression, it will determine the degree of osmotic pressure, the possibility of chemical reactions etc. The osmotic pressure will be the higher, the higher the concentration is; but for the osmotic pressure to act freezing has to occur, which requires the lowest concentration possible. Therefore a pessimum concentration exists around 1-3% according to laboratory and field experiments from the literature. The laboratory tests always apply this concentration in order to reach the highest damage possible, but the question of how often this very concentration is present under real conditions remains open,

- The action of SO_2 in the presence of humidity

The mechanism of this process is probably the clearest and most well documented in the literature out of all the tested weathering agents. It consist of the deposition of the SO_2 on the surface of the stone, the formation of sulphurous acid, the oxidation process to form sulphuric acid and the acidic attack of the mineral phases. The susceptibility of carbonates to this process is well known; while silicate minerals are considered to be more resistant to acid-base reactions. However, in this research it was proved that this question cannot be simplified to the level of silicate or carbonate minerals, as significant differences were observed in the degradation of two silicate

rocks during the test, one of which suffered very severe damage. The type of the silicate minerals and the presence of catalysers have a determining influence on the degree of degradation caused by the acid. The type of minerals is clearly a material property, while the catalysers may be both extrinsic, like NOx gases of particulate deposition, which are usually not present in the laboratory test, or intrinsic, determined by the chemical composition of the material, as happened in this research and as discussed among the material properties. The concentration of the SO_2 was not proved to have large influence on the degree of weathering, but the length of exposition seems to be more important.

5) To identify those petrophysical parameters of the stone that are most responsible for the decay

The stone properties that determine the degree of damage are specific in the case of each weathering agent. Hereby, they are summarized altogether.

- Mineralogical composition
    - The mineralogical composition has a dominant importance in the action of SO_2. The resistance of a stone material to this process is mostly determined by the resistance of its mineral phases to the acidic attack. The quantity of carbonates, of Ca-bearing mineral phases and of Fe-bearing mineral phases was proved to be fundamental in the degree of damage. The discoloration suffered by the stone during this test also depends on the quantity of Fe-bearing phases.
    - The presence of calcite has an importance whenever salt solutions are present, as the solubility of this mineral in solutions is higher than in pure water and therefore calcite dissolution may take place.
    - The quantity of phillosilicates has an importance in the salt crystallization processes, mostly in the salt mist weathering, because of the high susceptibility of these minerals to physical damage.
    - The thermal properties – discussed below – are mostly determined by the mineralogical composition also.
- Chemical composition

The chemical composition is strongly connected to the mineralogical composition. Nevertheless, there are a few aspects where the chemical composition alone is decisive. This was the case in the action of SO_2, where the chemical composition of the plagioclase (more or less Ca content) and the quantity of Fe, because of the catalytic

effect of this element on the oxidation of S-oxides, controlled the degree of damage. The andesite with significantly higher Ca and Fe content suffered notably more severe damage than the granite, although the mineralogical composition of the two stones is not that extremely different.

- Thermal properties

The thermal properties are determined by the mineralogical composition and the void space. Under real conditions the colour and the surface finish also plays a crucial part because of the albedo of the material but these aspects were not investigated in this project. Thermal weathering is an independent issue within the stone degradation field, however in this research it was experimented as a side-effect of other processes. In all the tests, where cyclic temperature changes occurred, the thermally most sensitive material, the marble suffered thermal degradation. Because of the anisotropic thermal expansion of the calcite, an important intergranular weakening was observed on this material already after 45 cycles of changes in the range of 20°C. The effect of the cycles was proved to be independent form the absolute temperature.

- Mechanical properties

The mechanical properties were not directly investigated in this research but, as they determine the resistance of the materials to physical damage, their contribution to durability is undeniable. The mechanically more resistant andesite proved to be significantly less susceptible to physical degradation than the weaker granite.

- Hydraulic properties

The most important hydraulic properties that have a control over the degradation processes are the followings:

  - The water uptake, which determines the quantity of salt solution or the quantity of water that can enter into the voids of the material. This will control the quantity of the crystallizing salt or ice, and thus the degree of damage. The water uptake is determined by the capillary uptake, which controls the velocity of the saturation and by the open porosity, which controls the amount of fluid.

  - The capillarity process does not only determine the uptake of liquids, but the velocity of propagation of the liquids inside the material also.

  - The permeability is responsible for the ease and velocity of fluids transport and movement inside the stone. This besides the material characteristics depends on the properties of the fluid itself; therefore we can talk about permeability to liquid water, permeability to water

vapour, permeability to salt solution etc., which all have crucial importance in one or more phases of degradation.

- The evaporation, which besides the permeability to vapour, depends on the surface characteristics of the material (and also of the fluid properties and environmental conditions) have a fundamental importance in the salt weathering, determining the place of salt crystallization

The hydraulic properties of a material are, almost exclusively, determined by the properties of the void space therefore they are also discussed in connection to them.

- Void space structure

The void space structure was found to be of utmost importance in more then one of the weathering processes so it is discussed independently in the next point.

6) To identify which feature of the porosity and void space structure most influences the degradation processes

A great number of properties are summarized under the concept of void space structure: the total porosity, open porosity, pore size distribution, pore shape, connectivity, tortuosity and specific surface. These features determine the hydraulic properties of the material and partly or completely control other important properties, such as the thermal or mechanical properties -; and aspects of weathering processes, such as the crystallization pressure, the freezing point depression etc.

The two most important of the void space properties were found to be the connectivity of the void space and the void/aperture size distribution.

- The connectivity of the porous space determines the liquid uptake and the permeability to liquids and vapours. These characteristics have an outstanding importance in all the weathering processes connected to the movement of fluids and they excessively overrule the importance of the open porosity for example, if we consider the differences in the durability of the examined granite and andesite with similar open porosity.

- The void/aperture size distribution has influence on the

  - hydraulic properties, above all on the fluid transport; see the void size dependence of the capillarity velocity or of the vapour permeability

  - the crystallization pressure that builds up during the precipitation of salt or formation of ice
  - freezing point temperature of water, therefore the quantity of ice that forms at a given temperature. The importance of the 0,1 – 10 μm void range was confirmed by the results of this research also.
  - damage of frost in the presence of soluble salts, which was observed to affect the >1 μm void size range mostly

- the open porosity will evidently have an influence on the amount of fluid that can enter into the material, and therefore on the degree of weathering, but it was proved to be of secondary importance
- the total porosity may have an influence on the mechanical and thermal properties but its importance was not proved neither disproved during this investigation
- the fissure density had a significant influence during the salt mist test
- the specific surface determines the surface area exposed to chemical weathering, however its effect was highly overshadowed by the chemical composition
- the role of pore shape was not clarified by the results of this project

7) To understand the principle mechanisms of deterioration of crystalline stones

The most important conclusion that should be mentioned under this point is that we cannot speak about the deterioration of crystalline stones exclusively as an independent and unanimous issue. The common characteristics of the crystalline rocks, such as the fissure like void space, low porosity etc. are usually overruled by other properties in the control of processes and degree of degradation. These other properties, as detailed above, may be connected to the void space and the texture or may not. Therefore, generalizing deterioration tendencies or mechanisms for the large group of crystalline rocks would be inexpedient. The assessment of durability of each crystalline rock must be carried out considering the properties of the very material and not based on the petrophysical classification.

8) To find the most adequate methodology both for the characterization and the durability assessment of crystalline stones

- Material characterization

The material characterization in the context of stone degradation must include those properties that were found to be decisive in the control of durability properties, meaning the mineralogical, chemical composition, the mechanical and thermal properties and the hydraulic and void space properties. The classical geological methods for the investigation of the compositions are equally adequate for crystalline or cemented rocks. The thermal and mechanical properties were not characterized in this research very thoroughly; therefore conclusions cannot be withdrawn about them. Nevertheless, the hydraulic and void space properties of the stones, which proved to be of utmost importance in weathering, is a peculiar issue as far as crystalline stones are concerned. In this project, Hg intrusion porosimetry, nitrogen adsorption and CLSM-DIP techniques were used for the void space-investigation; and standardized methods of water absorption under vacuum and atmospheric pressure, capillary uptake, water vapour permeability, evaporation, and the non-standardized liquid water permeability for the hydraulic properties.

  - For the void space characterization, Hg porosimetry was found to be the most adequate simply because it has the widest detection range. Nevertheless, the fact that this technique carries out the calculations of the void aperture distribution supposing cylindrical pores should not be forgotten. Therefore, the value of the open porosity is reliable but the distribution must be considered an estimation and the use of the other additional methods, mostly microscopic techniques, is indispensable. Moreover, the microscopy techniques give further information about the geometry of the voids, the connectivity, tortuosity etc. which are also necessary for the characterization of solids. By all means, the methodology always has to be chosen as a function of the known or expected material properties.

  - For the hydraulic characterization the reliability of the standardized methods becomes questionable in the case of stones with very low porosity (like the marble in this research), when the most minimal changes in the execution of the measurement can introduce significant errors. Therefore, the automation of these methods would be favourable.

- Durability assessment

There are two important points within the durability assessment of stone materials: the durability tests themselves, and the monitoring and evaluation of the damages caused by the tests.

- The durability tests are standardized processes, which aim at the acceleration of weathering by means of the extreme exaggeration of the deteriorating agents. Due to this aim these tests will never use perfectly realistic approaches. However, the introduction of mechanisms which are not parts of the examined weathering process can lead to the erroneous assessment of the materials applicability. The most extreme example for this is the thermal effect during the salt crystallization test. Also, the length of wetting-drying phases or of freezing-thawing phases can considerably change the caused damage. Therefore, the specification of these periods according to the material properties or according to the conditions of probable application of the stone could provide more reliable information about the durability.

- The evaluation of the changes in most of the standards is based on the weight loss. During this research the weight loss several times proved to be misleading either under- or overestimating the caused damage. It is a reliable measure of deterioration only if the material loss is high enough, which is often not the case in crystalline rocks, which does not mean that no damage occurs. The monitoring of ultrasonic propagation and of hydraulic properties, especially the capillary uptake on the other hand proved to describe the ongoing damage quite correctly. In the case of superficial damage the colour can be recommendable to measure – determining the limits of acceptability of colour change – and the XPS technique proved to be useful for the monitoring of the chemical changes of the surface. This later is not recommended for the industry but may be suitable for academic research.

In summary, the durability of stone is a function of several material properties, the most important ones of which are the mineralogical composition, the void aperture size and distribution, the connectivity of the void space, the hydraulic properties and the thermal and mechanical properties. This is true as much for the crystalline stones, investigated in this research and characterized by relatively low and fissure like porosity, as for the non-crystalline or cemented stones with higher proportions of spherical pores. No properties or weathering processes can be pointed out as especially determining for crystalline stones, as the variation of material properties within this group is very high. For the correct and reliable assessment, a thorough characterization of the most fundamental material properties and the testing of the material by several types of ageing tests is necessary, as the response of a given stone type may be very distinct to different weathering agents. The standardized processes are very useful for the comparison of different investigations and materials, however due to the necessary generalizations they may be misleading in some cases. Both the characterization and the

durability assessment of the stone materials must happen by a methodology that takes into account the material properties and the conditions of application.

The results of this thesis contribute to the knowledge about the mechanisms of stone deterioration and about the most important stone properties influencing these processes. In the field of Stone Conservation, a solid background of these ideas helps the interpretation of the weathering forms and types observed on materials of monuments and also the selection of the most adequate methods and treatments of conservation interventions.

Bibliography

– Ábalos B, Carreras J., Druguet E., Escuder Viruete J., Gómez Pugnaire M.T., Lorenzo Alvarez S., Quesada C., Rodríguez Fernández L.R. and Gil-Ibarguchi J.I (2002): Variscan and Pre –Variscan Tectonics in The Geology of Spain, Gibbons W. and Moreno T. eds. The Geological Society, London p.649

– Al-Harthi A.A. (1997): Effect of planar structures on the anisotropy of Ranyah sandstone, Saudi Arabia – Engineering Geology 50 pp. 49-57

– Allison R.J. (1988): A non-destructive method of determining rock strength – Earth Surface Processes and Landforms 13 pp. 729-736

– Alonso E. and MArtínez L. (2003): The role of the environmental sulfur on degradation of ignimbrites of the Cathedral in Morelia, Mexico (2003): Building and Environment 38 pp. 861-867

– Alonso F.J., Suárez del Río L.M. (1985) – Velocidad de propagación de ondas en rocas carbonatadas – Trabajos de Geología 15 pp 315-324

– Alonso F.J., Vázquez P., Esbert R.M. and Ordaz J. (2008): Ornamental granite durability: evaluation of damage caused by salt crystallization test – Materiales de Construcción 58 pp. 191-202

– Amoroso G.G. and Fassina V. (1983): Stone decay and conservation – Elsevier Science Publishers, Amsterdam, p.1453

– Anom, I. G. N. and Samidi, S. (1993) Conservation of stone monuments in Indonesia - In. Conservation of Stone and Other Materials, Proceedings of the international RILEM/UNESCO congress held at the UNESCO headquarters, Paris, ed.: Thiel, M.-J., pp. 853-859

– Anon. (1983): The selection of natural building stone – Digest 260. Watford: Building Research Establishment. Her Majesty's Stationary Office

– Aranda A.L., Ruiz-Agudo E., Cultrone G. and Sebastián E. (2008): Análisis superficial mediante VPSEM y XPS de mármoles alterados por acción de SO_2 – MACLA – Revista de la Sociedad Española de Mineralogía 9 pp. 147-148

– Arikan F., Ulusay R. and Aydin N. (2007): Characterization of weathered acidic volcanic rocks and a weathering classification based on a rating system – Bulletin of Engineering Geology and the Environment 66 pp. 415-430

– Arnfelt H. (1943): Damage to concrete pavements by wintertime salt treatment – Meddelande 66 Statens Väginstitut, Stockholm pp. 4-28

– Arnold A. (1975): Soluble salts and stone weathering – The Conservation of Stone I. Proceedings of the International Symposium, Bologna, Italy pp. 133-135

– Arnold A. (1981): Nature and reactions of saline minerals in walls – Conservation of Stone II. – Preprint of the Contributions to the International Symposium, Bologna, Italy pp. 13-23

– Arnold A. and Kueng A. (1985): Crystallization and habits of salt efflorescences on walls I. Methods of investigation and habits – 5th International Congress on Deterioration and Conservation of Stone, Lausanne

– ASTM Standard C672 (1992) Standard test method for scaling resistance of concrete surfaces exposed to deicing chemicals – Annual Book of ASTM Standards, 04.02., American Society for Testing and Materials, Philadelphia, pp. 341-343

– Ausset P., Crovisier J.L., Del Monte M., Furlan V., Girardet F., Hammecker C., Jeannette D. and Lefevre R.A. (1996): Experimental study of limestone and sandstone sulphation in polluted realistic conditions: the Lausanne Atmospheric Simulation Chamber (LASC) – Atmospheric Environment 30/18 pp. 3197-3207

– Azañón J.M., Galindo-Zaldívar J., Gracía-Dueñas V., Jabaloy A. (2002): Alpine tectonics II: Betic Cordillera and Balearic Islands – in The Geology of Spain, Gibbons W. and Moreno T. eds., The Geological Society, London pp. 401-416

– Bai Y., Thompson G.E. and Martinez-Ramirez S. (2006): Effects of NO_2 on oxidation mechanisms of atmospheric pollutant SO_2 over

Baumberger sandstone – Building and Environment 41 pp. 486-491

– Bams V. and Dewaele S. (2007): Staining of white marble – Materials Characterization 58 pp. 1052-1062

– Barbin, V., Zezza, U., Sebastián Pardo, E. (1995): The cathodomicrofacies of Macael white marbles (Almeria, Spain) – in The study of marble and other stones used in Antiquity eds. Maniatis, Y., Herz, N., Basiakos Y., Archetype, Athens, pp. 131-135

– Battaglia S., Franzini M., Mango F. (1993): High sensitivity apparatus for measuring linear thermal expansion: preliminary results on the response of marbles to thermal cycles - Il Nuovo Cimento 16 pp. 453-461.

– Beck K., Al.Mukhtar M., Rozenbaum O., Rautureau M. (2003): Characterization, water transfer properties and deterioration in tuffeau: building material in the Loire valley—France – Building and Environment 38 pp. 1151-1162

– Begonha A. and Braga M.A.S. (2002): Weathering of the Oporto granite: geotechnical and physical properties – Catena 49 pp. 57-76

– Bell F.G., and DearmanW.R. (1988): Assesment of the durability of sandstones with illustrations from some buildings in the North of England – Engineering Geology of Ancient Works, Monuments and Historical Site, Rotterdam pp. 707-716

– Bello, M.A., Martin L., Martin A.(1992): Decay and treatment of Macael white marble – Studies in Conservation **37** pp.193-200

– Benavente D., Martínez-Verdú F., Bernabeu A., Viquiera V., Fort R., García del Cura M.A., Illueca C., Ordóñez S. (2003a): Influence of surface roughness on colour changes in building stones – COLOR Research and Application 28/5 pp. 343-351

– Benavente D., García del Cura M.A., Ordóñez S. (2003b) – Salt influence on evaporation from porous building rocks – Construction and Building Materials 17 pp. 117-122

– Benavente D., García del Cura M.A., Fort R., Ordóñez S. (2004): Durability estimation of porous building stones from pore structure and strength – Engineering Geology 74 pp. 113-127

– Benavente D., Martínez-MArtínez J., Jáuregui P., Rodríguez M.A., García del Cura M.A. (2006): Assessment of the strength of building rocks using signal processing procedures – Construction and Building Materials 20 pp.562-568

– Benavente D., Cueto N., Martínez-Martínez J., García del Cura M.A. and Cañaveras J.C. (2007): The influence of petrophysical properties on the salt weathering of porous building rocks – Environmental Geology 52 pp. 215-224

– Benavente D., Cultrone G. and Gómez-Heras M. (2008): The combined influence of mineralogical, hygric and termal properties on the durability of porous building stones – European Journal of Mineralogy 20 pp. 673-685

– Benson P. M., Meredith P.G., Platzman E.S., White R.E (2005): Pore fabric shape anisotropy in porous sandstones and its relation to elastic wave velocity and permeability anisotropy under hydrostatic pressure – International Journal of Rock Mechanics and Mining Sciences 42 pp. 890-899

– Pérez Bernall J.L. and Bello López M.A. (2004): Dióxido de Azufre. Química Atmosférica y Destrucción del Patrimonio – Fundación El Monte, Sevilla

– Bing H., He P., Yang C., Shi Y., Zhao S. and Bian X. (2007): Impact of sodium sulphate on soil frost heaving in an open system – Applied Clay Science 35 pp. 189-193

– Birginie J.M. (2000): Sea water absorption, permeability evolution and deterioration assessment of building stones subjected to marine exposure – 9th International Congress on Deterioration and Conservation of Stone, Venice pp. 313-321

– Blanchard D. and Woodcock A. (1957): Bubble formation and modification in the sea and its meteorological significance – Tellus 9 pp. 145-158

– Bourgès A. (2006): Holistic correlation of physical and mechanical properties of selected natural stones for assessing durability and weathering in the natural environment – PhD Thesis, Fakultät für Geowissenschaften der Ludwigs-Maximilians-Universität, München

– Bousquie P. (1979): Texture et porosité de roches calcaires – Thesis doctoral, Université Pierre et Marie Curie, Paris

– Böke H., Göktürk E.H., Caner-Saltik E.N. and Demirci Ş. (1999) : Effect of airborne particle on SO_2—calcite reaction – Applied Surface Science 140 pp. 70-82

– Brandi C. (1977): Teoría de la restauración – Alianza Editorial

– Bromblet P., Bernabé E. and Vergès-Belmin V. (1996): Petrophysical investigation on the origin of scaling of a microgranular magmatic rock associated to granite in the monuments from Brittany (France) – Environmental Protection and Conservation of the European Cultural Heritage – Degradation and Conservation of Granitic Rocks, European Commission pp. 73-78

– Brunauer S., Emmett P. H., Teller E. (1938): Adsorption of Gases in Multimolecular Layers – Journal of the American Chemical Society 60 pp 309–319

– Bubics I. (1969): A szobi Csákhegyi és Malomvölgyi bányák andezit és dácit területének kutatási terve – Visegrád

– Bugini R., Laurenzi Tabasso M. and Realini M. (2000): Rate of formation of black crusts on marble. A cas stugy – Journal of Cultural Heritage 1 pp. 111-116

– Burdick L.R. and Barkley J.F. (1939): Effect of sulphur compounds on various materials – In Circular 7064, U.S. Bureau of Mines Information, Washington D.C.

– Bustillo Revuelta M. (1996) "Potencial geológico de granitos en España" in Manual de Rocas Ornamentales, ed. J. Carlos López, Madrid, , p. 696

– Camerman C. (1945): Study of the stones of Brussels' monuments: effects of air pollution - Bulletin de la Societe Belge de Geologie de Paleontologie et d'Hydrologie 54 cpp. 133-139

– Camuffo D., Del Monte M., Sabbioni C. (1983): Origin and growth mechanisms of the sulphated crusts on urban limestone – Water Air Soil Pollution 19 pp. 351-359

– Camuffo D. (1995): Physical weathering of stones - The Science of the Total Environment 167 pp. 1-14

– Camuffo D. (1996): Limits of stone sensitivity to freezing-thawing cycles - In: Vicente MA, Delgado-Rodrigues J, Acevedo J, editors. Proceedings of the European Commission Research Workshop on Degradation and Conservation of Granitic Rocks in Monuments: Spain pp.455 – 462

– Caneva G., Nugari M.P. and Salvadori O. (1991): Biology in the Conservation of Works of Art - ICCROM

– Cantisani E., Pecchioni E., Fratini F., Garzonio C.A., Malesani P. and Molli G. (2009): Thermal stress in the Apuan marbles: Relationship between microstructure and petrophysical characteristics – International Journal of Rock Mechanics and Mining Sciences 46 pp. 128-137

– Cardell C., Rivas T., Mosquera M.J., Birginie J.M., Moropoulou A., Prieto B., Silva B. and Van Grieken R. (2003a): Patterns of damage in igneous and sedimentary rocks under conditions simulating sea-salt weathering – Earth Surface and Landforms 28 pp.1-14

– Cardell C., Delalieux F., Roumpopoulos K., Moropoulou A., Auger F., Van Grieken R. (2003b) : Salt-induced decay in calcareous stone monuments and building in a marine environment in SW France – Construction and Building Materials 17 pp. 165-179

– Cardell C., Benavente D. and Rodríguez-Gordillo J. (2008): Weathering of limestone building material by mixed sulphate solutions. Characterization of stone microstructure, reaction products and decay forms – Materials Characterization 59 pp. 1371-1385

– CDF Test (1996) Test method for the freeze-thaw resistance of concrete – test with sodium chloride solution – Recommendation by Setzer

M.J., Fagerlung G. and Janssen D.J. published online: http://www.uni-due.de/ibpm/Projekte/CDF_eng.pdf

– Cerepi A., Humbert L., Burlot R. (2002): Dynamics of capillary flow and transport properties in porous media by time-controlled porosimetry – Colloids and Surfaces A: Physicochemical and Engineering Aspects 206 pp. 425-444

– Ceryan S., Tudes S. and Ceryan N. (2008): Influence of weathering on the engineering properties of Harsit granitic rocks (NE Turkey) – Bulletin of Engineering Geology and the Environment 67 pp. 97-104

– Chabas A. and Jeannette D. (2001) : Weathering of marbles and granites in marine environment : petrophysical properties and special role of atmospheric salts – Environmentyl Geology 40 (3) pp. 359-368

– Chae B.G., Ichikawa Y., Jeong G.C., Seo Y.S., Kim B.C. (2003) : Roughness measurement of rock discontinuities using a confocal laser scanning microscope and the Fourier spectral analysis - Engineering Geology 72 pp. 181-199

– Chan C.K., Ha Z. and Choi M.Y. (2000): Study of water activities of aerosols of mixtures of sodium and magnesium salts – Atmospheric Environment 34 pp. 4795-4803

– Charola A.E. (2000): Salts in the deterioration of porous materials: an overview – Journal of the American Institute for Conservation 39 pp. 327-343

– Charola A.E. and Weber J. (1992): The hydration-dehydration mechanism of sodium sulphate - 7th International Congress on Deterioration and Conservation of Stone, Lisbon, pp. 581-590

– Chatterji S. and A.D. Jensen (1989): Efflorescence and breakdown of building materials - Nordic Concrete Research, Oslo 8 pp. 56–61.

– Chatterji S. (2005): Aspects of generation of destructive crystal growth pressure – Journal of Crystal Growth 277 pp. 566-577

– Chen T.C., Yeung M.R. and Mori N. (2004): Effect of water saturation on deterioration of welded tuff due to freeze-thaw action – Cold Regions Science and Technology 38 pp. 127-136

– Chigira M. and Oyama T. (1999): Mechanism and effect of chemical weathering of sedimentary rocks – Engineering Geology 55 pp. 3-14

– Claxton N.S., Fellers T.J., Davidson M.W. (net access 2008.oct.): Laser Scanning Confocal Microscopy - http://www.olympusconfocal.com/theory/LSCMIntro.pdf

– Correns (1949): Growth and dissolution of crystals under linear pressure, Discussions of the Faraday Society. 5 pp. 267-271

– Coussy O. (2005): Poromechanics of freezing materials – Journal of the Mechanics and Physics of Solids 53 pp. 1689-1718

– Coussy O. (2006): Deformation and stress from in-pore drying-induced crystallization of salt – Journal of the Mechanics and Physics of Solids 52 pp. 1517-1547

– Coussy O. and Monteiro P. (2007): Unsaturated poroelasticity for crystallization in pores – Computers and Geotechnics 34 pp. 279-290

– Coussy O. and Monteiro P.J.M. (2008): Poroelastic model for concrete exposed to freezing temperatures – Cement and Concrete Research 38 pp. 40-48

– Cueto N., Benavente D., Martínez-Martínez J., Garcia del Cura M.A. (2009): Rock fabric, pore geometry and mineralogy effects on water transport in fractured dolostones – Engineering Geology 107 pp. 1-15

– Cultrone G., Russo L.G., Calabró C., Urošsevič M. and Pezzino A. (2008): Influence of pore system characteristics on limestone vulnerability: a laboratory study – Environmental Geology 54 pp. 1271-1281

– Cwajna J. and Roskosz S. (2001): Application of confocal laser scanning microscopy, atomic force microscopy and the profilometric method in quantitative fractography – Materials Characterisation 46 pp.183-187

– Çopuroğlu O. and Schlangen E. (2008): Modeling of frost salt scaling – Cement and Concrete Research 38 pp. 27-39

– Darrow M.M., Huang S.L. and Akagawa S. (2009): Adsorbed cation effects on the frost susceptibility of natural soils – Cold Region Science and Technology 55/3 pp. 263-277

– Delgado Rodrigues J. (1983): Laboratory study of thermally fissured rocks - Memória 583, LNEC, Lisboa pp. 281-294

– Delgado Rodriguez J. (2000): Decay of granite – in: Croci G. and Delgado Rodriguez J. Surface and structural stability for the conservation of historical buildings. EC Advanced Study Course, Sustainable Heritage. Londres, UCL Centre for Sustainable Heritage – Technical Notes for Sessions 14-15

– Del Monte M. and Rossi P. (1997): Fog and gypsum crystals on building materials – Atmospheric Environment 31/11 pp. 1637-1646

– Dessandier D. (2000): Durability of tuffeau stone buildings: Influence of mineralogical composition and microstructural properties – 9th International Congress on Deterioration and Conservation of Stone, Venice 19-24- June 2000. pp. 69-78

– D'Have R. and Motteu H. (1968): Etude de la résistance au gel des matériaux de construction – Buil. Bâtiment International 1. pp. 26-31

– Doehne E. (2002): Salt weathering: a selective review – In: Siegesmund A., Weiss T. and Vollbrecth A: Natural Stone, Weathering Phenomena, Conservation Strategies and Case Studies. Geological Society, London, Special Publications 205, pp. 51-64

– Dolske D.A. (1995): Deposition of atmospheric pollutants to monuments statues, and building – The Science of the Total Environment 167 pp. 15-31

– Dubois C., Couchot P., Alvarez Calleja A., Boeglin E., Chambaudet A. (1998): Specific mercury porosimetry for low-porosity materials – Measurement Science and Technology 9 pp. 2016-2022

– Duffy A.P. and O'Brien P.F. (1996): A basis for evaluating the durability of new building stone – In: Processes of Urban Stone Decay Eds.: Smith B.J. and Warke P.A., Donhead, London, pp. 253-260

– Dürrast H. and Siegesmund S. (1999): Correlation between rock fabricks and physical properties of carbonate rocks – International Journal of Earth Sciences 88 pp. 392-408

– Eberhardt E., Stimpson B. and Stead D. (1999): Effects of grain size on the initiation and propagation thresholds of stress induced brittle fractures – Rock Mechanics and Rock Engineering 32 pp. 81-99

– Eggleston C.M., Hug S., Stumm W., Sulzberger B. and Dos Santo sAfonso M. (1998): Surface complexation on sulphate by hematite surface: FTIR and STM observations – Geochimica et Cosmochimica Acta 62/4 pp. 585-593

– Elek I. (1973): Szobi andezitek kőzettani vizsgálatának technológiai értelmezése – Miskolc

– EN 1925 (1999): Natural stone test methods. Determination of water absorption coefficient by capillarity

– EN 1936 (1999): Natural stone test methods. Determination of real density and apparent density, and of total and open porosity

– EN 13755 (2002): Natural stone test methods. Determination of water absorption at atmospheric pressure

– EN 14066 (2003): Natural stone test methods. Determination of resistance to ageing by thermal shock

– Erdogan M. (2000): Measurement of polished rock surface brightness by image analysis method – Engineering Geology 57 pp. 65-72

– Eriksson E. (1960): The yearly circulation of chloride and sulfur in nature: meteorological, geochemical and pedological implications (part II) – Tellus 12 pp. 63-109

– Esbert R.M. (2004): Deterioro del granito en los monumentos de Santiago – ACTAS II Congreso Internacional Antiguos espacios para nuevos tiempos – El material pétreo y sus

fábricas en el patrimonio, Consorcio de Santiago, Santiago de Compostela, Spain pp. 49-69

– Esbert R.M (2007): Alteración de rocas graníticas utilizadas en edificación – Materiales de Construcción 57/288 pp. 77-89

– Esbert R.M. and Ordaz J. (1985): Alteración y alterabilidad de las piedras de la constricción: criterios petrophísicos y ensayos de laboratorio – I Congreso de Patología de la Edificación, C.O.A.C., Barcelona, p 15

– Esbert R.M. and Valdeón L. (1985): Relación entre porosidad, contenido en arcillas y durabilidad de areniscas – Materiales de construcción 35 pp. 15-22

– Esbert R.M., Ordaz J., Alonso F.J., Montoto M. (1997): Manual de diagnosis y tratamiento de materiales pétreos y cerámicos – Collegi d'Aparelladors i Arquitecets Tècnics de Barcelona, Barcelona p. 139

– Esbert R.M. and Losada J.M. (2003): Intervention criteria in masonry materials – Instituto del Patrimonio Histórico Español 2 pp. 1-35

– Everett D.H. (1961): The thermodynamics of frost damage to porous solids – Transactions of the Faraday Society 57. pp. 1541-1551

– Exadaktylos G. (1998): Characterization of mechanical properties and damage of natural building stones in historical monuments – Report of the MONUMENTS PROJECT – SMT4-CT96-2130 published online: http://www.mred.tuc.gr/projects/monuments/monuments.html

– Fagerlund G. (1975): The significance critical degrees of saturation at freezing of porous and brittle materials – Durability of Concrete, ACI SP 47-2. American Concrete Institute, Detroit, Michigan

– Flatt R.J. (2002): Salt damage in porous materials: how high supersaturation are generated – Journal of Crystal Growth 242 pp. 435-454

– Fitzner B. and Snethlage R. (1982): Über Zuzammenhange zwischen Salzcristallisationsdruck und Porenradien-verteilung – GP News Letter 3 pp. 13-24

– Friedrich J.T. (1999): 3D imaging of porous media using laser scanning confocal microscopy with application to microscale transport processes - Physics and Chemistry of the Earth 24 pp. 551-561

– Franke W.A. and Teschner-Steinhardt R. (1994): An experimental approach to the sequence of the stability of rock forming minerals towards chemical weathering – Catena 21 pp. 279-290

– Friedrich J.T., Menéndez B., Wong T.F. (1995): Imaging the pore structure of geomaterials - Science 268 pp. 276-297

– Gómez Heras M. (2005): Procesos y formas de deterioro térmico en piedra natural del patrimonio arquitectónico – Thesis doctoral, Departamento de Petrología y Geoquímica, Facultad de Ciencias Geológicas, Universidad Compultense de Madrid, p.339

– Gómez-Heras M., Smith B.J. and Fort R. (2006): Surface temperature differences between minerals in crystalline rocks: Implications for granular disaggregation of granites through thermal fatigue – Geomorphology 78 pp. 236-249

– Good R.J. and Mikhail R. SH. (1981): The contact angel in mercury intrusion porosimetry – Powder Technology 29 pp. 53-62

– Goudie A.S. (1974): Further experimental investigation of rock weathering by salt and other mechanical processes – Zeitschrift für Geomorphologie Supplementband 21 pp. 1-12

– Goudie A.S. (1977): Sodium sulphate weathering and disintegration of the Mohenjo-Daro, Pakistan – Earth Surface Processes and Landforms 2 pp. 75-86

– Goudie A.S. (1999): Experimental salt weathering of limestones in relation to rock properties – Earth Surface Processes and Landforms 24 pp. 715-724

– Goudie A.S. and Viles H.A. (1997): Salt weathering hazards. John Wiley, Chichester

– Grinzato E., Marinetti S., Bison P.G., Concas M., Fais S. (2004): Comparison of ultrasonic velocity and IR thermography for the characterization of stones – Infrared Physics and Technology 46 pp. 63-68

– Grossi C.M. and Esbert R.M. (1994): Las sales en el deterioro de rocas monumentales. Revisión bibliográfica – Materiales de Construcción 44/235 pp. 15-30

– Grossi C.M., Esbert R.M., Butlin R.N. and Lewry A.J. (1994): Weathering of building carbonate rocks under SO2 polluted atmospheres – 7th International Congress of the International Association of Engineering Geology, Balkema, pp. 3573-3582

– Grossi C.M. and Murray M. (1999): Characteristics of carbonate building stones that influence the dry deposition of acidic gases – Construction and Building Materials 13 pp. 101-108

– Grossi C.M., Brimblecombe P., Esbert R.M. and Alonso F.J. (2007a) : Color changes in architectural limestones from pollution and cleaning – Color Research and Application 32/4 pp. 320-331

– Grossi C.M., Brimblecombe P. and Harris I. (2007b): Predicting long term freeze-thaw risk on Europe built heritage and archaeological sites in a changing climate – Science of the Total Environment 377 pp. 273-281

– Gruszkiewicz M.S., Horita J., Simonson J.M., Mesmer R.E., Hulen J.B. (2001): Water adsorption at high temperature on core samples from The Geysere geothermal fiels, California, USA – Geothermics 30 pp. 269-302

– Guil Pinto J.M. (2007): Determinación del area superficial de sólidos - Técnicas de Caracterización de Sólidos, Curso de Especialización de Postgrado, CSIC, Oviedo

– Gupta A.S. and Seshagiri Rao K. (1998): Index properties of weathered rocks: inter-relationship and applicability – Bulletin of Engineering Geology and the Environment 57 pp. 161-172

– Hall K. (1988): A laboratory simulation of rock breakdown due to freeze-thaw in maritime Antarctic environment – Earth Surface Processes and Landforms 13 pp. 369-382

– Hall K. (1999): The role of thermal stress fatigue in the breakdown of rock in cold regions – Geomorphology 31 pp. 47-63

– Hall K. and André M.F. (2001): New insights into rock weathering from high-frequency rock temperature data: an Antarctic study of weathering by thermal stress – Geomorphology 41 pp. 23-35

– Hammecker C. (1995): The importance of the petrophysical properties and external factors in the stone decay on monuments – Pure and Applied Geophysics 145 pp. 337-361

– Hatsagortsian Z. (1985): Principes expérimentaux et théoriques pour l'évaluation de durabilité de la pierre – 5th International Congress on Deterioration and Conservation of Stone, Lausanne, pp. 195-202

– Hirschwald J. (1908): Die Prufung der naturlichen Bausteine auf ihre Wetterbestandigkeit – Ernst and Sohn, Berlin

– Hoffmann D. and Niesel K. (1992): Pore structure of rendering as a feature of its weathering – 7th International Congress on the Deterioration and Conservation of Stone, Lisbon, pp. 611-620

– Hudec P.P. (1998): Rock properties and physical processes of rapid weathering and deterioration – 8th International IAEG Congress, Rotterdam pp. 335-341

– ICR CNR NORMAL 21/85 (1985): Alterazioni dei materiali Lapidei e Trattamenti Conservativi. Proposte per L'Unificazione dei Metodi Sperimentali di Studio e di Controlo. Permeabilita al vapor d'acqua, Roma

– ICR CNR NORMAL 29/88 (1988): Misura Dell'Indice di Asciugamento, Roma

– IGME (1975) Mapa Geológico 1:50 000, MAGNA, hoja 1013. (Macael)

– IGME (1981) Mapa Geológico 1:50 000, MAGNA, hoja 261 (Tuy)

– Ingham J.P. (2005): Predicting the frost resistance of building stone – Quarterly Journal of Engineering Geology and Hydrogeology 38 pp. 387-399

– Inkpen R.J., Petley D. and Murohy W. (2004): Durability and rock properties – In: Stone Decay – Its Causes and Controls Eds.: Smith B.J. and Turkington A.V., Donhead Publishing, pp. 33-52

– Iñigo A.C., Vicente M.A., Rives V. (2000): Weathering and decay of granitic rocks: its relation to their pore network – Mechanics of Materials 32 pp. 555-560

– Ip K.H., Stuart B.H., Ray A.S. and Thomas P.S. (2008): A spectroscopic investigation of the weathering of a heritage Sydney sandstone – Spectrochimica Acta Part A: Molecular and Biomolecular Spectroscopy 71 pp. 1032-1035

– Jeannette D. (1997) – Importance of the pore structures during the weathering process of stones in monuments – In. Soils and Sediments, Mineralogy and Geochemistry; Paquet, H., Clauer, N., Eds.; Springer: Berlin, Germany, pp.177-190

– Johansson L.G., Lindqvist O. and Mangio R.E. (1988): Corrosion of calcareous stones in humid air containing NO2 and SO2 – Dur. Building Material 5 pp. 439-449

– Johnson J.B., Montgomery M., Thompson G.E., Wood G.C., Sage P.W. and Cooke M.J. (1996): The influence of combustion-derived pollutants on limestone deterioration: 2. The wet deposition of pollutant species – Corrosion Science 38/2 pp. 267-278

– Kahraman S. (2001): Evaluation of simple methods for assessing the uniaxial compressive strength of rock – International Journal of Rock Mechanics and Mining Sciences 38 pp. 981-994

– Kahraman S. (2002): The effects of fracture roughness on P-wave velocity – Engineering Geology 63 pp. 347-350

– Kahraman S. (2007): The correlations between the saturated and dry P-wave velocity of rocks – Ultrasonics 46 pp. 341-348

– Kapruz C. and Paşamehmetoğlu A.G. (1992): Rock mechanics characteristics of Ankara andesites in relation to teir degree of weathering – in eds.: Delgado-Rodrigues et al. Proceedings of 7th International Congress on Degradation and Conservation of Stone, Lisbon, Portugal pp. 39-46

– Kate J.M. and Gokhale C.S. (2006): A simple method to estimate complete pore size distribution of rocks – Engineering Geology 84 pp. 48-69

– Kertész P. (1985): Neogene mineral resources in the Carpathian basin – In: 8th Conference of the Regional Committee on Mediterranean Neogene Stratigraphy, Ed.: Hála J., Hungarian Geological Survey, Budapest pp. 397-426

– Koch A. and Siegesmund S. (2004): The combined effect of moisture and temperature on the anomalous expansion behaviour of marble – Environmental Geology 46 pp. 350-363

– Korpás L. (ed.) (1998): Magyarázó a Börzsöny és a Visegrádi-hegység földtani térképéhez. A Magyar Állami Földtani Intézet Térképmagyarázói. - Magyar Állami Földtani Intézet, Budapest, p.216

– Kovács I. (2006): Az Ónodi vár palotaszárhyának kötöredékei – Örökségvédelmi Hírmondó Published on-line: http://www.koh7.hu/6_szerkeszto/04_kpisti/090128_onod/onod.html

– Kovács T. (2008): Use of confocal laser scanning microscopy in the characterization of the void space of natural stones - in Török Á. and Vásárhelyi B. eds. Mérnökgeológia - Kőzetmechanika 2008 Budapest, Hungary pp. 177-184

– Kovács T., Esbert R.M., Montoto M. (2008): Characterization of the pore space of crystalline monumental stones – Proceedings 9th International Congress on Architectural Heritage and Building Rehabilitation , Sevilla, Spain pp. 63-68

– Kühnel R.A. (2002): Driving forces of rock degradation – Protection and Conservation of the Cultural Heritage of Mediterranean Cities, Eds.: Galán and Zezza, Swets and Zeitlinges, Lisse pp. 11-17

– Kühnel R.A. (2004): Cause and consequence: volume changes behing building material deterioration – Materials Characterization 53 pp. 171-180

– La Iglesia A., González V., López-Acevedo V. and Viedma C. (1997): Salt crystallization in porous construction materials I. Estimation of crystallization pressure – Journal of Crystal Growth 177 pp.111-118

– Lee S.Y., Kim S.J. and Baik M.H. (2008): Chemical weathering of granite under acid rainfall environment, Korea – Environmental Geology 55 pp. 853-862

– Leiss B. and Weiss T. (2000): Fabric anisotropy and its influence on physical weathering on different types of Carrara marbles – Journal of Structural Geology 22 pp. 1737 - 1745

– Lewin S.Z. (1982): The mechanism of masonry decay through crystallization – Conservation of Historic Stone Buildings and Monuments pp. 120 – 144

– Lewin S.Z. (1983): Foreword to Stone Decay and Conservation – Materials Science Monographs 11. Eds.: Amoroso G.G and Fassina V., Elsevier

– Lewin S.Z. (1989): The susceptibility of calcareous stones to salt decay

– Lindberg S.E. and Lovett G.M. (1992): Deposition and forest canopy interactions of airborn sulphur: results from the integrated forest study – Atmospheric Environment 26A pp. 1477-1492

– Lindqvist J.E., Åkesson U., Malaga K. (2007a): Microstructure and functional properties of rock materials – Materials Characterization 58 pp. 1183-1188

– Lindqvist J.E., Malaga K., Middendorf B., Savukoski M. and Pétursson P. (2007b): Frost resistance of natural stone, the importance of micro- and nano-porosity – published online: http://www.sgu.se/dokument/fou_extern/Lindqvist-et-al_2007.pdf

– Liu S.; Anwar A.H.M.F., Kim B.C., Ichikawa Y. (2006): Observation of micro-cracks in granite using a confocal laser scanning microscope – International Journal of Rock Mechanics and Mining Sciences 43 pp. 1293-1305

– Logan J.M., Hadedt M., Lehnert D. and Denton M. (1993): A case study of the properties of marble as building veneer – International Journal of Rock Mechanics, Mining Sciences and Geomechanics 30 pp. 1531-1537

– López-Arce P., García-Guinea J. and Fierro J.L.G. (2003): Manganese micro-nodules on ancient brick walls – The Science of the Total Environment 302 pp. 267-274

– López Burgos M.A. (2002): Los mármoles, la minería en España y la geología de Granada en la obre de E. Cook, un viajero inglés de 1830 – Cuadernos Geográficos, Universidad de Granada 32 pp. 229-248

– Lubelli B., Van Hees R.P.J., Groot C.J.W.P. (2004): The role of sea salts in the occurrence of different damage mechanisms and decay patterns on brick masonry – Construction and Building Materials 18 pp. 119-124

– MacAdam D.L. (1985): Colour Measurement – Theme and Variationas, Second Revised Edition, Springer-Verlag, p.228

– McMahon D.J., Sandberg P., Folliard K., Mehta P.K. (1992): Deterioration mechanisms of sodium sulfate - 7th International Congress on Deterioration and Conservation of Stone, Lisbon pp. 705-714

– Mahmutoğlu Y. (2006): The effects of strain rate and saturation on micro-cracked marble – Engineering Geology 82 pp. 137-144

– Malaga-Starzec K., Panas I., Lindqvist J.E., Lindqvist O. (2003): Efflorescence on thin sections of calcareous stones – Journal of Cultural Heritage 4 pp. 313-318

– Maravelaki-Kalaitzaki P. (2005): Black crusts and patinas on Pentelic marble from the Parthenon and Erechtheum (Acropolis, Athens): characterization and origin – Analytica Chimica Acta 532 pp. 187-198

– Maravelaki-Kalaitzaki P., Bertoncello R., Biscontin G. (2002): Evaluation of the initial weathering rate of Istria stone exposed to rain

action, in Venice, with X-ray photoelectron spectroscopy – Journal of Cultural Heritage 3 pp. 273-282

– Martínez Martínez J. (2008): Influencia de la alteración sobre las propriedades mecánicas de calizas, dolomías y mármoles. Evaluación mediante estimadores no destructivos (ultrasonidos) – Thesis doctoral. Universidad de Alicante

– Martínez-Martínez J., Benavente D., García del Cura M.A. (2007): Petrographic quantification of brecciated rock by image analysis. Application to the interpretation of elastic wave velocities – Engineering Geology 90 pp. 41-54

– Martínez-Nistal A. (1993): Discriminación, cuantificación y cartografiado de componentes petrográficos mediante proceso digital de multi-imágenes microscópicas - Tesis doctoral, Facultad de Geología, Universidad de Oviedo (Oviedo, Spain)

– Martínez-Nistal A., Veniale F., Setti M., Cotecchia F. (1999): A scanning electron microscopy image processing method for quantifying fabric orientation of clay geomaterials – Applied Clay Science 14 pp. 235-243

– Mateos F.J., Esbert R.M., Rojo A., Valdeón L. (2006): Evaluación del grado de penetración de tratamientos consolidantes mediante la determinación de las variaciones en la velocidad de propagación de ondas longitudinales – RECOPAR. Revista Electrónica de Conversación 3 pp. 33-38

– Mateos F. and Esbert R.M. (in press): Durability of ornamental granite exposed to saltwater spray – Materiales de Construcción

– Matsuoka N. (1990): Mechanisms of rock breakdown by frost action: an experimental approach – Cold Regions Science and Technology 17 pp. 253-270

– Mattila S., Leiro J.A. and Heinonen M. (2004): XPS study of the oxidized pyrite surface – Surface Science 566-568 pp. 1097-1101

– Mauko A., Muck T., Mirtič B., Mladenovič A., Kreft M. (2009): Applicability of Confocal Laser Scanning Microscopy (CLSM) to Geomaterials Characterization with Practical Example of Determination of Porosity in Marble - Materials Characterization doi: 10.1016/j.matchar.2009.01.008

– McAlister J.J., Smith B.J. and Török Á. (2008): Transition metals and water-soluble ions in deposits on a building and their potential catalysis of stone decay – Atmospheric Environment 42 pp. 7657-7668

– McGreevy J.P. (1982): 'Frost and salt' weathering: further experimental results – Earth Surface Processes and Landforms 7 pp. 475-488

– Menéndez B., David C., Darot M. (1999): A study of the crack network in thermally and mechanically cracked granite samples using confocal laser scanning microscopy - Physics and Chemistry of the Earth 24 pp. 627-632

– Menéndez B., David C., Nistal A. (2001) : Confocal laser scanning microscopy applied to the study of pore and crack networks in rocks - Computers Geosciences 27 pp. 1101-1109

– Metaxa E., Agelakopoulou T., Bassiotis I., Karagianni Ch. and Roubani-Kalantzopoulou (2008): Gas chromatographic study of degradation phenomena concerning building and cultural heritage materials – Journal of Hazardous Materials 164 pp. 592-599

– Miglio B. and Willmott Tony (1997): Durability of stone for construction – In: International Conference on Building Envelope Systems and Technology Eds.: Ledbetter S. and Harris R. published on.line: http://www.bath.ac.uk/cwct/cladding_org/icbest97/paper31.pdf

– Montoto M. (1983): Petrophysics: The petrographic interpretation of the physical properties of rocks – 5th International Congress of the International Society of Rock Mechanics, Melbourne, B: 93-98

– Montoto M. (2003): Petrophysics at the rock matrix scale: hydraulic properties and petrographic interpretation – ENRESA, Madrid p. 297

– Montoto M., Martínez-Nistal A., Rodríguez-Rey A., Fernández-Merayo N., Soriano P. (1995): Microfractography of granitic rocks under

confocal scanning laser microscopy - *Journal of Microscopy* 177 pp. 138-149.

– Montoto M., Mateos F. (2006): Characterization of water pathways in low permeable rocks at the rock matrix scale: Methodological review - Journal of Iberian Geology 32 pp. 197-213

– Moropoulou A., Theoulakis P. and Chrysophakis T. (1995): Correlation between stone weathering and environmental factors in marine atmosphere – Atmospheric Environment 29/8. pp. 895-903

– Moropoulou A., Bisbikou K., Torfs K., Van Grieken R., Zezza F. and Macrí F. (1998): Origin and growth of weathering crusts on ancient marbles in industrial atmosphere – Atmospheric Environment 32/6 pp. 967-982

– Moropoulou A., Polikreti K., Ruf V., Deodatis G. (2002a) : San Fransisco Monastery, Quito, Equador : characterisation of building materials, damage assessment and conservation considerations – Journal of Cultural Heritage 4 pp. 101-108

– Moropoulou A., Koui M., Theoulakis P., Bakolas A., Roumpopoulos K. and Michailidis (2002b): Microstructural criteria for the evaluation of stone susceptibility to sea-salt decay – In: Protection and Conservation of the Cultural Heritage of Mediterranean Cities Eds.: Galán and Zezza, Swets and Zeitlinger, Lisse p. 339- 345

– Moropoulou A., Kouloumbi N., Haralampopoulos G., Konstanti A. and Michailidis P. (2003a): Criteria and methodology for the evaluation of conservation interventions on treated porous stone susceptible to salt decay – Progress in Organic Coatings 48 pp. 259-270

– Mortensen H. (1933): Die Salzsprengung und ihre Bedeutung für die regionalklimatische GLiederung der Wüsten – Petermann's Mitteilungen aus Justus Perthes geographischer Anstalt 79 pp. 130-135

– Mosquera M.J., Rivas T., Priet B. and Silva B. (2000): Capillary rise in granitic rocks: Interpretation of kinetics on the basis of pore structure – Journal o fColloid and Interface Science 222 pp. 41-45

– Mottershead D., Gorbushina A., Lucas G. and Wright J. (2003): The influence of marine salts, aspect and microbes in the weathering of sandstone in two historic structures – Building and Environment 38 pp. 1193-1204

– Müller U. (2008): The mineralogical composition of sandstone and its effect on sulphur dioxide deposition – Materiales de Construcción 58 pp. 81-95

– Namorado Rosa R. (1996): Contributions to the characterization of the fissure network in granitic rocks - In: Vicente MA, Delgado-Rodrigues J, Acevedo J, editors. Proceedings of the European Comisión Research Workshop on Degradation and Conservation of Granitic Rocks in Monuments: Spain pp. 261-264

– Neugebauer, J. (1973): The diagenetic problem of chalk. The role of pressure solution and pore fluid - Neues Jahrbuch fur Geologie und Palaontologie 143 pp. 223-245

– Nicholson D.T. (2001): Pore properties as indicators of breakdown mechanisms in experimentally weathered limestones – Earth Surface Processes and Landforms 26 pp. 819-838

– Nicholson D.T. (2002): Quantification of rock breakdown for experimental weathering studies – In: Understanding and managing stone decay Eds.: Přikryl R. and Viles H., Karolinum Press, pp. 115-130

– Nicholson D.T. and Nicholson F.H. (2000): Physical deterioration of sedimentary rocks subjected to experimental freeze-thaw weathering – Earth Surface Processes and Landforms 25 pp. 1295-1307

– Nieminen P. and Uusinoka R. (1988): The role of pore properties of rocks in the decay problem of building stones – Engineering Geology of Ancient Works, Monuments and Historical Sites, Marinos and Koukis (eds.), Rotterdam pp. 809-813

– Nireki T. (1980): Examination of durability test methods for building materials based on performance evaluation – In: Durability of Building Materials and Components Eds.: Sereda P.J. and Litvan P.P. ASTM STP 691 pp. 119-130

– Nishinura T. (1986): Conservation of rock-cliff sculptures in Japan - in Case studies in the conservation of stone and wall paintings: preprints of the contributions to the Bologna Congress, eds. Brommelle, N.S.; Smith, P., pp. 155-158

– Norton D. and Knapp R. (1977): Transport phenomena in hydrothermal systems: The nature of porosity – American Journal of Science 277. pp. 913-936

– NT BUILD 485 Aggregates: frost resistance using 1% NaCl. Published online www.nordicinnovation.net

– Onishi C.T., Shimizu I. (2005): Microcrack networks in granite affected by a fault zone: Visualization by confocal laser scanning microscopy - Journal of Structural Geology 27 pp. 2268-2280

– Ordaz J., Esbert R.M and Montoto M. (1985): Estados de alteración y alterabilidad futura de la piedra de Villamayor de los monumentos salamantinos: interpretación petrográfica – Estudio sobre las alteraciones y tratamiento de la piedra de Villamayor. Edic. de la Caja Ahorros M. de P. de Salamanca, serie monografías. pp. 93-102

– Ordoñez S., Fort R., García del Cura M.A. (1997): Pore size disrtibution and the durability of a porous limestone – Quarterly Journal of Engineering Geology 30 pp. 221-230

– Orkoula M.G. and Koutsoukos P.G. (2001): Dissolution effects on specific surface area, particle size, and porosity of Pentelic marble – Journal of Colloid Interface Science 239 pp-483-488

– Pacheco F.A.L. and Alencoão A.M.P. (2006): Role of fractures in weathering of solid rocks: narrowing tje gap between laboratory and field weathering rates – Journal of Hydrology 316 pp. 248-265

– Papp F. (1950): A szobi Csákhegy és környéke kőzeteiről – Építőanyag 2, pp. 184-188

– Parra Soto J.B. (2007): Macro, Meso y Microporosidad de Sólidos – Técnicas de Caracterización de Sólidos, Curso de Especialización de Postgrado, CSIC, Oviedo, Spain

– Pender R.J. (2004): The behaviour of water in porous building materials and structures – Reviews in Conservation 5 pp. 49-62

– Peruzzi R., Poli T., Toniolo L. (2003): The experimental test for the evaluation of protective treatments: a critical survey of the "capillary absorption index" – Journal of Cultural Heritage 4 pp. 251-254

– Petford N., Davidson G., Miller J.A. (1999): Pore structure determination using confocal laser scanning microscopy, Physics and Chemistry of the Earth 24 pp. 563-567

– Pétursson P. (2005): Frost resistance test on aggregates with and without salt – Published online www.nordicinnovation.net

– Pigeon M., Zuber B. and Marchand J. (2003): Freeze/thaw resistance – in. Advanced Concrete Technology: Concrete Properties eds.: Newmann J. and Choo B.S., Butterworth-Heinemann pp. 11/2-11/17

– Pinto A.P.F. and Rodrigues J.D. (2008): Stone consolidation: The role of treatment procedures – Journal of Cultural Heritage) pp. 38-53

– Poblador M.P. (2001): Legislación intenacional sobre patrimonio y restauración: Convenios y Cartas Internacionales. In: I jJornadas se Caracterización y Restauración de Materiales Pétreos en Arquitectura, Escultura y Restauración. Ed.: J. Gisbert Aguilar, Universidad de Zaragoza pp. 3-58

– Poschold K. and Grimm W.D. (1988): The characterization of the pore space of crystalline natural stones - Engineering Geology of Ancient Works, Monuments and Historical Sites, Marinos and Koukis (eds.), Rotterdam pp. 815-818

– Powers T.C. (1945): A working hypothesis for further studies of frost resistance of concrete – American Concrete Institute Journal Proc 41 pp. 245-272

– Prasad K.M.M.K., Raheem S., Vijayalekshmi P., Kamala Sastri C. (1996): Basic aspects and applications of tristimulus colorimetry – Review – Talanta 43 pp. 1187-1206

– Prieto B., Aira N. and Silva B. (2007): Comparative study of dark patinas on granitic outcrops and buildings – Science of the Total Environment 381 pp. 280-289

– Přikrly R., Lokajíček T., Svobodová J. and Weishauptová Z. (2003): Experimental weathering of marlstone from Přední Kopanina (Check Republic) – historical building stone of Prague – Building and Environment 38 pp. 1163-1171

– Pühringer J. (1983): Salt disintegration. Salt migration and degradation by salts – a hypothesis – Swedish Coulcil for Building Research, Stockholm p.159

– Raeburn S.P., Ilton E.S., and Veblen D.R. (1997a): Quantitative determination of the oxidation state of iron in biotite using X-ray photoelectron spectroscopy: I. Calibration – Geochimica et Cosmochimica Acta 61/21. pp. 4519-4530

– Raeburn S.P., Ilton E.S., and Veblen D.R. (1997b): Quantitative determination of the oxidation state of iron in biotite using X-ray photoelectron spectroscopy: II. In situ analyses – Geochimica et Cosmochimica Acta 61/21. pp. 4531-4537

– Rigby S.P., Fletcher R.S., Riley S.N. (2004): Characterisation of porous solids using integrated nitrogen sorption and mercury porosimetry – Chemical Engineering Science 59 pp. 41-51

– RILEM II.1 (1980): Essais recommandés pour mesurer l'altération des pierres et évaluer l'efficacité des méthodes de traitement / Recommended tests to measure the deterioration of stone and to assess the effectiveness of treatment methods - Coefficient de saturation – Materials and Structures 13/75 pp. 175-253

– RILEM II.7 (1980): Essais recommandés pour mesurer l'altération des pierres et évaluer l'efficacité des méthodes de traitement / Recommended tests to measure the deterioration of stone and to assess the effectiveness of treatment methods – Dilatation linéaire par absorption d'eau – Materials and Structures 13/75 pp. 175-253

– RILEM TC 117 FDC (1995): Test method for the freeze-thaw resistance of concrete, Slab Test and cube test, Draft of recommendation. Materials and Structures 28 pp. 366-71

– Rivas Brea T., Prieto Lamas B. and Silva Hermo B. (2008): Artificial weathering of granite – Materiales de Construcción 58 pp. 179-189

– Rivera M.H. and Melo M.E.R. (2001): La rugosidad de las superficies: Topometría – Ingenierías IV/11. pp. 27-33

– Robertson E.C (1982): Physical properties of building stone – in Conservation of Historic Stone Buildings and Monuments, Proceedings of a conference held Feb. 2-4, 1981 at the National Academy of Sciences in Washington, D.C., pp. 62-86

– Robinson D.A and Williams R.B.G. (2000): Experimental weathering of sandstone by combination of salts – Earth Surface Processes and Landforms 25 pp. 1309-1315

– Rodríguez-Gordillo, J., Sáez-Pérez, M.P., (2006): Effects of thermal changes on Macael marble: Experimental study - Construction and Building Materials **20**, pp. 355-365

– Rodriguez-Navarro C. and Doehne E. (1999): Salt weathering: influence of evaporation rate, supersaturation and crystallization pattern – Earth Surface Processes and Landforms 24 pp. 191-209

– Rodriguez-Navarro C., Doehne E. and Sebastian E. (2000): How does sodium sulfate crystallize? Implications for the decay and testing of building materials – Cement and Concrete Research 30 pp. 1527-1534

– Roels S., Elsen J., Carmeliet J., Hens H. (2001): Characterisation of pore structure combining mercury porosimetry and micrography – Materials and Structures / Matériaux et Constructions 34 pp. 76-82

– Rossi-Manaresi R. and Tucci A. (1991): Pore structure and the disruptive or cementing effect of salt crystallization in various types of stone – Studies in Conservation 36 pp.53-58

– Royer-Carfagni G.F (1999): On the thermal degradation of marble – International Journal of

Rock Mechanics and Mining Sciences 36 pp. 119-126

– Ruedrich J. and Siegesmund S. (2007): Salt and ice crystallization in porous sandstones – Environmental Geology 52/2 pp. 225-249

– Ruiz-Agudo E., Mees F., Jacobs P. and Rodríguez-Navarro C. (2007): The role of saline solution properties on porous limestone salt weathering by magnesium and sodium sulfates – Environmental Geology 52 pp.269-281

– Ruiz de Argandoña V.G., Rodríguez Rey A., Celorio C., Suárez del Río L.M., Calleja L. and Llavota J. (1999): Characterization by computed X-ray tomography of the evolution of the pore structure of a dolomite rock during freeze-thaw cyclic test – Physics and Chemistry of the Earth 24/7 pp. 633-637

– Sabbioni C. (1995): Contribution of atmospheric deposition to the formation of damage layers – The Science of Total Environment 167 pp. 49-55

– Sáez Pérez M.P. (2003): Estudio de elementos arquitectónicos y composición de materiales del Patio de los Leones. Interacciones en sus causas de deterioro – Tesis doctoral, Departamento de Construcciones Arquitectónicas, Universidad de Granada, Spain

– Sáez-Pérez M.P. and Rodríguez-Gordillo J. (2009): Structural and compositional anisotropy in Macael marble (Spain) by ultrasonic, XRD and optical microscopy methods – Construction and Building Materials 23 pp 2121-2126

– Schafarzik F. (1904): A Magyar szent korona országainak területén létező kőbányák részletes ismertetése – Magyar Kiráyli Földtani Intézet, Budapest p. 412

– Scherer G.W. (1999): Crystallization in pores – Cement and Concrete Research 29 pp. 1347-1358

– Scherer G.W. (2004): Stress from crystallization of salt – Cement and Concrete Research 34 pp. 1613-1624

– Schiavon N., Chiavari G., Schiavon G. and Fabbri D. (1995): Nature and decay effects of urban soiling on granitic building stones – The Science of the Total Environment 167 pp. 87-101

– Sebastián Pardo, E., Rodríguez-Navarro, A., Cultrone G., Uroševiè M., Rodríguez-Navarro C. (2006): Caracterización de la anisotropía textural de mármoles comerciales – MACLA 6 pp. 453-456

– Sebastián E., Gultrone G., Benavente D., Linares Fernandez L., Elert K. and Rodríguez-Navarro C. (2008): Swelling damage in clay-rich sandstones used in the church of San Mateo in Tarifa (Spain) – Journal of Cultural Heritage 9 pp. 66-76

– Siegesmund S., Ullemeyer K., Weiss T. and Tschegg E.K. (2000): Physical weathering of marbles caused by anisotropic thermal expansion – International Journal of Earth Sciences 89 pp. 170-182

– Siegesmund S., Weiss T. and Vollbrecht A. (eds.) (2002): Natural Stone, Weathering Phenomena, Conservation Strategies and Case Studies – Geological Society Special Publication No. 25 Londodn, p. 448

– Silva B., Rivas T. and Prieto B. (2003): Soluble salts in granitic monuments: origin and decay effects – In. Applied study of cultural heritage and clays. Editor: Perez-Rodriguez J.L. Madrid CSIC pp. 113-131

– Silva B., Rivas T., García-Rodeja E. and Prieto B. (2007): Distribution of ions of marine origin in Galicia (NW Spain) as a function of distance from the sea – Atmospheric Environment 41 pp. 4396-4407

– Simão J., Ruiz-Agudo E., Rodríguez-Navarro C. (2006): Effects of particulate matter from gasolina and diesel vehicle exhaust emission on silicate stone sulfation – Atmospheric Environment 40 pp. 6905-6917

– Smith B.J., Warke P.A., McGreevy J.P. and Kane H.L. (2005): Salt-weathering simulations under hot desert conditions: agents of enlightenment or perpetuators of preconceptions? – Geomorphology 67 pp. 211-227

– Sousa L.M.O, Calleja L., Suárez del Río L.M, Rodríguez Rey A. (2002): Anisotropia de propagação das ondas sísmicas em granitos – 8°

Congreso Nacional de Geotecnia, Lisboa, pp. 507-516

– Sousa L.M.O, Suárez del Río L.M, Calleja L., Ruiz de Argandoña, Rodríguez Rey A. (2005): Influence of microfractures and porosity on the physico-mechanical properties and weathering of ornamental granites – Engineering Geology 77 pp. 153-168

– Spetzler H. (1978): Seismic velocity changes during fracture and frictional sliding – Pure and Applied Geophysics 116 pp. 732-742

– Spiker E.C., Comer V.J., Hosker R.P. and Sherwood S.I. (1992): Dry deposition of SO_2 on limestone and marble: role of humidity – 7th International Congress on Deterioration and Conservation of Stone, Lisbon, pp. 397-406

– Stefanis N.A., Theoulakis P. and Pilinis C. (2009): Dry deposition effect of marine aerosol to the building stone of the medieval city of Rhodes, Greece – Building and Environment 44 pp. 260-270

– Steiger M. (2005a): Crystal growth in porous materials—I: The crysatllization pressure of large crystals – Journal of Crystal Growth 282 pp. 455-469

– Steiger M. (2005b): Crystal growth in porous materials—II: Influence of crystal size on the crystallization pressure – Journal of Crystal Growth 282 pp. 470-481

– Steiger M. and Asmussen S. (2008): Crystallization of sodium sulfate phases in porous materials: The phase diagram Na_2SO_4-H_2O and the generation of stress – Geochimica et Cosmochimica Acta 72 pp. 4291-4306

– Stipp S.L.S. (1999): Toward the conceptual model of the calcite surface: Hydratation, hydrolysis and surface potential – Geochimica et Cosmochimica Acta 63/19-20 pp. 3121-3131

– Sun W., Mu R., Luo X., Miao C. (2002): Effect of chloride salt, freeze-thaw cycling and externally applied load on the performance of the concrete – Cement and Concrete Research 32 pp. 1859-1864

– Swedish Standard 13 72 44 (1992) Concrete Testing-Hardened Concrete-Frost Resistance – Standardiserings-kommissionen i Sverige

– Tabasso M.L. and Simon S. (2006): Testing methods and criteria for the selection/evaluation of products for the conservation of porous building materials – Reviews in Conservation 7 pp. 67-82

– Takarli M., Prince W. and Siddique R. (2008): Damage in granite under heating/cooling cycles and water freeze-thaw condition – International Journal of Rock Mechanics and Mining Sciences 45 pp. 1164-1175

– Theoulakis P. and Moropoulou A. (1997): Microstructural and mechanical parameters determinig the susceptibility of porous building stones to salt decay – Construction and Building Materials 11/1 pp.65-71

– Tittarelli F., Moriconi G. and Bonazza A. (2008): Atmospheric deterioration of cement plaster in a building exposed to a urban environment – Journal of Cultural Heritage 9 pp. 203-206

– Torfs K. and Van Grieken R. (1997): Chemical relations between atmospheric aerosols, deposition and stone decay layers on historic buildings at the Mediterranean coast – Atmospheric Environment 32/15. pp. 2179-2192

– Torraca G. (1982): Porous building materials – Materials science for architectural conservation ICCROM, Rome, Italy p. 145

– Tourenq C., Fourmaintraux D., Denis A. (1971): Propagation des ondes et discontinuities des roches – Proceedings of International Symposium on Rock Mechanics, Nancy, I-1.

– Török Á., Stück H., Quetscher A., Glätzner P., Siegesmund S. (2008): Comparative study of weathering features of stones in Hungarian castles: morphological characteristics and changes in physical properties – Z. dt. Ges. Geowiss, 158/4 pp. 931-955

– Tsui N., Flatt R.J., Scherer G.W. (2003): Crystallization damage by sodium sulphate – Journal of Cultural Heritage 4 pp. 109-115

– Tuğrul A. (2004): The effect of weathering on the pore geometry and compressive strenght of selected rock types from Turkey – Engineering Geology 75 pp. 215-227

– Turkington A.V. (2002): Perceprion and prediction of stone durability – In: Annual Meeting of Decay and Conservation of Stone Buildings and Monuments, Denver Paper No. 37-6

– Turkington A.V., Martin E., Viles H.A. and Smith B.J. (2003): Surface change and decay of sandstone samples exposed to a polluted urban atmosphere over a six-year period: Belfast, Northern Ireland – Building and Environment 38 pp. 1205-1216

– Yasar E., Erdogan Y. (2004): Correlating sound velocity with the density, compressive strength and Young's modulus of carbonate rocks - International Journal of Rock Mechanics and Mining Sciences 41 pp. 871-875

– Valdeón L., Esbert R.M. and Grossi C.M. (1992): Hydric properties of some Spanish building stones: a petrophysical interpretation – Proceedings of the Symposium of Materials Research Society Vol. 267, Materials Research Society pp. 911-916

– Valdeón L., de Freitas M.H., King M.S. (1996): Assessment of the quality of building stones using signal processing procedures – Quarterly Journal of Engineering Geology 29 pp. 299-308

– Valdeón L., Montoto M., Calleja L. and Esbert R.M. (1997): A method to assess spatial coordinates in art and archaeological objects: Application of tomography to a dolmen – Journal of Archaeolicical Science 24 pp. 337-346

– Valenza J.J. II (2005): Mechanism for salt scaling – PhD Thesis, Princeton University www.jvalenza.com/thesis.html

– Valenza J.J. II and Scherer G.W. (2006): Mechanism of salt scaling – Journal of the American Ceramic Society 89 pp. 1161-1179

– Valenza J.J. II and Scherer G.W. (2007a): A review of salt scaling I. Phenomenology – Cement and Concrete Research 37 pp. 1007-1021

– Valenza J.J. II and Scherer G.W. (2007b): A review of salt scaling II. Mechanisms – Cement and Concrete Research 37 pp. 1022-1034

– Vallet J.M., Gosselin C., Bromblet P., Rolland O., Vergès-Belmin V., Kloppmann W. (2006): Origin of salts in stone monument degradation using sulphur and oxygen isotopes: First results of the Bourges cathedral (France) – Journal of Geochemical Exploration 88 pp. 358-362

– Van Brakel J., Modrý S. and Svatá M. (1981): Mercury Porsimetry: State of Art – Powder Technology 29 pp. 1-12.

– Vasconcelos G., Lourenço P.B., Alves C.A.S., Pamplona J. (2008): Ultrasonic evaluation of the physical and mechanical properties of granites – Ultrasonics 48 pp. 453-466

– Verbeck G.J. and Klieger P. (1957): Studies of salt scaling of concrete – Highway Research Board Bulletin 150 pp. 1-17

– Vicente M.A., Delgado-Rodrigues J., Acevedo J. eds. (1996): Degradation and conservation of granitic rocks in monuments – Proceedings of EC workshop Environmental protection and conservation of the European cultural heritage, Santiago de Compostela, Spain, p. 471

– Viscarra Rossel R.A., Minasny B., Roudier P., McBratney A.B. (2006): Colour space models for soil science – Geoderma 133 pp. 320-337

– Wagner C.D., Riggs W. M., Davis L. E. and J. F. Moulder (1979): Handbook of X-ray Photoelectron Spectroscopy 1st ed – Ed.: G. E. Muilenberg, Perkin-Elmer Corporation Physical Electronics

– Walsh J.B., Brace W. (1966): Cracks and pores in rocks – Proceedings of the first Congress of the International Society of Rock Mechanics pp. 643-646

– Weast R.C. (1985): CRC Handbook of Chemistry and Physics – 66th ed., CRC Press, Boca Raton, Florida, pp. D213-D214

– Weiss T., Siegesmund S., Fuller E.R. Jr. (2003): Thermal degradation of marble: indications from fine-element modelling – Building and Environment 38 pp. 1251-1260

– Wellmann H.V. and Wilson A.T. (1965): Salt weathering, neglected geological erosive agent in coastal and arid environments – Nature 205 pp. 1097-1098

– Wessman L. (1997): Studies on the frost resistance of natural stone – Licentiate Thesis, Lund University, Lund Institute of Technology p.199

– Williams R.G.B. and Robinson D.A (1981): Weathering of sandstone by the combined action of frost and salt – Earth Surface Proceses and Landforms 6 pp. 1-9

– Williams R.G.B. and Robinson D.A. (1991): Frost weathering of rocks in the presence of salts – a review – Permafrost and Periglacial Processes 2 pp. 347-353

– Williams R.G.B. and Robinson D.A. (2001): Experimental frost weathering of sandstone by various combinations of salts – Earth Surface Processes and Landforms 26. pp. 811-818

– Wilson-Yang K.M and Burns G. (1986): The X-ray photoelectron spectroscopy of ancient murals in the tombs at Beni Hasan, Egypt – Canadian Journal of Chemistry 65 pp. 1058-1064

– Winkler E.M. (1996): Properties of marble as building veneer – International Journal of Rock Mechanics, Mining Sciences and Geomechanics Abstracts 33 pp. 215-218

– Winkler, E.M. (1997): Stone in Architecture. Properties. Durability. Springer – Verlag, Wien, New York. p.313

– Winkler E.M. and Wilhelm E.J. (1970): Salt burst by hydration pressures in architectural stone in urban atmospheres – Geological Society of America Bulletin 81 pp. 567-572

– Winkler K.W. and Murphy W.F. III. (1995): Acoustic Velocity and Attenuation in Porous Rocks – In: Rock Physics and Phase Relations – A Handbook of Physical Constants Ed.: Ahrens T. J., American Geophysical Union, Washington, pp. 20-34

– Xie P. and Beaudoin J.J. (1992): Mechanism of sulphate expansion I. Thermodynamic principle of crystallization pressure – Cement and Concrete Research 22 pp. 631-641

– Xie S., Qi L. and Zhou D. (2004): Investigation of th effects of acid rain on the deterioration of cement concrete using accelerated tests established in laboratory – Atmospheric Environment 38 pp. 4457-4466

– Yasar E. and Erdoğan Y. (2004): Correlating sound velocity with density, compressive strength and Young modulus of carbonate rocks – International Journal of Rocks Mechanics and Mining Sciences 41 pp. 871-875

– Yavuz A.B. and Topal T. (2007): Thermal and salt crystallization effects on marble deterioration: Examples from Western Anatolia, Turkey – Engineering Geology 90 pp. 30-40

– Yuan Q., Shi C., De Schutter G., Audenaert K. and Deng D. (2009): Chloride binding of cement-based materials subjected to external chloride environment – A review – Construction and Building Materials 23 pp. 1-13

– Zappia G., Sabbioni C. and Gobbi G. (1993): Non-carbonate carbon content on black and white areas of damages stone monuments – Atmospheric Environment 27A pp. 1117-1121

– Zedef V., Kocak K., Doyen A., Ozsen H., Kekec B. (2007): Effect of salt crystallization on stones of historical buildings and monuments, Konya, Central Turkey – Building and Environment 42 pp. 1453-1457

– Zehnder K. and Arnold A. (1989): Crystal growth in salt efflorescence – Journal of Crystal Growth 97 pp. 513-521

– Zelenka T. and Földessy J. (2005): A Szob-Malomkőbánya összefoglaló földtani jelentése a 2005. évi kutatások alapján – Miskolci Egyetem Földtan-Teleptani Tanszék, Miskolc

– Zezza U. and Sebastián Pardo E. (1992): El mármol Macael (Almería) en los monumentos históricos de Granada (España) – I. Congreso Internacional Rehabilitación del Patrimonio Arquitectónico y Edificación. Islas Canarias. Tomo I. pp. 153-160

– Zezza U. and Macri F. (1995): Marine aerosol and stone decay – The Science of the Total Environment 167 pp. 123-143

Appendices

Appendix I.

Stone characterization – P-wave velocity

Macael marble

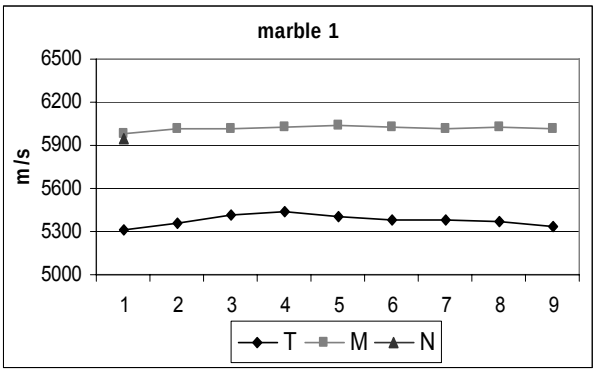

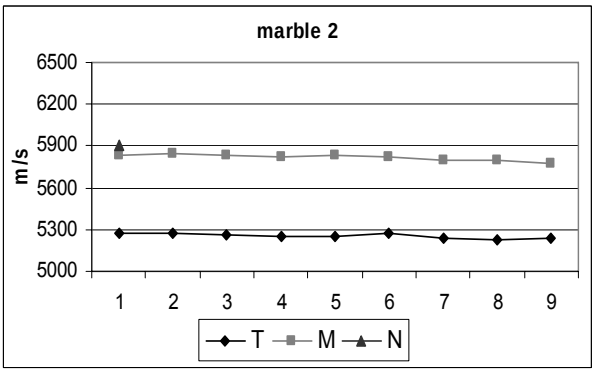

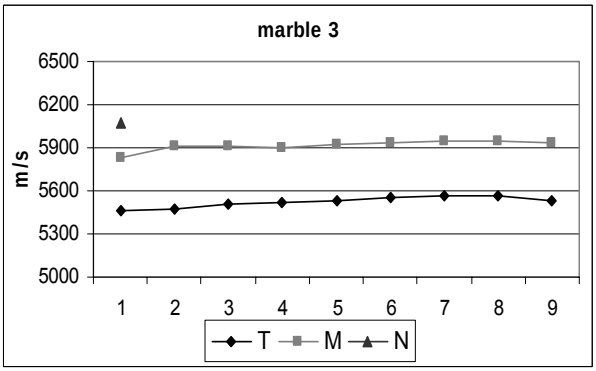

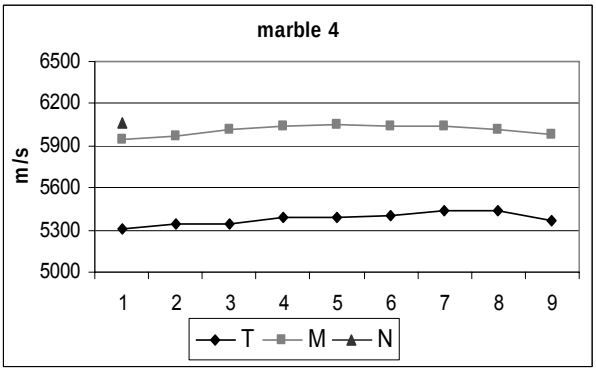

Silvestre Vilachán

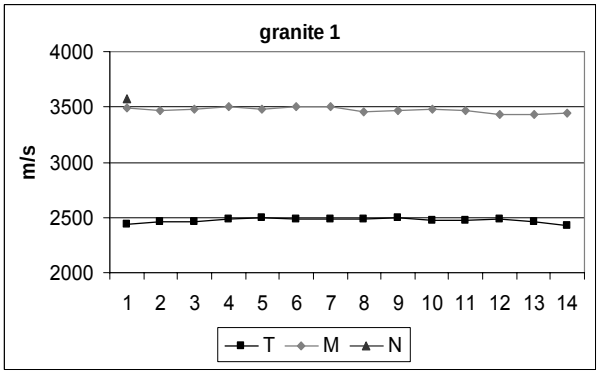

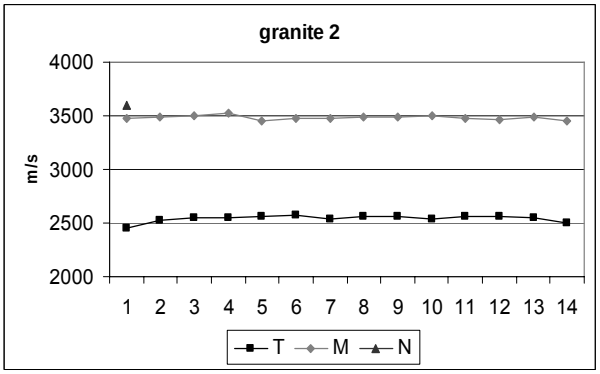

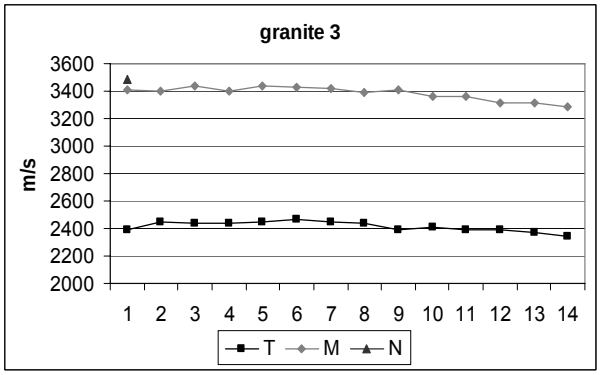

Szob andesite

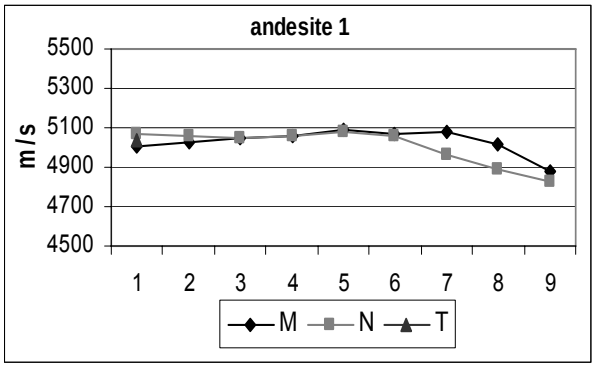

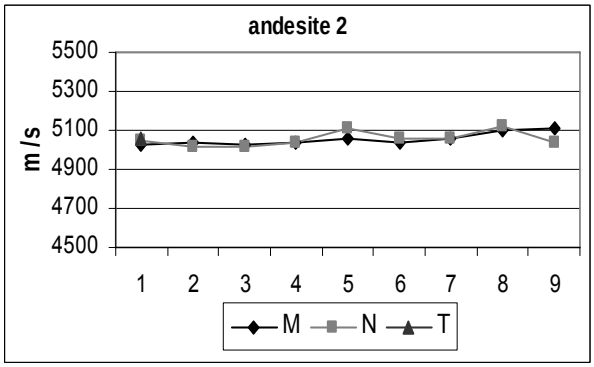

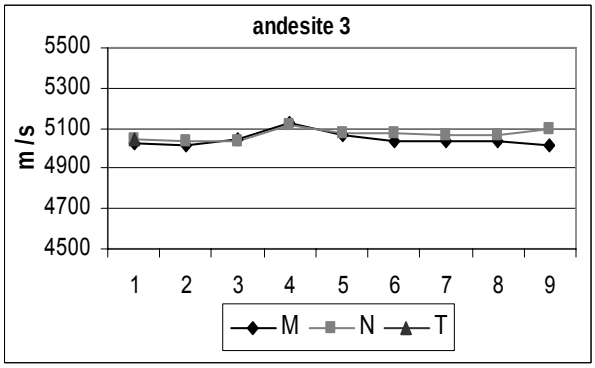

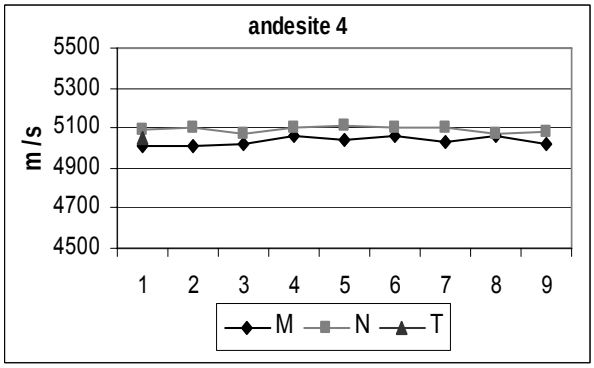

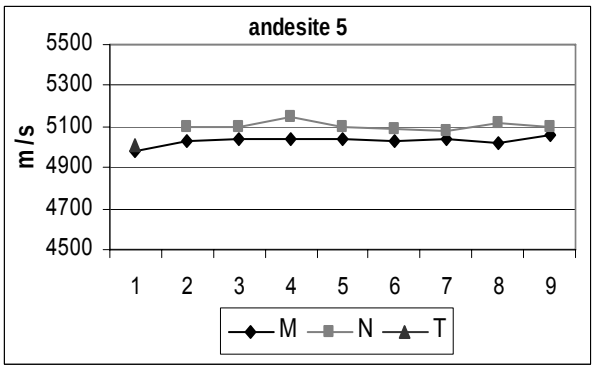

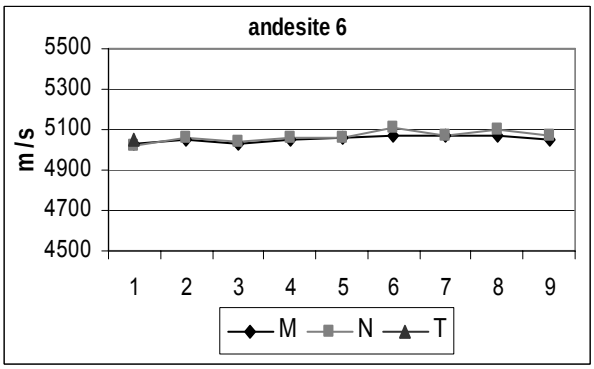

	Pore shape factor								
	Vilachán granite			Macael marble			Szob andesite		
	T	M	N	T	M	N	T	M	N
1	0,34	0,31	0,32	0,32	0,23	0,25	0,07	0,05	0,02
2	0,35	0,31	0,34	0,33	0,27	0,26	0,01	0,01	0,03
3	0,32	0,30	0,32	0,34	0,25	0,27	0,03	0,02	0,03
4	0,36	0,30	0,32	0,31	0,24	0,25	0,03	0,03	0,02
5	0,39	0,32	0,33	0,32	0,23	0,25	0,02	0,01	0,02
6	0,35	0,32		0,32	0,26	0,24	0,02	0,03	0,02
average	**0,35**	**0,31**	**0,32**	**0,32**	**0,25**	**0,25**	**0,03**	**0,03**	**0,02**
st.dev	0,02	0,01	0,01	0,01	0,01	0,01	0,02	0,01	0,00

Appendix II.

Evolution of hydraulic properties

Salt crystallization – Macael marble

Water absorption

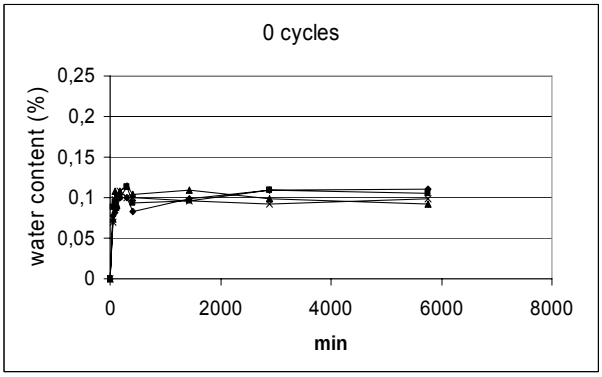

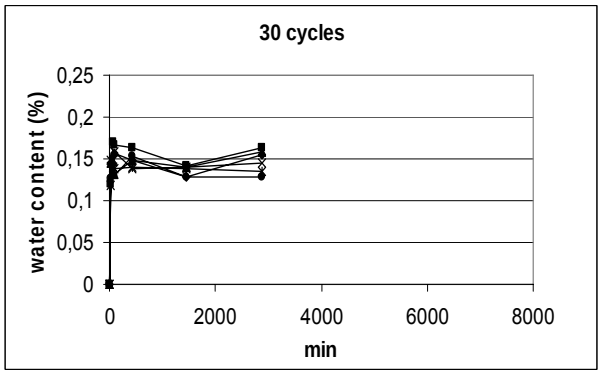

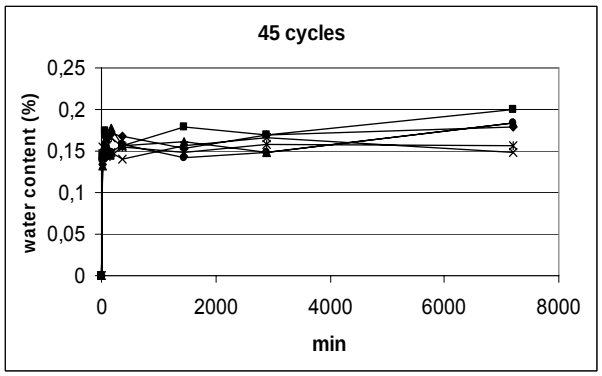

Capillary uptake

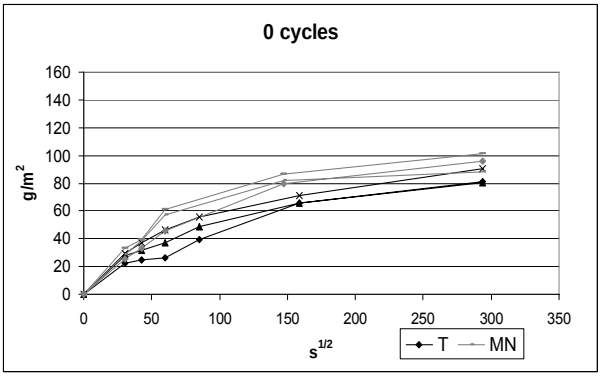

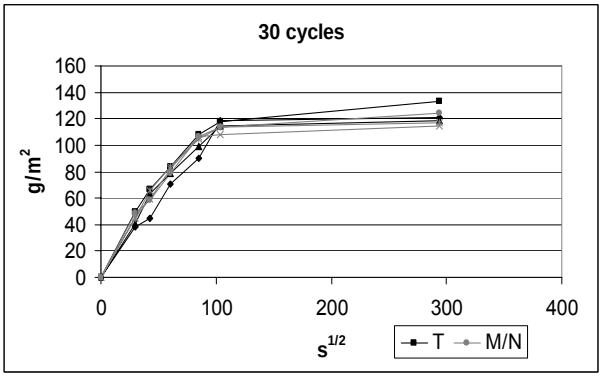

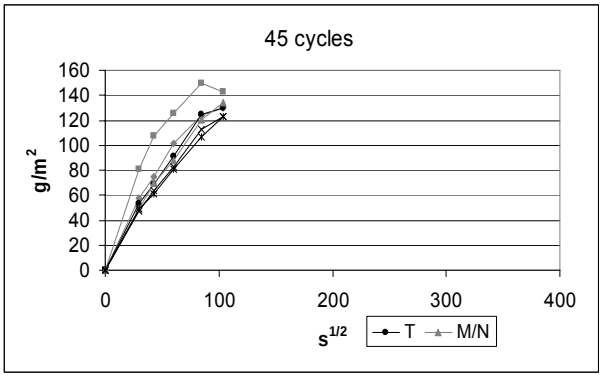

Salt crystallization – Vilachán granite

Water absorption

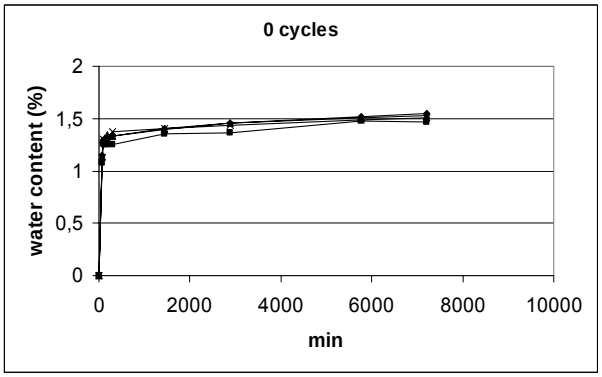

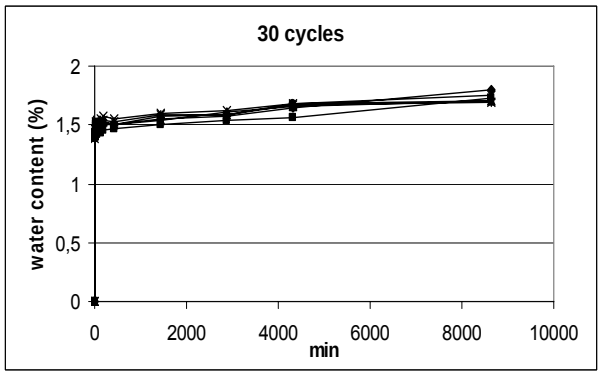

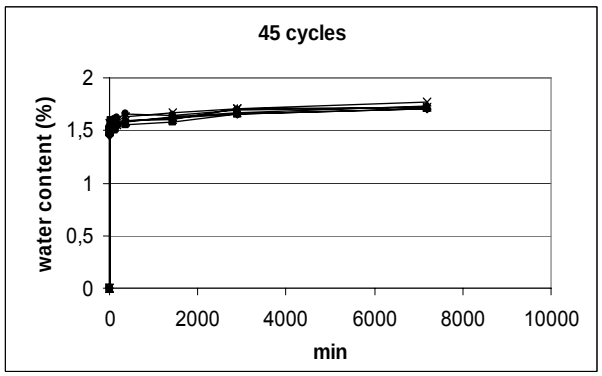

Capillary uptake

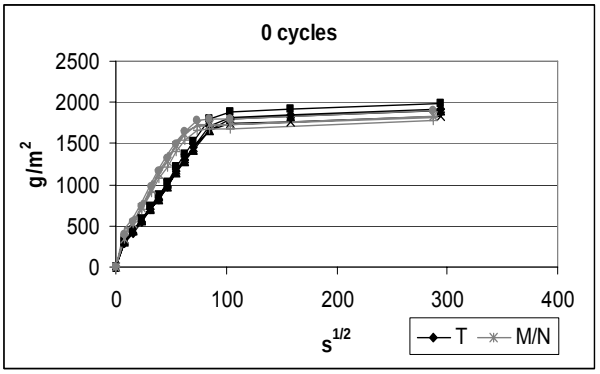

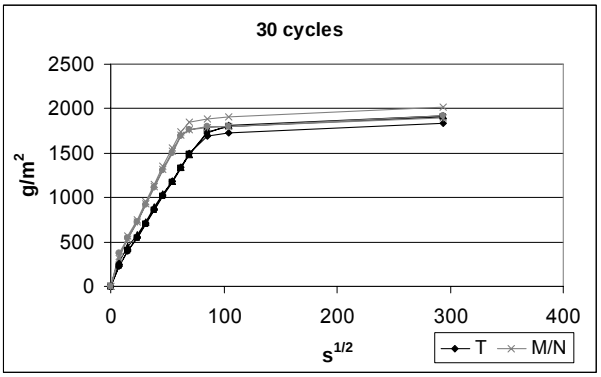

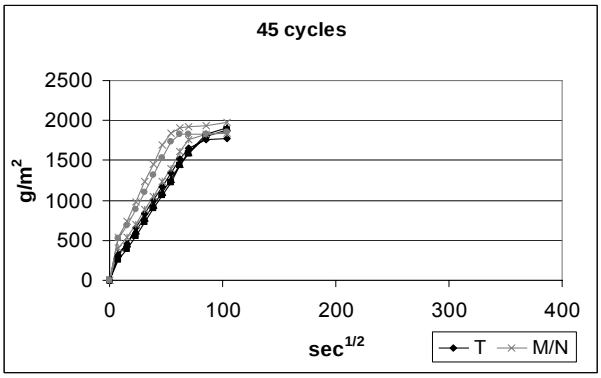

Salt crystallization – Szob andesite

Water absorption

Capillary uptake

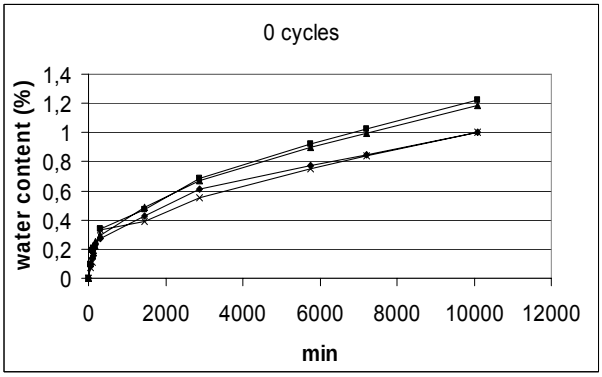

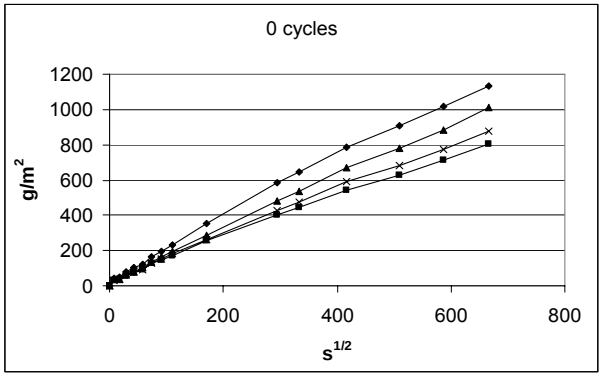

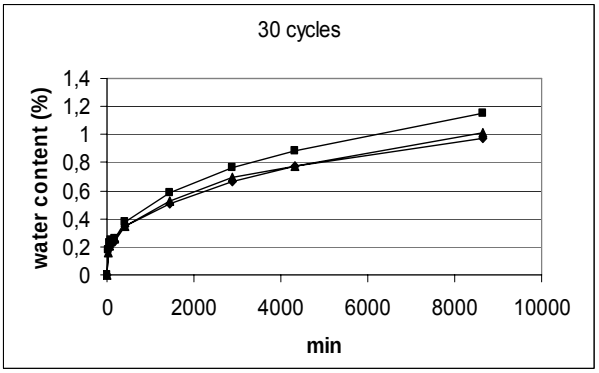

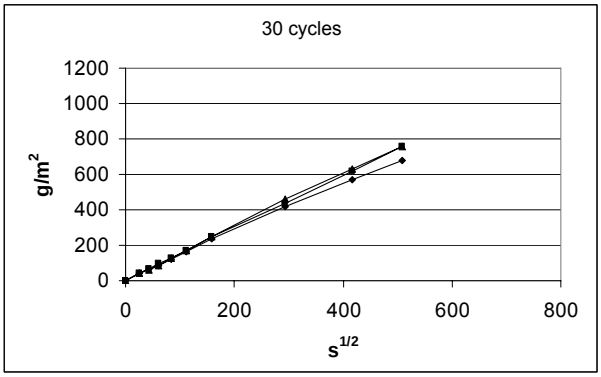

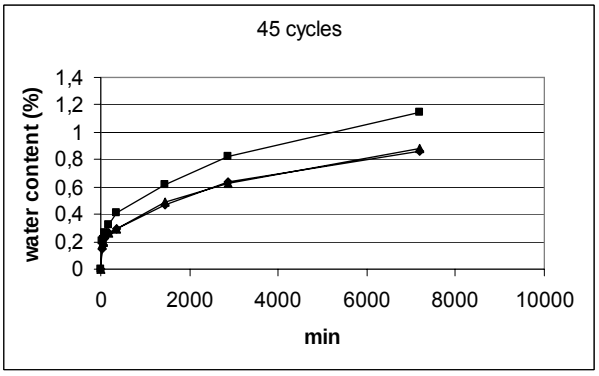

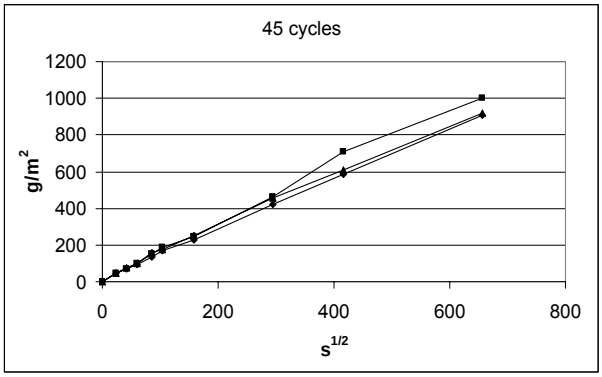

Freeze-thaw – Macael marble

Water absorption

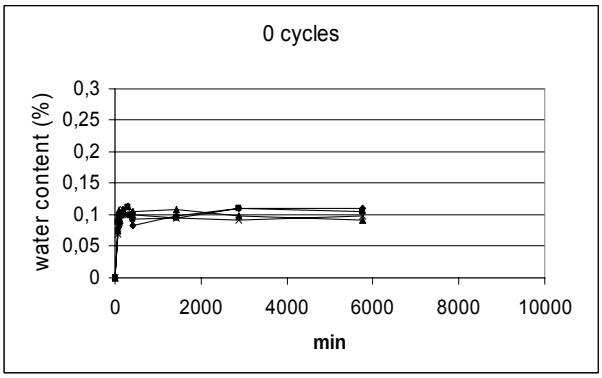

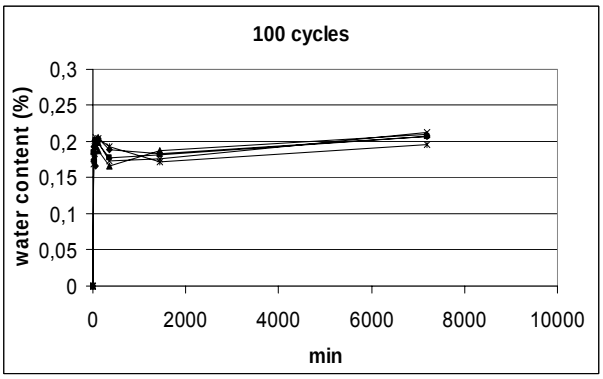

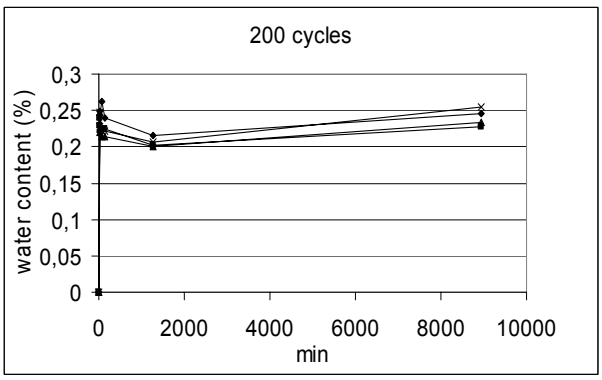

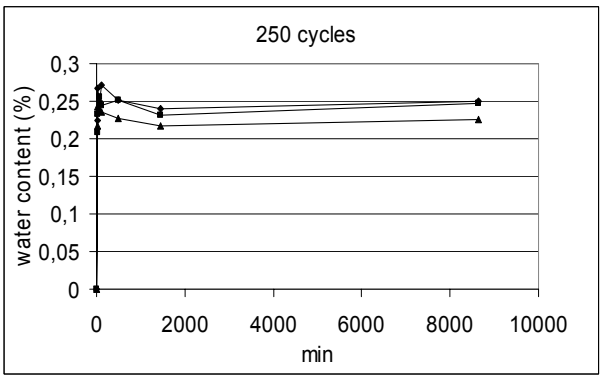

Capillary uptake

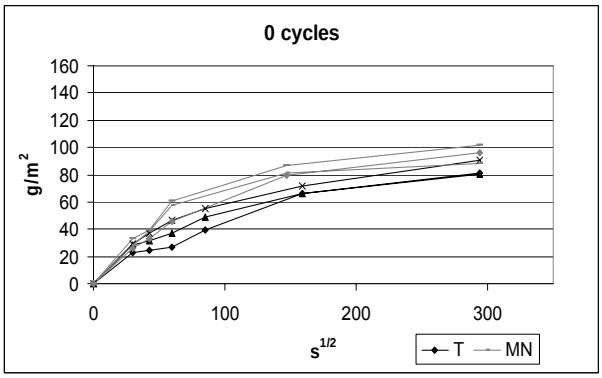

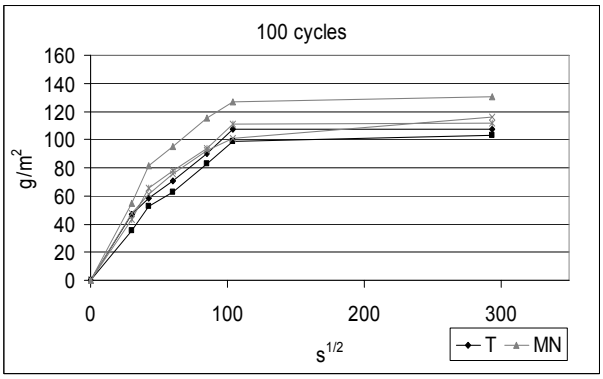

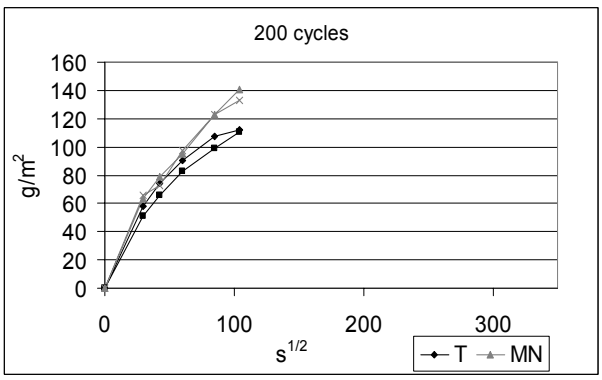

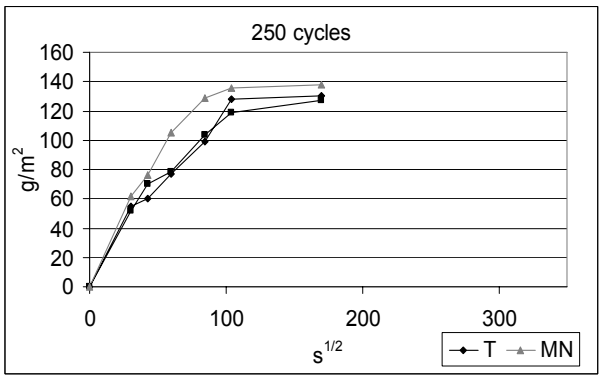

Freeze-thaw – Vilachán granite

Water absorption

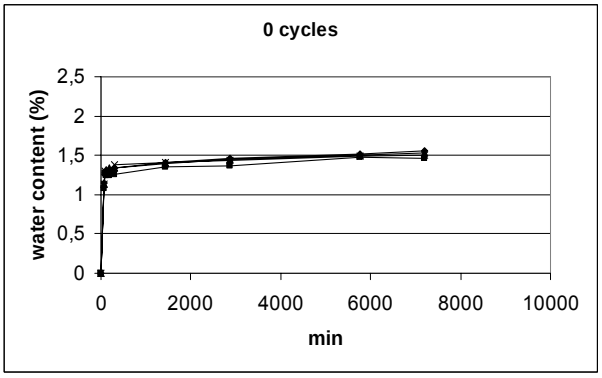

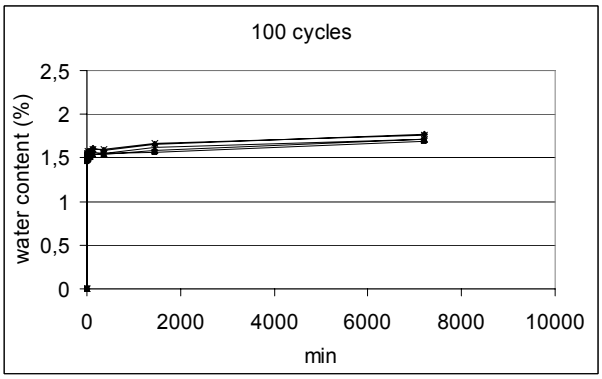

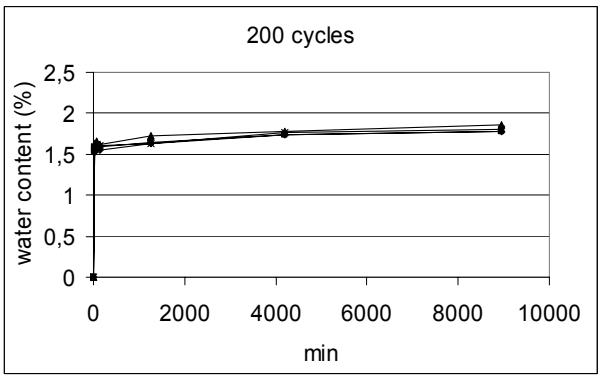

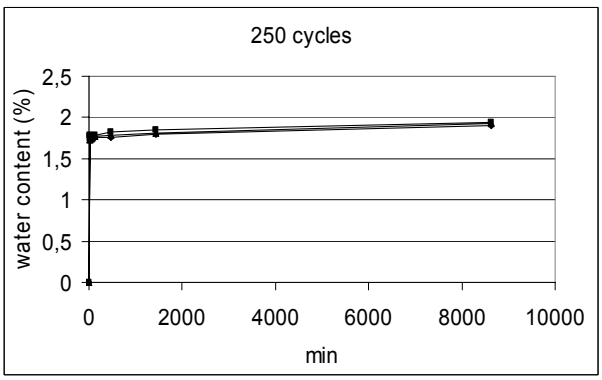

Capillary uptake

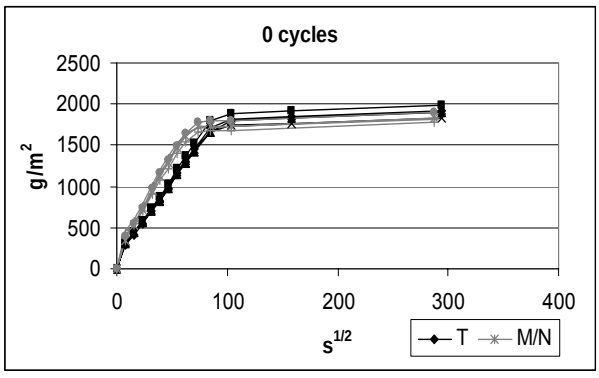

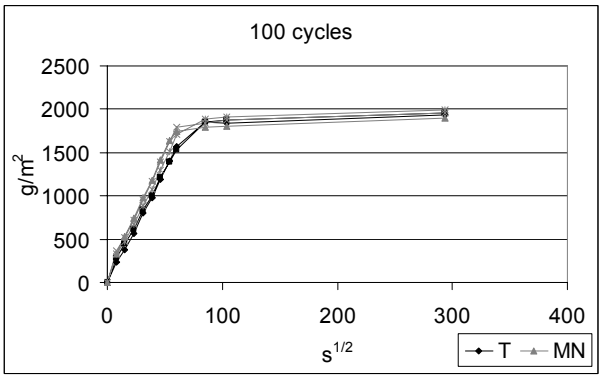

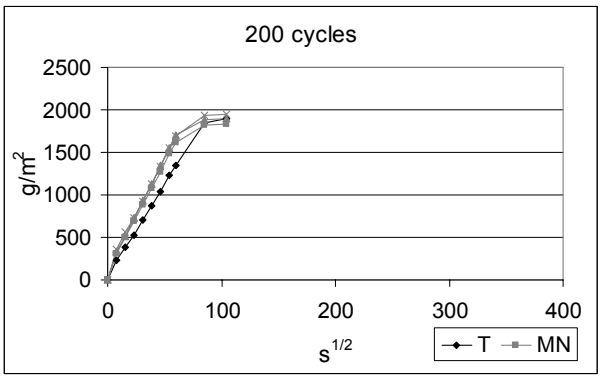

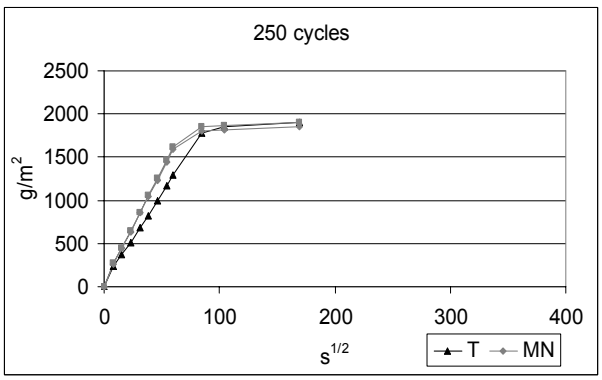

Freeze-thaw – Szob andesite

Water absorption

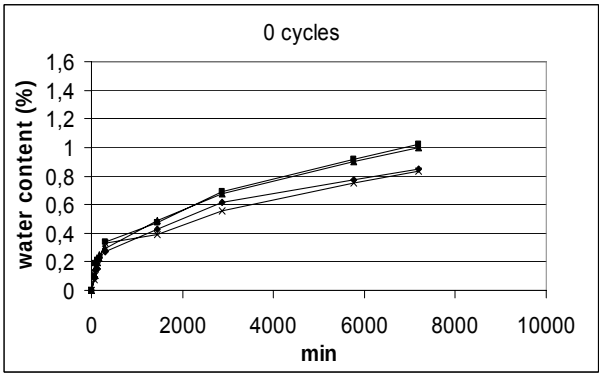

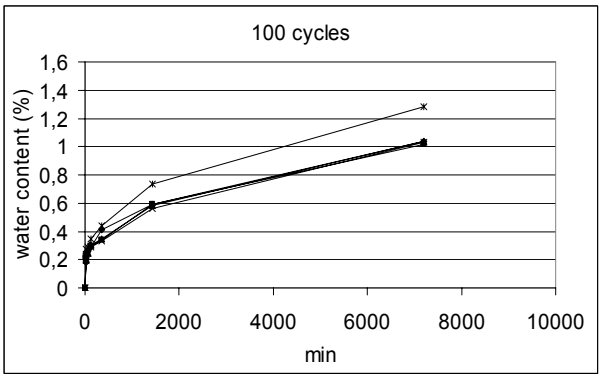

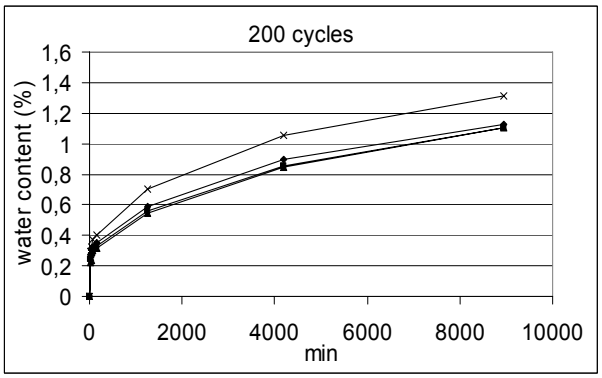

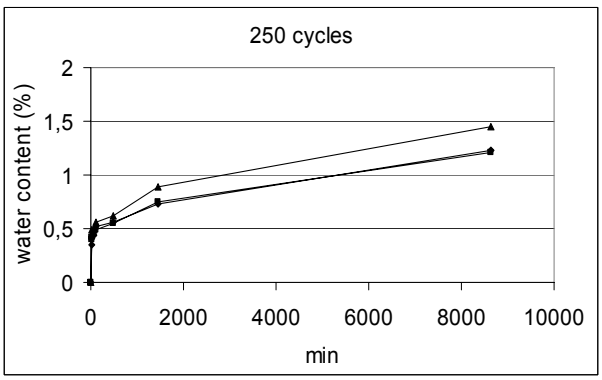

Capillary uptake

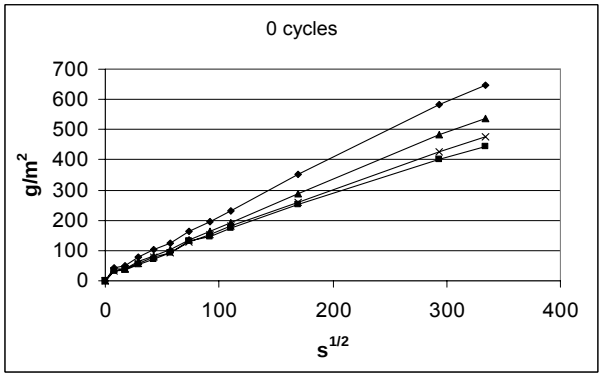

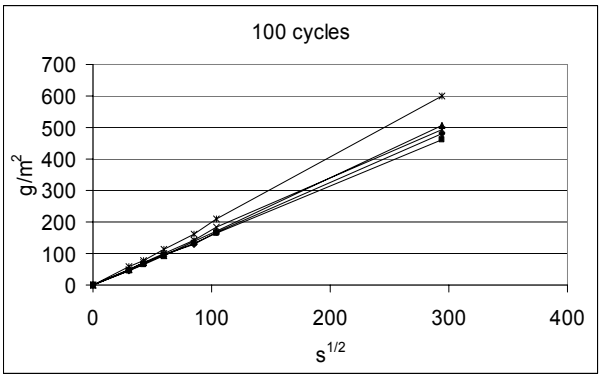

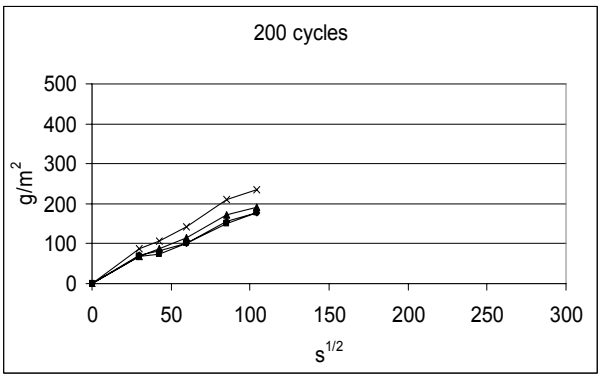

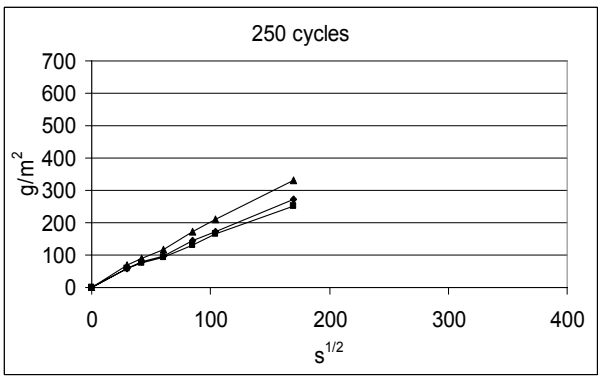

Freeze-thaw with salt – Macael marble

Water absorption

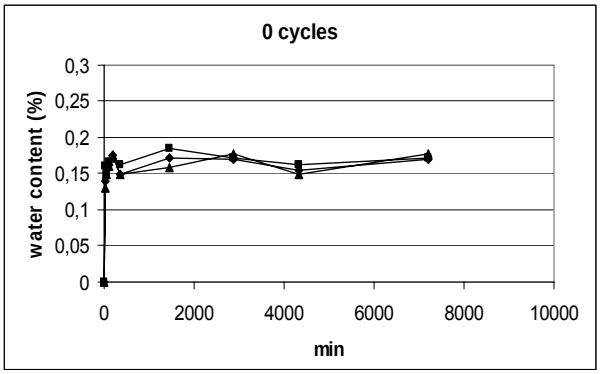

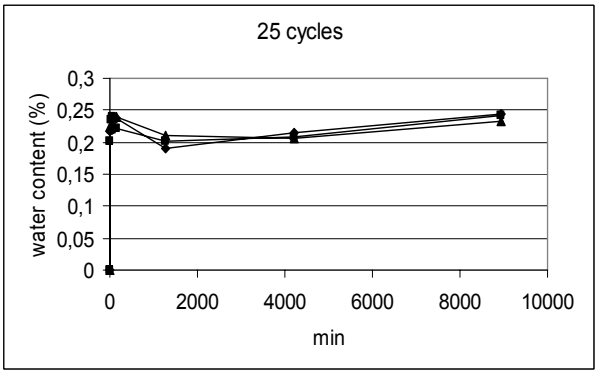

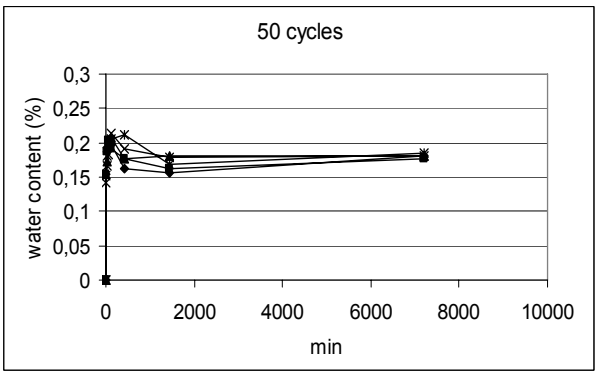

Capillary uptake

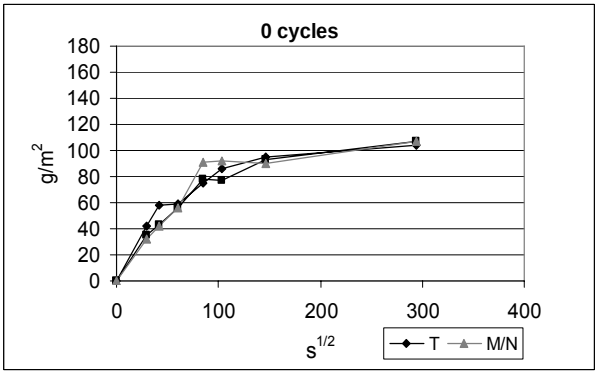

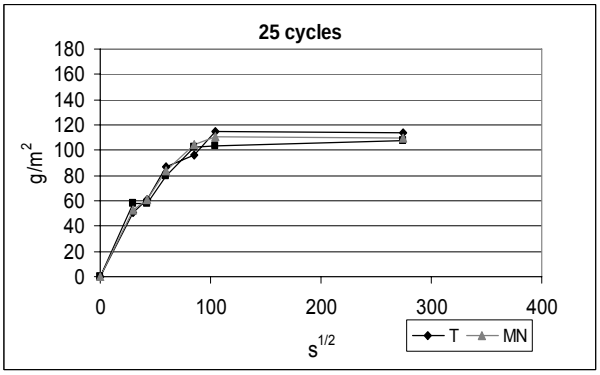

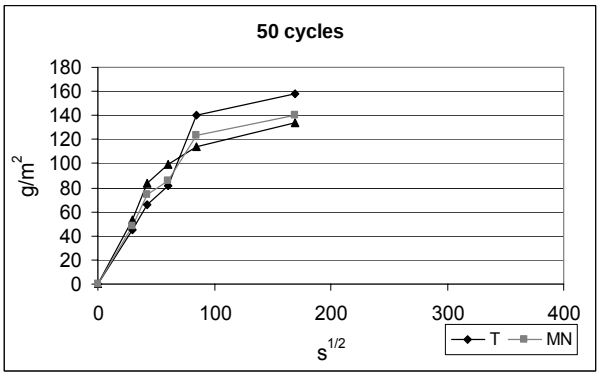

Freeze-thaw with salt – Vilachán granite

Water absorption

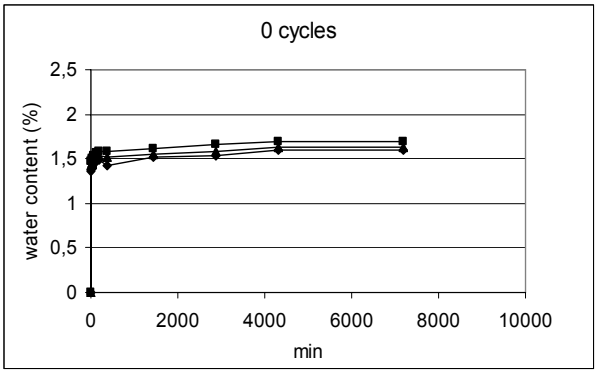

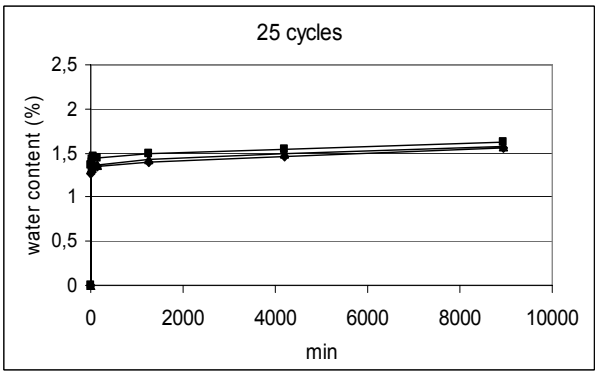

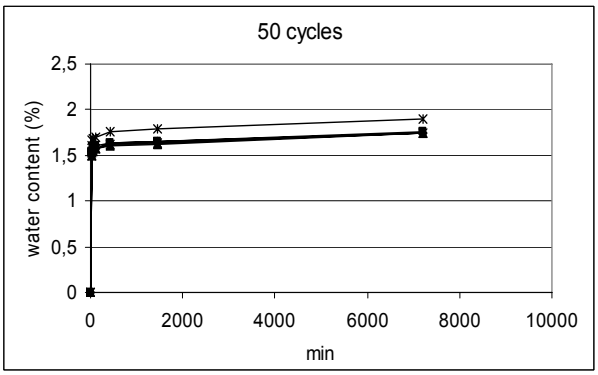

Capillary uptake

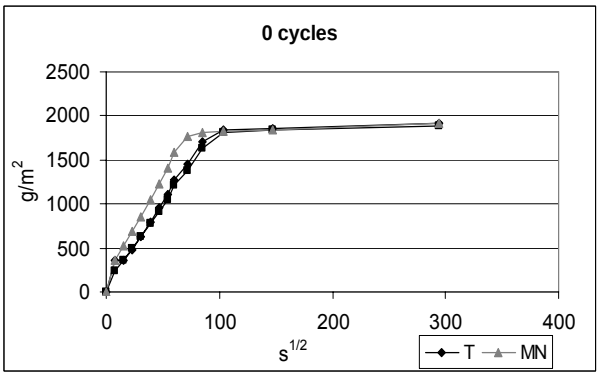

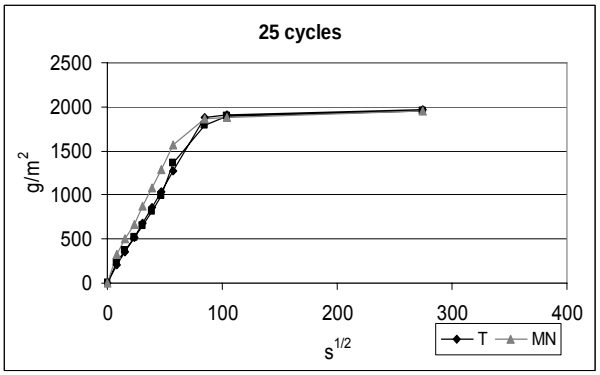

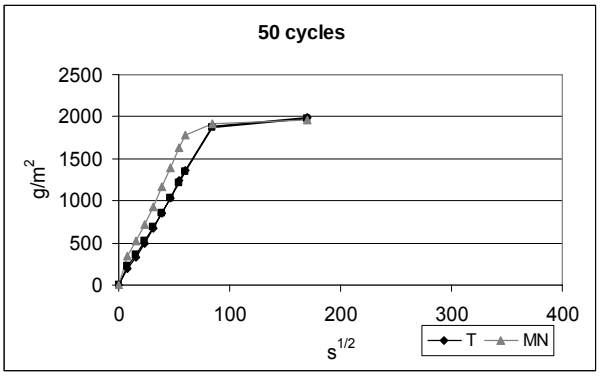

Freeze-thaw with salt – Szob andesite

Water absorption

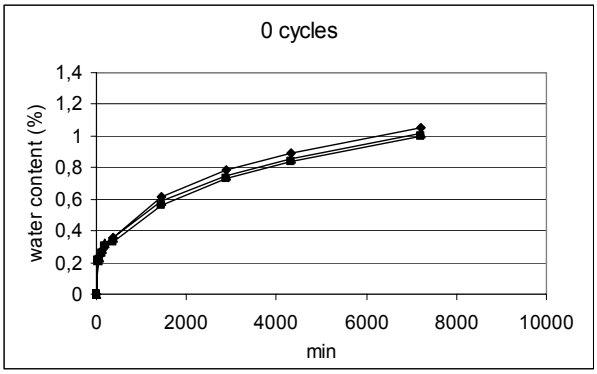

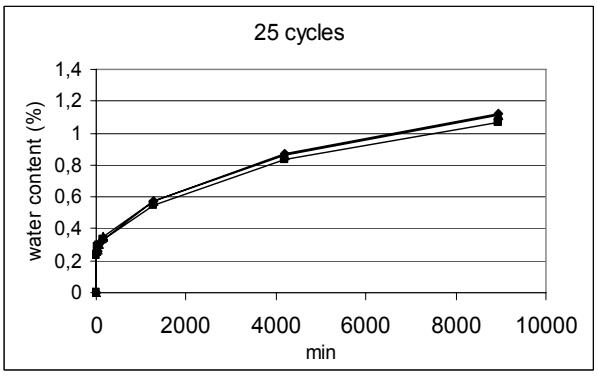

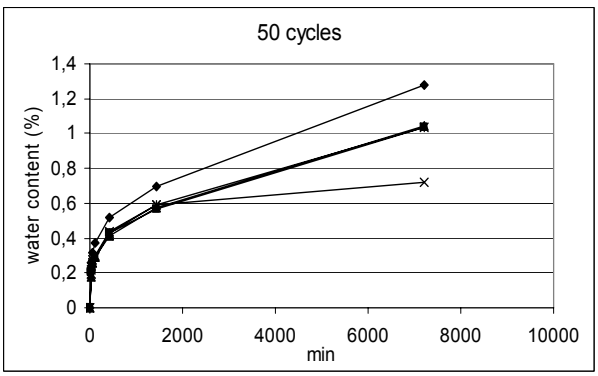

Capillary uptake

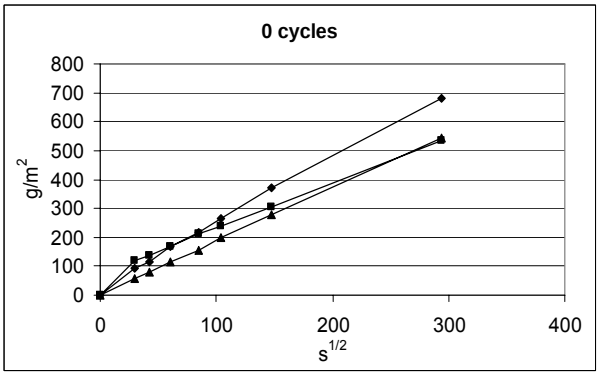

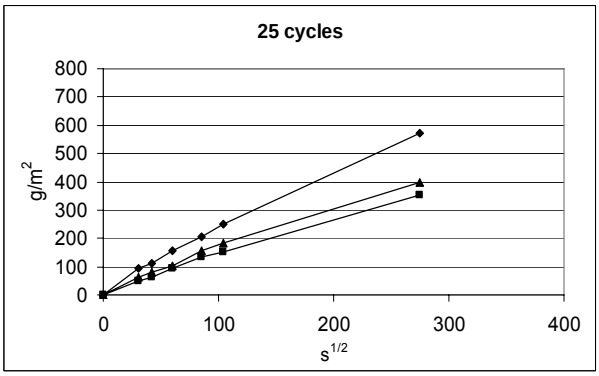

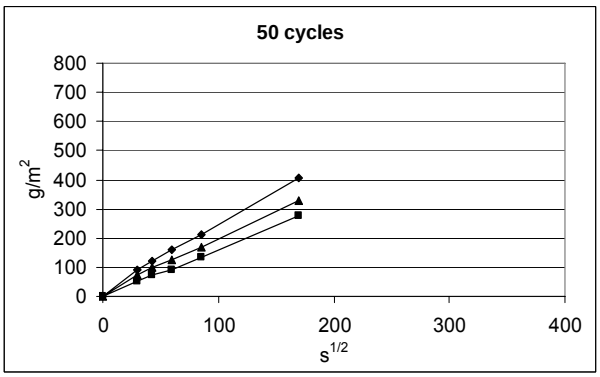

Appendix III.

Evolution of the void space properties

Measurements by Hg porosimetry

		original		after 45 salt crystallization cycles		after 200 freeze-thaw cycles		after 250 freeze-thaw cycles		after 50 freeze-thaw cycles with salt	
		average	st.dev	average	st.dev	average	st.dev	average	st.dev	average	st.dev
Macael marble	**total pore area (m^2/g)**	0,51	0,03	0,59	0,03	0,53	0,001	0,49	0,04	0,53	0,12
	average pore radius (μm)	0,014	0,002	0,014	0,001	0,020	0,002	0,017	0,002	0,019	0,002
	porosity (%)	0,97	0,11	1,11	0,03	1,38	0,08	1,11	0,02	1,35	0,45
Vilachán granite	**total pore area (m^2/g)**	1,01	0,02	1,08	0,10	1,15	0,19	1,18	0,21	1,19	0,25
	average pore radius (μm)	0,025	0,001	0,035	0,001	0,035	0,004	0,033	0,0004	0,034	0,003
	porosity (%)	3,3	0,1	4,8	0,3	5,0	0,2	4,9	0,9	5,0	0,7
Szob andesite	**total pore area (m^2/g)**	3,32	0,07	3,39	0,13	3,65	0,09	3,53	0,32	3,63	0,07
	average pore radius (μm)	0,0081	0,0001	0,0091	0,0007	0,0085	0,0003	0,0090	0,0001	0,0089	0,0002
	porosity (%)	3,47	0,09	3,98	0,18	4,00	0,00	4,17	0,11	4,13	0,02

Measurements by CLSM-DIP

	number of cycles		Macael marble				Silvestre Vilachán granite				Szob andesite			
			porosity (%)	Sv	mean aperture (μm)	LCD	porosity (%)	Sv	mean aperture (μm)	LCD	porosity (%)	Sv	mean aperture (μm)	LCD
	0	median	0,18	0,002	2,02	0,94	2,43	0,028	2,84	11,1	0,27	0,004	2,98	1,78
		st.dev.	0,27	0,004	2,33	1,68	4,54	0,037	1,02	11,6	0,54	0,006	1,24	3,31
salt crystallization	15	median	0,40	0,006	2,48	1,76	2,13	0,023	2,85	9,7	0,24	0,003	2,98	1,13
		st.dev.	0,49	0,005	0,91	2,49	3,86	0,032	1,45	10,8	0,21	0,003	1,42	1,91
	25	median	0,57	0,008	2,48	1,94	2,94	0,030	2,97	10,3	0,14	0,003	2,10	1,35
		st.dev.	0,51	0,006	0,90	2,53	4,85	0,045	1,48	11,9	0,44	0,006	1,15	2,55
	35	median	0,41	0,006	2,45	2,48	2,60	0,024	3,27	10,0	0,33	0,005	2,29	-
		st.dev.	0,47	0,006	1,08	4,83	5,11	0,034	1,72	10,3	0,29	0,005	1,21	-
	45	median	0,74	0,010	3,52	2,14	3,55	0,035	3,00	14,1	0,24	0,003	2,59	1,95
		st.dev.	1,18	0,007	1,75	3,76	5,36	0,049	1,38	13,8	0,50	0,008	1,90	3,11
freeze - thaw	50	median	1,39	0,018	2,58	5,61	3,54	0,033	3,35	10,6	0,19	0,003	2,32	0,99
		st.dev.	1,53	0,013	1,61	5,16	5,39	0,042	1,35	12,6	0,56	0,008	1,78	2,30
	100	median	0,37	0,006	2,19	2,44	2,73	0,028	3,17	11,4	0,28	0,004	3,04	2,98
		st.dev.	0,60	0,007	1,48	3,65	5,33	0,041	1,10	12,7	0,89	0,009	1,66	4,82
	150	median	0,44	0,008	2,11	2,89	1,59	0,021	2,66	7,0	0,65	0,009	2,77	3,68
		st.dev.	0,62	0,006	0,93	4,60	2,50	0,024	0,76	7,8	1,09	0,016	1,13	6,29

	number of cycles		Macael marble				Silvestre Vilachán granite				Szob andesite			
			porosity (%)	Sv	mean aperture (μm)	LCD	porosity (%)	Sv	mean aperture (μm)	LCD	porosity (%)	Sv	mean aperture (μm)	LCD
freeze - thaw	200	median	1,18	0,012	3,15	3,11	3,14	0,019	3,80	10,2	0,92	0,013	2,68	3,48
		st.dev.	1,32	0,009	1,16	3,11	5,25	0,041	3,54	12,9	0,74	0,009	0,77	4,37
	250	median	1,18	0,014	2,81	2,53	3,14	0,036	2,87	8,0	1,19	0,013	3,18	2,67
		st.dev.	0,80	0,008	0,79	3,55	5,30	0,045	0,68	14,7	1,23	0,015	1,02	6,44
freeze - thaw with salt	13	median	0,42	0,008	2,20	0,00	5,57	0,045	3,90	8,0	0,82	0,011	2,75	2,67
		st.dev.	0,42	0,005	0,97	3,62	5,26	0,037	0,95	13,7	0,61	0,009	0,88	4,39
	25	median	0,77	0,009	2,85	0,00	5,38	0,049	3,79	14,7	0,51	0,008	3,35	2,67
		st.dev.	0,86	0,007	1,11	3,86	5,75	0,044	1,11	14,3	0,67	0,008	1,14	3,61
	37	median	1,10	0,012	2,67	3,31	3,64	0,030	3,55	8,0	1,33	0,014	3,68	2,67
		st.dev.	1,14	0,007	1,80	3,50	6,13	0,047	3,42	15,7	0,91	0,010	1,02	4,54
	50	median	0,79	0,011	2,90	2,67	5,39	0,051	3,36	13,3	1,84	0,019	3,89	5,34
		st.dev.	0,83	0,008	1,11	5,19	7,12	0,058	1,35	18,0	1,45	0,015	0,84	6,67